



**DESIGN AND SYNTHESIS OF COUMARIN BASED ORGANIC  
FLUOROPHORES AND INVESTIGATION OF THEIR APPLICATIONS AS  
FLUORESCENT PROBES VIA SPECTROSCOPIC METHODS**

**A THESIS SUBMITTED TO  
THE GRADUATE SCHOOL OF NATURAL AND APPLIED SCIENCES  
OF  
GAZI UNIVERSITY**

**BY**

**Issah YAHAYA**

**IN PARTIAL FULFILLMENT OF THE REQUIREMENTS  
FOR  
THE DEGREE OF DOCTOR OF PHILOSOPHY  
IN  
CHEMISTRY**

**AUGUST 2018**

The thesis study titled "DESIGN AND SYNTHESIS OF COUMARIN BASED ORGANIC FLUOROPHORES AND INVESTIGATION OF THEIR APPLICATIONS AS FLUORESCENT PROBES VIA SPECTROSCOPIC METHODS" is submitted by Issah YAHAYA in partial fulfillment of the requirements for the degree of Doctor of Philosophy in the Department of Chemistry, Gazi University by the following committee.

**Supervisor:** Prof. Dr. Zeynel SEFEROĞLU

Chemistry Department, Gazi University

I certify that this thesis is a graduate thesis in terms of quality and content

**Chairman:** Prof. Dr. Hülya ŞENÖZ

Chemistry Department, Hacettepe University

I certify that this thesis is a graduate thesis in terms of quality and content

**Member:** Prof. Dr. Erden BANOĞLU

Professional Pharmaceutical Sciences, Gazi University

I certify that this thesis is a graduate thesis in terms of quality and content

**Member:** Assoc. Prof. Barış TEMELLİ

Chemistry Department, Hacettepe University

I certify that this thesis is a graduate thesis in terms of quality and content

**Member:** Assoc. Prof. Serkan YAVUZ

Chemistry Department, Gazi University

I certify that this thesis is a graduate thesis in terms of quality and content

Date: 09/08/2018

I certify that this thesis, accepted by the committee, meets the requirements for being a Doctor of Philosophy Thesis.

.....

Prof. Dr. Sena YAŞYERLİ

Director of Graduate School of Natural and Applied Sciences

## **ETHICAL STATEMENT**

I hereby declare that in this thesis study I prepared in accordance with thesis writing rules of Gazi University Graduate School of Natural and Applied Sciences;

- All data, information and documents presented in this thesis have been obtained within the scope of academic rules and ethical conduct,
  - All information, documents, assessments and results have been presented in accordance with scientific ethical conduct and moral rules,
  - All material used in this thesis that are not original to this work have been fully cited and referenced,
  - No change has been made in the data used,
  - The work presented in this thesis is original,
- or else, I admit all loss of rights to be incurred against me.

Issah YAHAYA

09/08/2018

KUMARİN TEMELLİ ORGANİK FLOROFORLARIN TASARIMI, SENTEZİ VE  
FLORESAN PROB OLARAK UYGULANABİLİRLİĞİNİN SPEKTROSKOPİK  
YÖNTEMLERLE İNCELENMESİ

(Doktora Tezi)

Issah YAHAYA

GAZİ ÜNİVERSİTESİ  
FEN BİLİMLERİ ENSTİTÜSÜ

Ağustos 2018

ÖZET

Bu çalışmada, mikrodalga ışıması destekli ve geleneksel sentez yöntemleri geliştirildi ve her iki yöntemin karşılaştırmalı analizi yapıldı. Her iki metot da etkili olmasına rağmen mikrodalga ışıması yöntemi kullanılarak geliştirilen metotun geleneksel metota göre çevre dostu, daha az zaman gerektiren, daha ucuz, ılıman koşullarda yapılabilmesi ve yüksek verim vb. üstünlüklerinden dolayı daha avantajlı olduğu görülmüştür. Mikrodalga ışıması yöntemi ile 3-asetilkumarin ve malonitril türevleri Knoevenagel tepkimesi ile kumarin-tiyofen türevleri ise Gewald reaksiyonu ile basamaklı ve tek kap yöntemi kullanılarak sentezlenmiştir. Bileşikler yüksek verimlerle sentezlenmiş ve sentezlenen tüm bileşiklerin yapıları <sup>1</sup>H-NMR, <sup>13</sup>C-NMR, HRMS, ve FTIR yöntemleriyle karakterize edilmiştir. Kumarin-tiyofen temelli bileşiklerin fotofiziksel özellikleri UV-GB ve Floresans spektroskopisi yöntemleriyle farklı polariteye sahip çeşitli çözücüler içerisinde belirlenmiştir. Ayrıca, 7-hidroksikumarin-tiyofen bileşiğinin floresan pH probu olma özelliği de araştırılmıştır. Son olarak, tüm kumarin-tiyofen temelli bileşiklerin potansiyel optik boyarmadde olarak kullanılabilirliğinin önemli bir ölçüsü olan ısıl kararlılık için bileşiklerin termal gravimetrik analizleri yapılmıştır.

Bilim Kodu : 20114

Anahtar Kelimeler : Kumarin, kumarin-tiyofen, geleneksel metot, çözücüsüz reaksiyon, mikrodalga destekli ışıma, gewald reaksiyonu, tek-kap üç bileşenli reaksiyon, fotofiziksel özellik, termogravimetrik analiz

Sayfa No : 205

Danışman : Prof. Dr. Zeynel SEFEROĞLU

DESIGN AND SYNTHESIS OF COUMARIN BASED ORGANIC FLUOROPHORES  
AND INVESTIGATION OF THEIR APPLICATIONS AS FLUORESCENT PROBES  
VIA SPECTROSCOPIC METHODS

(Ph. D. Thesis)

Issah YAHAYA

GAZI UNIVERSITY

GRADUATE SCHOOL OF NATURAL AND APPLIED SCIENCES

August 2018

ABSTRACT

In this study, two synthetic protocols have been developed; the microwave-assisted irradiation and the conventional procedures, and comparative analyses on the procedures were conducted. Even though both protocols were found to be efficient, the microwave-assisted irradiation reactions were identified to be the best, environmentally friendly, cost-effective, mild, efficient, with high yields, less time consuming but with high purity for the synthesis of 3-acetylcoumarins and their malononitrile derivatives via Knoevenagel condensation, and the coumarin-thiophene derivatives via Gewald reaction in stepwise and one-pot three-component. The compounds were synthesized in good to excellent yields and their structures were characterized using spectroscopic methods such as  $^1\text{H-NMR}$ ,  $^{13}\text{C-NMR}$ , HRMS, and FTIR. Photophysical activities of all the target coumarin-thiophene hybrids were determined using a combination of UV-vis and fluorescence spectroscopy in various solvents with varying polarities. In addition, 7-hydroxycoumarin-thiophene derivative was also investigated for use as fluorescence pH probe. The thermal properties of all the coumarin-thiophene based compounds were also evaluated with TGA in order to test their potency and applicability as optical dyes.

Science Code : 20114

Key Words : Coumarins, coumarin-thiophene, conventional method, solvent-free condition, microwave-assisted irradiation, gewald reaction, one-pot three-component reaction, photophysical property, thermogravimetric analysis

Page Number : 205

Supervisor : Prof. Dr. Zeynel SEFEROĞLU

## ACKNOWLEDGEMENT

This thesis is first and foremostly dedicated to The Glory, Greatness, and Oneness of ALLAH (SWT), my lovely wife, Sharifatu Abdul-Samed, for her wonderful support and encouragement, and my children; Raiyan Issah, Farida Issah, and Faleehah Issah.

I thank the Turkish Government Scholarships (Türkiye Bursları) for given me scholarship as well the opportunity to study a Ph.D. programme in one of the best universities in Turkey, Gazi University.

I am particularly appreciative to Professor Doctor Zeynel SEFEROĞLU, my advisor, for introducing me into the World of Synrthetic Organic Chemistry, guiding me through various academic endeavours, providing with novel trends and unique scientific environment as a whole, and Fluorescence applications to solving varieties of issues facing Humans, Animals, and the Environment. He is such a mentor. The first time I met this humble but intelligent man, I knew that I had met the right person for my dream academic advancement. My choice became obvious as this learned Professor guided and helped me both academically and socially (Me and family living in Turkey)-Thank you so much Professor Doctor SEFEROĞLU may Allah reward you in various ways and make your aspirations easier and achievable for you, aameen.

I am also grateful and appreciative to Professor Nurgül SEFEROĞLU, the wife of Professor SEFEROĞLU, also at Gazi University, for being there for my advisor in terms of the lots of support for me and my family living in Turkey-Thanks Professor Nurgül SEFEROĞLU.

I wish to express my profound gratitude to the members of my Proficiency Examination as well as the thesis Jury members. My gratitude can not be ended withiout acknowledging all members of the Synthesis Group of Target Organic Molecules (SYNGTOM).

## TABLE OF CONTENTS

	<b>Page</b>
ÖZET .....	iv
ABSTRACT.....	v
ACKNOWLEDGEMENT .....	vi
TABLE OF CONTENTS.....	vii
LISTS OF TABLES.....	xii
LISTS OF FIGURES .....	xiii
LIST OF SYMBOLS AND ABBREVIATIONS .....	xvii
<b>1. INTRODUCTION.....</b>	<b>1</b>
1.1. Justification for the Study .....	5
1.2. Objectives of the Research.....	5
<b>2. GENERAL INFORMATON AND LITERATURE SUMMARY OF THE STUDY .....</b>	<b>7</b>
2.1. Structure and Properties of The Molecules Synthesized in Thesis .....	7
2.2. Coumarin Derivatives and Their Applications .....	10
2.3. Malononitrile Derivatives and Their Applications .....	14
2.4. 2-Aminothiophenes and Their Uses .....	15
2.5. Amide Derivatives and Their Applications.....	16
2.6. Sulfonamide Derivatives and Their Applications .....	17
2.7. Urea Derivatives and Their Applications.....	18
2.8. Microwave-Assisted Irradiation in Organic Synthesis .....	20
2.8.1. Microwave irradiation versus conventional method.....	21
2.9. Some Literature Mechanisms for The Formation of The Target Molecules.....	23
2.9.1. Literature mechanisms for the formation of 3-acetylcoumarin derivatives .....	23
2.9.2. Formation of malonitrile derivative published by our group .....	28

	<b>Page</b>
2.9.3. Mechanism for the formation of 2-aminothiophenes.....	29
<b>3. MATERIALS AND METHODS .....</b>	<b>31</b>
3.1. Materials and Tools.....	31
3.1.1. Chemical substances used.....	31
3.1.2. Devices used .....	31
3.2. Synthesis of Initial 3-Acetylcoumarins.....	32
3.2.1. General procedure for the synthesis of 3-acetylcoumarins via conventional procedure .....	33
3.2.2. General procedure for the synthesis of 3-acetylcoumarins via microwave-assisted irradiation procedure .....	33
3.3. Synthesis of Malononitrile Derivatives.....	35
3.3.1. General procedure for the synthesis of malononitrile derivatives via conventional procedure .....	36
3.3.2. General procedure for the synthesis of malononitrile derivatives of the synthesized coumarins via microwave-assisted irradiation procedure.....	36
3.4. Synthesis of Coumarin-Thiophene Derivatives .....	39
3.4.1. General procedure for the synthesis of coumarin-thiophene hybrids via conventional procedure in stepwise .....	39
3.4.2. General procedure for the synthesis of coumarin-thiophene hybrids via microwave-assisted irradiation procedure in stepwise.....	40
3.5. Synthesis of Coumarin-Thiophene Hybrids Via One-Pot Three-Component ....	40
3.5.1. General procedure for the synthesis of coumarin-thiophene hybrids via conventional procedure in one-pot three-component.....	41
3.5.2. General procedure for the synthesis of coumarin-thiophene hybrids via microwave-assisted irradiation procedure in one-pot three- component.....	41
3.6. Synthesis of Amides, Disulfonamide, and Urea derivatives of Benzocoumarin-Thiophene derivative .....	43
3.6.1. Synthesis of the amide derivatives.....	43
3.6.2. Synthesis of disulfonamide derivative of benzo[f]coumarin-thiophene derivatives .....	47

	<b>Page</b>
3.6.3. Synthesis of urea derivative of Benzo[f]coumarin--thiophene derivative.....	49
3.7. The Structural Characterizations and Elucidations of the Synthesized 3-Acetylcoumarins (1-10).....	51
3.7.1. Structural elucidation for 3-Acetyl-2 <i>H</i> -chromen-2-one (1).....	51
3.7.2. Structural elucidation for 3-Acetyl-6-bromo-2 <i>H</i> -chromen-2-one (2).....	52
3.7.3. Structural elucidation for 3-Acetyl-6-chloro-2 <i>H</i> -chromen-2-one (3).....	53
3.7.4. Structural elucidation for 3-Acetyl-6-hydroxy-2 <i>H</i> -chromen-2-one (4)....	54
3.7.5. Structural elucidation for 3-Acetyl-7-(diethylamino)-2 <i>H</i> -chromen-2-one (5) .....	55
3.7.6. Structural elucidation for 3-Acetyl-7-methoxy-2 <i>H</i> -chromen-2-one (6) ...	56
3.7.7. Structural elucidation for 3-Acetyl-7-hydroxy-2 <i>H</i> -chromen-2-one (7)....	57
3.7.8. Structural elucidation for 3-Acetyl-8-ethoxy-2 <i>H</i> -chromen-2-one (8) .....	58
3.7.9. Structural elucidation for 3-Acetyl-8-methoxy-2 <i>H</i> -chromen-2-one (9) ...	59
3.7.10. Structural elucidation for 2-Acetyl-3 <i>H</i> -benzo[f]chromen-3-one (10) ....	60
3.8. The Structural Characterizations and Elucidations of the synthesized Malononitriles.....	61
3.8.1. Structural elucidation for 2-(1-(2-Oxo-2 <i>H</i> -chromen-3-yl)ethylidene)malononitrile (11) .....	61
3.8.2. Structural elucidation for 2-(1-(6-bromo-2-oxo-2 <i>H</i> -chromen-3-yl)ethylidene) malononitrile (12).....	62
3.8.3. Structural elucidation for 2-(1-(6-chloro-2-oxo-2 <i>H</i> -chromen-3-yl)ethylidene) malononitrile (13).....	63
3.8.4. Structure elucidation for 2-(1-(6-hydroxy-2-oxo-2 <i>H</i> -chromen-3-yl)ethylidene) malononitrile (14).....	64
3.8.5. Structural elucidation for (1-(7-(Diethylamino)-2-oxo-2 <i>H</i> -chromen-3-yl)ethylidene)malononitrile (15).....	65
3.8.6. Structural elucidation for 2-(1-(7-methoxy-2-oxo-2 <i>H</i> -chromen-3-yl)ethylidene) malononitrile (16).....	66
3.8.7. Structural elucidation for 2-(1-(7-hydroxy-2-oxo-2 <i>H</i> -chromen-3-yl)ethylidene) malononitrile (17).....	67

	<b>Page</b>
3.8.8. Structural elucidation of 2-(1-(8-ethoxy-2-oxo-2 <i>H</i> -chromen-3-yl)ethylidene) malononitrile (18) .....	68
3.8.9. Structural elucidation for 2-(1-(8-methoxy-2-oxo-2 <i>H</i> -chromen-3-yl)ethylidene) malononitrile (19) .....	70
3.8.10. Structural elucidation for 2-(1-(3-oxo-3 <i>H</i> -benzo[ <i>f</i> ]chromen-2-yl)ethylidene) malononitrile (20) .....	71
3.9. The Structural Characterizations and Elucidations of the synthesized 2-Aminothiophenes .....	72
3.9.1. Structural elucidation for 2-Amino-4-(2-oxo-2 <i>H</i> -chromen-3-yl)thiophene-3-carbonitrile (21).....	72
3.9.2. Structural elucidation for 2-Amino-4-(6-bromo-2-oxo-2 <i>H</i> -chromen-3-yl) thiophene-3-carbonitrile (22) .....	73
3.9.3. Structural elucidation for 2-Amino-4-(6-chloro-2-oxo-2 <i>H</i> -chromen-3-yl)thiophene-3-carbonitrile (23) .....	74
3.9.4. Structural elucidation for 2-Amino-4-(6-hydroxy-2-oxo-2 <i>H</i> -chromen-3-yl) thiophene-3-carbonitrile (24) .....	75
3.9.5. Structural elucidation for 2-Amino-4-(7-(diethylamino)-2-oxo-2 <i>H</i> -chromen-3-yl) thiophene-3-carbonitrile (25) .....	76
3.9.6. Structural elucidation for 2-Amino-4-(7-methoxy-2-oxo-2 <i>H</i> -chromen-3-yl) thiophene-3-carbonitrile (26) .....	78
3.9.7. Structural elucidation for 2-Amino-4-(7-hydroxy-2-oxo-2 <i>H</i> -chromen-3-yl) thiophene-3-carbonitrile (27) .....	79
3.9.8. Structural elucidation for 2-Amino-4-(8-ethoxy-2-oxo-2 <i>H</i> -chromen-3-yl)thiophene-3-carbonitrile (28) .....	80
3.9.9. Structural elucidation for 2-Amino-4-(8-methoxy-2-oxo-2 <i>H</i> -chromen-3-yl) thiophene-3-carbonitrile (29) .....	82
3.9.10. Structural elucidation for 2-Amino-4-(3-oxo-3 <i>H</i> -benzo[ <i>f</i> ]chromen-2-yl)thiophene-3-carbonitrile (30) .....	83
3.10. The Structural Characterizations and Elucidations of the synthesized Amide derivatives .....	84
3.10.1. Structural elucidation for N-(3-cyano-4-(3-oxo-3 <i>H</i> -benzo[ <i>f</i> ]chromen-2-yl) thiophen-2-yl)acetamide (31) .....	84
3.10.2. Structure elucidation for N-(3-cyano-4-(3-oxo-3 <i>H</i> -benzo[ <i>f</i> ]chromen-2-yl)thiophen-2-yl)benzamide (32) .....	86

	<b>Page</b>
3.10.3. Structure elucidation for N-(3-cyano-4-(3-oxo-3H-benzo[f]chromen-2-yl)thiophen-2-yl)-4-nitrobenzamide (33).....	87
3.11. The Structural Characterization and Elucidation of the synthesized Diulfonamide derivative (34) .....	88
3.11.1. Structural elucidation for N-(3-cyano-4-(3-oxo-3H-benzo[f]chromen-2-yl) thiophen-2-yl)-N-(methylsulfonyl)methanesulfonamide (34) .....	88
3.12. The Structural Characterization and Elucidation of the synthesized Urea derivative (35).....	90
3.12.1. Structural elucidation for 1-(3-cyano-4-(3-oxo-3H-benzo[f]chromen-2-yl)thiophen-2-yl)-3-phenylurea (35) .....	90
<b>4. RESULTS AND DISCUSSION .....</b>	<b>93</b>
4.1. Photophysical activities of dyes 21-35.....	102
4.2. Thermal properties of dyes 21-35 .....	116
<b>5. CONCLUSION AND RECOMMENDATIONS.....</b>	<b>119</b>
<b>REFERENCES .....</b>	<b>121</b>
<b>APPENDICES .....</b>	<b>141</b>
Appendix-1. FT-IR, <sup>1</sup> H-NMR, <sup>13</sup> C-NMR, HR-MS of the 3-Acetylcoumarins (1)-(10).....	142
Appendix-2. FT-IR, <sup>1</sup> H-NMR, <sup>13</sup> C-APT, HRMS of the Malononitriles 11-20.....	152
Appendix-3. FT-IR, <sup>1</sup> H-NMR, <sup>13</sup> C-APT, HRMS of the 2-Aminothiophenes 21-30.....	170
Appendix-4. FT-IR, <sup>1</sup> H-NMR, <sup>13</sup> C-APT, HRMS for the Amides, the Sulfonamide, and the Urea 31-35.....	188
Appendix-5. Results Tables, Physicochemical Properties, Comparative Analyses of Data for all the Synthesized compounds.....	198
<b>CURRICULUM VITAE.....</b>	<b>205</b>

**LISTS OF TABLES**

<b>Table</b>	<b>Page</b>
Table 2.1. Some biologically active coumarins .....	13
Table 4.1. Comparative analysis of data of 3-acetylcoumarins synthesized via conventional and microwave irradiation procedures.....	94
Table 4.2. Optimization of the reaction conditions for synthesis of 11 .....	95
Table 4.3. Comparative analysis of data of malononitriles synthesized via conventional and microwave irradiation procedures.....	96
Table 4.4. Optimization of the reaction conditions for synthesis of 21 .....	97
Table 4.5. Comparative analysis of data of coumarin-thiophenes synthesized via conventional and microwave irradiation procedures in stepwise.....	98
Table 4.6. Optimization of the one-pot three-component reaction conditions for synthesis of 30 .....	99
Table 4.7. Comparative analysis of data of coumarin-thiophene synthesized via conventional and microwave-assisted irradiation procedures in one-pot three-component .....	100
Table 4.8. Comparative analysis of data of compounds synthesized via conventional and microwave-assisted irradiation procedures.....	101
Table 4.9. Photophysical activities of 21-23.....	109
Table 4.10. Photophysical activities of 24-26.....	110
Table 4.11. Photophysical activities of 27-29.....	110
Table 4.12. Photophysical activities of 30 .....	110

## LISTS OF FIGURES

<b>Figure</b>	<b>Page</b>
Figure 1.1. Structures and numbering of coumarin and benzocoumarins .....	4
Figure 1.2. Biologically active and commercially important coumarin derivatives ....	4
Figure 2.1. Structures of some industrially important coumarins .....	8
Figure 2.2. Synthes of ylides via different strategies .....	9
Figure 2.3. Variation of the gewald reaction .....	10
Figure 2.4. Substituent effect on the coumarin core and applications of coumarins....	11
Figure 2.5. Some sources of coumarins.....	12
Figure 2.6. Plant sources of coumarins.....	12
Figure 2.7. Drugs in the market that contain coumarins .....	13
Figure 2.8. Structures of substituted 2-aminothiophenes T1-4 .....	15
Figure 2.9. 2-Ureido-thiophene-3-carboxylate 18 antibacterial agent against S. aureus .....	15
Figure 2.10. General structure of an amide.....	16
Figure 2.11. Microwave procedure for the synthesis amides .....	17
Figure 2.12. General structure of sulfonamides.....	18
Figure 2.13. General synthetic pathway for sulfonamides .....	18
Figure 2.14. Structure of urea .....	19
Figure 2.15. Synthesis of the anthraquinone urea derivatives UD1-2 .....	20
Figure 2.16. Synthesis of UD3.....	20
Figure 2.17. Comparison between conventional method and microwave-assisted irradiation .....	22
Figure 2.18. Pechmann condensation .....	24
Figure 2.19. Claisen rearrangement for the synthesis of coumarin .....	25
Figure 2.20. Synthesis of coumarin via the perkin reaction .....	26
Figure 2.21. Synthesis of coumarin via wittig reaction .....	26

<b>Figure</b>	<b>Page</b>
Figure 2.22. Preparation of coumarin via knoevenagel condensation.....	27
Figure 2.23. General mechanism for knoevenagel condensation .....	28
Figure 2.24. The synthesis of 3-acetylcoumarin .....	28
Figure 2.25. The synthetic pathway for Malononitriles.....	29
Figure 3.1. General synthetic rout for the 3-acetylcoumarins 1-10 .....	33
Figure 3.2. Structures of the salisaldehydes (S1-10) and the 3-acetylcoumarins 1-10...	34
Figure 3.3. Plausible mechanism for the synthesized 3-acetylcoumarins .....	35
Figure 3.4. General synthetic pathways for the malononitriles 11-20.....	36
Figure 3.5. Structures of the synthesized malononitriles 11-20.....	37
Figure 3.6. Plausible mechanism for the synthesized malononitriles .....	38
Figure 3.7. General synthetic pathways for the coumarin-thiophene hybrids .....	39
Figure 3.8. General synthetic pathways for the coumarin-thiophene hybrids in one- pot three-component.....	40
Figure 3.9. Structures of the synthesized coumarin-thiophene hybrids 21-30 .....	42
Figure 3.10. Plausible mechanism for the synthesized of coumarin-thiophenes 21- 30.....	42
Figure 3.11. Synthetic routs for the amide, sulfonamide, and urea derivatives 31-35 ...	43
Figure 3.12. Plausible mechanism for the synthesized amide derivatives.....	46
Figure 3.13. Plausible mechanism for the synthesized disulfonamide derivative .....	48
Figure 3.14. Plausible mechanism for the synthesized urea derivative .....	50
Figure 3.15. Structures of the synthesized amide, sulfonamide, and urea derivatives 31-35 .....	50
Figure 3.16. Structure of 3-Acetyl-2 <i>H</i> -chromen-2-one (1) .....	51
Figure 3.17. Structure of 3-Acetyl-6-bromo-2 <i>H</i> -chromen-2-one (2) .....	52
Figure 3.18. Structure of 3-Acetyl-6-chloro-2 <i>H</i> -chromen-2-one (3).....	53
Figure 3.19. Structure of 3-Acetyl-6-hydroxy-2 <i>H</i> -chromen-2-one (4) .....	54
Figure 3.20. Structure of 3-Acetyl-7-(diethylamino)-2 <i>H</i> -chromen-2-one (5).....	55

<b>Figure</b>	<b>Page</b>
Figure 3.21. Structure of 3-Acetyl-7-methoxy-2 <i>H</i> -chromen-2-one (6).....	56
Figure 3.22. Structure of 3-Acetyl-7-hydroxy-2 <i>H</i> -chromen-2-one (7) .....	57
Figure 3.23. Structure of 3-Acetyl-8-ethoxy-2 <i>H</i> -chromen-2-one (8).....	58
Figure 3.24. Structure of 3-Acetyl-8-methoxy-2 <i>H</i> -chromen-2-one (9).....	59
Figure 3.25. Structure of 2-Acetyl-3 <i>H</i> -benzo[ <i>f</i> ]chromen-3-one (10) .....	60
Figure 3.26. Structure of 2-(1-(2-Oxo-2 <i>H</i> -chromen-3-yl)ethylidene)malononitrile (11) .....	61
Figure 3.27. Structure of 2-(1-(6-bromo-2-oxo-2 <i>H</i> -chromen-3- yl)ethylidene)malononitrile (12) .....	62
Figure 3.28. Structure of 2-(1-(6-chloro-2-oxo-2 <i>H</i> -chromen-3- yl)ethylidene)malononitrile (13) .....	63
Figure 3.29. Structure of 2-(1-(6-hydroxy-2-oxo-2 <i>H</i> -chromen-3- yl)ethylidene)malononitrile (14) .....	65
Figure 3.30. Structure of (1-(7-(Diethylamino)-2-oxo-2 <i>H</i> -chromen-3- yl)ethylidene)malononitrile (15) .....	66
Figure 3.31. Structure of 2-(1-(7-methoxy-2-oxo-2 <i>H</i> -chromen-3- yl)ethylidene)malononitrile (16) .....	67
Figure 3.32. Structure of 2-(1-(7-hydroxy-2-oxo-2 <i>H</i> -chromen-3- yl)ethylidene)malononitrile (17) .....	68
Figure 3.33. Structure of 2-(1-(8-ethoxy-2-oxo-2 <i>H</i> -chromen-3- yl)ethylidene)malononitrile (18) .....	69
Figure 3.34. Structure of 2-(1-(8-methoxy-2-oxo-2 <i>H</i> -chromen-3- yl)ethylidene)malononitrile (19) .....	70
Figure 3.35. Structure of 2-(1-(3-oxo-3 <i>H</i> -benzo[ <i>f</i> ]chromen-2- yl)ethylidene)malononitrile (20) .....	72
Figure 3.36. Structure of 2-Amino-4-(2-oxo-2 <i>H</i> -chromen-3-yl)thiophene-3- carbonitrile (21).....	73
Figure 3.37. Structure of 2-Amino-4-(6-bromo-2-oxo-2 <i>H</i> -chromen-3-yl)thiophene- 3-carbonitrile (22) .....	74
Figure 3.38. Structure of 2-Amino-4-(6-chloro-2-oxo-2 <i>H</i> -chromen-3-yl)thiophene- 3-carbonitrile (23) .....	75

<b>Figure</b>	<b>Page</b>
Figure 3.39. Structure of 2-Amino-4-(6-hydroxy-2-oxo-2 <i>H</i> -chromen-3-yl)thiophene-3-carbonitrile (24).....	76
Figure 3.40. Structure of 2-Amino-4-(7-(diethylamino)-2-oxo-2 <i>H</i> -chromen-3-yl)thiophene-3-carbonitrile (25) .....	77
Figure 3.41. Structure of 2-Amino-4-(7-methoxy-2-oxo-2 <i>H</i> -chromen-3-yl)thiophene-3-carbonitrile (26).....	79
Figure 3.42. Structure of 2-Amino-4-(7-hydroxy-2-oxo-2 <i>H</i> -chromen-3-yl)thiophene-3-carbonitrile (27).....	80
Figure 3.43. Structure of 2-Amino-4-(8-ethoxy-2-oxo-2 <i>H</i> -chromen-3-yl)thiophene-3-carbonitrile (28) .....	81
Figure 3.44. Structure of 2-Amino-4-(8-methoxy-2-oxo-2 <i>H</i> -chromen-3-yl)thiophene-3-carbonitrile (29).....	82
Figure 3.45. Structure of 2-Amino-4-(3-oxo-3 <i>H</i> -benzo[ <i>f</i> ]chromen-2-yl)thiophene-3-carbonitrile (30) .....	84
Figure 3.46. Structure of <i>N</i> -(3-cyano-4-(3-oxo-3 <i>H</i> -benzo[ <i>f</i> ]chromen-2-yl)thiophen-2-yl)acetamide (31) .....	85
Figure 3.47. Structure of <i>N</i> -(3-cyano-4-(3-oxo-3 <i>H</i> -benzo[ <i>f</i> ]chromen-2-yl)thiophen-2-yl)benzamide (32) .....	87
Figure 3.48. Structure of <i>N</i> -(3-cyano-4-(3-oxo-3 <i>H</i> -benzo[ <i>f</i> ]chromen-2-yl)thiophen-2-yl)-4-nitrobenzamide (33).....	88
Figure 3.49. Structure of <i>N</i> -(3-cyano-4-(3-oxo-3 <i>H</i> -benzo[ <i>f</i> ]chromen-2-yl)thiophen-2-yl)- <i>N</i> -(methylsulfonyl) methanesulfonamide (34).....	90
Figure 3.50. Structure of 1-(3-cyano-4-(3-oxo-3 <i>H</i> -benzo[ <i>f</i> ]chromen-2-yl)thiophen-2-yl)-3-phenylurea (35).....	91

## LIST OF SYMBOLS AND ABBREVIATIONS

The symbols and abbreviations used in this thesis are presented in below with explanations.

<b>Symbols</b>	<b>Explanations</b>
<b>A</b>	Absorbance
$\lambda_{ab}$	absorption wavelength
$^{\circ}\text{C}$	Degrees celcius
<i>c</i>	molar concentration of solute in mol L <sup>-1</sup>
$\delta$	NMR chemical shift / ppm
$\lambda_{em}$	emission wavelength
$\epsilon$	molar absorptivity or the molar extinction coefficient in cm <sup>-1</sup> M <sup>-1</sup>

<b>Abbreviations</b>	<b>Explanations</b>
<b><sup>13</sup>C-APT</b>	Carbon-13 Attached Proton Test
<b>AcOEt</b>	Ethyl acetate
<b>AcOH</b>	Acetic acid
<b>AlCl<sub>3</sub></b>	Aluminium chloride
<b>CAN</b>	Cerium (IV) ammonium nitrate
<b>CDCl<sub>3</sub></b>	Deuterated chloroform
<b>CF<sub>3</sub>CO<sub>2</sub>H</b>	Trifluoroacetic acid
<b>CH<sub>2</sub>Cl<sub>2</sub></b>	Dichlormethane
<b>CHCl<sub>3</sub></b>	Chloroform
<b>DCM</b>	Dichloromethane
<b>DMAP</b>	Dimethylaminopyridine
<b>DMF</b>	<i>N,N</i> -Dimethylformamide
<b>DMSO</b>	Dimethyl sulfoxide
<b>DMSO-<i>d</i><sub>6</sub></b>	Deuterated dimethyl sulfoxide
<b>Et<sub>2</sub>NH</b>	Diethylamine

<b>Abbreviations</b>	<b>Explanations</b>
<b>Et<sub>2</sub>O</b>	Diethyl ether
<b>Et<sub>3</sub>N</b>	Triethylamine
<b>EtOAc</b>	Ethyl acetate
<b>EtOH</b>	Ethanol
<b>FT-IR</b>	Fourier-transform Infrared
<b>FVP</b>	Flash Vacuum Pyrolysis
<b>g</b>	Gram
<b>h</b>	Hour
<b>HCl</b>	Hydrochloric acid
<b>HIV</b>	Human immunodeficiency virus
<b>hrs.</b>	Hours
<b>Hz</b>	Hertz
<b>IR</b>	Infra-red
<b>K<sub>2</sub>CO<sub>3</sub></b>	Potassium carbonate
<b>KBr</b>	Potassium bromide
<b>KOH</b>	Potassium hydroxide
<b>LiH<sub>2</sub>PO<sub>4</sub></b>	Lithium dihydrogenphosphate
<i>m/e</i>	mass/electron
<b>MeCN</b>	Acetonitrile
<b>MeOH</b>	Methanol
<b>mg</b>	Milligram
<b>MgSO<sub>4</sub></b>	Magnesium sulphate
<b>MHz</b>	Megahertz
<b>min</b>	Minutes
<b>mL</b>	Milliliter
<b>mm</b>	millimolar
<b>mmol</b>	Millimole
<b>mol</b>	Mole
<b>mol<sup>-1</sup>. cm<sup>-1</sup></b>	Per mol per centimeter
<b>mp</b>	Melting point
<b>MSA</b>	Methanesulfonic acid
<b>MW</b>	Microwave

<b>Abbreviations</b>	<b>Explanations</b>
<b>MWI</b>	Microwave Irradiation
<b>Na<sub>2</sub>SO<sub>4</sub></b>	Sodium sulphate
<b>NaCl</b>	Sodium chloride
<b>NaH</b>	Sodium hydride
<b>NaHCO<sub>3</sub></b>	Sodium hydrogen carbonate
<b>NaOEt</b>	Sodium ethoxide
<b>NaOH</b>	Sodium hydroxide
<b>NH<sub>4</sub>Cl</b>	Ammonium chloride
<b>NH<sub>4</sub>OAc</b>	Ammonium acetate
<b>nM</b>	Nanomolar
<b>nm</b>	Nanometer
<b>NMR</b>	Nuclear magnetic resonance
<b>NOAC</b>	Ammonium acetate
<b>PhMe</b>	Toluene
<b>ppm</b>	Parts per million
<b>RT</b>	Room temperature
<b>s</b>	seconds
<b>S<sub>8</sub></b>	Elemental sulfur
<b>SO<sub>2</sub>NH<sub>2</sub></b>	Sulfuramidite
<b>TBAC</b>	tetra-Butylammonium chloride
<b>TBAF</b>	tetra-Butylammonium fluoride
<b>TEA</b>	Trimethylamine
<b>TFA</b>	Trifluoroacetate
<b>TFAA</b>	Trifluoroacetic acid
<b>TGA</b>	Thermogravimetric Analysis
<b>THF</b>	Tetrahydrofuran
<b>TLC</b>	Thin layer chromatography
<b>TMS</b>	Trimethylsilyl
<b>TMSOAc</b>	trimethylsilyl acetate
<b>UV</b>	Ultraviolet
<b>UV-Vis</b>	Ultraviolet Visible
<b>W</b>	Watt

## 1. INTRODUCTION

A great number of naturally occurring compounds contain heterocyclic rings as an essential and useful part of their structure. These include alkaloids, flavonoids, coumarins and terpenoids, and they are mostly used as medicines. Among the large number of heterocycle compounds, coumarin and its derivatives have remarkable activities against bacteria [1], fungi [2], tumours [3], viruses [4], and importantly against HIV protease [5]. They are also used as anti-coagulants [6], free radical scavengers [7], lipoxygenase [8], and cyclooxygenase [9] inhibitors.

Coumarin was first isolated in 1822 from the tonka bean [10]. Coumarins were also isolated from sweet clover, bison grass, and woodruff [11]. They are found in a variety of plant sources in the form of benzopyrene derivatives. Coumarin and its derivatives have useful effects in plant biochemistry and physiology; are involved in the actions of plant growth hormones and growth regulators, in the control of respiration, photosynthesis, and as defense against infection [12]. Compounds containing the coumarin nucleus (2H-1-benzopyran-2-one) constitute an important class of heterocycles, which occupy an important place in the realm of natural products and synthetic organic chemistry [13,14]. Some marine alkaloid coumarin derivatives such as ningalin B and lamellarin D are known to exhibit HIV-1 integrase inhibition, immunomodulatory activity, and cytotoxicity [15-17]. Moreover, (+)-calanolide A is a nonnucleoside reverse transcriptase inhibitor (NNRTI) which has potent activity against HIV-1 [18,19]. NNRTI was first isolated from *Calophyllum lanigerum* in Malaysia [18]. Again, (+)-calanolide A has been employed for anti-HIV activity, but (-)-calanolide A was found to be inactive. The isolation of (+)-inophyllum B from *C. inophyllum*, a known most active component for inhibition against HIV-reverse transcriptase, was reported by Patil et al [20]. In 1985, tetracyclic coumarin, (+)-cordatolide A, was isolated from the light petrol extract of the leaves of *C. cordatooblangum* [21]. Coumarins are classified according to four main parts. Simple coumarins are the first, which includes the hydroxylated, alkoxyated, or alkylated on the benzene ring e.g., umbelliferone [22,23]. Furanocoumarins are the second, which contain a five-membered furan ring attached to the coumarin nucleus and are subdivided into the linear furanocoumarins e.g., xanthotoxin [24] and the angular furanocoumarins e.g., angelicin [25]. Pyranocoumarins are the third, which contain a six-membered ring attached

to the coumarin moiety e.g., seselin and xanthyletin [26]. Last but not the least, the fourth are coumarins with substituents in the pyrone ring e.g., warfarin [27]. Other important coumarin derivatives are the benzocoumarins. Benzocoumarin derivatives can be classified into four types depending on the position of the fused benzene ring [28]: benzo[*c*]coumarin, benzo[*f*]coumarin, benzo[*g*]coumarin, and benzo[*h*]coumarin types (Figure 1.1). All coumarin derivatives shown in Figure 1.2 have some biological importance.

Nitrile derivatives, especially those of malononitrile, have different and proved to be useful in their utilization in the synthesis of heterocyclic compounds. They are usually used as an intermediary part in variety of synthetic reactions. Malononitrile derivatives show synergistic toxicity in the toxic-dynamic and toxic-kinetic interactions with aldehyde components [29]. A number of malononitrile derivatives show significant antimicrobial [30], antibacterial [31], antifungal [32,33], and anti-proliferative activities on human breast adenocarcinoma, ovarian adenocarcinoma and lymphoblastic leukemia cell [34]. Additionally, they are used and act as anticancer [35], molluscicidal [36], anti-inflammatory [37], and anti-oxidant agents [38]. Furthermore, complexes of malononitrile derivatives of copper metal are known to exhibit anticancer activities [39] and also act as G protein-coupled receptor 35 (GPR<sub>35</sub>) agonists [40].

Highly substituted thiophene derivatives are heterocycles with varieties of applications and are found in a great number of natural products as well as biologically active compounds [41-45]. Their applications vary from dye chemistry [46] to modern drug design [47], biodiagnostics [48], electronic and optoelectronic devices [49], conductivity-based sensors [50] and self-assembled superstructures [51]. 2-Amino-3-arylthiophenes are agonist allosteric enhancers at the A1 adenosine receptor [52,53]. Some thiophene-derived antagonists of the human glucagon receptor have been discovered [54]. Generally, polysubstituted 2-aminothiophenes with an electron-withdrawing groups such as cyano, ethoxycarbonyl or aminocarbonyl at the 3-position and alkyl, aryl or hetaryl groups in the 4- and 5-position are synthesized by the Gewald reaction [55].

Organic synthesis and reactions under solvent-free [56,57] and aqueous [58-60] conditions have continuingly attracted the interests of many chemists, especially from the viewpoint

of green chemistry [61]. Microwave irradiation has been utilized as one of the most convenient and efficient ways to promote organic reactions [62,63].

Microwave-assisted irradiation technique has revolutionized organic synthesis, and has attracted huge interests as a tool for design and synthetic protocols. In the past 30 years, an appreciable number of climate change; temperatures are rising, weather severely erratic, and glaciers melting continuously due to a higher level of greenhouse gas (GHG) emissions. Several researches concluded that, increasing anthropogenic GHG emissions are largely caused by the use of fossil fuels, and therefore there is a need for a range of renewable technology options to meet stringent global warming targets (e.g., keeping CO<sub>2</sub> concentration below 440 ppm by 2050) [64]. Of late, rapid increase in the rates of chemical reactions due to the utilization of microwave-assisted irradiation has become of great interest to researchers, especially the chemists. Early researchers reported that the microwave-assisted rates of reaction, when compared to the conventional reactions, increased by a factor of 5 to 1000 [65,66]. The entire scientific and industrial communities have been attracted and are interested in the application of microwave-assisted irradiation reactions, not only as a result of its increased reaction rates, but also for its capability to completely changing the chemical reactions with unimaginable results. Additionally, there are a lot of advantages in the use of microwave-assisted reactions, such as rapid heating, relatively lower energy consumption, and environmental friendliness, higher yield of products, controllable processing, shorter reaction time, high purity, quality and improved properties of the products [67-69].

In this thesis, a facile and expeditious synthesis of 3-acetylcoumarin and its derivatives, malononitrile derivatives of the 3-acetylcoumarins, and coumarins substituted at the position-3 by cyano substituted 2-aminothiophene, have been designed and utilized under microwave-assisted irradiation procedure. Since reactions under microwave irradiation require accuracy, versatility, and special attention, several preliminary experiments were performed in order to establish the optimal conditions. The second strategy was the development and used of conventional procedure for the synthesis of the target compounds. Finally, comparative analyses of the various results from the Microwave-assisted Irradiation and Conventional procedures were made.

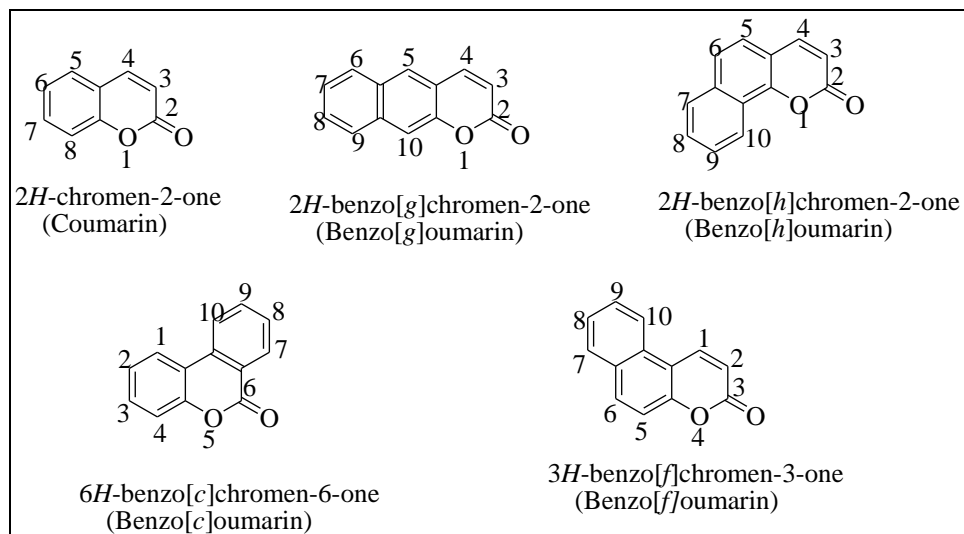


Figure 1.1. Structures and numbering of coumarin and benzocoumarins

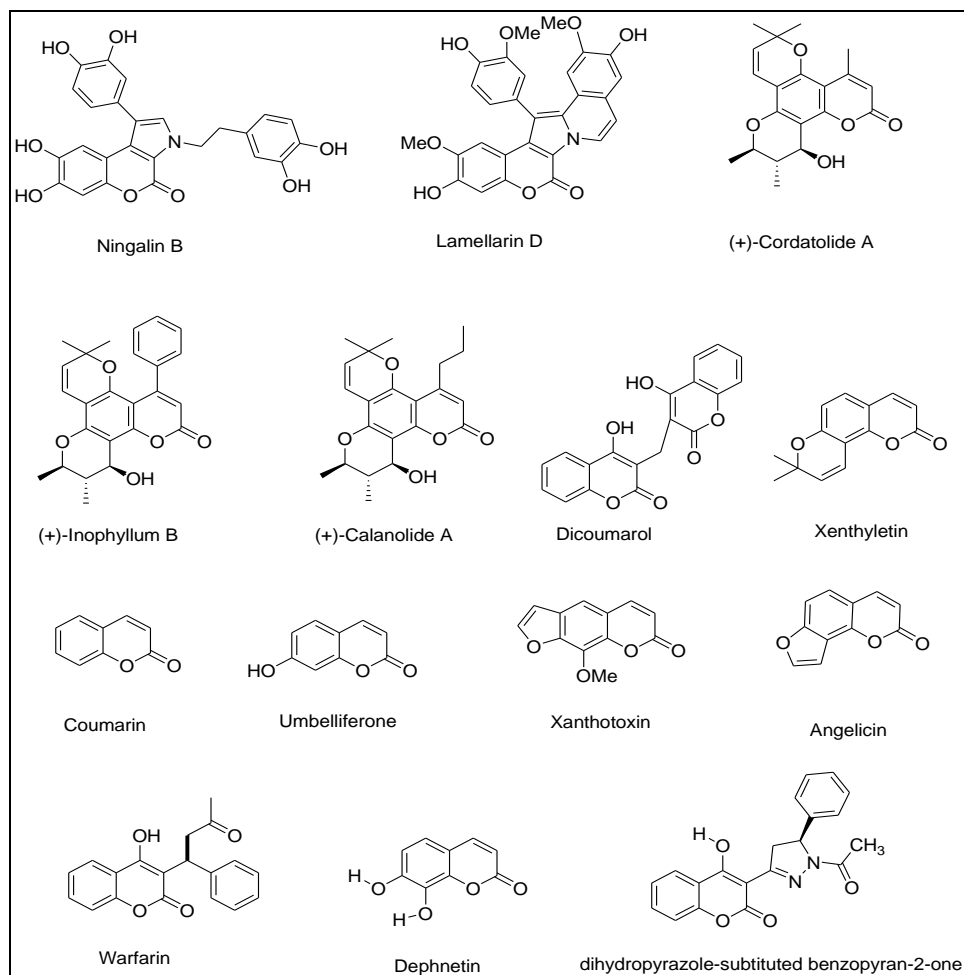


Figure 1.2. Biologically active and commercially important coumarin derivatives

## 1.1. Justification for the Study

- Several attempts are being made to find efficient antitumor agents such as coumarin derivatives because remain among the most vibrant compounds against cancer cell lines and are vital components among the molecules in drug discovery.
- Coumarins are known to exhibit antibiotic and antifungal activities.
- Effective and facile synthetic protocols for the synthesis of organic compounds, as drug candidates, have become the yastic for morden industrial set-up.
- Environmentally friendly procedures for synthesis are being sort for as the globe is become warmer.
- One-pot three-component synthetic strategies have become the current trends in synthetic organic chemistry.

## 1.2. Objectives of the Research

Because of the biological importance and usefulness of the coumarins, they became synthetically important molecules. In the past years, a lot of protocols have developed for preparing coumarin and its derivatives. Malononitriles have also been identified as intermediates of several synthetic procedures. Multi-substituted 2-aminothiophenes are good candidates for drug development and delivery. The main aim of this thesis was to develop new synthetic protocols for the synthesis of 3-acetylcoumarins, their malonitrile derivatives, and their coumarin-thiophene derivatives using cost-effective and environmentally friendly protocols. It was also to enable the synthesis of the coumarin-thiophene derivatives in one-pot three-component. Finally, to be able to synthesize all the compounds using two protocols- the conventional method (CM) and the microwave-assisted irradiation (MWI) method in good to excellent yields. In 2014, Devulapally Srikrishna and Pramod Kumar Dubey [70] reported a closely related protocol for the synthesis of coumarin-thiophene compounds, but their protocol involved the use of conventional procedure only. However, in this study, two methods, thus the conventional and the microwave-enhanced procedures, were used in the preparation of all the molecules.



## 2. GENERAL INFORMATION AND LITERATURE SUMMARY OF THE STUDY

In this section of the thesis gives general information about the structures and properties of the synthesized compounds and possible applications in different areas.

### 2.1. Structure and Properties of The Molecules Synthesized in Thesis

Basically, this thesis describes the synthesis, photophysical properties, and thermal stabilities of six main products. The products are coumarins, malononitriles, 2-aminothiophenes, amides, sulfonamides, and urea.

Coumarins can generally be synthesised by methods including Claisen rearrangement, Perkin reaction, Pechmann reaction, and Knoevenagel condensation [71]. Some industrially important coumarins that can be prepared through the Pechman reaction, using readily available 1,3-disubstituted compounds and their acetoacetic esters, contain a 4-methyl substituted group [e.g., 7-hydroxy-4-methylcoumarin (Coumarin 47 or Coumarin 460) and 7-diethylamino-4-methylcoumarin (Figure 2.1) [72].

Recently, it was reported that the Pechman reaction can successfully be applied using microwave irradiation of the reagents by the use of a household microwave oven [73]. Knoevenagel reaction [74] and synthesis of coumarin via the Knoevenagel condensation [75] have become the subject of microwave-enhanced reactions. For coumarins, only the synthesis of 7-hydroxy-4-methylcoumarin (Coumarin 47 or Coumarin 460), Ethyl 2-oxo-2H-1-benzopyran-3-carboxylate, 7-diethylamino-4-methylcoumarin, and 9-methyl-2,3,6,7-tetrahydro-1*H*,5*H*,11*H*-pyrano[2,3-*f*]pyrido[3,2,1-*ij*]quinolin-11-one (Coumarin 153) (Figure 2.1.1).

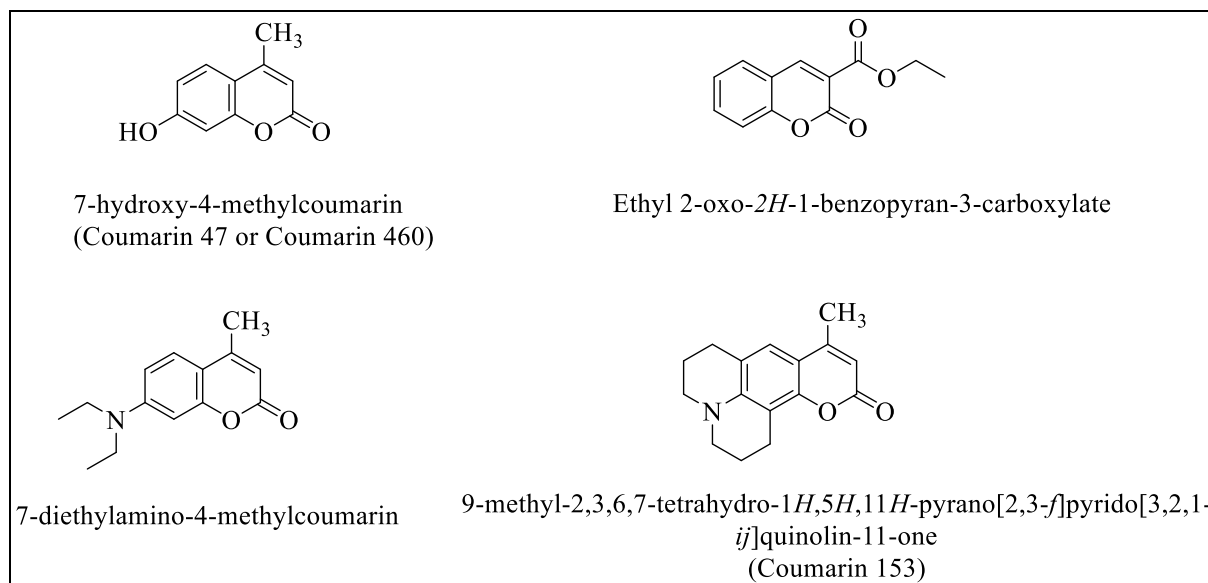


Figure 2.1. Structures of some industrially important coumarins

The synthesis of 2-(1-(4-nitrophenyl)ethylidene)malononitrile via literature method [76] and other similar ylidene molecules which involves mixing of a ketone, malononitrile, and a catalyst (e.g., ammonium acetate) in benzene or toluene (Figure 2.2). The mixture is then warmed to reflux and water is removed via azeotropic distillation employing a Dean–Stark apparatus. The ylidene, 2-(1-(4-nitrophenyl)ethylidene)malononitrile is thermally unstable, hydrolytically sensitive, and decomposes in the presence of weak bases (i.e., sodium bicarbonate). This instability is most likely due to the combination of an unhindered enolizable methyl group and an electron withdrawing nitro-substituted aromatic ring. Analogous compounds derived from acetophenone or 40-nitropropiophenone are much less prone to degradation. At the elevated temperatures required for azeotropic distillation, dimerization to form adduct 5'-amino-1',6'-dimethyl-4,4''-dinitro-1',6'-dihydro-[1,1':3',1''-terphenyl]-4',6'-dicarbonitrile was significant; this dimerization resulted in highly variable yields of 2-(1-(4-nitrophenyl)ethylidene)malononitrile ranging from 10–70% (Figure 2.2). Using lower boiling solvents such as THF or EtOAc resulted in even more ylidene dimerization. In addition, 2-(1-(4-nitrophenyl)ethylidene)malononitrile isolated by silica gel chromatography from these standard Knoevenagel reaction conditions was an unstable oil, which dimerized to 5'-amino-1',6'-dimethyl-4,4''-dinitro-1',6'-dihydro-[1,1':3',1''-terphenyl]-4',6'-dicarbonitrile upon standing. Lowering the reaction temperature to ~60 °C in toluene did show promise; however, the reaction stalled (~50% conversion); longer reaction times resulted only in significant dimerization. Isolated 2-(1-(4-nitrophenyl)ethylidene)malononitrile hydrolyzes to starting ketone 1-(4-nitrophenyl)ethan-1-one under mild acidic conditions (LiH<sub>2</sub>PO<sub>4</sub>, THF/ water) indicating that the condensation reaction is

reversible, and that the removal of the water is necessary to drive the reaction to completion. Addition of inorganic desiccants ( $\text{MgSO}_4$ ,  $\text{Na}_2\text{SO}_4$ , 4 Å molecular sieves) at 60 °C failed to improve the reaction. On the other hand, an organic desiccant, namely trimethylsilyl acetate ( $\text{TMSOAc}$  [77], 1.5 equiv relative to ketone) afforded full conversion with only 5% dimerization in 6 h at 60 °C (toluene,  $\text{NH}_4\text{OAc}$ ). However, 2-(1-(7-(diethylamino)-2-oxo-2H-chromen-3-yl)ethylidene)malononitrile has been successfully synthesized using a buffer ( $\text{NH}_4\text{OAc}/\text{AcOH}$ ) as the catalyst and benzene as the solvent, in good yield (Figure 2.2) [78]. All these procedures have their peculiar setbacks. These setbacks have addressed in one way or another in the protocols established in this thesis.

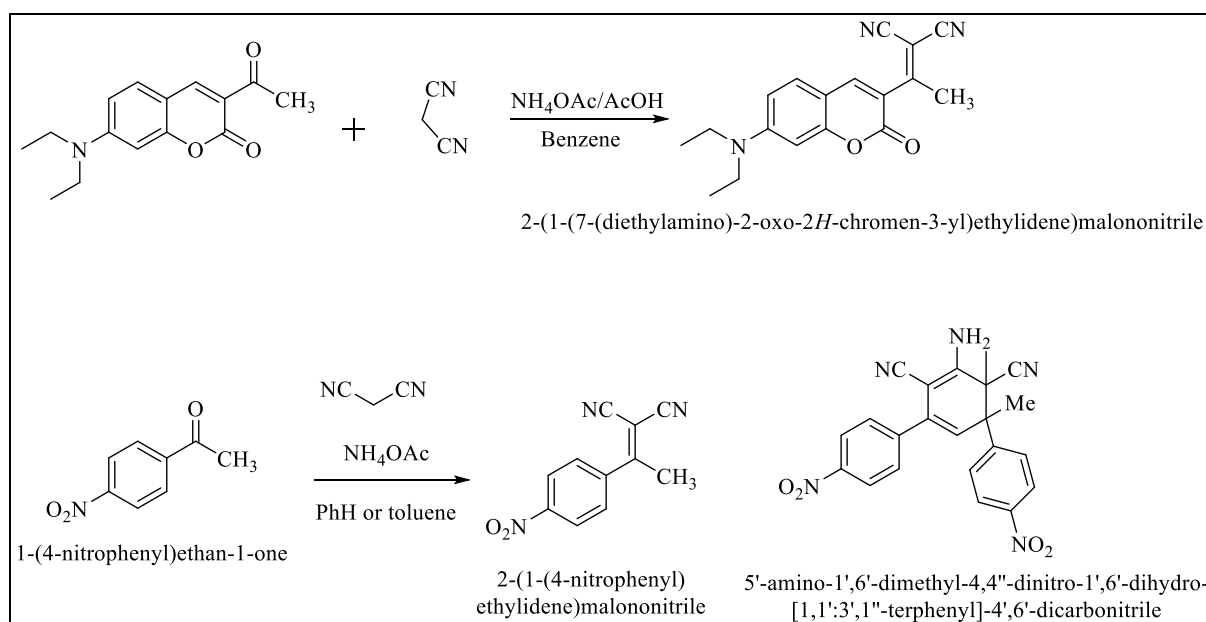


Figure 2.2. Synthesis of ylides via different strategies

The Gewald reaction represents a multi-component procedure for the preparation substituted 2-aminothiophenes usually in high yields. The reaction is carried using  $\alpha$ -substituted acetonitriles carrying electron withdrawing groups and  $\alpha$ -methylene carbonyl compounds (aldehydes or ketones) in the presence of the base. The organic bases that are normally utilized in this process include secondary or tertiary amines such as diethylamine, morpholine, triethylamine, pyridine, and inorganic bases such as  $\text{NaHCO}_3$ ,  $\text{K}_2\text{CO}_3$ ,  $\text{NaOH}$ . Polar solvents, such as DMF, alcohols (i.e. methanol, ethanol), 1,4-dioxane assist the condensation of intermediates –  $\alpha,\beta$ -unsaturated nitriles with sulfur, which are either synthesized in situ or externally. Depending on the starting substrates being employed and the reaction protocols, three basic strategies of the Gewald

reaction have been developed [79-82], which were further enriched with a fourth one (Figure 2.3) [83].

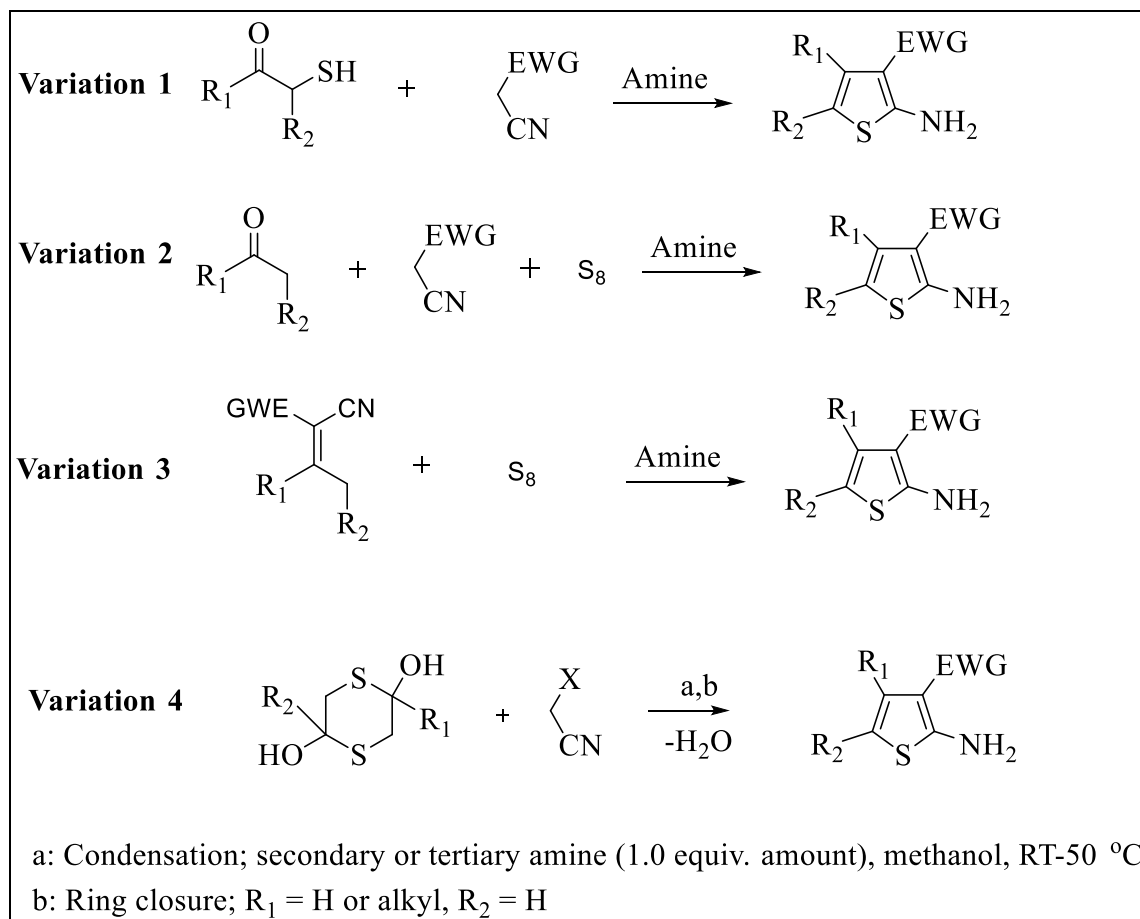


Figure 2.3. Variation of the gewald reaction

## 2.2. Coumarin Derivatives and Their Applications

Substituents which differ in size, length, and electronic or lipophilic characteristics, on the coumarin compound, could regulate its biological behaviour. Introduction of a large array of compounds, of a carboxamido spacer between a substituted coumarin [84] and a lateral (aromatic or aliphatic) chain, showed IC<sub>50</sub> values in the nanomolar range [85]. Merging methylketone, arylketone, ethyl ester, carboxylic acid, and carboxyhydrazido [86] functionalities at position C3, and different substituents at positions C5, C6, C7, and C8 of the coumarin nucleus could be utilized for assay of varieties of *in vitro* assays as shown in Figure 2.4.

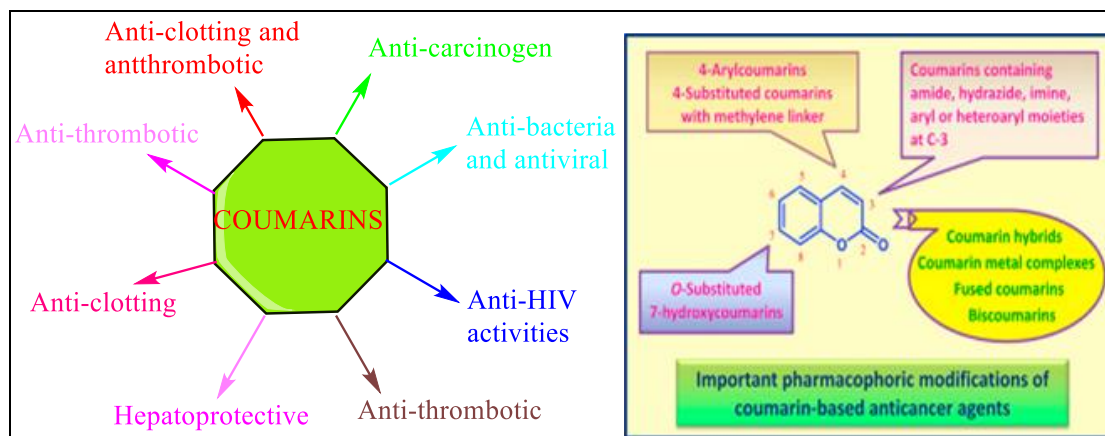


Figure 2.4. Substituent effect on the coumarin core and applications of coumarins

Coumarin can occur either free or combined with the sugar glucose (coumarin glycoside). The glycosides are non-reducing organic compounds that on hydrolysis with acids, alkalis or enzymes yield, a sugar part (glycone, formed of one or more sugar units and a non-sugar part (aglycone, also called genin). The glycoside of umbelliferone is called skimmion. These compounds are used to protect skin from UV light. Umbelliferone occurs in many familiar plants from the Apiaceae (Umbelliferae) family such as carrot, coriander and garden angelica, as well as in plants from other families, such as the mouse-ear hawkweed (*Hieracium pilosella*, Asteraceae) or the bigleaf hydrangea (*Hydrangea macrophylla*, Hydrangeaceae). anticoagulants (has blood-thinning), anti-fungicidal, anti-tumor and anti-inflammatory activities, treatment for skin disease, Psoriasis, Eczema. It is used in the treatment of asthma and lymphedema, as a food additive and ingredient in perfume. Ammi majus contains a group of furanocoumarins, the parent compound is called Psoralene. They are used for the treatment of Psoriasis and leucoderma. Furanochromones are benzo- $\gamma$ -pyrone derivatives that resist alkalis. Ammi visnaga contain furanochromones, the major is Khellin. Khellin is a smooth muscle relaxant used as, Bronchodilator, Antispasmodic, Renal colic, and Coronary vasodilator. Xanthotoxin or Methoxsalen is extracted from Ammi majus, a plant of the family Umbelliferae. It modifies the way skin cells receive the UV radiation. Warfarin is widely used as anticoagulant (Figure 2.5). Coumarins are found in several plants, including tonka beans, lavender, licorice, strawberries, apricots, cherries, cinnamon, and sweet clover (Figure 2.6). Drugs found in market that contain coumarins are shown in Figure 2.7 [87-89]. Some biologically active coumarin compounds are shown in Table 2.1.

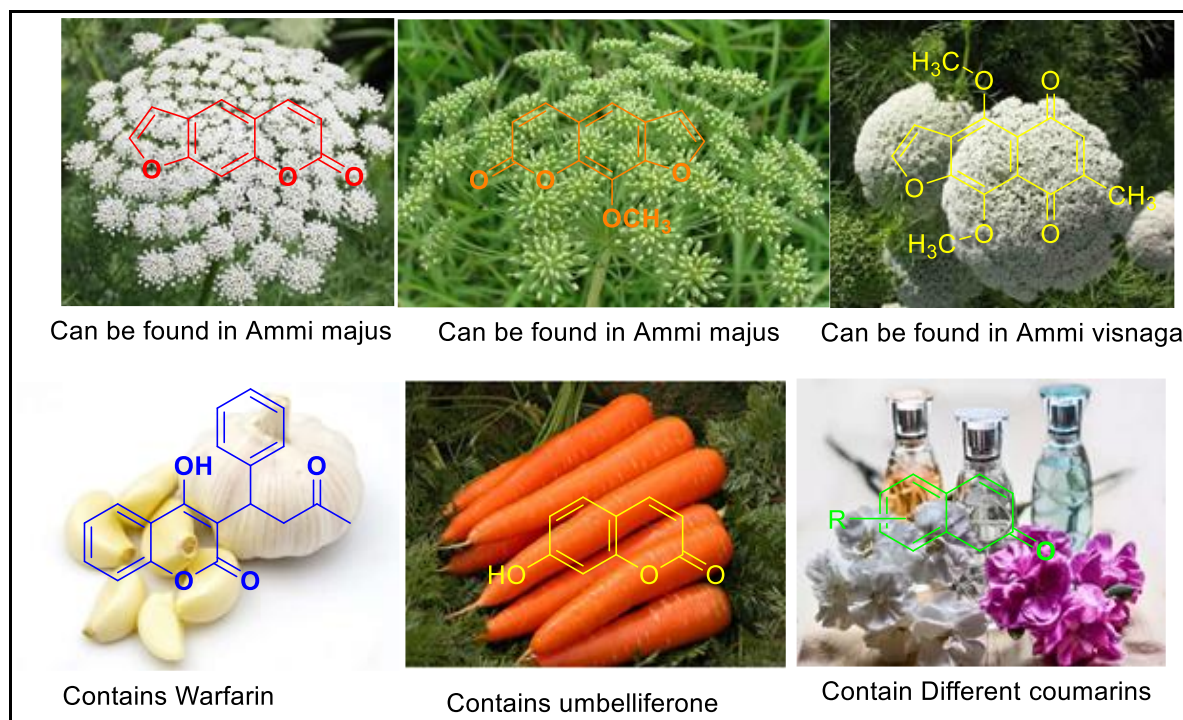


Figure 2.5. Some sources of coumarins

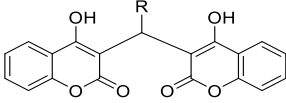
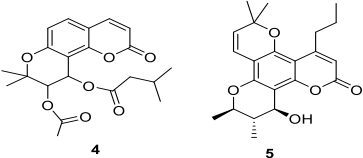
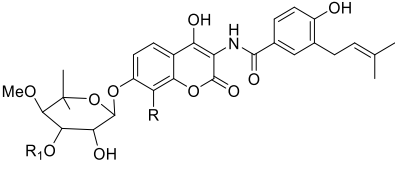
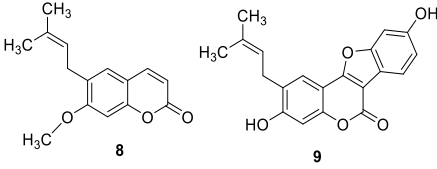


Figure 2.6. Plant sources of coumarins



Figure 2.7. Drugs in the market that contain coumarins

Table 2.1. Some biologically active coumarins

Examples	Biological Properties
 <p>1: R = H, 2: R = CH<sub>3</sub>, 3: R = CO<sub>2</sub>Et</p>	Anticoagulant
	Anti-HIV (Reverse transcriptase inhibitors)
 <p>6: R = CH<sub>3</sub>, R<sub>1</sub> = CONH<sub>2</sub>, 7: R = Cl, R<sub>1</sub> = C<sub>6</sub>H<sub>5</sub>N</p>	Antibiotic and Antibacterial (DNA gyrase inhibitors)
	Anticancer (Breast cancer, Stomach cancer, Colon cancer and Renal cancer)

### 2.3. Malononitrile Derivatives and Their Applications

Malononitrile able to intercalate with Vanadyl phosphate and forms an organic compound has a Lewis base character [90]. Malononitrile derivatives such as benzylidene malononitrile and its p-chloro derivative are used for synthesizing a new class of photo-cross linkable main chain liquid crystalline polymers. A blood group centigenic oligosaccharide monomer containing a benzylidene moiety was chemically synthesized [90]. Malononitrile derivative such as (*E*)-2-(3-(4-aminostyryl)-5,5-dimethylcyclohex-2-enylidene)malononitrile which is organic non-linear optical (NLO) compound has been intensively studied in recent years because of its potential application in telecommunications and optical information processes [92].

In recent years, chromophores-functionalized electro-optic (EO) polymeric materials have been intensively investigated for their potential application in high speed photonic devices. This had led to expensive explorations of 'push-pull' type chromophores with high molecular building blocks commonly used for NOL (nonlinear optic) chromophores [93] (electron donor, conjugated bridge and electron acceptor), the development of electron donors and conjugated bridges is already so mature that they can meet most of the synthetic and physical requirements [93]. Malononitrile derivative (2-dicyanomethylene-4,5,5-trimethyl-2,5-dihydrofuran-3-carbonitrile) which is a strong electron acceptor for nonlinear optics [93] was synthesized. It is a molecular building block for NLO material [93]. NOL polymers are considered candidate materials [94], mainly because they offer many advantages such as mechanical endurance, light weight, and good process ability to form optical devices [95]. Merocyanine dyes are donor-acceptor compounds exhibiting intermolecular charge transfer from the donor end group through the conjugated polymethine chain [96]. Depending on the charge of these groups [96,97] and the length of the polymethine chain, as well as the nature of the solvent, the electronic excitation of these compounds can cause either a sharp increase or decrease in their dipole moment. Therefore, the spectral and fluorescent properties of merocyanines are very sensitive to charges in their chemical structure and the polarity of the medium [98,99]. For this reason, these dyes are widely used in various fields of science and engineering connected with the transformation of light energy [96-99].

## 2.4. 2-Aminothiophenes and Their Uses

Substituted 2-aminothiophenes are important intermediates in the synthesis of a variety of agrochemicals, dyes and pharmacologically active compounds [100]. The thiophene ring as is bioisosteric replacement for phenyl group broadly present in active drugs. The thiophene core exists in many natural and synthetic pharmaceuticals. The positions of substituents in the 2-aminothiophenes in the field of drug design and synthesis of pharmaceuticals comes from their important properties. Substituted 2-aminothiophenes of structure T1–4, with alkyl, aryl and cycloalkyl substituents in C-4 and C-5 position and aroyl substituent in C-3 position (Figure 2.8), maintained the best allosteric enhancer activity [101,102]. A high-throughput screening program based on this enzyme from *Staphylococcus aureus* had identified a 2-ureido-thiophene-3-carboxylate (Figure 2.9) as a low micro-molar inhibitor. The inhibitor was said to have displayed good antibacterial activity against *S. aureus* and *S. epidermidis*. Based on these observations, the authors reported a facile synthesis of the number of analogs of 2-ureido-thiophene-3-carboxylate via the Gewald reaction and evaluated for cytotoxic activity against Rifampicin-resistant *S. aureus* [103].

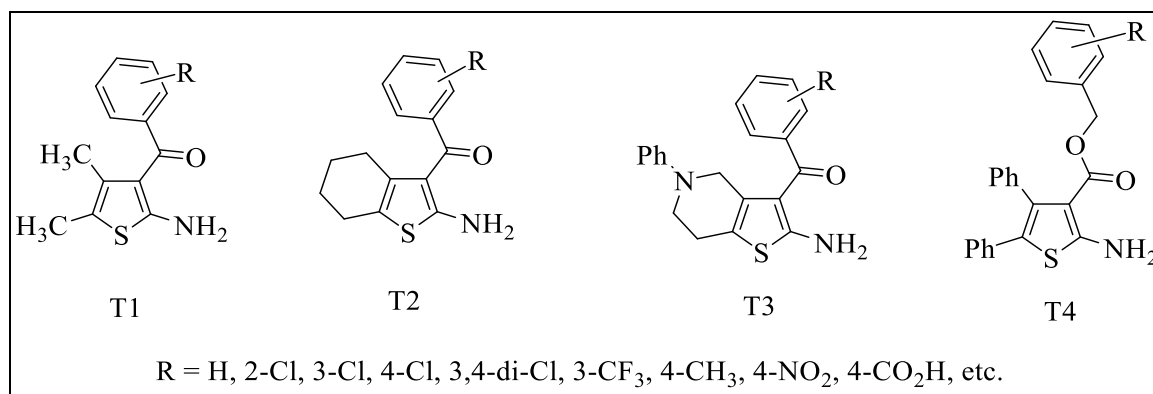


Figure 2.8. Structures of substituted 2-aminothiophenes T1-4

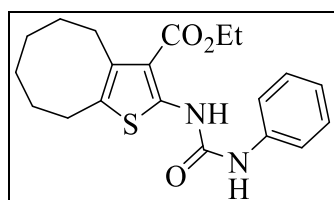


Figure 2.9. 2-Ureido-thiophene-3-carboxylate 18 antibacterial agent against *S. aureus*

## 2.5. Amide Derivatives and Their Applications

Amides have been associated with a wide range of biological activities such as antituberculosis [104], anticonvulsant [105], analgesicantiinflammatory [106], insecticidal [107], antifungal [108], and antitumor [109] activities. Those bearing morpholine are known for their antimicrobial property and show anthelmintic, bactericidal and insecticidal activity [110]. They are again utilized as the intermediate product in the synthesis of therapeutic agents. Additionally, amides exhibit anti-platelet activity [111]. Aromatic amides appended with aromatic and heterocyclic acids have been synthesized in search for new antagonists of excitatory amino acids receptors with anticonvulsant property. Benzylamides were generally more active than other amides. The most effective ones were the amides of the following acids: picolinic, nicotinic, isonicotinic, nipecotic and isonipecotic [112]. When amides are conjugates with different aliphatic, aromatic and heterocyclic ring various types of biological activities are produced. General structure of amide is given below.

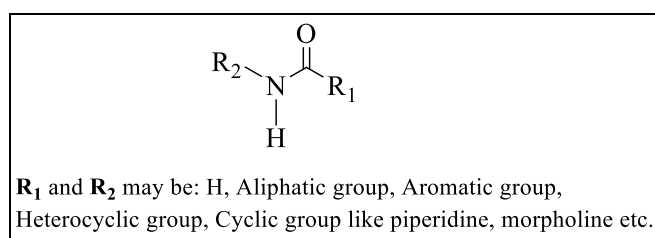


Figure 2.10. General structure of an amide

Among the lanthanide reagents cerium (IV) ammonium nitrate (CAN) is one of the most important catalyst in organic synthesis [6]. Accordingly, herein is reported the carboxylic acid-urea reaction in the presence of catalytic amount of CAN (2 mol%) under microwave irradiation with high yields and short reaction time (Figure 2.11). Neerja Gupta and Ruby Naaz successfully carried out the reaction of benzoic acid with urea in the presence of CAN (2 mol%) under microwave irradiation which afforded the product in 90% yield. Without CAN or any catalyst, the reaction did not yield any product even after irradiating for a longer time, and they therefore concluded that CAN indeed catalysed the reaction [113].

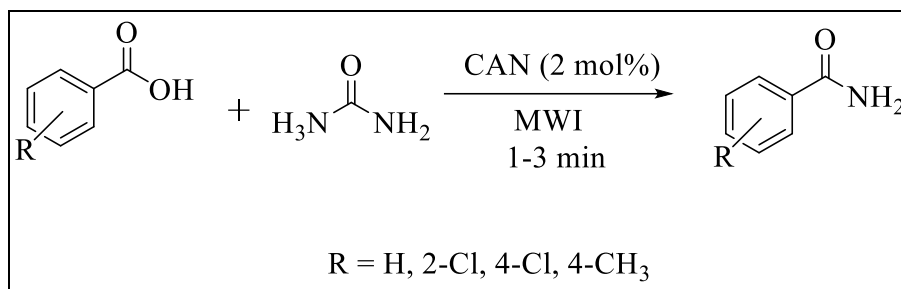


Figure 2.11. Microwave procedure for the synthesis amides

## 2.6. Sulfonamide Derivatives and Their Applications

Sulfonamides (mostly as sulfa drugs) were the first drugs largely employed and systematically used as preventive and chemotherapeutic agents against various diseases [114]. Over 30 drugs containing this functionality are in clinical use, including antihypertensive agent bosentan [115], antibacterial [116], antiprotozoal [117], antifungal [118], anti-inflammatory [119], nonpeptidic vasopressin receptor antagonists [120] and translation initiation inhibitors [121]. Some important sulfonamide derivatives used as carbonic anhydrase inhibitors of commercial importance [122]. They are also effective for the treatment of urinary, intestine, and ophthalmic infections, scalds, ulcerative colitis [123], rheumatoid arthritis [124], male erectile dysfunction as the phosphodiesterase-5 inhibitor sildenafil—better known under its commercial name, Viagra [125], and obesity [126]. More recently, sulfonamides are used as an anticancer agent [127], as the antiviral HIV protease inhibitor amprenavir [128] and in Alzheimer's disease [129]. Sulfonamides are compounds, which have a general structure represented by Figure 2.12. After sulfanilamide discovery, thousands of chemical variations were studied and the best therapeutic results were obtained from the compounds in which one hydrogen atom of the SO<sub>2</sub>NH<sub>2</sub> group was replaced by heterocyclic ring [130]. To date more than twenty thousand sulfanilamide derivatives have been synthesized. These syntheses have resulted in the discovery of new compounds with varying pharmacological properties in this main structure, R, R1 may be hydrogen, alkyl, aryl or hetero aryl etc. The lipophilicity of the N1 group has the largest effect on protein binding, and generally, the more lipids soluble a sulfonamide is the more of it will be protein bound [131]. The aniline (N4) amino group is very important for activity because any modification of it other than to make prodrugs results in a loss of activity [132]. Moreover sulfonamides are also inactive if *p*-amino group is acylated, benzene is substituted, sulfonamide group not attached directly to

benzene ring. More advanced studies revealed that modified sulphonamides showing high to moderate antibacterial activity [133]. Aliphatic sulfonamides have highest powerful antibacterial activity for Gram (-) bacteria than Gram (+) and antibacterial activity decreases as the length of the carbon chain increases [134]. Also, novel macrocyclic bis-sulfonamides showed antimicrobial activities [135].

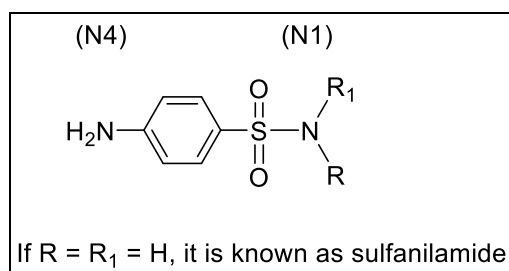


Figure 2.12. General structure of sulfonamides

Generally, sulphonamides can be synthesized through the reaction pathways shown in Figure 2.13. depending on the equivalents of the starting reagents, the reaction afford either a disulfonamide ( thus, via pathway 1) or a monosulfonamide (thus, via pathway 2). A comprehensive review on the synthesis of sulfonamide derivatives through different protocols has been reported [136].

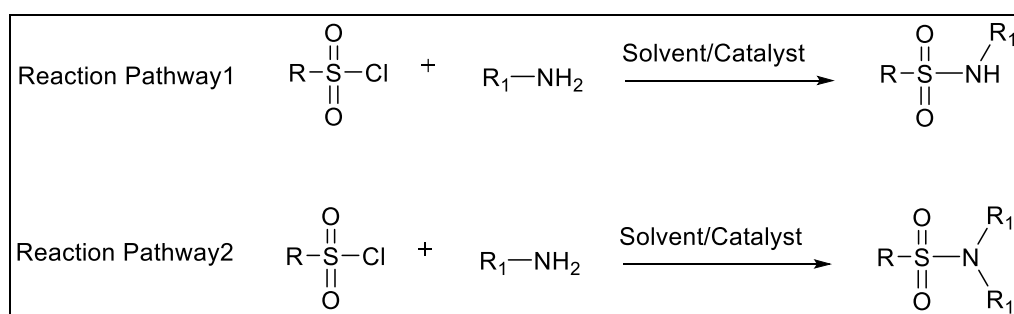


Figure 2.13. General synthetic pathway for sulfonamides

## 2.7. Urea Derivatives and Their Applications

Among them, the thiourea group often chosen as anion binding sites as a functional group is a good hydrogen-bond donor and therefore results in quite stable strongly hydrogen-bonded complexes with different anions such as acetate, phosphate or fluoride. Therefore, large numbers of anion receptors containing the thiourea subunits have been designed, synthesized and tested for anion recognition and sensing during the past decades. For

example, Aneta et al [137] have synthesized some receptors by integrating two p-nitrophenylthiourea groups into 4, 5-dimethyl-1,2-diaminobenzene, which have been proven to be efficient and colorimetric chemosensors for fluoride and acetate. Urea is a natural chemical compound, produced in human organism as a metabolite of proteins and other nitrogen- containing compounds [138]. It is released in urine and sweat in amount 20–30 mg per day. Urea is a carbonic acid diamide (carbamide, CAS number: 57–13–6) (Figure 2.14). It occurs in the form of odourless, colourless crystals whose melting point is 133°C, highly soluble in water and ethanol. It was for the first time synthesised in 1828 by a German chemist Friedrich Wöhler [138]. The keratolytic properties of urea are also used in cosmetology and dermatology. It is used as a component of cosmetic formulas reducing skin roughness and discolorations. In particular, urea is commonly used in foot skin care products, in which its concentration is 2–10 %wt [139]. Dermatological products containing carbamide in higher concentrations are recommended to patients suffering from psoriasis and other skin conditions with excessive and abnormal skin keratinization [140].

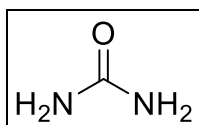


Figure 2.14. Structure of urea

One of the most popular urea derivative used in cosmetic industry is allantoin (5-ureidohydantoin). This heterocyclic derivative of urea is produced from ureic acid by tissues of Leguminosae roots that are in symbiosis with nodule bacteria. In cosmetic industry synthetic allantoin is used as keratolytic ingredient applied for stimulation of epidermis regeneration and assistance in wound healing process. Allantoin- containing products are used for the treatment of psoriasis, decubitus and other skin disorders [141].

A novel colorimetric receptors for selective fluoride ion sensing containing anthraquinone as chromogenic signalling subunit and urea derivatives UD1-2 (Figure 2.15) as the binding sites have been successfully prepared and reported by Amitava Das et al [142].

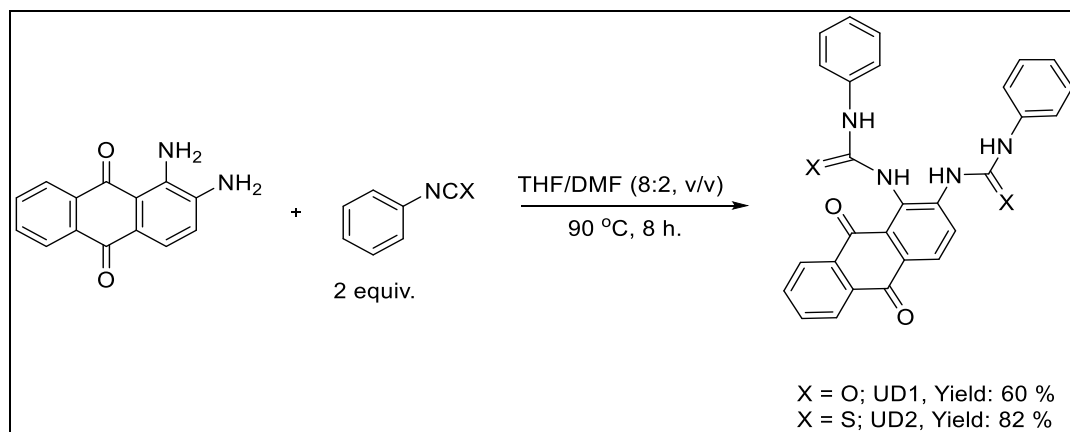


Figure 2.15. Synthesis of the anthraquinone urea derivatives UD1-2

A group of researchers have designed and synthesized a fluoride selective fluorescent as well as chromogenic chemosensor UD3, based on a naphthalene urea derivative, which shows a unique fluorescent and absorption peak in the presence of fluoride ions. The synthesis of UD3 was carried out by refluxing the solution of 1,8-diaminonaphthalene with phenylisocyanate in THF/DMF (2:1 ratio) for 5 h (80% yield) as shown in Figure 2.16 [143].

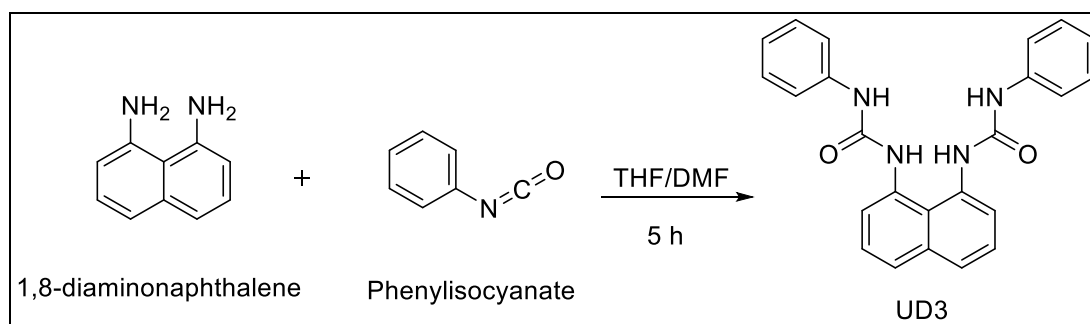


Figure 2.16. Synthesis of UD3

## 2.8. Microwave-Assisted Irradiation in Organic Synthesis

The continuous urge to design economically viable as well as environmentally friendly synthetic chemical procedures has encouraged synthetic chemists to look for methods that are more versatile, such as microwave method, for conducting chemical reactions within a shorter reaction time and little or negligible waste [144,145]. Considering the experimental data from different studies, it has been found that microwave-assisted irradiation chemical reaction rates are more rapid than those of the conventional heating reactions, by as high as a 1000-fold [146]. Microwave-enhanced synthesis has been employed in the synthesis of

molecules of biological interest due to the faster rates at which such compounds are obtained [147-150]. Recently, success was achieved in the use of microwave- assisted irradiation method for the fast synthesis of some thiazoles, which are of biological interest [151,152]. The synthesis of coumarins, both on small and large scale as also been achieved using this same versatile and rapid procedure [153-157], as well as in the synthesis of thiazolyl coumarin Schiff bases [158]. Microwave-enhanced irradiation organic reactions is an emerging green technology that could make industrially important organic synthesis more eco-friendly than conventional reactions [159]. For example, Ceric Ammonium Nitrate (CAN) can provide both an inexpensive and nontoxic green solution to the synthesis of many amide derivatives of pharmaceutical uses [160]. Microwave may be considered as more efficient source of heating than conventional systems [161,162] The reactions in solid phase occur more efficiently and more selectivity compared to reactions carried out in conventional solvents. Such reactions are simple to handle, reduce pollution, comparatively cheaper to operate and are especially important in pharmaceutical industry. Attempts have been made to design synthesis for manufacturing processes in such a way that the waste products are minimum, they have no effects on the environment and their disposal is convenient [163].

### **2.8.1. Microwave irradiation versus conventional method [164]**

Traditionally, organic synthesis is carried out by conductive heating with an external heat source (e.g. an oil-bath or heating mantle). This is a comparatively slow and inefficient method for transferring energy into the system since it depends on convection currents and on the thermal conductivity of the various materials that must be penetrated, and generally results in the temperature of the reaction vessel being higher than that of the reaction mixture (Figure 2.17). This is particularly true if reactions are performed under reflux conditions, whereby the temperature of the bath fluid is typically kept at 10–30 °C above the boiling point of the reaction mixture in order to ensure an efficient reflux. In addition, a temperature gradient can develop within the sample and local overheating can lead to product, substrate or reagent decomposition. In contrast, microwave irradiation produces efficient internal heating (in core volumetric heating) by direct coupling of microwave energy with the molecules (solvents, reagents, catalysts) that are present in the reaction mixture. Microwave irradiation, therefore, raises the temperature of the whole volume simultaneously (bulk heating) whereas in the conventionally heated vessel, the reaction

mixture in contact with the vessel wall is heated first (Figure 2.17). Since the reaction vessels employed in modern microwave reactors are typically made out of (nearly) microwave transparent materials such as borosilicate glass, quartz or Teflon, the radiation passes through the walls of the vessel and an inverted temperature gradient as compared to conventional thermal heating results. If the microwave cavity is well designed, the temperature increase will be uniform throughout the sample. The very efficient internal heat transfer results in minimized wall effects (no hot vessel surface which may lead to the observation of so-called specific microwave effects, for example in the context of diminished catalyst deactivation). It should be emphasized that microwave dielectric heating and thermal heating by convection are totally different processes, and that any comparison between the two is inherently difficult. Characteristics of microwaves and microwave–matter interaction are summarized as:

- i. Electromagnetic waves.
- ii. Low energy photon (does not break chemical bonds).
- iii. Causes movement of molecules (dipole rotation).
- iv. Causes movement of ions (ionic conduction).
- v. Will be reflected, transmitted or absorbed.
- vi. Volumetric heating throughout an absorbing material.

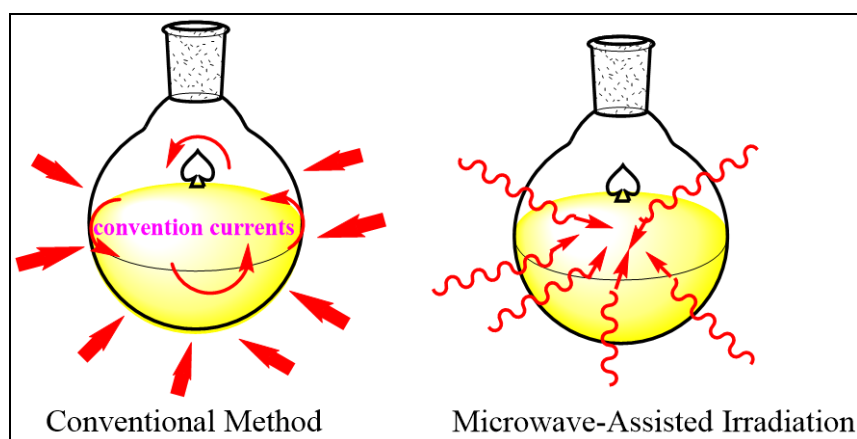


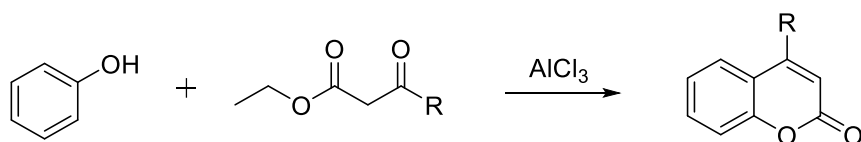
Figure 2.17. Comparison between conventional method and microwave-assisted irradiation

## 2.9. Some Literature Mechanisms for The Formation of The Target Molecules

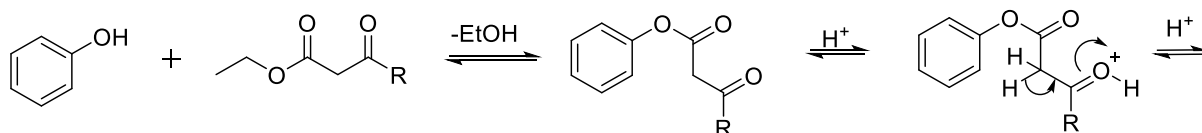
### 2.9.1. Literature mechanisms for the formation of 3-acetylcoumarin derivatives

A lot of synthetic pathways have been successfully designed and reported for the syntheses of coumarins. Some of them are the Pechmann condensation, Claisen rearrangement, Perkin, Reformatsky, and Knoevenagel condensation.

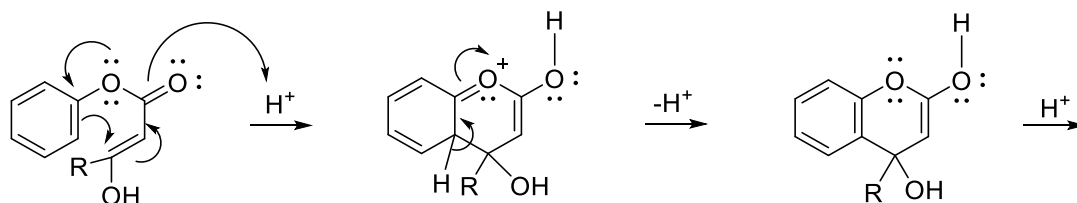
**Pechmann Condensation:** The Pechmann Condensation allows the synthesis of coumarins by reaction of phenols with  $\beta$ -keto esters as illustrated in Figure 2.18.



**Mechanism of the Pechmann Condensation:** The reaction is conducted with a strong Brønsted acid such as methanesulfonic acid or a Lewis acid such as  $\text{AlCl}_3$ . The acid catalyses and induces transesterification as well as keto-enol tautomerisation:



A Michael Addition leads to the formation of the coumarin skeleton. This addition is followed by re-aromatisation:



Subsequent acid-induced elimination of water gives the product:

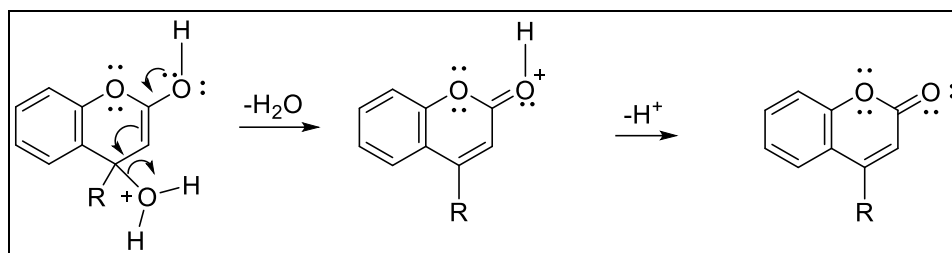


Figure 2.18. Pechmann condensation

Furthermore, the Pechmann reaction is a widely used method for preparing coumarins in good yield; it involves reacting a phenol with a  $\beta$ -oxo ester in the presence of a catalyst. The Pechmann reaction has been carried out using both homogeneous acid catalysts (such as sulphuric [165,166], hydrochloric, phosphoric and trifluoroacetic acids [167], and with Lewis acids, such as zinc chloride [168], iron (III) chloride, tin(IV) chloride, titanium chloride and aluminium chloride[169]) and heterogeneous catalysts (such as cationexchange resins, Nafion-H, zeolite-HBEA and other solid acids) [170]. Recently, microwave irradiation has also been applied to accelerate this reaction [171].

Zhan-Hui Zhang et al [172] reported the synthesis of coumarins via the Pechmann reaction catalysed by montmorillonite K-10 or KSF in yields of up to 96%. This procedure is environmentally friendly and inexpensive compared to previous methods. They reported that K-10 worked better than KSF in terms of reaction time and yield, and that the use of montmorillonite clays as heterogeneous catalysts is a viable alternative. Furthermore, this method has the advantages of easy separation of the product, minimal environmental effect and recyclability of the catalyst.

The use of the cation exchange resins, Zeokarb 225 and Amberlite IR.120, as condensing agents in the synthesis of hydroxycoumarins has also been reported [173]. The main advantages of cation exchange resins are that they simplify the isolation of the product and tend to be relatively inexpensive. In order to obtain a maximum yield of the coumarin, between 20 and 40% of the resin by weight of the total reactants is used. The reaction is considered to involve the following steps:- (i) addition across the double bond of the enolic form of the  $\beta$ -keto ester; (ii) ring closure; and (iii) dehydration [174].

Claisen rearrangement: Fadia et al [175] reported the synthesis of 4-methyl-3-methylene-3,4-dihydrocoumarin 3ii via the intramolecular Claisen-rearrangement of the aryl ether 1ii

in the presence of trifluoroacetic acid (Figure 2.19). Such compounds had been synthesised previously by other routes, but Drewes' method is more efficient, because the precursor alkyl 3-acetoxy-2-methylene butanoate is readily prepared via acetylation of a Baylis-Hillman product and cyclization may be affected in the presence of trifluoroacetic acid to afford the coumarin 3ii in 86% yield in a one-pot procedure.

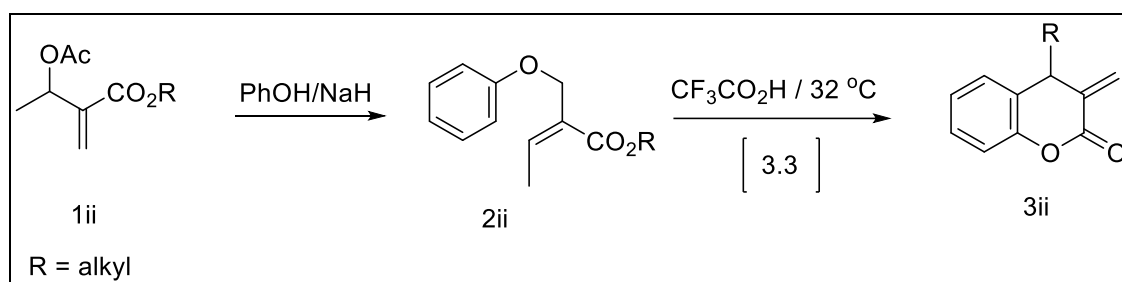


Figure 2.19. Claisen rearrangement for the synthesis of coumarin

Previously, a similar approach to 3-methylenecoumarin was reported, which involves Lewis-acid catalysed Claisen rearrangement of an  $\alpha$ -aryloxymethylacrylate ester [176]. A small amount of a dimer is also produced, which is assumed to form via an ene reaction of the highly reactive methylenecoumarin.

In an attempt to overcome the deficiencies and difficulties encountered with the Pechmann synthesis of coumarin derivatives Rapoport et al [165] developed a new application of the Claisen rearrangement using allyl or propargyl aryl ethers in which the allylic or propargylic  $\alpha$ -carbon is oxygenated. This method has been applied in cases where formation of the coumarin could not be achieved using the Pechmann reaction. The approach is based on the rearrangement of  $\alpha$ -oxygenated allyl aryl ether. The intermediate alkoxychroman was then oxidized to the corresponding coumarin.

Perkin reaction: Perkin, in the mid-nineteenth century discovered the transformation now known as the Perkin reaction [177], a reaction which involves heating an O-hydroxybenzaldehyde with acetic anhydride in the presence of sodium acetate at a high temperature (ca. 200 °C) to afford a trans-cinnamic acid. Optimum yields of coumarins are obtained when a 1:2 molar ratio of aldehyde to anhydride is used. Isomerization of the trans-cinnamic acid by irradiation or treatment with iodine followed by cyclization affords the coumarin 2iii (Figure 2.20) [178]. The disadvantage of this approach is the generally

poor yield of the coumarin obtained, due to the production of tarry materials under the severe reaction conditions of the Perkin synthesis. However, the obvious advantage is that the formation of isomeric chromones is not possible, as is the case with the Pechmann reaction [179].

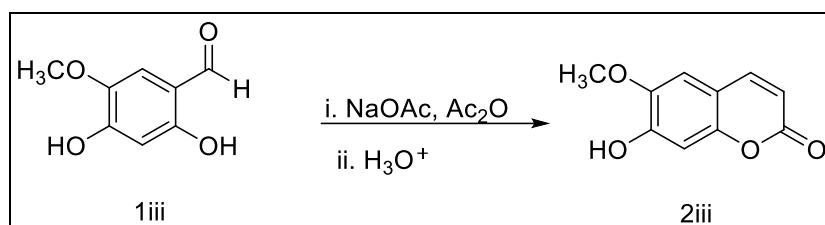


Figure 2.20. Synthesis of coumarin via the perkin reaction

Coumarin can also be formed in the reaction of acetic anhydride and salicylaldehyde in the presence of triethylamine as the base catalyst [180].

Wittig reaction: Mali and Yadav [181,182] developed a preparation of coumarins via Wittig olefination-cyclisation of 3-(2-hydroxyaryl)propenoic esters (Figure 2.21). Cyclization under olefination conditions depends on formation of the *Z*-alkene intermediate 3iv, and concomitant formation of the *E*-alkenes is often a problem. This difficulty may be addressed by heating the reaction mixture, or by photochemical isomerization, but these methods suffer from variable yields, inconvenient work-up, or both [183]. In an attempt to solve these problems, McNab and co-workers [183,184] showed that the cyclization takes place in consistently high yield when the isolated 3-(2-hydroxyaryl)propenoic esters 3iv are subjected to flash vacuum pyrolysis (FVP). While the *E*-configuration of the double bond precludes cyclization, the barrier to isomerization is overcome by the high-temperature.

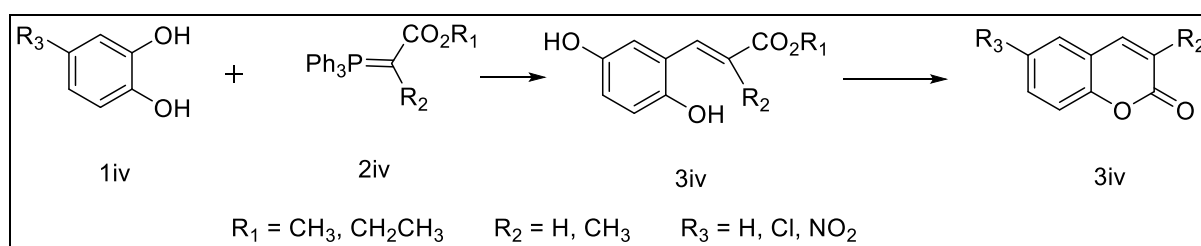


Figure 2.21. Synthesis of coumarin via wittig reaction

The synthesis of coumarins by condensing *o*-hydroxybenzaldehydes or *o*-hydroxyacetophenones with the stable phosphorane, (ethoxycarbonylmethylene)-triphenylphosphorane has also been reported [179,181,185]. Uriarte et al [186] have also made use of the Wittig reaction in the synthesis of potential antipsychotic compounds containing the coumarin moiety by subjecting keto diphenols to a Wittig reaction with (ethoxycarbonylmethylene)triphenylphosphorane to give the expected 7ethoxycoumarin in rather poor yield (24%) and 7-hydroxycoumarin in 70% yield.

**Knoevenagel condensation:** The Knoevenagel reaction involves the condensation of benzaldehydes with activated methylene compounds in the presence of an amine, and is used to overcome the inherent difficulties associated with the synthesis of coumarins via the Perkin reaction. In order to obtain coumarin rather than the usual cinnamic acid, a 2-hydroxy substituent must be present in the aromatic aldehyde and the conditions for the Knoevenagel reaction are less severe than those required for the Perkin reaction. Various coumarins have been prepared via Knoevenagel condensation of salicylaldehyde with activated methylene compounds as illustrated in Figure 2.22 [179].

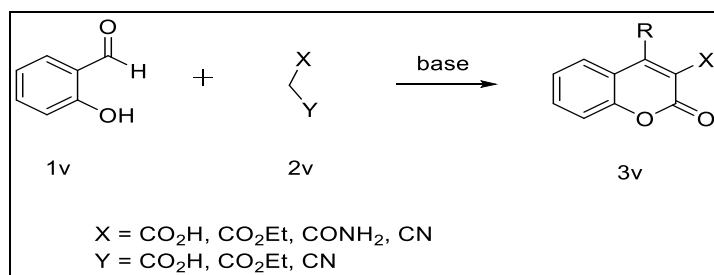


Figure 2.22. Preparation of coumarin via Knoevenagel condensation

Two different mechanisms have been proposed for the above Knoevenagel reaction [187]. In the first (Figure 2.23), formation of an imine or iminium salt 4v with the amine (e.g. piperidine) is followed by reaction with the enolate of the active methylene compound, elimination of the amine and intramolecular ring closure to give the coumarin 5v. The second proposal involves attack by the carbanion, produced by deprotonation of the active methylene compound by the amine, on the carbonyl group to give the intermediate 6v. Proton transfer, ring-closure via acyl substitution and dehydration then gives the coumarin 5v.

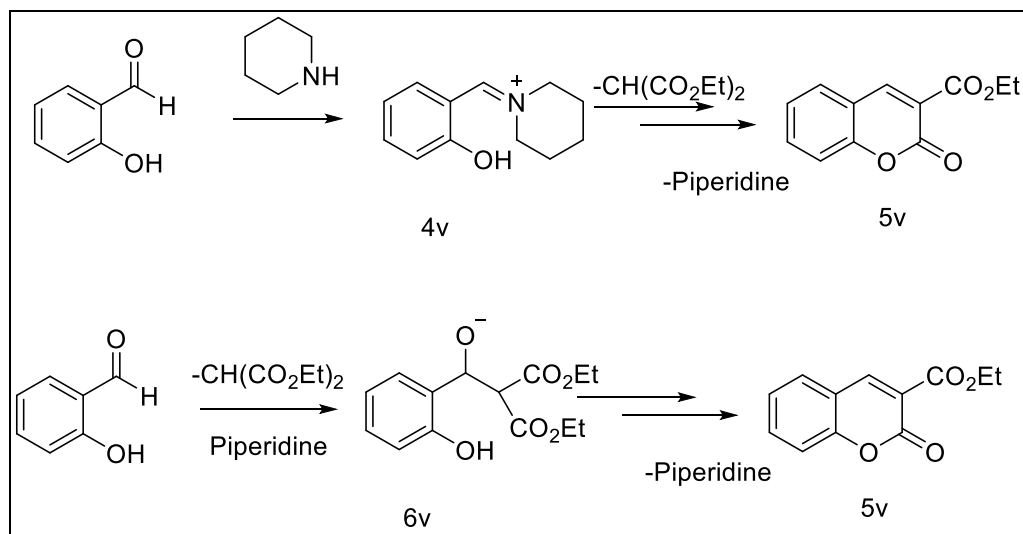


Figure 2.23. General mechanism for Knoevenagel condensation

Bogdal [188] has shown that, under microwave irradiation, the Knoevenagel condensation can be successfully applied to the synthesis of a number of coumarins with yields up of 94%. This reaction involves the condensation of salicylaldehydes 7v with carboxylic esters in the presence of piperidine under solvent-free conditions.

Previous 3-acetylcoumarin synthesized and published by our group: Recently, 7-(diethylamino)coumarin was synthesized by our group via the Knoevenagel condensation and the synthetic pathway is illustrated in Figure 2.24 [79].

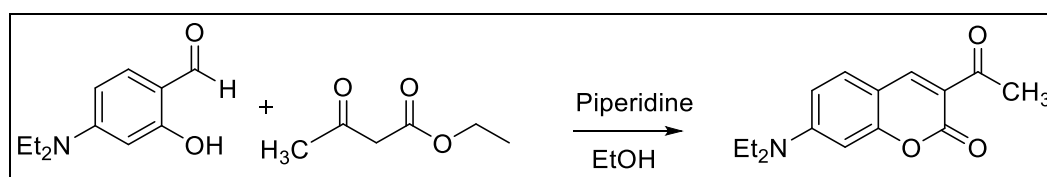


Figure 2.24. The synthesis of 3-acetylcoumarin

### 2.9.2. Formation of malonitrile derivative published by our group

Again, the Knoevenagel condensation was also employed, by our group [79], in the synthesis of malonitrile derivatives as shown in Figure 2.25.

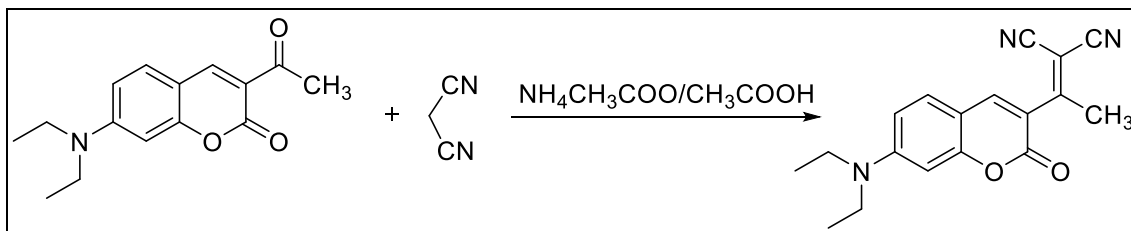
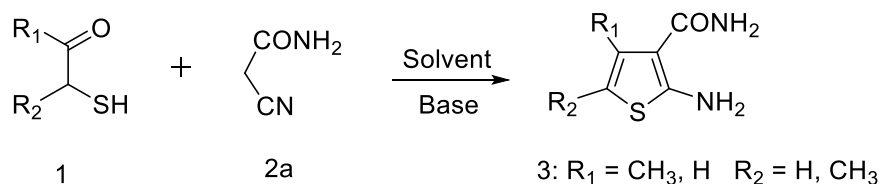


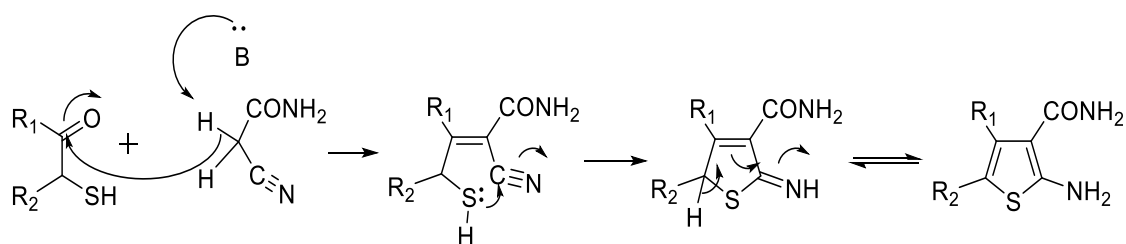
Figure 2.25. The synthetic pathway for Malononitriles

### 2.9.3. Mechanism for the formation of 2-aminothiophenes

Gewald devised the most facile and promising set of synthetic routes leading to 2-aminothiophene with a carboxamide group in position 3 and alkyl, aryl, cycloalkyl, and hetaryl groups in positions 4 and 5. Three major variations of this reaction have been described in detail. The first version [182-219] consists of a single step, by treatment of  $\alpha$ -mercaptoaldehyde or an  $\alpha$ -mercaptoketone with cyanoacetamide 2a in a solvent such as ethanol, dimethylformamide (DMF), dioxane, or water, in the presence of a basic catalyst such as trimethylamine (TEA) or piperidine at 50 °C.

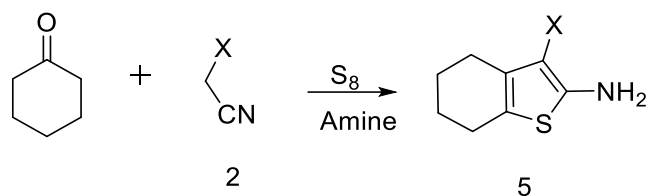


$\alpha$ -Mercaptoaldehyde or  $\alpha$ -mercaptoketone is often generated in situ by the reaction of alkali sulfides with the corresponding  $\alpha$ -halocarbonyl compounds. This version has a few drawbacks; the starting compounds are unstable and difficult to prepare. The mechanism of this reaction is as follows [191-205].



The second version of the Gewald reaction [187,195-200] consists of a one-pot procedure that is very extensively used for this synthesis. The convenient technique includes the

condensation of ketones with cyanoacetamide or *N*-substituted derivatives of compound 2 and a sulfur element in a solvent such as ethanol, DMF, or dioxane in the presence of amine as dimethylamine, morpholine, or TEA at room temperature.



2, 5a: X = CONH<sub>2</sub>; b: X = CONHCH<sub>3</sub>, c: X = CONHC<sub>2</sub>H<sub>5</sub>  
 d: X = CONHC<sub>6</sub>H<sub>5</sub>, e: X = CSNH<sub>2</sub>, f: X = CONHNH<sub>2</sub>

Aldehydes such as phenylacetaldehyde were used instead of ketones in the above reaction to give 2-amino-5-phenylthiophene-3-carboxamide 5 and the mechanism for this reaction has been illustrated in literature [181,195-200].

### 3. MATERIALS AND METHODS

#### 3.1. Materials and Tools

##### 3.1.1. Chemical substances used

All the chemicals used in the synthesis of the compounds were procured from Aldrich Chemical Company and were used without further purification. The solvents used were of spectroscopic grade.

##### 3.1.2. Devices used

###### <sup>1</sup>H-NMR and <sup>13</sup>C-NMR

<sup>1</sup>H-NMR and <sup>13</sup>C-NMR spectra were recorded on NMR spectrometer Bruker Avance and Ultra-Shield, using either DMSO-*d*<sub>6</sub> or CDCl<sub>3</sub> as the solvents. Chemical shifts (δ) are given in parts per million (ppm) using the residue solvent peaks as reference relative to TMS. Coupling constants (J) are given in hertz (Hz). Signals are abbreviated as follows: broad, br; singlet, s; doublet, d; doublet-doublet, dd; doublet-triplet, dt; triplet of doublet, td; triplet, t; multiplet, m.

###### FT-IR

FT-IR Spectra were recorded on a Mattson 1000 FT-IR spectrophotometer in KBr (ν are in cm<sup>-1</sup>).

###### Mass spectrometer

High resolution mass spectra (HRMS) were recorded at Gazi University, Faculty of Pharmacy, using electron ionization (EI) mass spectrometry (Waters-LCT-Premier-XE-LTOF (TOF-MS) instruments; in m/z (rel. %).

#### UV-Vis mass spectrometer

The electronic absorption spectra were obtained on Varian Cary 100 Bio spectrometer and CD spectra on JASCO J815 spectrophotometer all in quartz cuvettes (1 cm).

#### Fluorescence mass spectrometer

Fluorescence spectra were recorded on HITACHI F-7000 FL Spectrofluorophotometer in the same range for all solvents with a slit width of 5 nm for both excitation and emission.

#### Microwave device

The microwave syntheses were carried out in a Milestone Start microwave reaction system.

#### Melting point device

The melting points were measured using Electrothermal IA9200 apparatus.

#### TLC plates

Thin-layer chromatography (TLC) was used for monitoring the domino reactions using precoated silica gel 60 F254 plates.

#### Thermogravimetric analysis device

Thermal analyses were performed with a Shimadzu DTG-60H system, up to 600 °C (10 °C min<sup>-1</sup>) under a dynamic nitrogen atmosphere (15 mL min<sup>-1</sup>).

### **3.2. Synthesis of Initial 3-Acetylcoumarins**

Synthesis of the 3-Acetylcoumarins was carried out using Knoevenagel condensation.

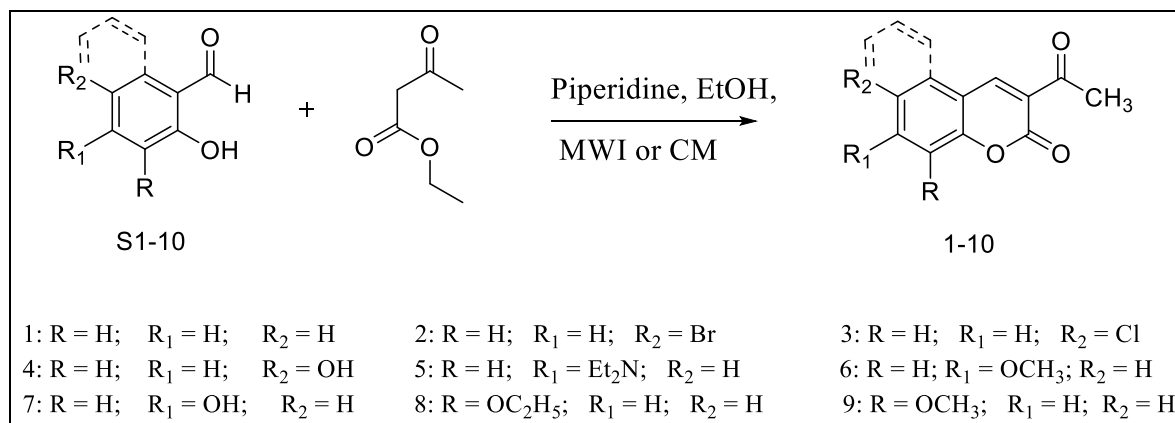


Figure 3.1. General synthetic route for the 3-acetylcoumarins 1-10

### 3.2.1. General procedure for the synthesis of 3-acetylcoumarins via conventional procedure

Synthesis of 3-Acetyl-2*H*-chromen-2-one (1): A mixture of 2-hydroxybenzaldehyde (S1) (10 mmol, 1.09 mL) and ethanol (20 mL) was stirred, and ethyl acetoacetate (12 mmol, 1.55 mL) was later added. Then, a catalytic amount of piperidine was added and swirled thoroughly. The mixture was stirred at room temperature for a specific period of time shown in Figure 3.1. The reaction was monitored by TLC (ethylacetate/n-hexane, 1:2) till completion. After completion, it was then allowed to cool for few minutes in iced water bath. A solid product was formed. After completion, it was then allowed to cool for few minutes in iced water bath. A solid product was formed. The product was filtered and dried to afford 3-acetyl-2*H*-chromen-2-one (1), whose physicochemical properties are shown in Appendix 5 (Table 5.1). The same procedure was followed in the synthesis of other derivatives 2-10.

### 3.2.2. General procedure for the synthesis of 3-acetylcoumarins via microwave-assisted irradiation procedure

Synthesis of 3-acetyl-2*H*-chromen-2-one (1): A mixture of 2-hydroxybenzaldehyde (2 mmol, 1.09 mL) and ethanol (20 mL) was stirred, and ethyl acetoacetate (2.4 mmol, 0.31 mL) was later added. Then, a catalytic amount of piperidine was added and swirled thoroughly. The reaction mixtures were added together in a microwave reaction vial and irradiated in microwave oven for a specific period of time and temperature as shown in Appendix 5 (Figure 3.1). The mixture was irradiated in microwave oven for a specific period of time and temperature as shown in Appendix 5. The reaction was monitored by

TLC (ethylacetate/n-hexane, 1:2) till completion. After completion, it was then allowed to cool for few minutes in iced water bath. A solid product was formed. The product was filtered and dried to afford 3-acetyl-2*H*-chromen-2-one (1), whose physicochemical properties are shown in Appendix 5 (Table 5.2). The same procedure was followed in the synthesis of other derivatives 2-10.

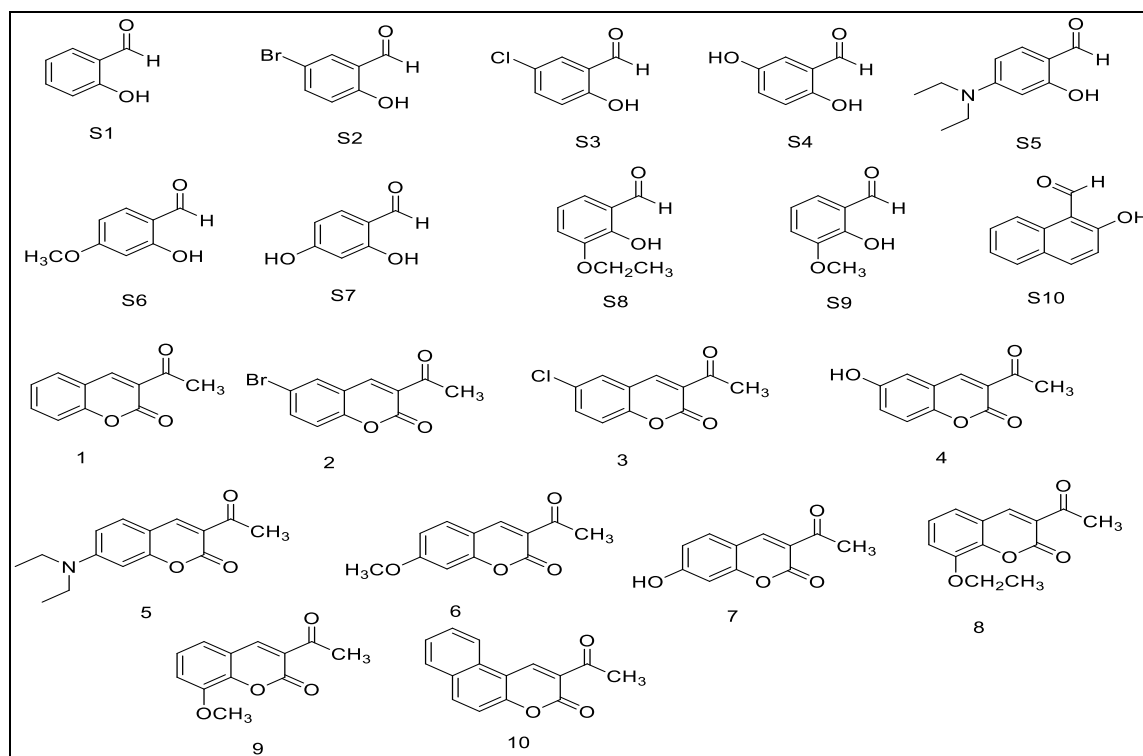


Figure 3.2. Structures of the salicylaldehydes (S1-10) and the 3-acetylcoumarins 1-10

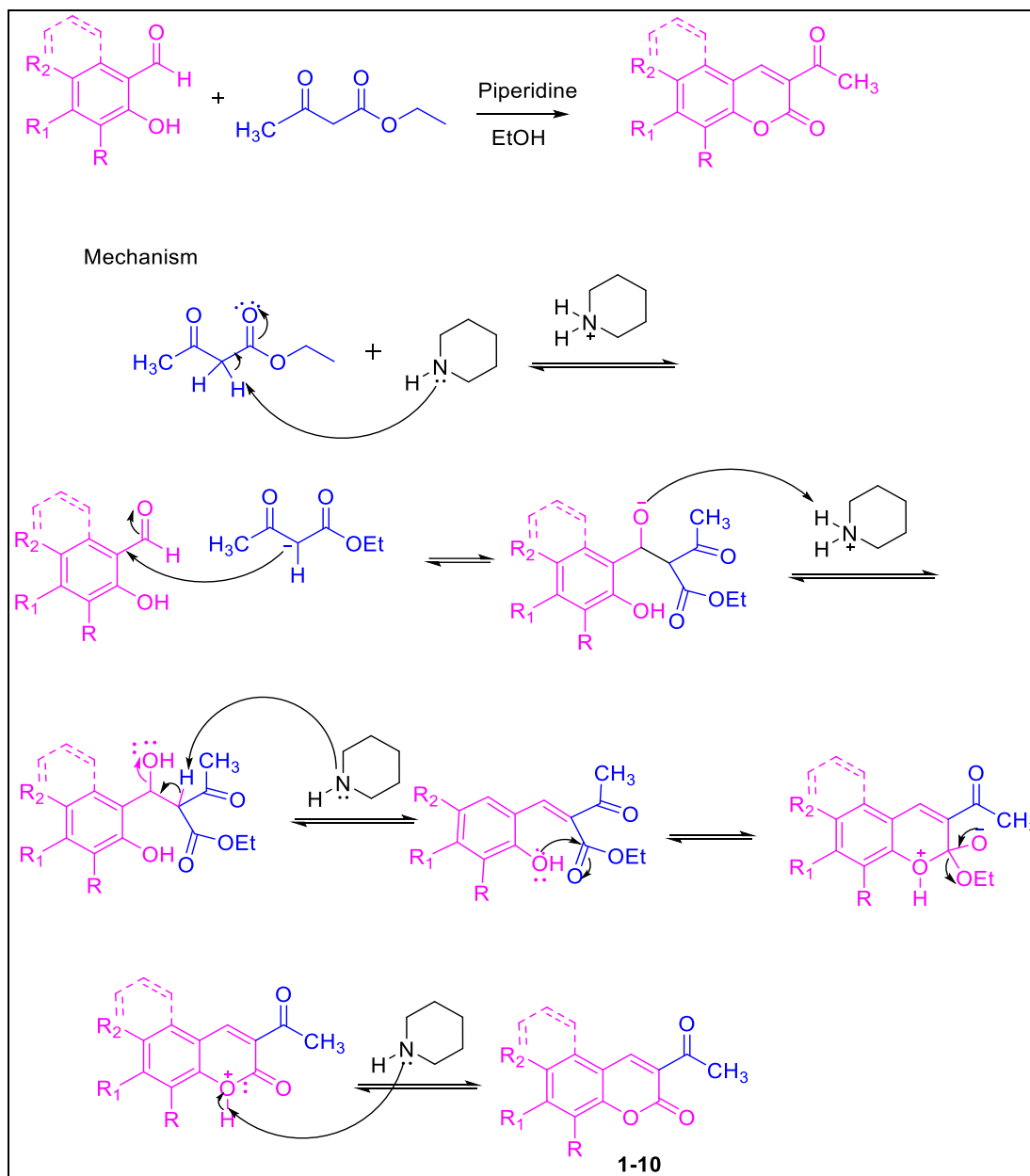


Figure 3.3. Plausible mechanism for the synthesized 3-acetylcoumarins

### 3.3. Synthesis of Malononitrile Derivatives

The synthesis of the Malononitrile derivatives was carried out by reacting 3-acetylcoumarin derivatives with Malononitrile using the Knoevenagel condensation under solvent-free conditions.

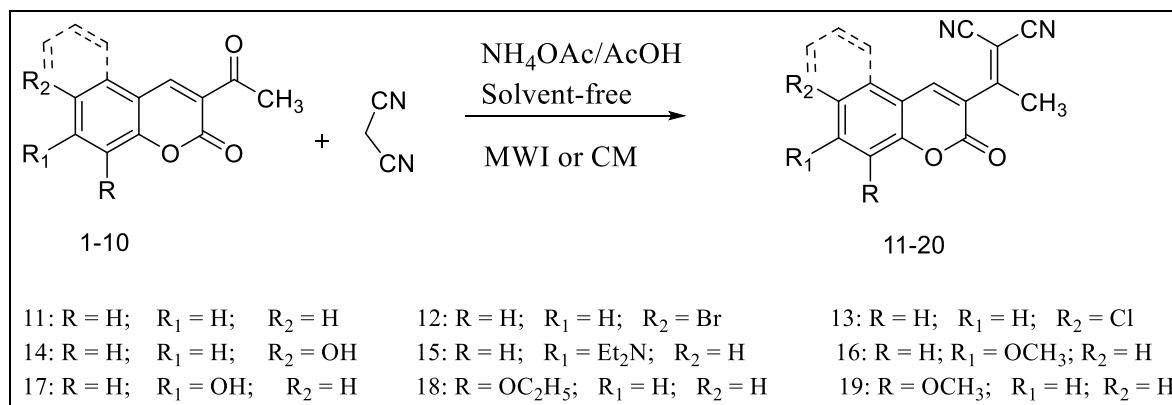


Figure 3.4. General synthetic pathways for the malononitriles 11-20

### 3.3.1. General procedure for the synthesis of malononitrile derivatives via conventional procedure

Synthesis of 2-(1-(2-oxo-2*H*-chromen-3-yl)ethylidene)malononitrile (11): To a mixture of 3-acetyl-6-bromo-2*H*-chromen-2-one (1) (2 mmol, 0.378 g) and malononitrile (4 mmol, 0.25 mL), an NH<sub>4</sub>OAc/AcOH buffer (5.00 mL) was added and swirled thoroughly. The mixture was stirred at room temperature for a specific period of time shown in Appendix 5 (Figure 3.4). The reaction was monitored by TLC (ethylacetate/n-hexane, 1:3) till completion. After completion, it was then allowed to cool for few minutes in iced water bath. A solid product was formed. The product was filtered and dried to afford 2-(1-(2-oxo-2*H*-chromen-3-yl)ethylidene)malononitrile (11), whose physicochemical properties are shown in Appendix 5 (Table 5.3). The same procedure was followed in the synthesis of other derivatives 12-20.

### 3.3.2. General procedure for the synthesis of malononitrile derivatives of the synthesized coumarins via microwave-assisted irradiation procedure

Synthesis of 2-(1-(2-oxo-2*H*-chromen-3-yl)ethylidene)malononitrile (11): To a mixture of 3-acetyl-2*H*-chromen-2-one (1) (2 mmol, 0.378 g) and malononitrile (4 mmol, 0.25 mL), an NH<sub>4</sub>OAc/AcOH buffer (5.00 mL) was added and swirled thoroughly. The reaction mixtures were added together in a microwave reaction vial and irradiated in microwave oven for a specific period of time and temperature as shown in Appendix 5 (Figure 3.4). The reaction was monitored by TLC (ethylacetate/n-hexane, 1:3) till completion. After completion, it was then allowed to cool for few minutes in iced water bath. A solid product was formed. The product was filtered and dried to afford the product whose

physicochemical properties are shown in Appendix 5 (Table 5.4). The same procedure was followed in the synthesis of other derivatives 12-20.

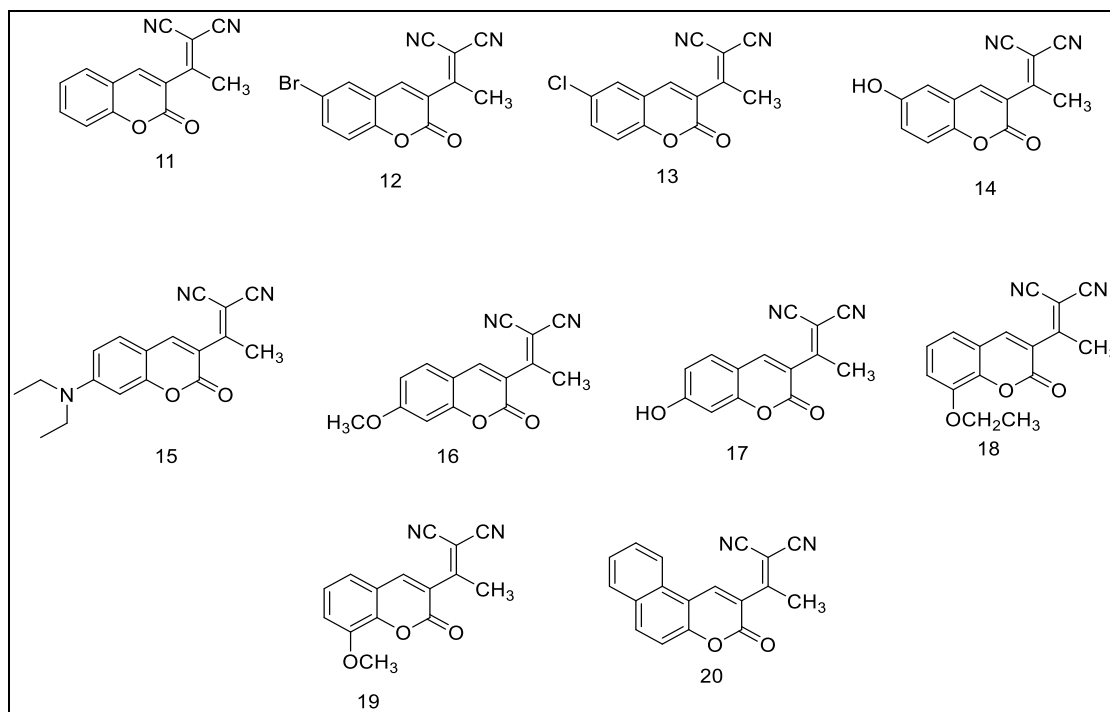


Figure 3.5. Structures of the synthesized malononitriles 11-20.

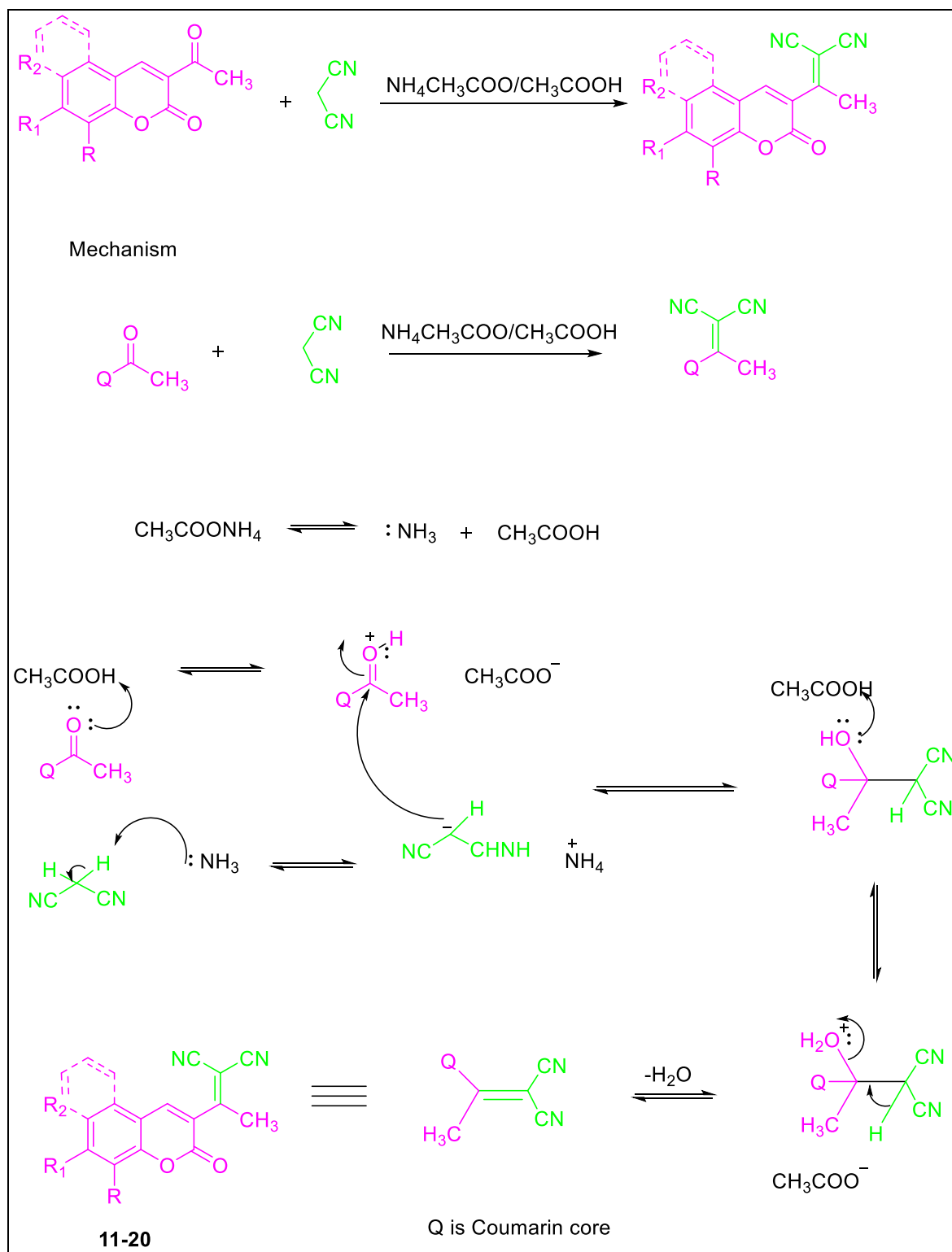


Figure 3.6. Plausible mechanism for the synthesized malononitriles

### 3.4. Synthesis of Coumarin-Thiophene Derivatives

Synthesis of coumarin-thiophene derivatives, in stepwise, was carried out using the Gewald reaction.

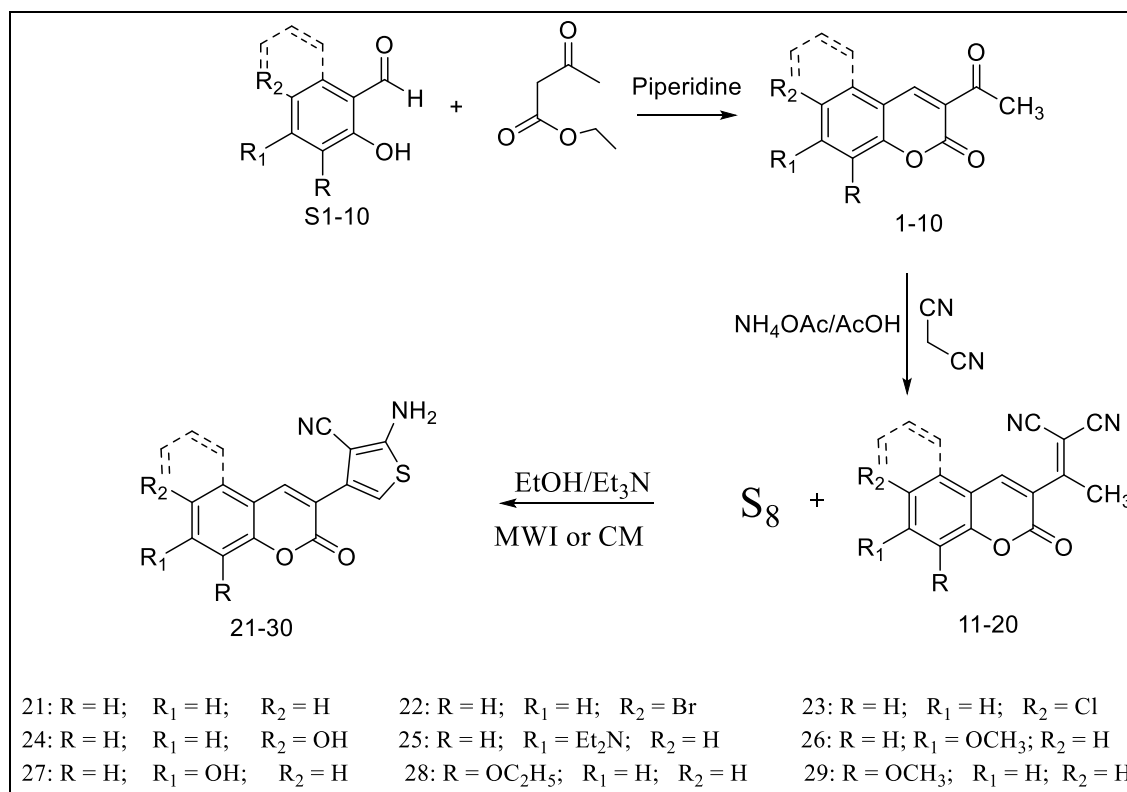


Figure 3.7. General synthetic pathways for the coumarin-thiophene hybrids

#### 3.4.1. General procedure for the synthesis of coumarin-thiophene hybrids via conventional procedure in stepwise

Synthesis of 2-Amino-4-(2-oxo-2*H*-chromen-3-yl)thiophene-3-carbonitrile (21): A mixture of 2-(1-(2-oxo-2*H*-chromen-3-yl)ethylidene)malononitrile (4 mmol) and elemental sulphur (5 mmol) in ethanol (25 mL) was mixed and stirred thoroughly. Triethylamine (1 mL) was added to the mixture and swirled thoroughly. The mixture was stirred at room temperature for a specific period of time shown in Appendix 5 (Figure 3.7). The reaction was monitored by TLC (ethylacetate/n-hexane, 1:3) till completion. After completion, it was then allowed to cool for few minutes in iced water bath. A solid product was formed. The product was filtered and dried to afford the product whose physicochemical properties are

shown in Appendix 5 (Table 5.5). The same procedure was followed in the synthesis of other derivatives 22-30.

### 3.4.2. General procedure for the synthesis of coumarin-thiophene hybrids via microwave-assisted irradiation procedure in stepwise

Synthesis of 2-Amino-4-(2-oxo-2*H*-chromen-3-yl)thiophene-3-carbonitrile (21): A mixture of 2-(1-(2-oxo-2*H*-chromen-3-yl)ethylidene)malononitrile (4 mmol) and elemental sulphur (5 mmol) in ethanol (25 mL) was mixed and stirred thoroughly. Triethylamin (1 mL) was added to the mixture and swirled thoroughly. The reaction mixtures were added together in a microwave reaction vial and irradiated in microwave oven for a specific period of time and temperature as shown in Appendix 5 (Figure 3.7). The reaction was monitored by TLC (ethylacetate/n-hexane, 1:3) till completion. After completion, it was then allowed to cool for few minutes in iced water bath. A solid product was formed. The product was filtered and dried to afford the product whose physicochemical properties are shown in Appendix 5 (Table 5.6). The same procedure was followed in the synthesis of other derivatives 22-30.

### 3.5. Synthesis of Coumarin-Thiophene Hybrids Via One-Pot Three-Component

Synthesis of Coumarin-thiophene derivative was carried out using the Gewald reaction.

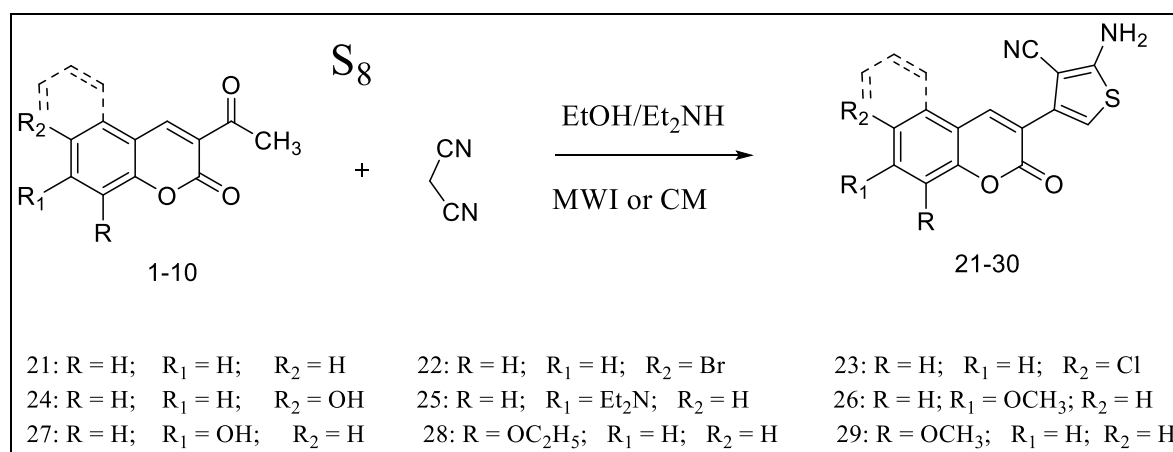


Figure 3.8. General synthetic pathways for the coumarin-thiophene hybrids in one-pot three-component

### **3.5.1. General procedure for the synthesis of coumarin-thiophene hybrids via conventional procedure in one-pot three-component**

Synthesis of 2-Amino-4-(2-oxo-2*H*-chromen-3-yl)thiophene-3-carbonitrile (21): In a 100 mL round-bottomed flask, 2-hydroxybenzaldehyde (1) (4 mmol, 0.753 g) and ethanol (30 mL) were mixed thoroughly. Malononitrile (4 mmol, 0.25 mL) was then added to the mixture and stirred again. After that, diethylamine (4 mmol, 0.416 mL) was added to the mixture and allowed to stir for sometime. After obtaining an homogeneous mixture, elemental sulfur (4 mmol, 0.128g) was finally added to the reaction mixture. The reaction mixture was stirred for 3 h at room temperature (Figure 3.8). After completion of the reaction, as monitored and seen on thin layer chromatography (ethylacetate/n-hexane, 1:3) conducted, the crude product was allowed to cool in an ice-bath. A solid product was formed, which was then filtered, dried, and recrystallized from hot ethanol to obtain pure product. The same procedure was followed in the synthesis of other derivatives 22-30.

### **3.5.2. General procedure for the synthesis of coumarin-thiophene hybrids via microwave-assisted irradiation procedure in one-pot three-component**

Synthesis of 2-Amino-4-(2-oxo-2*H*-chromen-3-yl)thiophene-3-carbonitrile (21): In a 100 mL round-bottomed flask, 2-hydroxybenzaldehyde (1) (2 mmol, 0.376 g) and ethanol (10 mL) were mixed thoroughly. Malononitrile (2 mmol, 0.125 mL) was then added to the mixture and stirred again. After that, diethylamine (2 mmol, 0.208 mL) was added to the mixture and allowed to stir for sometime. After obtaining an homogeneous mixture, elemental sulfur (2 mmol, 0.064 g) was finally added to the reaction mixture. The reaction mixtures were added together in a microwave reaction vial and irradiated in microwave oven for a specific period of time and temperature as shown in Table 4.7 (Figure 3.8). The reaction was monitored by TLC (ethylacetate/n-hexane, 1:3) till completion. After completion, it was then allowed to cool for few minutes in iced water bath. A solid product was formed, which was then filtered, dried, and recrystallized from hot ethanol to obtain pure product. The same procedure was followed in the synthesis of other derivatives 22-30.

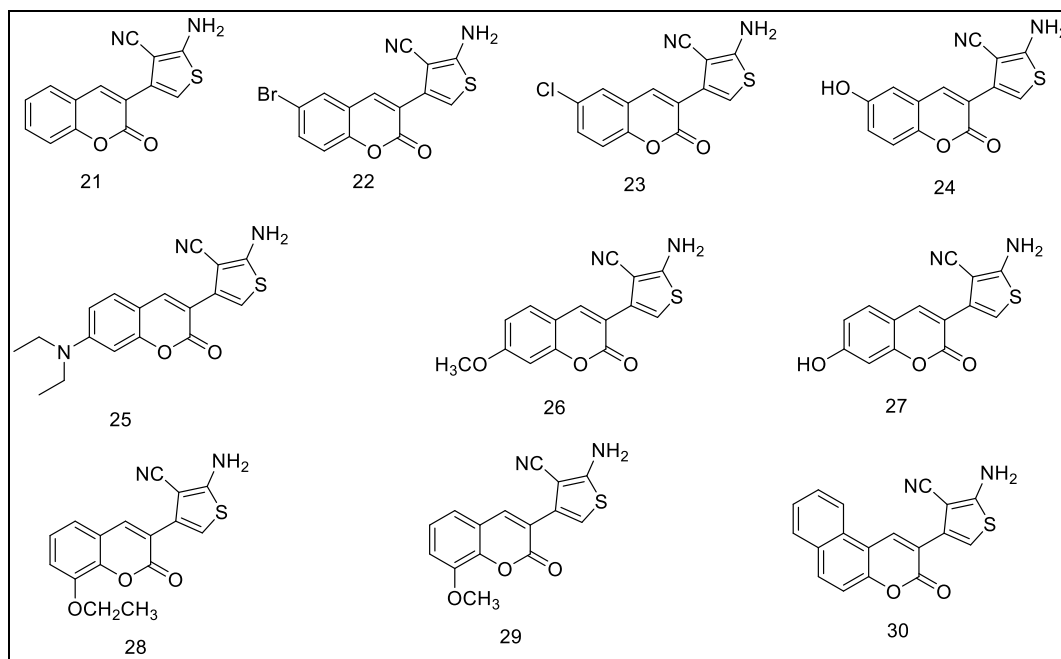


Figure 3.9. Structures of the synthesized coumarin-thiophene hybrids 21-30

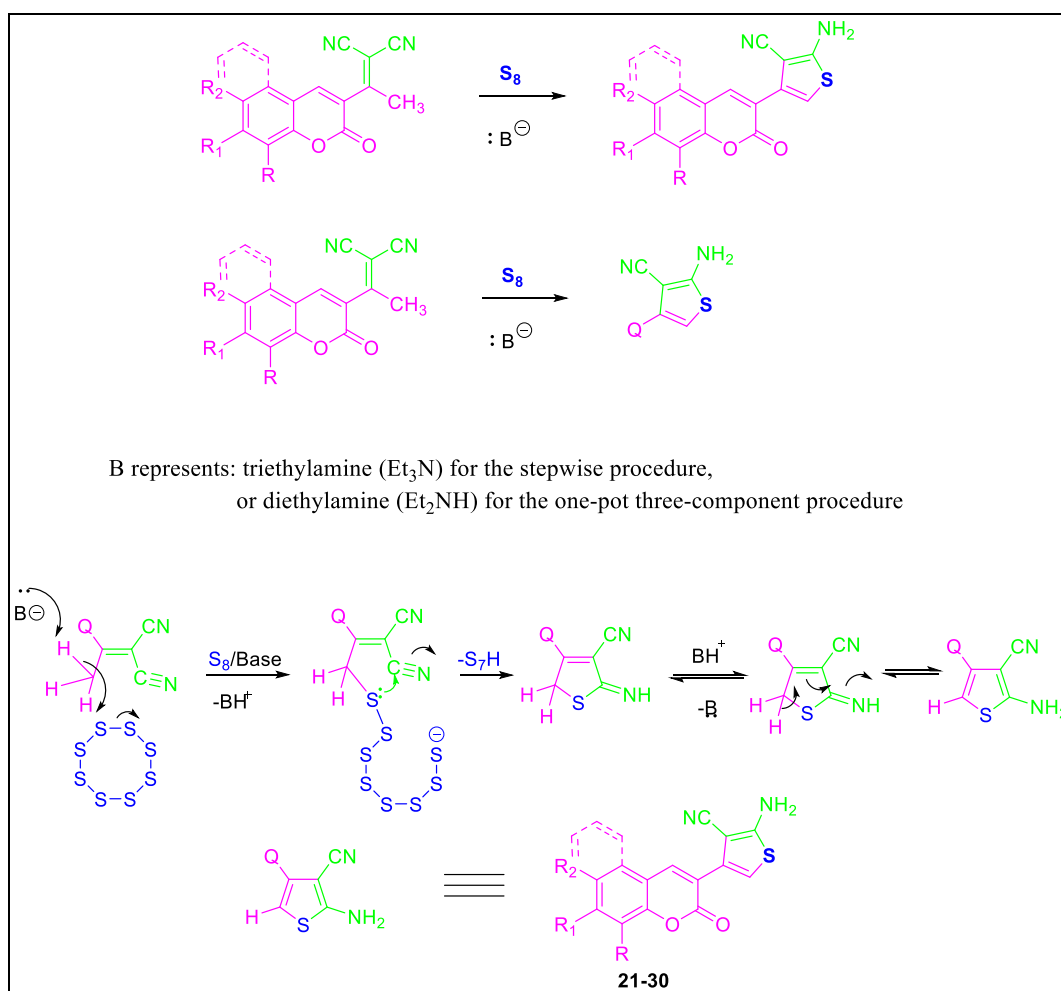


Figure 3.10. Plausible mechanism for the synthesized of coumarin-thiophenes 21-30

### 3.6. Synthesis of Amides, Disulfonamide, and Urea derivatives of Benzocoumarin-Thiophene derivative

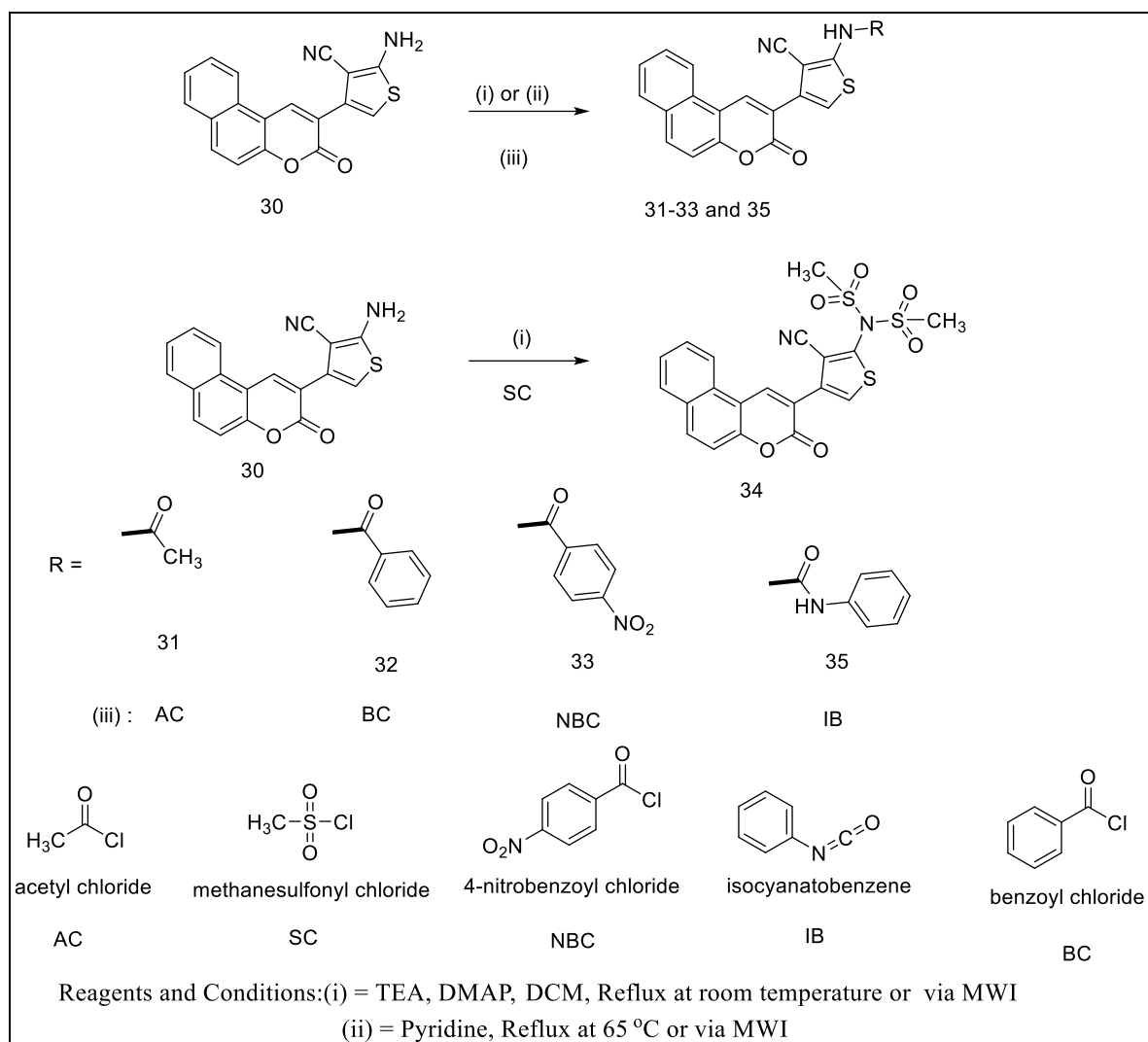


Figure 3.11. Synthetic routes for the amide, sulfonamide, and urea derivatives 31-35

#### 3.6.1. Synthesis of the amide derivatives

##### Synthesis of the amide derivatives via conventional procedure

##### *Synthesis of N-(3-cyano-4-(3-oxo-3H-benzo[f]chromen-2-yl)thiophen-2-yl)acetamide (31)*

To a mixture of 2-Amino-4-(3-oxo-3H-benzo[f]chromen-2-yl)thiophene-3-carbonitrile (30) (1 mmol, 0.318 g) and DCM (10 mL), a solution of DMAP (0.20 mmol, 0.024g) in DCM (5 mL) was added dropwise and the mixture was mixed thoroughly for some time. After that, TEA (3 mmol, 0.42 mL) was gradually added to the mixture. The mixture was stirred

at room temperature for a while. Finally, acetyl chloride (1.25 mmol, 0.098 g) was added and the reaction mixture was refluxed for 18 hours as shown in Figure 3.11. The reaction was monitored by TLC (ethylacetate/n-hexane, 1:3) till completion. A solid product was formed. At the end of the period, diisopropyl ether (10 mL) was added to the product solution. A solid product was formed. The solid product was filtered, dried, and washed with hot DCM to afford the pure *N*-(3-cyano-4-(3-oxo-3*H*-benzo[*f*]chromen-2-yl)thiophen-2-yl)acetamide whose physicochemical properties are shown in Appendix 5 (Table 5.7).

*Synthesis of N-(3-cyano-4-(3-oxo-3H-benzo[f]chromen-2-yl)thiophen-2-yl)benzamide (32)*

Using (30) (1 mmol, 0.318 g) and benzoyl chloride (1.25 mmol, 0.176 g) as the starting compounds, the reaction was carried out under the same conditions as that of compound 31 as shown in Figure 3.11. A solid product was formed. The solid product was filtered, dried, and washed with hot DCM to afford the pure *N*-(3-cyano-4-(3-oxo-3*H*-benzo[*f*]chromen-2-yl)thiophen-2-yl)benzamide whose physicochemical properties are shown in Appendix 5 (Table 5.7).

*Synthesis of N-(3-cyano-4-(3-oxo-3H-benzo[f]chromen-2-yl)thiophen-2-yl)-4-nitrobenzamide (33)*

Using (30) (1 mmol, 0.318 g) and 4-nitrobenzoyl chloride (1.25 mmol, 0.231 g) as the starting compounds, the reaction was carried out under the same conditions as that of compound 31 as shown in Figure 3.11. A solid product was formed. The solid product was filtered, dried, and washed with hot DCM to afford the pure *N*-(3-cyano-4-(3-oxo-3*H*-benzo[*f*]chromen-2-yl)thiophen-2-yl)-4-nitrobenzamide whose physicochemical properties are shown in Appendix 5 (Table 5.7).

*Synthesis of amide derivatives via microwave-irradiation procedure*

*Synthesis of N-(3-cyano-4-(3-oxo-3H-benzo[f]chromen-2-yl)thiophen-2-yl)acetamide (31)*

To a mixture of 2-amino-4-(3-oxo-3*H*-benzo[*f*]chromen-2-yl)thiophene-3-carbonitrile (30) (1 mmol, 0.318 g) and DCM (10 mL), a solution of DMAP (0.20 mmol, 0.024g) in DCM (5 mL) was added dropwise and the mixture was mixed thoroughly for some time. After that, TEA (3 mmol, 0.42 mL) was gradually added to the mixture. The mixture was stirred

at room temperature for a while. Finally, acetyl chloride (1.25 mmol, 0.098 g) was added and the reaction mixture was stirred at 130 °C for 3 min, 450W as shown in Figure 3.11. The reaction mixtures were added together in a microwave reaction vial and irradiated in microwave oven for a specific period of time and temperature as shown in Appendix 5. The reaction was monitored by TLC (ethylacetate/n-hexane, 1:3) till completion. At the end of the period, diisopropyl ether (10 mL) was added to the product solution. A solid product was formed. The solid product was filtered, dried, and washed with hot DCM to afford the pure *N*-(3-cyano-4-(3-oxo-3*H*-benzo[*f*]chromen-2-yl)thiophen-2-yl)acetamide whose physicochemical properties are shown in Appendix 5 (Table 5.8).

*Synthesis of N-(3-cyano-4-(3-oxo-3H-benzo[f]chromen-2-yl)thiophen-2-yl)benzamide (32)*

Using (30) (1 mmol, 0.318 g) and benzoyl chloride (1.25 mmol, 0.176 g) as the starting compounds, the reaction was carried out under the same conditions as that of compound 31 as shown in Figure 3.11. A solid product was formed. The solid product was filtered, dried, and washed with hot DCM to afford the pure *N*-(3-cyano-4-(3-oxo-3*H*-benzo[*f*]chromen-2-yl)thiophen-2-yl)benzamide whose physicochemical properties are shown in Appendix 5 (Table 5.8).

*Synthesis of N-(3-cyano-4-(3-oxo-3H-benzo[f]chromen-2-yl)thiophen-2-yl)-4-nitrobenzamide (33)*

Using (30) (1 mmol, 0.318 g) and 4-nitrobenzoyl chloride (1.25 mmol, 0.231 g) as the starting compounds, the reaction was carried out under the same conditions as that of compound 31 as shown in Figure 3.11. A solid product was formed. The solid product was filtered, dried, and washed with hot DCM to afford the pure *N*-(3-cyano-4-(3-oxo-3*H*-benzo[*f*]chromen-2-yl)thiophen-2-yl)-4-nitrobenzamide whose physicochemical properties are shown in Appendix 5 (Table 5.8).

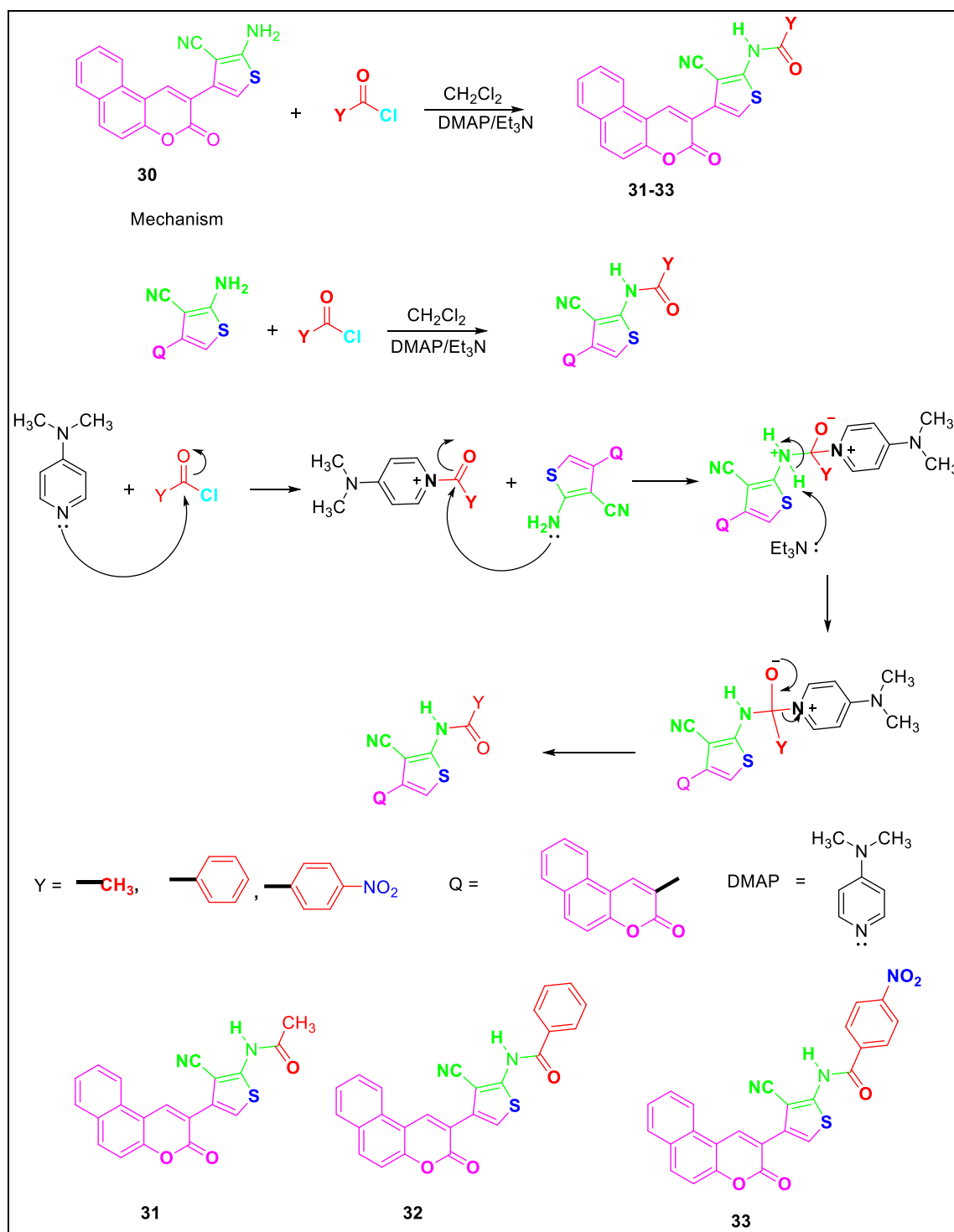


Figure 3.12. Plausible mechanism for the synthesized amide derivatives

### 3.6.2. Synthesis of disulfonamide derivative of benzo[f]coumarin-thiophene derivatives

#### Synthesis of disulfonamide derivative (34) via conventional procedure

To a mixture of 2-amino-4-(3-oxo-3*H*-benzo[f]chromen-2-yl)thiophene-3-carbonitrile (30) (1 mmol, 0.318 g) and DCM (10 mL), another DCM (5 mL) was added dropwise and the mixture was mixed thoroughly. A DMAP (0.20 mmol, 0.024g) was added. After that, TEA (3 mmol, 0.42 mL) was added. The mixture was stirred at room temperature for a while. Finally, methanesulfonyl chloride (2.5 mmol, 0.286 g) was added, and the reaction mixture was refluxed for 18 hours as shown in Figure 3.11. The reaction was monitored by TLC (ethylacetate/n-hexane, 1:3) till completion. At the end of the period, diisopropyl ether (10 mL) was added to the product solution. A solid product was formed. The solid product was filtered, dried, and washed with hot methanol to afford pure *N*-(3-cyano-4-(3-oxo-3*H*-benzo[f]chromen-2-yl)thiophen-2-yl)-*N*-(methylsulfonyl) methanesulfonamide whose physicochemical properties are shown in Appendix 5 (Table 5.7).

#### *Synthesis of disulfonamide derivative (34) via micro-wave-assisted irradiation procedure*

To a mixture of 2-Amino-4-(3-oxo-3*H*-benzo[f]chromen-2-yl)thiophene-3-carbonitrile (30) (1 mmol, 0.318 g) and DCM (10 mL), another DCM (5 mL) was added dropwise and the mixture was mixed thoroughly. A DMAP (0.20 mmol, 0.024g) was added. After that, TEA (3 mmol, 0.42 mL) was added. The mixture was stirred at room temperature for a while. Finally, methanesulfonyl chloride (2.5 mmol, 0.286 g) was added. The reaction mixtures were added together in a microwave reaction vial and irradiated in microwave oven at 130°C for 3 min (450 W) as shown in Figure 3.11. The reaction was monitored by TLC (ethylacetate/n-hexane, 1:3) till completion. At the end of the period, diisopropyl ether (10 mL) was added to the product solution. A solid product was formed. The solid product was filtered, dried, and washed with hot methanol to afford the pure *N*-(3-cyano-4-(3-oxo-3*H*-benzo[f]chromen-2-yl)thiophen-2-yl)-*N*-(methylsulfonyl) methanesulfonamide whose physicochemical properties are shown in Appendix 5 (Table 5.8).



### 3.6.3. Synthesis of urea derivative of Benzo[f]coumarin--thiophene derivative

*Synthesis of 1-(3-cyano-4-(3-oxo-3H-benzo[f]chromen-2-yl)thiophen-2-yl)-3-phenylurea (35) via Conventional Procedure*

To a mixture of 2-amino-4-(3-oxo-3H-benzo[f]chromen-2-yl)thiophene-3-carbonitrile (1 mmol, 0.318 g) and pyridine (4 mL), an isocyanatobenzene (2.3 mmol, 0.274 g) was added and swirled thoroughly. The reaction mixture was placed in an oil bath set to 65 ° C and stirred for 18 hours as shown in Figure 3.11. The reaction was monitored by TLC (ethylacetate/n-hexane, 1:3) till completion. At the end of the period, 30mL of 20% HCl was added to the product. A solid product was formed. The aqueous portion was discarded. The solid portion was filtered, washed with hot ethanol and dried, to afford pure 1-(3-cyano-4-(3-oxo-3H-benzo[f]chromen-2-yl)thiophen-2-yl)-3-phenylurea whose physicochemical properties are shown in Appendix 5 (Table 5.7).

*Synthesis of 1-(3-cyano-4-(3-oxo-3H-benzo[f]chromen-2-yl)thiophen-2-yl)-3-phenylurea (35) via Micro-wave-Assisted Irradiation Procedure*

To a mixture of 2-amino-4-(3-oxo-3H-benzo[f]chromen-2-yl)thiophene-3-carbonitrile (30) (1 mmol, 0.318 g) and pyridine (4 mL), an isocyanatobenzene (2.3 mmol, 0.274 g) was added and swirled thoroughly. The reaction mixtures were added together in a microwave reaction vial and irradiated in a microwave oven at 180°C (350 W) for 3 min as shown in Figure 3.11. The reaction was monitored by TLC (ethylacetate/n-hexane, 1:3) till completion. At the end of the period, 30mL of 20% HCl was added to the product. A solid product was formed. The aqueous portion was discarded. The solid portion was filtered, washed with hot ethanol and dried, to afford pure 1-(3-cyano-4-(3-oxo-3H-benzo[f]chromen-2-yl)thiophen-2-yl)-3-phenylurea whose physicochemical properties are shown in Appendix 5 (Table 5.8).

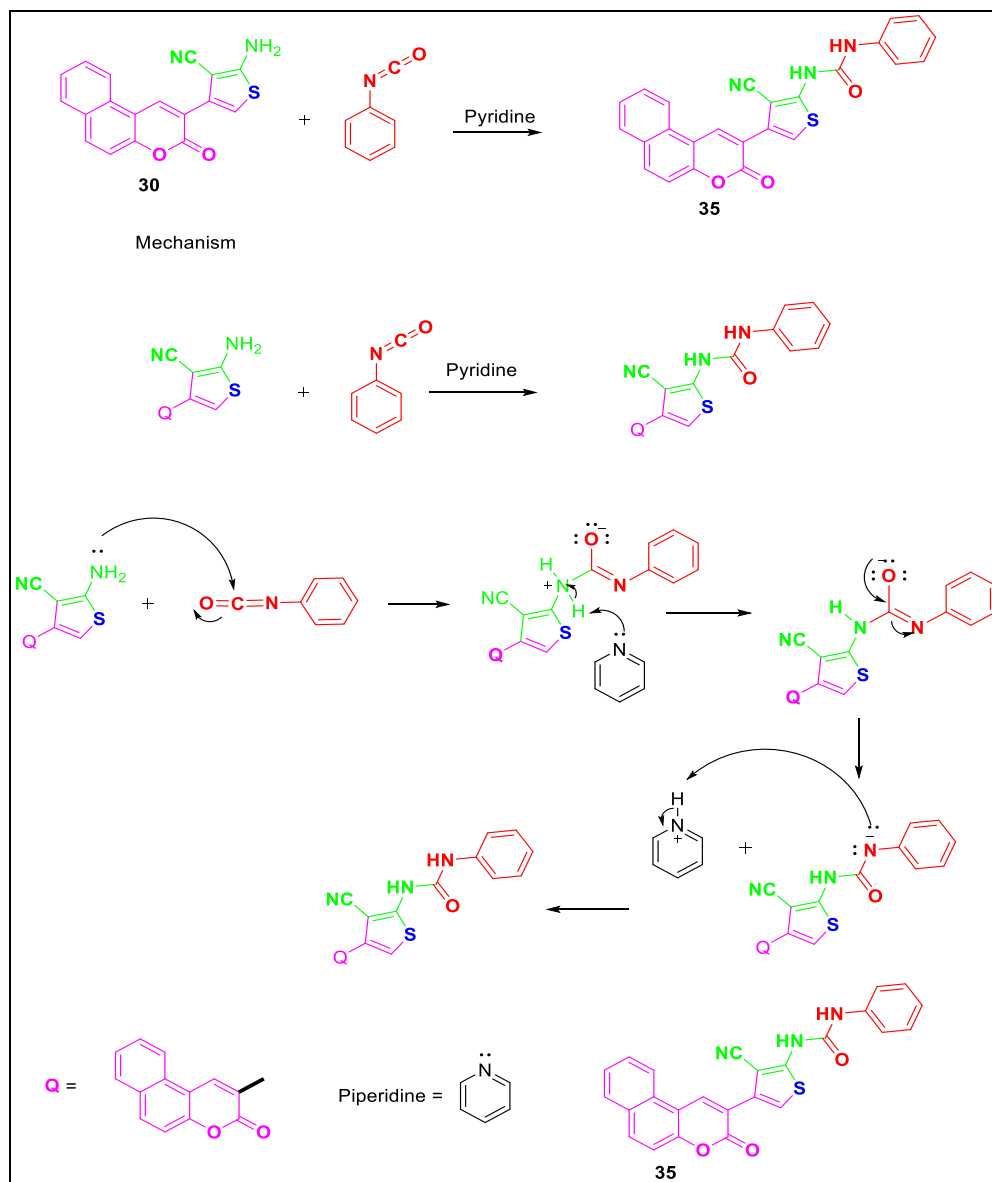


Figure 3.14. Plausible mechanism for the synthesized urea derivative

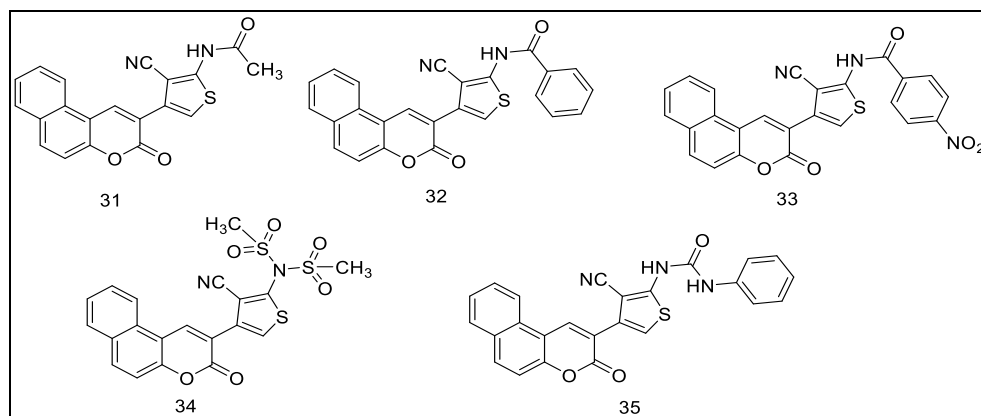


Figure 3.15. Structures of the synthesized amide, sulfonamide, and urea derivatives 31-35

### 3.7. The Structural Characterizations and Elucidations of the Synthesized 3-Acetylcoumarins (1-10)

#### 3.7.1. Structural elucidation for 3-Acetyl-2*H*-chromen-2-one (1)

Solvent of recrystallization: Ethanol; FT-IR ( $\nu_{\max}$ ,  $\text{cm}^{-1}$ ): 3030 (Aromatic C-H), 2975 (Aliphatic C-H), 1735 (C=O, lactone), 1665 (C=O), 1554 (C=C), 1289 (C-O-C);  $^1\text{H-NMR}$  (DMSO- $d_6$ , 300 MHz)  $\delta$ : 2.65 (s, 3H, CH<sub>3</sub>), 7.40-7.98 (complex, m, 4H, Ar-H), 8.65 (s, 1H, Ar-H).

The chemical structure of (1) was identified and can be explained by using its IR, NMR, and MS spectra as shown in Appendix 1 (Figures 1.1.1 and 1.1.2).

For the IR spectrum, recorded in KBr pellets, the vibration bands of (1) appear at 3030, 2975, 1735, 1665, 1554, and 1289  $\text{cm}^{-1}$ . The band at 3030 corresponds to the stretching vibrations of the conjugated system. The vibration bands at 2975, 1735, 1665, 1554, and 1280  $\text{cm}^{-1}$  can be related to aliphatic  $\nu(\text{C-H})$ , lactone  $\nu(\text{C=O})$ , carbonyl  $\nu(\text{C=O})$ , aromatic  $\nu(\text{C=C})$ , and lactone  $\nu(\text{C-O-C})$  stretching vibrations, respectively. The NMR spectrum of (1) was recorded in DMSO- $d_6$  using tetramethylsilane (TMS). The CH<sub>3</sub> protons are easily distinguishable as a singlet linked to the monocyclic carbonyl group of 3 protons at 2.65 ppm in the  $^1\text{H-NMR}$  spectrum. The complex multi-peak located at 7.40-7.98 ppm representing the protons; Hb, Hc, Hd, and He of the coumarin ring. The spectrum also shows a Ha proton in the singlet peak of coumarin ring at 8.45 ppm. With respect to these data and the explanation given above, the following structural formula is proposed for compound 3-acetyl-2*H*-chromen-2-one (1)

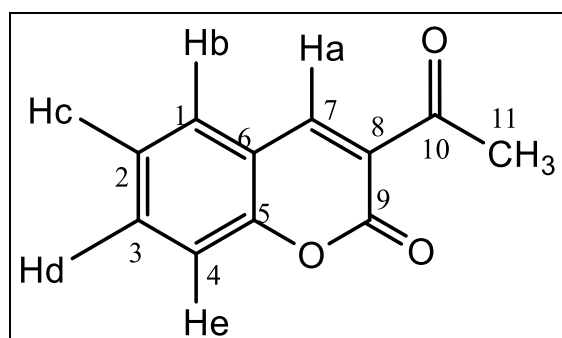


Figure 3.16. Structure of 3-Acetyl-2*H*-chromen-2-one (1)

### 3.7.2. Structural elucidation for 3-Acetyl-6-bromo-2*H*-chromen-2-one (2)

Solvent of recrystallization: Ethanol; FT-IR ( $\nu_{\max}$ ,  $\text{cm}^{-1}$ ): 3048 (Aromatic C-H), 2924 (Aliphatic C-H), 1730 (C=O, lactone), 1672 (C=O), 1546 (C=C), 1280 (C-O-C), 658 (C-Br);  $^1\text{H-NMR}$  (DMSO- $d_6$ , 300 MHz)  $\delta$ : 2.58 (s, 3H, CH<sub>3</sub>), 7.45 (d,  $J = 8.8$  Hz, 1H, Ar-H), 7.89 (dd,  $J = 8.9, 2.4$  Hz, 1H, Ar-H), 8.22 (d,  $J = 2.4$  Hz, 1H, Ar-H), 8.60 (s, 1H, Ar-H).

The chemical structure of (2) was identified and can be explained by using its IR and NMR spectra as shown in Appendix 1 (Figures 1.2.1 and 1.2.2).

For the IR spectrum, recorded in KBr pellets, the vibration bands of (2) appear at 3098, 2924, 1730, 1672, 1546, 1280, and 658  $\text{cm}^{-1}$ . The band at 3098 corresponds to the stretching vibrations of the conjugated system. The vibration bands at 2924, 1730, 1672, 1546, 1280, and 658  $\text{cm}^{-1}$  can be related to aliphatic  $\nu(\text{C-H})$ , lactone  $\nu(\text{C=O})$ , carbonyl  $\nu(\text{C=O})$ , aromatic  $\nu(\text{C=C})$ , lactone  $\nu(\text{C-O-C})$ , and (C-Br) stretching vibrations, respectively. The NMR spectrum of (2) was recorded in DMSO- $d_6$  using tetramethylsilane (TMS) as the reference. The CH<sub>3</sub> protons are easily distinguishable as a singlet linked to the monocyclic carbonyl group of 3 protons at 2.58 ppm in the  $^1\text{H-NMR}$  spectrum. A doublet proton at 7.45 ppm corresponds to Hd (d,  $J = 8.9$  Hz) of an aromatic proton, and the doublet of doublet at 7.89 ppm can be linked to Hc (dd,  $J = 8.9, 2.4$  Hz), also an aromatic proton. Another doublet proton at 8.22 ppm corresponds to Hd ( $J = 2.4$  Hz), and the Ha proton in the singlet peak of coumarin ring at 8.60 ppm. With respect to these data and the explanation given above, the following structural formula is proposed for compound 3-acetyl-6-bromo-2*H*-chromen-2-one (2).

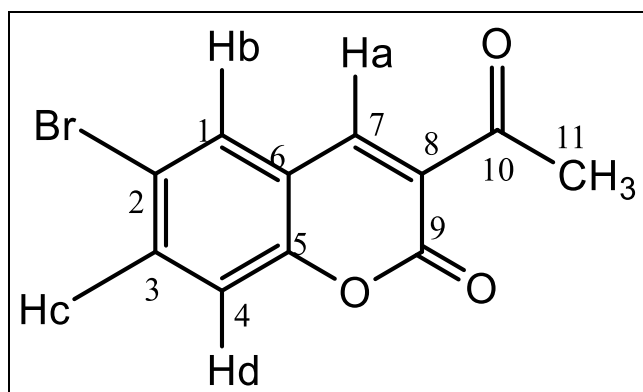


Figure 3.17. Structure of 3-Acetyl-6-bromo-2*H*-chromen-2-one (2)

### 3.7.3. Structural elucidation for 3-Acetyl-6-chloro-2*H*-chromen-2-one (3)

Solvent of recrystallization: Ethanol; FT-IR ( $\nu_{\max}$ ,  $\text{cm}^{-1}$ ): 3042 (Aromatic C-H), 2924 (Aliphatic C-H), 1732 (C=O, lactone), 1673 (C=O), 1550 (C=C), 1228 (C-O-C), 562 (C-Cl);  $^1\text{H-NMR}$  (DMSO, 300 MHz)  $\delta$ : 2.58 (s, 3H,  $\text{CH}_3$ ), 7.51 (d,  $J = 8.9$  Hz, 1H, Ar-H), 7.79 (dd,  $J = 8.9, 2.5$  Hz, 1H, Ar-H), 8.08 (d,  $J = 2.5$  Hz, 1H, Ar-H), 8.61 (s, 1H, Ar-H).

The chemical structure of (3) was identified and can be explained by using its IR, NMR, and MS spectra as shown in Appendix 1 (Figures 1.3.1 and 1.3.2).

For the IR spectrum, recorded in KBr pellets, the vibration bands of (3) appear at 3042, 2924, 1732, 1673, 1550, 1228, and 562  $\text{cm}^{-1}$ . The band at 3042 corresponds to the stretching vibrations of the conjugated system. The vibration bands at 2924, 1732, 1673, 1550, 1228, and 562  $\text{cm}^{-1}$  can be related to aliphatic  $\nu(\text{C-H})$ , lactone  $\nu(\text{C=O})$ , carbonyl  $\nu(\text{C=O})$ , aromatic  $\nu(\text{C=C})$ , lactone  $\nu(\text{C-O-C})$ , and (C-Cl) stretching vibrations, respectively. The NMR spectrum of (3) was recorded in  $\text{CDCl}_3$  using tetramethylsilane (TMS). The  $\text{CH}_3$  protons are easily distinguishable as a singlet linked to the monocyclic carbonyl group of 3 protons at 2.58 ppm in the  $^1\text{H-NMR}$  spectrum. A doublet proton at 7.51 ppm corresponds to Hd (d,  $J = 8.9$  Hz) of an aromatic proton, and the doublet of doublet at 7.79 ppm can be linked to Hc (dd,  $J = 8.9, 2.4$  Hz), also an aromatic proton. Another doublet proton at 8.08 ppm corresponds to Hd ( $J = 2.4$  Hz), and the Ha proton in the singlet peak of coumarin ring at 8.61 ppm. With respect to these data and the explanation given above, the following structural formula is proposed for compound 3-acetyl-6-chloro-2*H*-chromen-2-one (3).

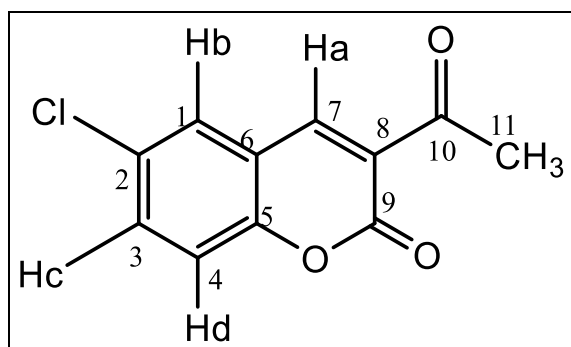


Figure 3.18. Structure of 3-Acetyl-6-chloro-2*H*-chromen-2-one (3)

### 3.7.4. Structural elucidation for 3-Acetyl-6-hydroxy-2*H*-chromen-2-one (4)

Solvent of recrystallization: Ethanol; FT-IR ( $\nu_{\max}$ ,  $\text{cm}^{-1}$ ): 3114 (Phenolic O-H), 3051 (Aromatic C-H), 2936 (Aliphatic C-H), 1737 (C=O, lactone), 1642 (C=O), 1564 (C=C), 1278 (C-O-C);  $^1\text{H-NMR}$  (DMSO- $d_6$ , 300 MHz)  $\delta$ : 2.57 (s, 3H, CH<sub>3</sub>), 7.15-7.33 (complex, *m*, 3H, Ar-H), 8.57 (s, 1H, Ar-H), 9.91 (s, 1H, O-H, exchangeable with D<sub>2</sub>O).

The chemical structure of (4) was identified and can be explained by using its IR and NMR spectra as shown in Appendix 1 (Figures 1.4.1 and 1.4.2).

For the IR spectrum, recorded in KBr pellets, the vibration bands of (4) appear at 3114, 3051, 2936, 1737, 1642, 1564, and 1278  $\text{cm}^{-1}$ . A broad band, characteristic of O-H stretching vibrations is in the range 2847-3366  $\text{cm}^{-1}$  in the spectrum of (4). The band at 3051 corresponds to the stretching vibrations of the conjugated system. The vibration bands at 2936, 1737, 1642, 1564, and 1278  $\text{cm}^{-1}$  can be related to aliphatic  $\nu(\text{C-H})$ , lactone  $\nu(\text{C=O})$ , carbonyl  $\nu(\text{C=O})$ , aromatic  $\nu(\text{C=C})$ , and lactone  $\nu(\text{C-O-C})$  stretching vibrations, respectively. The NMR spectrum of (4) was recorded in DMSO- $d_6$  using tetramethylsilane (TMS). The CH<sub>3</sub> protons are easily distinguishable as a singlet linked to the monocyclic carbonyl group of 3 protons at 2.57 ppm in the  $^1\text{H-NMR}$  spectrum. The complex multiplet located at 7.15-7.33 ppm represents the 3 protons; Hb, Hc, and Hd, of the coumarin ring. The spectrum also shows a Ha proton in the singlet peak of coumarin ring at 8.57 ppm. An O-H proton, which is exchangeable with D<sub>2</sub>O, is observed at 9.91 ppm. With respect to these data and the explanation given above, the following structural formula is proposed for compound 3-acetyl-6-hydroxy-2*H*-chromen-2-one (4).

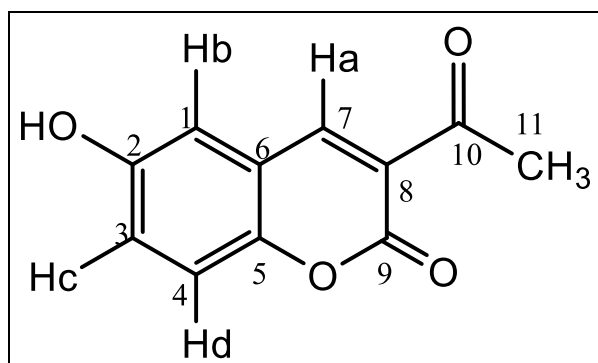


Figure 3.19. Structure of 3-Acetyl-6-hydroxy-2*H*-chromen-2-one (4)

### 3.7.5. Structural elucidation for 3-Acetyl-7-(diethylamino)-2H-chromen-2-one (5)

Solvent of recrystallization: Ethanol; FT-IR ( $\nu_{\max}$ ,  $\text{cm}^{-1}$ ): 3314 (Aromatic C-H), 3117 (Aliphatic C-H), 1708 (C=O, lactone), 1658 (C=O), 1563 (C=C), 1274 (C-O-C);  $^1\text{H-NMR}$  (DMSO- $d_6$ , 300 MHz)  $\delta$ : 1.14 (t, 6H,  $J = 7.0$  Hz), 2.50 (s, 3H, CH<sub>3</sub>), 3.50 (q, 4H,  $J = 7.0$  Hz), 6.58 (d, 1H,  $J = 2.3$  Hz), 6.80 (dd, 1H,  $J = 2.4$  Hz and  $J = 2.5$  Hz), 7.67 (d, 1H,  $J = 9.5$  Hz), 8.49 (s, 1H).

The chemical structure of (5) was identified and can be explained by using its IR and NMR spectra as shown in Appendix 1 (Figures 1.5.1 and 1.5.2).

For the IR spectrum, recorded in KBr pellets, the vibration bands of (3) appear at 3314, 3117, 1708, 1658, 1563, and 1274  $\text{cm}^{-1}$ . The band at 3314 corresponds to the stretching vibrations of the conjugated system. The vibration bands at 3117, 1708, 1658, 1563, and 1274  $\text{cm}^{-1}$  can be related to aliphatic  $\nu(\text{C-H})$ , lactone  $\nu(\text{C=O})$ , carbonyl  $\nu(\text{C=O})$ , aromatic  $\nu(\text{C=C})$ , and lactone  $\nu(\text{C-O-C})$  stretching vibrations, respectively. The NMR spectrum of (5) was recorded in DMSO- $d_6$  using tetramethylsilane (TMS). In the (-N(CH<sub>2</sub>CH<sub>3</sub>)<sub>2</sub>), the two ethyl groups attached to the nitrogen atom have six protons belonging to 2 $\times$ CH<sub>3</sub> in the (-N(CH<sub>2</sub>CH<sub>3</sub>)<sub>2</sub>) at 1.14 ppm in the  $^1\text{H-NMR}$  spectrum. The CH<sub>3</sub> protons are easily distinguishable as a singlet linked to the monocyclic carbonyl group of 3 protons at 2.50 ppm in the  $^1\text{H-NMR}$  spectrum. The 2 quartet protons at 3.50 ppm (q,  $J = 7.0$  Hz) correspond to the 2 $\times$ CH<sub>2</sub> in the (-N(CH<sub>2</sub>CH<sub>3</sub>)<sub>2</sub>). A doublet proton at 6.58 ppm belongs to Hd (d,  $J = 2.3$  Hz) of an aromatic proton, and the doublet of doublet at 6.80 ppm can be linked to Hc (dd,  $J = 2.4, 2.5$  Hz), also an aromatic proton. Another doublet proton at 7.67 ppm corresponds to Hb ( $J = 9.5$  Hz), and the Ha proton in the singlet peak of coumarin ring at 8.49 ppm. With respect to these data and the explanation given above, the following structural formula is proposed for compound 3-acetyl-7-(diethylamino)-2H-chromen-2-one (5).

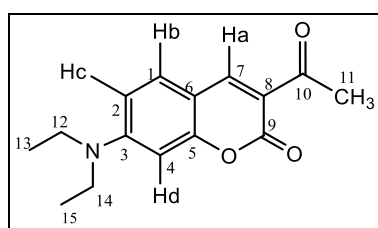


Figure 3.20. Structure of 3-Acetyl-7-(diethylamino)-2H-chromen-2-one (5)

### 3.7.6. Structural elucidation for 3-Acetyl-7-methoxy-2H-chromen-2-one (6)

Solvent of recrystallization: Ethanol; FT-IR ( $\nu_{\max}$ ,  $\text{cm}^{-1}$ ): 3042 (Aromatic C-H), 2980 (Aliphatic C-H), 1738 (C=O, lactone), 1669 (C=O), 1544 (C=C), 1295 (C-O-C);  $^1\text{H-NMR}$  (DMSO- $d_6$ , 300 MHz)  $\delta$ : 2.60 (s, 3H,  $\text{CH}_3$ ), 3.90 (s, 3H,  $\text{OCH}_3$ ), 7.03 (dd, 1H, Ar-H,  $J = 2.4$  Hz,  $J = 2.4$  Hz), 7.08 (d, 1H, Ar-H,  $J = 2.4$  Hz), 7.88 (d, 1H, Ar-H,  $J = 8.7$  Hz), 8.65 (s, 1H, Ar-H).

The chemical structure of (6) was identified and can be explained by using its IR and NMR spectra as shown in Appendix 1 (Figures 1.6.1 and 1.6.2).

For the IR spectrum, recorded in KBr pellets, the vibration bands of (6) appear at 3042, 2980, 1738, 1669, 1544, and 1295  $\text{cm}^{-1}$ . The band at 3042 corresponds to the stretching vibrations of the conjugated system. The vibration bands at 2980, 1738, 1669, 1544, and 1295  $\text{cm}^{-1}$  can be related to aliphatic  $\nu(\text{C-H})$ , lactone  $\nu(\text{C=O})$ , carbonyl  $\nu(\text{C=O})$ , aromatic  $\nu(\text{C=C})$ , and lactone  $\nu(\text{C-O-C})$  stretching vibrations, respectively. The NMR spectrum of (6) was recorded in DMSO- $d_6$  using tetramethylsilane (TMS). The  $\text{CH}_3$  and  $\text{OCH}_3$  protons are easily distinguishable as two singlets linked to the monocyclic carbonyl group and the coumarin, each with 3 protons at 2.60 ppm and 3.90 ppm, respectively, in the  $^1\text{H-NMR}$  spectrum. The spectrum also shows a doublet of doublet proton at 7.03 ppm which belongs to Hd (dd,  $J = 2.4$ , 2.4 Hz) of an aromatic proton, and a doublet at 7.08 ppm can be linked to Hc (d,  $J = 2.4$  Hz), which is also an aromatic proton. Another doublet proton at 7.88 ppm corresponding to Hb ( $J = 8.6$  Hz), and there is the Ha proton in the singlet peak of coumarin ring at 8.65 ppm. With respect to these data and the explanation given above, the following structural formula is proposed for compound 3-acetyl-7-methoxy-2H-chromen-2-one (6).

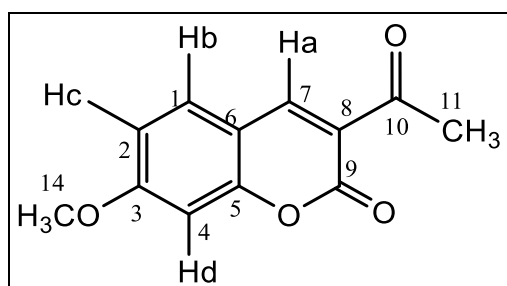


Figure 3.21. Structure of 3-Acetyl-7-methoxy-2H-chromen-2-one (6)

### 3.7.7. Structural elucidation for 3-Acetyl-7-hydroxy-2H-chromen-2-one (7)

Solvent of recrystallization: Ethanol; FT-IR ( $\nu_{\max}$ ,  $\text{cm}^{-1}$ ): 3400 (Phenolic O-H), 3054 (Aromatic C-H), 2926 (Aliphatic C-H), 1700 (C=O, lactone), 1677 (C=O), 1569 (C=C), 1292 (C-O-C);  $^1\text{H-NMR}$  (DMSO- $d_6$ , 300 MHz)  $\delta$ : 2.60 (s, 3H, CH<sub>3</sub>), 6.74 (d, 1H,  $J = 2.0$  Hz), 6.84 (dd, 1H,  $J = 2.2$  Hz and  $J = 2.6$  Hz), 7.79 (d, 1H,  $J = 5.2$  Hz), 8.60 (s, 1H), 11.10 (s, 1H, OH, exchanged with D<sub>2</sub>O). The chemical structure of (7) was identified and can be explained by using its IR and NMR spectra as shown in Appendix 1 (Figures 1.7.1 and 1.7.2).

For the IR spectrum, recorded in KBr pellets, the vibration bands of (7) appear at 3400, 3054, 2926, 1700, 1677, 1569, and 1292  $\text{cm}^{-1}$ . A broad band, characteristic of O-H stretching vibrations is in the range 2865-3400  $\text{cm}^{-1}$  in the spectrum of (7). The band at 3054 corresponds to the stretching vibrations of the conjugated system. The vibration bands at 2926, 1700, 1677, 1569, and 1292  $\text{cm}^{-1}$  can be related to aliphatic  $\nu(\text{C-H})$ , lactone  $\nu(\text{C=O})$ , carbonyl  $\nu(\text{C=O})$ , aromatic  $\nu(\text{C=C})$ , and lactone  $\nu(\text{C-O-C})$  stretching vibrations, respectively. The NMR spectrum of (7) was recorded in DMSO- $d_6$  using tetramethylsilane (TMS). The CH<sub>3</sub> protons are easily distinguishable as a singlet linked to the monocyclic carbonyl group of 3 protons at 2.60 ppm in the  $^1\text{H-NMR}$  spectrum. A doublet proton at 6.74 ppm belongs to Hd (d,  $J = 2.0$  Hz) of an aromatic proton, and the doublet of doublet at 6.84 ppm can be linked to Hc (dd,  $J = 2.2, 2.6$  Hz), also an aromatic proton. Another doublet proton at 7.79 ppm corresponds to Hb ( $J = 5.2$  Hz), and the Ha proton in the singlet peak of coumarin ring at 8.60 ppm. An OH proton, which is expected to have appeared around 11.10 ppm, has been exchanged with D<sub>2</sub>O, and appeared at 3.40 ppm with the D<sub>2</sub>O. With respect to these data and the explanation given above, the following structural formula is proposed for compound 3-acetyl-7-hydroxy-2H-chromen-2-one (7).

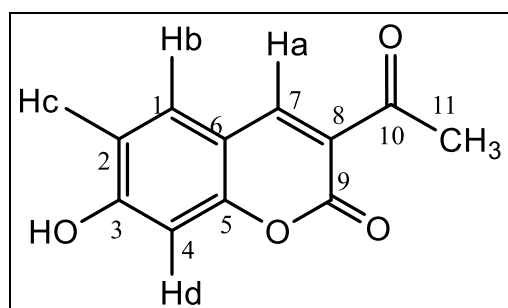


Figure 3.22. Structure of 3-Acetyl-7-hydroxy-2H-chromen-2-one (7)

### 3.7.8. Structural elucidation for 3-Acetyl-8-ethoxy-2*H*-chromen-2-one (8)

Solvent of recrystallization: Ethanol; FT-IR ( $\nu_{\max}$ ,  $\text{cm}^{-1}$ ): 3040 (Aromatic C-H), 2978 (Aliphatic C-H), 1714 (C=O, lactone), 1683 (C=O), 1566 (C=C), 1283 (C-O-C);  $^1\text{H-NMR}$  ( $\text{CDCl}_3$ , 300 MHz)  $\delta$ :  $^1\text{H NMR}$  (300 MHz,  $\text{DMSO-}d_6$ )  $\delta$ : 1.42 (t,  $J = 7.0$  Hz, 3H,  $\text{CH}_3$ ), 2.58 (s, 3H,  $\text{CH}_3$ ), 4.19 (q,  $J = 7.0$  Hz, 2H,  $\text{OCH}_2$ ), 7.29 –7.49 (complex, m, 3H, Ar-H), 8.63 (s, 1H, Ar-H).

The chemical structure of (8) was identified and can be explained by using its IR and NMR spectra as shown in Appendix 1 (Figures 1.8.1 and 1.8.2).

For the IR spectrum, recorded in KBr pellets, the vibration bands of (8) appear at 3098, 2978, 1714, 1683, 1566, and 1283  $\text{cm}^{-1}$ . The band at 3098 corresponds to the stretching vibrations of the conjugated system. The vibration bands at 2978, 1714, 1683, 1566, and 1283  $\text{cm}^{-1}$  can be related to aliphatic  $\nu(\text{C-H})$ , lactone  $\nu(\text{C=O})$ , carbonyl  $\nu(\text{C=O})$ , aromatic  $\nu(\text{C=C})$ , and lactone  $\nu(\text{C-O-C})$  stretching vibrations, respectively. The NMR spectrum of (8) was recorded in  $\text{CDCl}_3$  using tetramethylsilane (TMS). In the ( $-\text{OCH}_2\text{CH}_3$ ), The 3 triplet protons at 1.42 ppm (t,  $J = 7.0$  Hz) correspond to the  $\text{CH}_3$  attached to the  $\text{OCH}_2$  group in the  $^1\text{H-NMR}$  spectrum. The  $\text{CH}_3$  protons are easily distinguishable as a singlet linked to the monocyclic carbonyl group of 3 protons at 2.58 ppm in the  $^1\text{H-NMR}$  spectrum. The 2 quartet protons at 4.19 ppm (q,  $J = 10.4$  Hz) correspond to the  $\text{CH}_2$  in the ( $-\text{OCH}_2\text{CH}_3$ ) group. The complex multi-peak located at 7.29-7.49 ppm represents the 3 protons; Hb, Hc, and Hd of the coumarin ring. The spectrum also shows a Ha proton in the singlet peak of coumarin ring at 8.63 ppm. With respect to these data and the explanation given above, the following structural formula is proposed for compound 3-acetyl-8-ethoxy-2*H*-chromen-2-one (8).

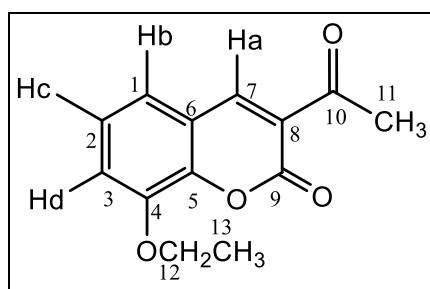


Figure 3.23. Structure of 3-Acetyl-8-ethoxy-2*H*-chromen-2-one (8)

### 3.7.9. Structural elucidation for 3-Acetyl-8-methoxy-2*H*-chromen-2-one (9)

Solvent of recrystallization: Ethanol; FT-IR ( $\nu_{\max}$ ,  $\text{cm}^{-1}$ ): 3077 (Aromatic C-H), 2968 (Aliphatic C-H), 1731 (C=O, lactone), 1678 (C=O), 1600 (C=C), 1283 (C-O-C);  $^1\text{H-NMR}$  (DMSO- $d_6$ , 300 MHz)  $\delta$ : 2.60 (s, 3H, CH<sub>3</sub>), 3.90 (s, 3H, OCH<sub>3</sub>), 7.31-7.49 (complex, m, 3H, Ar-H), 8.60 (s, 1H, Ar-H).

The chemical structure of (9) was identified and can be explained by using its IR and NMR spectra as shown in Appendix 1 (Figures 1.9.1 and 1.9.2).

For the IR spectrum, recorded in KBr pellets, the vibration bands of (9) appear at 3077, 2968, 1731, 1678, 1600, and 1283  $\text{cm}^{-1}$ . The band at 3077 corresponds to the stretching vibrations of the conjugated system. The vibration bands at 2968, 1731, 1678, 1600, and 1280  $\text{cm}^{-1}$  can be related to aliphatic  $\nu(\text{C-H})$ , lactone  $\nu(\text{C=O})$ , carbonyl  $\nu(\text{C=O})$ , aromatic  $\nu(\text{C=C})$ , and lactone  $\nu(\text{C-O-C})$  stretching vibrations, respectively. The NMR spectrum of (9) was recorded in DMSO- $d_6$  using tetramethylsilane (TMS). The CH<sub>3</sub> and OCH<sub>3</sub> protons are easily distinguishable as singlets linked to the monocyclic carbonyl group and the coumarin moiety, respectively, each with 3 protons at 2.60 ppm and 3.90 ppm, respectively, in the  $^1\text{H-NMR}$  spectrum. The complex multi-peak located at 7.31-7.49 ppm represents the 3 protons; Hb, Hc, and Hd of the coumarin ring. The spectrum also shows a Ha proton in the singlet peak of coumarin ring at 8.60 ppm. With respect to these data and the explanation given above, the following structural formula is proposed for compound 3-acetyl-8-methoxy-2*H*-chromen-2-one (9).

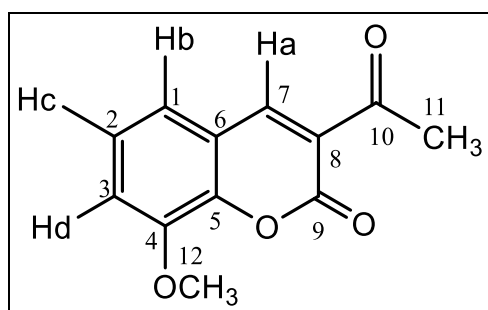


Figure 3.24. Structure of 3-Acetyl-8-methoxy-2*H*-chromen-2-one (9)

### 3.7.10. Structural elucidation for 2-Acetyl-3H-benzo[f]chromen-3-one (10)

Solvent of recrystallization: Ethanol; FT-IR ( $\nu_{\max}$ ,  $\text{cm}^{-1}$ ): 3065 (Aromatic C-H), 2935 (Aliphatic C-H), 1735 (C=O, lactone), 1672 (C=O), 1597 (C=C), 1292 (C-O-C);  $^1\text{H-NMR}$  (DMSO- $d_6$ , 300 MHz)  $\delta$ : 2.70 (s, 3H, CH<sub>3</sub>), 7.45-7.82 (complex, m, 3H, Ar-H), 8.10 (d, 1H, Ar-H,  $J = 8.1$  Hz), 8.34 (d, 1H, Ar-H,  $J = 9.1$  Hz), 8.64 (d, 1H, Ar-H,  $J = 7.4$  Hz), 9.30 (s, 1H, Ar-H).

The chemical structure of (10) was identified and can be explained by using its IR and NMR spectra as shown in Appendix 1 (Figures 1.10.1 and 1.10.2).

For the IR spectrum, recorded in KBr pellets, the vibration bands of (10) appear at 3065, 2935, 1735, 1672, 1597, and 1292  $\text{cm}^{-1}$ . The band at 3065 corresponds to the stretching vibrations of the conjugated system. The vibration bands at 2935, 1735, 1672, 1597, and 1292  $\text{cm}^{-1}$  can be related to aliphatic  $\nu(\text{C-H})$ , lactone  $\nu(\text{C=O})$ , carbonyl  $\nu(\text{C=O})$ , aromatic  $\nu(\text{C=C})$ , and lactone  $\nu(\text{C-O-C})$  stretching vibrations, respectively. The NMR spectrum of (10) was recorded in DMSO- $d_6$  using tetramethylsilane (TMS). The CH<sub>3</sub> protons are easily distinguishable as a singlet linked to the monocyclic carbonyl group of 3 protons at 2.70 ppm in the  $^1\text{H-NMR}$  spectrum. The complex multi-peak located at 7.45-7.82 ppm representing the 3 protons; Hc, Hd, and He, of the coumarin ring. A doublet proton at 8.10 ppm belongs to Hg (d,  $J = 8.1$  Hz) of an aromatic proton, and the another doublet at 8.34 ppm can be linked to Hb (d,  $J = 9.1$  Hz), also an aromatic proton. A third doublet proton at 8.64 ppm corresponding to Hf ( $J = 7.4$  Hz), and the Ha proton in the singlet peak of coumarin ring at 9.30 ppm. With respect to these data and the explanation given above, the following structural formula is proposed for compound 2-acetyl-3H-benzo[f]chromen-3-one (10).

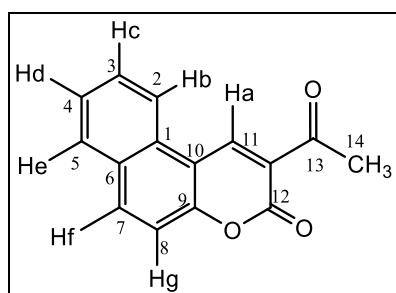


Figure 3.25. Structure of 2-Acetyl-3H-benzo[f]chromen-3-one (10)

### 3.8. The Structural Characterizations and Elucidations of the synthesized Malononitriles

#### 3.8.1. Structural elucidation for 2-(1-(2-Oxo-2*H*-chromen-3-yl) ethylidene)malononitrile (11)

Recrystallization solvent: Ethanol; FT-IR ( $\nu_{\max}$ ,  $\text{cm}^{-1}$ ): 3083 (Aromatic C-H), 2997 (Aliphatic C-H), 2231 ( $\text{C}\equiv\text{N}$ ), 1714 ( $\text{C}=\text{O}$ , lactone), 1561 ( $\text{C}=\text{C}$ ), 1268 ( $\text{C}-\text{O}-\text{C}$ );  $^1\text{H-NMR}$  ( $\text{DMSO-}d_6$ , 300 MHz)  $\delta$ : 2.65 (s, 3H,  $\text{CH}_3$ ), 7.44-7.87 (complex, m, 4H, Ar-H), 8.52 (s, 1H, Ar-H); HRMS ( $m/e$ ):  $[\text{M}+\text{H}]^+$ :  $\text{C}_{14}\text{H}_9\text{N}_2\text{O}_2$ , Calculated: 237.0664; Found: 237.0671.

The chemical structure of (11) was identified and can be explained by using its IR, NMR, and MS spectra as shown in Appendix 2 (Figures 2.1.1-2.1.3).

For the IR spectrum, recorded in KBr pellets, the vibration bands of (11) appear at 3083, 2997, 2231, 1714, 1607, 1561, and 1268  $\text{cm}^{-1}$ . The band at 3083 corresponds to the stretching vibrations of the conjugated system. The vibration bands at 2997, 2231, 1714, 1607, 1561, and 1268  $\text{cm}^{-1}$  can be related to aliphatic  $\nu(\text{C-H})$ , nitrile tensile  $\nu(\text{C}\equiv\text{N})$ , lactone  $\nu(\text{C}=\text{O})$ , aromatic  $\nu(\text{C}=\text{C})$ , and lactone  $\nu(\text{C}-\text{O}-\text{C})$  stretching vibrations, respectively. The NMR spectrum of (11) was recorded in  $\text{DMSO-}d_6$  using tetramethylsilane (TMS). The  $\text{CH}_3$  protons are easily distinguishable as a singlet linked to the monocyclic carbonyl group of 3 protons at 2.65 ppm in the  $^1\text{H-NMR}$  spectrum. The complex multi-peak located at 7.44-7.87 ppm representing the protons; Hb, Hc, Hd, and He, of the coumarin ring. The spectrum also shows a Ha proton in the singlet peak of coumarin ring at 8.52 ppm. According to this, the following structural formula is proposed for Compound 2-(1-(2-Oxo-2*H*-chromen-3-yl) ethylidene) malononitrile (11).

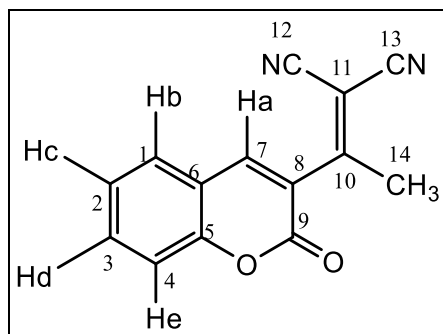


Figure 3.26. Structure of 2-(1-(2-Oxo-2*H*-chromen-3-yl)ethylidene)malononitrile (11)

### 3.8.2. Structural elucidation for 2-(1-(6-bromo-2-oxo-2H-chromen-3-yl)ethylidene) malononitrile (12)

Recrystallization solvent: Ethanol; FT-IR ( $\nu_{\max}$ ,  $\text{cm}^{-1}$ ): 3042 (Aromatic C-H), 2921 (Aliphatic C-H), 2228 ( $\text{C}\equiv\text{N}$ ), 1729 ( $\text{C}=\text{O}$ , lactone), 1546 ( $\text{C}=\text{C}$ ), 1280 ( $\text{C}-\text{O}-\text{C}$ ), 659 ( $\text{C}-\text{Br}$ );  $^1\text{H-NMR}$  ( $\text{DMSO-}d_6$ , 300 MHz)  $\delta$ : 2.58 (s, 3H,  $\text{CH}_3$ ), 7.45 (d,  $J = 8.8$  Hz, 1H, Ar-H), 7.89 (dd,  $J = 8.9, 2.4$  Hz, 1H, Ar-H), 8.22 (d,  $J = 2.4$  Hz, 1H, Ar-H), 8.61 (s, 1H, Ar-H); HRMS ( $m/e$ ):  $[\text{M}+\text{H}]^+$ :  $\text{C}_{14}\text{H}_6\text{N}_2\text{O}_2\text{Br}$ , Calculated: 312.9400; Found: 312.9399.

The chemical structure of (12) was identified and can be explained by using its IR, NMR, and MS spectra as shown in Appendix 2 (Figures 2.2.1-2.2.3).

For the IR spectrum, recorded in KBr pellets, the vibration bands of (12) appear at 3042, 2921, 2228, 1729, 1672, 1546, 1280, and 659  $\text{cm}^{-1}$ . The band at 3042 corresponds to the stretching vibrations of the conjugated system. The vibration bands at 2921, 2228, 1729, 1672, 1548, 1280, and 659  $\text{cm}^{-1}$  can be related to aliphatic  $\nu(\text{C}-\text{H})$ , nitrile tensile  $\nu(\text{C}\equiv\text{N})$ , lactone  $\nu(\text{C}=\text{O})$ , aromatic  $\nu(\text{C}=\text{C})$ , lactone  $\nu(\text{C}-\text{O}-\text{C})$ , and ( $\text{C}-\text{Br}$ ) stretching vibrations, respectively. The NMR spectrum of (12) was recorded in  $\text{DMSO-}d_6$  using tetramethylsilane (TMS). The  $\text{CH}_3$  protons are easily distinguishable as a singlet linked to the monocyclic carbonyl group of 3 protons at 2.58 ppm in the  $^1\text{H-NMR}$  spectrum. A doublet proton at 7.45 ppm corresponds to Hd (d,  $J = 8.9$  Hz) of an aromatic proton, and a doublet of doublet at 7.89 ppm can be linked to Hc (dd,  $J = 8.9, 2.4$  Hz), also an aromatic proton. Another doublet proton at 8.22 ppm corresponds to Hb ( $J = 2.4$  Hz), and the Ha proton in the singlet peak of coumarin ring at 8.61 ppm. With respect to these data and the explanation given above, the following structural formula is proposed for compound 2-(1-(6-bromo-2-oxo-2H-chromen-3-yl)ethylidene)malononitrile (12).

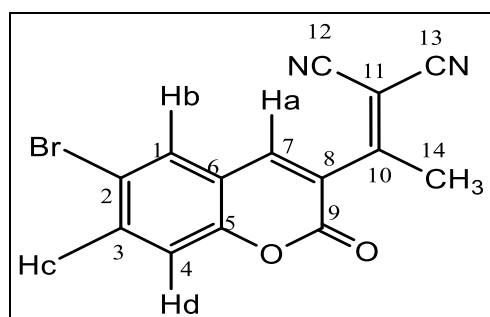


Figure 3.27. Structure of 2-(1-(6-bromo-2-oxo-2H-chromen-3-yl)ethylidene)malononitrile (12)

### 3.8.3. Structural elucidation for 2-(1-(6-chloro-2-oxo-2H-chromen-3-yl)ethylidene)malononitrile (13)

Recrystallization solvent: Ethanol; FT-IR ( $\nu_{\max}$ ,  $\text{cm}^{-1}$ ): 3042 (Aromatic C-H), 2930 (Aliphatic C-H), 2234 ( $\text{C}\equiv\text{N}$ ), 1728 ( $\text{C}=\text{O}$ , lactone), 1552 ( $\text{C}=\text{C}$ ), 1245 ( $\text{C}-\text{O}-\text{C}$ ), 585 ( $\text{C}-\text{Cl}$ );  $^1\text{H-NMR}$  ( $\text{DMSO-}d_6$ , 300 MHz)  $\delta$ : 2.58 (s, 3H,  $\text{CH}_3$ ), 7.51 (d,  $J = 8.9$  Hz, 1H, Ar-H), 7.77 (dd,  $J = 8.9, 2.5$  Hz, 1H, Ar-H), 8.08 (d, 1H,  $J = 2.5$  Hz, Ar-H), 8.61 (s, 1H, Ar-H); HRMS ( $m/e$ ):  $[\text{M}+\text{H}]^+$ :  $\text{C}_{14}\text{H}_6\text{N}_2\text{O}_2\text{Cl}$ , Calculated: 269.0118; Found: 269.0111.

The chemical structure of (13) was identified and can be explained by using its IR, NMR, and MS spectra as shown in Appendix 2 (Figures 2.3.1-2.3.3).

For the IR spectrum, recorded in KBr pellets, the vibration bands of (15) appear at 3042, 2930, 2234, 1728, 1671, 1552, 1245, and 585  $\text{cm}^{-1}$ . The band at 3042 corresponds to the stretching vibrations of the conjugated system. The vibration bands at 2983, 2234, 1728, 1609, 1552, 1245, and 772  $\text{cm}^{-1}$  can be related to aliphatic  $\nu(\text{C}-\text{H})$ , nitrile tensile  $\nu(\text{C}\equiv\text{N})$ , lactone  $\nu(\text{C}=\text{O})$ , aromatic  $\nu(\text{C}=\text{C})$ , lactone  $\nu(\text{C}-\text{O}-\text{C})$ , and ( $\text{C}-\text{Cl}$ ) stretching vibrations, respectively. The NMR spectrum of (13) was recorded in  $\text{DMSO-}d_6$  using tetramethylsilane (TMS). The  $\text{CH}_3$  protons are easily distinguishable as a singlet linked to the monocyclic nitrile carbon of 3 protons at 2.58 ppm in the  $^1\text{H-NMR}$  spectrum. A doublet proton at 7.51 ppm corresponds to Hd (d,  $J = 8.9$  Hz), and a doublet of doublet at 7.77 representing Hc (dd,  $J = 8.9, 2.5$  Hz), both are aromatic protons. There is another doublet at 8.08 ppm which can be linked to Hb (d,  $J = 2.5$  Hz), also an aromatic proton. There is a Ha proton in the singlet peak of coumarin ring at 8.61 ppm. With respect to these data and the explanation given above, the following structural formula is proposed for compound 2-(1-(6-chloro-2-oxo-2H-chromen-3-yl)ethylidene)malononitrile (13).

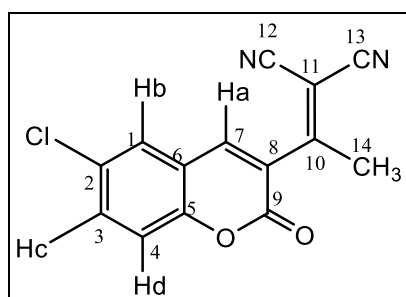


Figure 3.28. Structure of 2-(1-(6-chloro-2-oxo-2H-chromen-3-yl)ethylidene)malononitrile (13)

### 3.8.4. Structure elucidation for 2-(1-(6-hydroxy-2-oxo-2H-chromen-3-yl)ethylidene)malononitrile (14)

Recrystallization solvent: Ethanol; FT-IR ( $\nu_{\max}$ ,  $\text{cm}^{-1}$ ): 3407 (Phenolic O-H), 3041 (Aromatic C-H), 2926 (Aliphatic C-H), 2234 ( $\text{C}\equiv\text{N}$ ), 1723 ( $\text{C}=\text{O}$ , lactone), 1570 ( $\text{C}=\text{C}$ ), 1280 ( $\text{C}-\text{O}-\text{C}$ );  $^1\text{H}$  NMR ( $\text{DMSO}-d_6$ , 300 MHz)  $\delta$ : 2.58 (s, 3H,  $\text{CH}_3$ ), 7.12 (d,  $J = 2.7$  Hz, 1H, Ar-H), 7.19 (d,  $J = 2.9$  Hz, 1H, Ar-H), 7.36 (d,  $J = 8.9$  Hz, 1H, Ar-H), 8.43 (s, 1H, Ar-H), 9.98 (s, 1H, O-H, exchangeable with  $\text{D}_2\text{O}$ );  $^{13}\text{C}$ -APT ( $\text{DMSO}-d_6$ , 75 MHz)  $\delta$ : 23.63 ( $\text{CH}_3$ ), 88.19 ( $\text{C}\equiv\text{N}$ ), 113.31, 113.39, 114.38, 118.25, 118.69, 119.51, 123.62, 123.99, 125.13, 146.36, 148.54, 155.76, 173.98 ( $\text{C}=\text{O}$ ); HRMS ( $m/e$ ):  $[\text{M}+\text{H}]^+$ :  $\text{C}_{14}\text{H}_9\text{N}_2\text{O}_3$ , Calculated: 253.0613; Found: 253.0612.

The chemical structure of (14) was identified and can be explained by using its IR, NMR, and MS spectra as shown in Appendix 2 (Figures 2.4.1-2.4.4).

For the IR spectrum, recorded in KBr pellets, the vibration bands of (14) appear at 3407, 3041, 2926, 2234, 1723, 1628, 1570, and 1280  $\text{cm}^{-1}$ . A broad band, characteristic of O-H stretching vibrations is in the range 3407  $\text{cm}^{-1}$  in the spectrum of (14). The band at 3041 corresponds to the stretching vibrations of the conjugated system. The vibration bands at 2926, 2234, 1723, 1628, 1570, and 1280  $\text{cm}^{-1}$  can be related to aliphatic  $\nu(\text{C}-\text{H})$ , nitrile tensile  $\nu(\text{C}\equiv\text{N})$ , lactone  $\nu(\text{C}=\text{O})$ , aromatic  $\nu(\text{C}=\text{C})$ , and lactone  $\nu(\text{C}-\text{O}-\text{C})$  stretching vibrations, respectively. The NMR spectrum of (14) was recorded in  $\text{DMSO}-d_6$  using tetramethylsilane (TMS). The  $\text{CH}_3$  protons are easily distinguishable as a singlet linked to the monocyclic carbonyl group of 3 protons at 2.58 ppm in the  $^1\text{H}$ -NMR spectrum. Three doublets are located at 7.12 ppm (d,  $J = 2.7$  Hz), 7.19 ppm (d,  $J = 2.9$  Hz), and 7.36 ppm (d,  $J = 8.9$  Hz), representing the 3 protons; Hb, Hc, and Hd, of the coumarin ring. The spectrum also shows a Ha proton in the singlet peak of coumarin ring at 8.43 ppm. An O-H proton, which is exchangeable with  $\text{D}_2\text{O}$ , is observed at 9.98 ppm. In addition, the  $^{13}\text{C}$ -APT spectrum revealed the presence of  $\delta$  23.63 ( $\text{CH}_3$ ),  $\delta$  88.19 ( $\text{C}\equiv\text{N}$ ),  $\delta$  173.98 ( $\text{C}=\text{O}$ ), beside the signals belonging to coumarin and the benzene carbons. With respect to these data and the explanation given above, the following structural formula is proposed for compound 2-(1-(6-hydroxy-2-oxo-2H-chromen-3-yl)ethylidene)malononitrile (14).

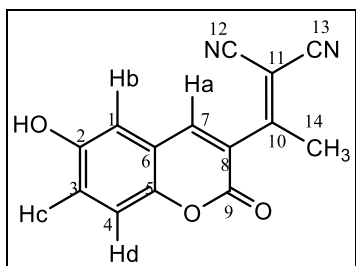


Figure 3.29. Structure of 2-(1-(6-hydroxy-2-oxo-2*H*-chromen-3-yl)ethylidene)malononitrile (14)

### 3.8.5. Structural elucidation for (1-(7-(Diethylamino)-2-oxo-2*H*-chromen-3-yl)ethylidene)malononitrile (15)

Recrystallization solvent: Ethanol; FT-IR ( $\nu_{\max}$ ,  $\text{cm}^{-1}$ ): 3128 (Aromatic C-H), 2973 (Aliphatic C-H), 2228 ( $\text{C}\equiv\text{N}$ ), 1710 ( $\text{C}=\text{O}$ , lactone), 1564 ( $\text{C}=\text{C}$ ), 1267 ( $\text{C}-\text{O}-\text{C}$ );  $^1\text{H-NMR}$  ( $\text{DMSO-}d_6$ , 300 MHz)  $\delta$ : 1.15 (q, 6H,  $J = 6.97$  Hz,  $\text{NCH}_2\text{CH}_3$ ), 2.55 (s, 3H,  $\text{CH}_3$ ), 3.50 (q, 4H,  $J = 6.95$  Hz,  $\text{CH}_2\text{CH}_3$ ), 6.63 (d, 1H,  $J = 2.1$  Hz, Ar-H), 6.83 (dd, 1H,  $J = 2.3$  Hz and  $J = 2.3$  Hz, Ar-H), 7.56 (d, 1H, Ar-H,  $J = 9.0$  Hz, Ar-H), 8.33 (s, 1H, Ar-H). HRMS ( $m/e$ ):  $[\text{M}+\text{H}]^+$ :  $\text{C}_{18}\text{H}_{18}\text{N}_3\text{O}_2$ , Calculated: 308.1399; Found: 308.1392.

The chemical structure of (15) was identified and can be explained by using its IR, NMR, and MS spectra as shown in Appendix 2 (Figures 2.5.1-2.5.3).

For the IR spectrum, recorded in KBr pellets, the vibration bands of (15) appear at 3128, 2973, 2228, 1710, 1609, 1564, and  $1267\text{ cm}^{-1}$ . The band at 3128 corresponds to the stretching vibrations of the conjugated system. The vibration bands at 2973, 2228, 1710, 1609, 1564, and  $1267\text{ cm}^{-1}$  can be related to aliphatic  $\nu(\text{C}-\text{H})$ , nitrile tensile  $\nu(\text{C}\equiv\text{N})$ , lactone  $\nu(\text{C}=\text{O})$ , aromatic  $\nu(\text{C}=\text{C})$ , and lactone  $\nu(\text{C}-\text{O}-\text{C})$  stretching vibrations, respectively. The NMR spectrum of (15) was recorded in  $\text{DMSO-}d_6$  using tetramethylsilane (TMS). In the (-N ( $\text{CH}_2\text{CH}_3$ )<sub>2</sub>), the two ethyl groups attached to the nitrogen atom have six protons (belonging to  $2\times\text{CH}_3$ ) at 1.15 ppm in the  $^1\text{H-NMR}$  spectrum. The  $\text{CH}_3$  protons are easily distinguishable as a singlet linked to the monocyclic carbonyl group of 3 protons at 2.55 ppm in the  $^1\text{H-NMR}$  spectrum. The 2 quartet protons at 3.50 ppm (q,  $J = 7.0$  Hz) correspond to the  $2\times\text{CH}_2$  in the (-N ( $\text{CH}_2\text{CH}_3$ )<sub>2</sub>). A doublet proton at 6.63 ppm belongs to Hd (d,  $J = 2.1$  Hz) of an aromatic proton, and the doublet of doublet at 6.83 ppm can be linked to Hc (dd,  $J = 2.3, 2.3$  Hz), also an aromatic proton.

Another doublet proton at 7.56 ppm corresponds to Hb ( $J = 9.5$  Hz), and the Ha proton in the singlet peak of coumarin ring at 8.33 ppm. The molecular mass spectrum of the compound shows a molecular ion peak (M-H)<sup>+</sup> 308,1392 (m / z) at 100% intensity [Calculated: 308,1399 (m / z)]. According to this, the following structural formula is proposed for Compound (1-(7-(Diethylamino) -2-oxo-2*H*-chromen-3-yl) ethylidene) malononitrile (15).

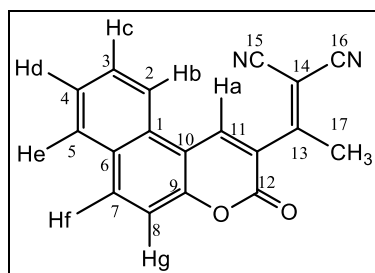


Figure 3.30. Structure of (1-(7-(Diethylamino)-2-oxo-2*H*-chromen-3-yl)ethylidene)malononitrile (15)

### 3.8.6. Structural elucidation for 2-(1-(7-methoxy-2-oxo-2*H*-chromen-3-yl)ethylidene) malononitrile (16)

Recrystallization solvent: Ethanol; FT-IR ( $\nu_{\max}$ ,  $\text{cm}^{-1}$ ): 3095 (Aromatic C-H), 2975 (Aliphatic C-H), 2230 ( $\text{C}\equiv\text{N}$ ), 1715 ( $\text{C}=\text{O}$ , lactone), 1561 ( $\text{C}=\text{C}$ ), 1275 ( $\text{C}-\text{O}-\text{C}$ ); <sup>1</sup>H-NMR (DMSO-*d*<sub>6</sub>, 300 MHz)  $\delta$ : 2.65 (s, 3H, CH<sub>3</sub>), 3.95 (s, 3H, OCH<sub>3</sub>), 7.07 (dd, 1H,  $J = 2.4$  Hz,  $J = 2.4$  Hz, Ar-H), 7.14 (d, 1H,  $J = 2.3$  Hz, Ar-H), 7.78 (d, 1H,  $J = 8.7$  Hz, Ar-H), 8.48 (s, 1H, Ar-H); <sup>13</sup>C-APT (DMSO-*d*<sub>6</sub>, 75 MHz)  $\delta$ : 21.86 (CH<sub>3</sub>), 56.90 (OCH<sub>3</sub>), 82.82 ( $\text{C}\equiv\text{N}$ ), 113.67, 115.78, 122.41, 123.59, 132.01, 143.38, 148.45, 158.23, 161.60, 164.72, 173.70 ( $\text{C}=\text{O}$ ); HRMS ( $m/e$ ): [M+H]<sup>+</sup>: C<sub>15</sub>H<sub>11</sub>N<sub>2</sub>O<sub>3</sub>, Calculated: 267.0770; Found: 267.0775.

The chemical structure of (16) was identified and can be explained by using its IR, NMR, and MS spectra as shown in Appendix 2 (Figures 2.6.1-2.6.4).

For the IR spectrum, recorded in KBr pellets, the vibration bands of (16) appear at 3095, 2975, 2230, 1715, 1561, and 1275  $\text{cm}^{-1}$ . The band at 3095 corresponds to the stretching vibrations of the conjugated system. The vibration bands at 2975, 2230, 1715, 1607, 1561, and 1275  $\text{cm}^{-1}$  can be related to aliphatic  $\nu(\text{C}-\text{H})$ , nitrile tensile  $\nu(\text{C}\equiv\text{N})$ , lactone  $\nu(\text{C}=\text{O})$ , carbonyl  $\nu(\text{C}=\text{O})$ , aromatic  $\nu(\text{C}=\text{C})$ , and lactone  $\nu(\text{C}-\text{O}-\text{C})$  stretching vibrations, respectively. The NMR spectrum of (16) was recorded in DMSO-*d*<sub>6</sub> using

tetramethylsilane (TMS). The CH<sub>3</sub> and OCH<sub>3</sub> protons are easily distinguishable as two singlets linked to the monocyclic carbonyl group and the coumarin, each with 3 protons at 2.65 ppm and 3.95 ppm, respectively, in the <sup>1</sup>H-NMR spectrum. The spectrum also shows a doublet of doublet proton at 7.07 ppm which belongs to Hd (dd, *J* = 2.4, 2.4 Hz) of an aromatic proton, and a doublet at 7.14 ppm can be linked to Hc (d, *J* = 2.3 Hz), which is also an aromatic proton. Another doublet proton at 7.78 ppm corresponding to Hb (*J* = 8.7 Hz), and there is the Ha proton in the singlet peak of coumarin ring at 8.48 ppm. In addition, the <sup>13</sup>C-APT spectrum revealed the presence of δ 21.86 (CH<sub>3</sub>), δ 56.90 (OCH<sub>3</sub>), δ 82.82 (C≡N), δ 173.70 (C=O), beside the signals belonging to coumarin and the benzene carbons. With respect to these data and the explanation given above, the following structural formula is proposed for compound 2-(1-(7-methoxy-2-oxo-2*H*-chromen-3-yl)ethylidene)malononitrile (16).

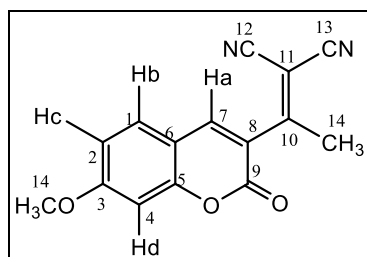


Figure 3.31. Structure of 2-(1-(7-methoxy-2-oxo-2*H*-chromen-3-yl)ethylidene)malononitrile (16)

### 3.8.7. Structural elucidation for 2-(1-(7-hydroxy-2-oxo-2*H*-chromen-3-yl)ethylidene)malononitrile (17)

Recrystallization solvent: Ethanol; FT-IR ( $\nu_{\max}$ , cm<sup>-1</sup>): 3163 (Phenolic O-H), 3040 (Aromatic C-H), 2836 (Aliphatic C-H), 2240 (C≡N), 1689 (C=O, lactone), 1516 (C=C), 1264 (C-O-C); <sup>1</sup>H-NMR (DMSO-*d*<sub>6</sub>, 300 MHz) δ: 2.60 (s, 3H, CH<sub>3</sub>), 6.78 (d, 1H, Ar-H, *J* = 8.0 Hz), 6.90 (dd, 1H, Ar-H, *J* = 8.6 Hz and *J* = 8.6 Hz), 7.68 (d, 1H, Ar-H, *J* = 8.6 Hz), 8.43 (s, 1H, Ar-H), 11.10 (s, 1H, O-H, exchangeable with D<sub>2</sub>O); <sup>13</sup>C-APT (DMSO-*d*<sub>6</sub>, 75 MHz) δ: 23.32 (CH<sub>3</sub>), 86.57 (C≡N), 102.79, 111.28, 113.46, 115.30, 119.52, 132.61, 147.02, 157.37, 158.25, 165.05, 173.73 (C=O); HRMS (*m/e*): [M+H]<sup>+</sup>: C<sub>14</sub>H<sub>7</sub>N<sub>2</sub>O<sub>3</sub>, Calculated: 251.0457; Found: 251.0448.

The chemical structure of (17) was identified and can be explained by using its IR, NMR, and MS spectra as shown in Appendix 2 (Figures 2.7.1-2.7.4).

For the IR spectrum, recorded in KBr pellets, the vibration bands of (17) appear at 3163, 3040, 2836, 2240, 1689, 1584, 1516, and 1264  $\text{cm}^{-1}$ . A broad band, characteristic of O-H stretching vibrations is located at 3163  $\text{cm}^{-1}$  in the spectrum of (17). The band at 3040 corresponds to the stretching vibrations of the conjugated system. The vibration bands at 2836, 2240, 1689, 1516, and 1264  $\text{cm}^{-1}$  can be related to aliphatic  $\nu(\text{C-H})$ , nitrile tensile  $\nu(\text{C}\equiv\text{N})$ , lactone  $\nu(\text{C=O})$ ,  $\nu(\text{C=O})$ , aromatic  $\nu(\text{C=C})$ , and lactone  $\nu(\text{C-O-C})$  stretching vibrations, respectively. The NMR spectrum of (17) was recorded in DMSO- $d_6$  using tetramethylsilane (TMS). The  $\text{CH}_3$  protons are easily distinguishable as a singlet linked to the monocyclic carbonyl group of 3 protons at 2.60 ppm in the  $^1\text{H-NMR}$  spectrum. A doublet proton at 6.78 ppm belongs to Hd (d,  $J = 8.0$  Hz) of an aromatic proton, and the doublet of doublet at 6.90 ppm can be linked to Hc (dd,  $J = 8.6, 8.6$  Hz), also an aromatic proton. Another doublet proton at 7.68 ppm corresponds to Hb ( $J = 8.6$  Hz), and the Ha proton in the singlet peak of coumarin ring at 8.43 ppm. An OH proton which can be observed at 11.10 ppm, and is exchangeable with  $\text{D}_2\text{O}$ , is vividly distinguishable as a singlet. In addition, the  $^{13}\text{C-APT}$  spectrum revealed the presence of  $\delta$  23.32 ( $\text{CH}_3$ ),  $\delta$  86.57 ( $\text{C}\equiv\text{N}$ ),  $\delta$  172.64 ( $\text{C=O}$ ), beside the signals belonging to coumarin and the benzene carbons. With respect to these data and the explanation given above, the following structural formula is proposed for compound 2-(1-(7-hydroxy-2-oxo-2*H*-chromen-3-yl)ethylidene)malononitrile (17).

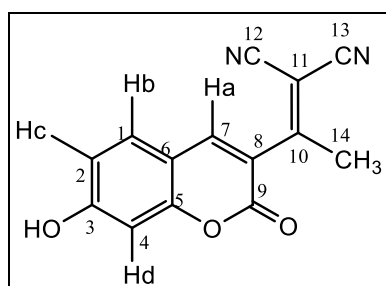


Figure 3.32. Structure of 2-(1-(7-hydroxy-2-oxo-2*H*-chromen-3-yl)ethylidene)malononitrile (17)

### 3.8.8. Structural elucidation of 2-(1-(8-ethoxy-2-oxo-2*H*-chromen-3-yl)ethylidene)malononitrile (18)

Recrystallization solvent: Ethanol; FT-IR ( $\nu_{\text{max}}$ ,  $\text{cm}^{-1}$ ): 3047 (Aromatic C-H), 2941 (Aliphatic C-H), 2232 ( $\text{C}\equiv\text{N}$ ), 1717 ( $\text{C=O}$ , lactone), 1575 ( $\text{C=C}$ ), 1278 ( $\text{C-O-C}$ );  $^1\text{H-NMR}$  ( $\text{CDCl}_3$ , 300 MHz)  $\delta$ : 1.51 (t, 3H,  $J = 7.0$  Hz,  $\text{OCH}_2\text{CH}_3$ ), 2.67 (s, 3H,  $\text{CH}_3$ ), 4.21 (q, 2H,  $J$

= 7.0 Hz,  $\text{OCH}_2\text{CH}_3$ ), 7.17-7.29 (complex, m, 3H, Ar-H), 7.92 (s, 1H, Ar-H);  $^{13}\text{C}$ -APT (DMSO- $d_6$ , 75 MHz)  $\delta$ : 15.09 ( $\text{CH}_3$ ), 23.57 ( $\text{OCH}_2\text{CH}_3$ ), 65.48 ( $\text{OCH}_2$ ), 88.34 ( $\text{C}\equiv\text{N}$ ), 113.27, 113.43, 118.34, 119.64, 121.83, 125.28, 126.59, 144.49, 147.70, 158.06, 173.67 ( $\text{C}=\text{O}$ ); HRMS ( $m/e$ ):  $[\text{M}+\text{H}]^+$ :  $\text{C}_{16}\text{H}_{11}\text{N}_2\text{O}_3$ , Calculated: 279.0770; Found: 279.0775.

The chemical structure of (18) was identified and can be explained by using its IR, NMR, and MS spectra as shown in Appendix 2 (Figures 2.8.1-2.8.4).

For the IR spectrum, recorded in KBr pellets, the vibration bands of (18) appear at 3047, 2941, 2232, 1717, 1606, 1575, and 1278  $\text{cm}^{-1}$ . The band at 3047 corresponds to the stretching vibrations of the conjugated system. The vibration bands at 2941, 2232, 1717, 1575, and 1278  $\text{cm}^{-1}$  can be related to aliphatic  $\nu(\text{C-H})$ , nitrile tensile  $\nu(\text{C}\equiv\text{N})$ , lactone  $\nu(\text{C}=\text{O})$ , aromatic  $\nu(\text{C}=\text{C})$ , and lactone  $\nu(\text{C-O-C})$  stretching vibrations, respectively. The NMR spectrum of (18) was recorded in  $\text{CDCl}_3$  using tetramethylsilane (TMS). In the ( $-\text{OCH}_2\text{CH}_3$ ), The 3 triplet protons at 1.51 ppm (t,  $J = 7.0$  Hz) correspond to the  $\text{CH}_3$  attached to the  $\text{OCH}_2$  group in the  $^1\text{H}$ -NMR spectrum. The  $\text{CH}_3$  protons are easily distinguishable as a singlet linked to the monocyclic carbonyl group of 3 protons at 2.67 ppm in the  $^1\text{H}$ -NMR spectrum. The 2 quartet protons at 4.21 ppm (q,  $J = 7.0$  Hz) correspond to the  $\text{CH}_2$  in the ( $-\text{OCH}_2\text{CH}_3$ ) group. The complex multi-peak located at 7.17-7.29 ppm represents the 3 protons; Hb, Hc, and Hd of the coumarin ring. The spectrum also shows a Ha proton in the singlet peak of coumarin ring at 7.92 ppm. In addition, the  $^{13}\text{C}$ -APT spectrum revealed the presence of  $\delta$  15.09 ( $\text{CH}_3$ ),  $\delta$  23.57 ( $\text{OCH}_2\text{CH}_3$ ),  $\delta$  65.48 ( $\text{OCH}_2$ ),  $\delta$  88.34 ( $\text{C}\equiv\text{N}$ ),  $\delta$  173.67 ( $\text{C}=\text{O}$ ), beside the signals belonging to coumarin and the benzene carbons. With respect to these data and the explanation given above, the following structural formula is proposed for compound 2-(1-(8-ethoxy-2-oxo-2H-chromen-3-yl)ethylidene)malononitrile (18).

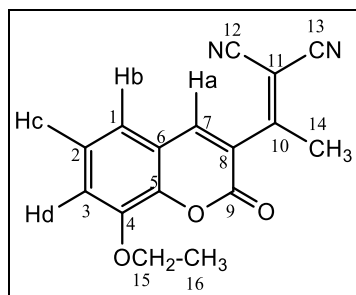


Figure 3.33. Structure of 2-(1-(8-ethoxy-2-oxo-2H-chromen-3-yl)ethylidene)malononitrile (18)

### 3.8.9. Structural elucidation for 2-(1-(8-methoxy-2-oxo-2H-chromen-3-yl)ethylidene) malononitrile (19)

Recrystallization solvent: Ethanol; FT-IR ( $\nu_{\max}$ ,  $\text{cm}^{-1}$ ): 3089 (Aromatic C-H), 2936 (Aliphatic C-H), 2234 ( $\text{C}\equiv\text{N}$ ), 1721 ( $\text{C}=\text{O}$ , lactone), 1583 ( $\text{C}=\text{C}$ ), 1252 ( $\text{C}-\text{O}-\text{C}$ );  $^1\text{H-NMR}$  ( $\text{DMSO-}d_6$ , 300 MHz)  $\delta$ : 2.60 (s, 3H,  $\text{CH}_3$ ), 3.98 (s, 3H,  $\text{OCH}_3$ ), 7.37-7.48 (complex, m, 3H, Ar-H), 8.50 (s, 1H, Ar-H); HRMS ( $m/e$ ):  $[\text{M}+\text{H}]^+$ :  $\text{C}_{15}\text{H}_{11}\text{N}_2\text{O}_3$ , Calculated: 265.0613; Found: 265.0623.

The chemical structure of (19) was identified and can be explained by using its IR, NMR, and MS spectra as shown in Appendix 2 (Figures 2.9.1-2.9.3).

For the IR spectrum, recorded in KBr pellets, the vibration bands of (19) appear at 3089, 2936, 2234, 1721, 1583, and  $1252\text{ cm}^{-1}$ . The band at 3089 corresponds to the stretching vibrations of the conjugated system. The vibration bands at 2936, 2234, 1721, 1583, and  $1252\text{ cm}^{-1}$  can be related to aliphatic  $\nu(\text{C}-\text{H})$ , nitrile tensile  $\nu(\text{C}\equiv\text{N})$ , lactone  $\nu(\text{C}=\text{O})$ , aromatic  $\nu(\text{C}=\text{C})$ , and lactone  $\nu(\text{C}-\text{O}-\text{C})$  stretching vibrations, respectively. The NMR spectrum of (19) was recorded in  $\text{DMSO-}d_6$  using tetramethylsilane (TMS). The  $\text{CH}_3$  and  $\text{OCH}_3$  protons are easily distinguishable as singlets linked to the monocyclic nitrile carbon and the coumarin, each with 3 protons at 2.60 ppm and 3.98 ppm, respectively, in the  $^1\text{H-NMR}$  spectrum. The complex multi-peak located at 7.37-7.48 ppm represents the 3 protons; Hb, Hc, and Hd, of the coumarin ring. The spectrum also shows a Ha proton in the singlet peak of coumarin ring at 8.50 ppm; HRMS ( $m/e$ ):  $[\text{M}+\text{H}]^+$ :  $\text{C}_{15}\text{H}_{10}\text{N}_2\text{O}_3$ , Calculated: 267.0770; Found: 267.0775. With respect to these data and the explanation given above, the following structural formula is proposed for compound 2-(1-(8-methoxy-2-oxo-2H-chromen-3-yl)ethylidene)malononitrile (19).

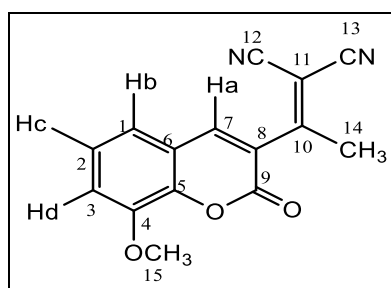


Figure 3.34. Structure of 2-(1-(8-methoxy-2-oxo-2H-chromen-3-yl)ethylidene)malononitrile (19)

### 3.8.10. Structural elucidation for 2-(1-(3-oxo-3*H*-benzo[*f*]chromen-2-yl)ethylidene)malononitrile (20)

Recrystallization solvent: Ethanol; FT-IR ( $\nu_{\max}$ ,  $\text{cm}^{-1}$ ): 3074 (Aromatic C-H), 2936 (Aliphatic C-H), 2225 ( $\text{C}\equiv\text{N}$ ), 1705 ( $\text{C}=\text{O}$ , lactone), 1561 ( $\text{C}=\text{C}$ ), 1273 ( $\text{C}-\text{O}-\text{C}$ );  $^1\text{H}$ -NMR (DMSO- $d_6$ , 300 MHz)  $\delta$ : 2.75 (s, 3H,  $\text{CH}_3$ ), 7.67-7.87 (complex, m, 3H, Ar-H), 8.14 (d, 1H,  $J = 8.1$  Hz, Ar-H), 8.37 (d, 1H,  $J = 9.1$  Hz, Ar-H), 8.62 (d, 1H,  $J = 8.5$  Hz, Ar-H), 9.20 (s, 1H, Ar-H);  $^{13}\text{C}$ -APT (DMSO- $d_6$ , 75 MHz)  $\delta$ : 23.52 ( $\text{CH}_3$ ), 88.25 ( $\text{C}\equiv\text{N}$ ), 96.27, 111.32, 113.43, 113.58, 117.68, 123.43, 127.91, 130.36, 131.28, 137.16, 142.97, 155.78, 158.22, 173.67 ( $\text{C}=\text{O}$ ); HRMS ( $m/e$ ):  $[\text{M}+\text{H}]^+$ :  $\text{C}_{18}\text{H}_{18}\text{N}_3\text{O}_2$ , Calculated: 308.1399; Found: 308.1392.

The chemical structure of (20) was identified and can be explained by using its IR, NMR, and MS spectra as shown in Appendix 2 (Figures 2.10.1-2.10.4).

For the IR spectrum, recorded in KBr pellets, the vibration bands of (20) appear at 3074, 2936, 2225, 1705, 1561, and 1273  $\text{cm}^{-1}$ . The band at 3074 corresponds to the stretching vibrations of the conjugated system. The vibration bands at 2936, 2225, 1705, 1628, 1561, and 1273  $\text{cm}^{-1}$  can be related to aliphatic  $\nu(\text{C}-\text{H})$ , nitrile tensile  $\nu(\text{C}\equiv\text{N})$ , lactone  $\nu(\text{C}=\text{O})$ , aromatic  $\nu(\text{C}=\text{C})$ , and lactone  $\nu(\text{C}-\text{O}-\text{C})$  stretching vibrations, respectively. The NMR spectrum of (20) was recorded in DMSO- $d_6$  using tetramethylsilane (TMS). The  $\text{CH}_3$  protons are easily distinguishable as a singlet linked to the monocyclic carbonyl group of 3 protons at 2.75 ppm in the  $^1\text{H}$ -NMR spectrum. The complex multi-peak located at 7.67-7.87 ppm representing the 3 protons; Hc, Hd, and He, of the coumarin ring. A doublet proton at 8.14 ppm which belongs to Hg (d,  $J = 8.1$  Hz) of an aromatic proton, and the another doublet at 8.37 ppm can be linked to Hb (d,  $J = 9.1$  Hz), also an aromatic proton. A third doublet proton at 8.62 ppm corresponding to Hf ( $J = 8.5$  Hz), and the Ha proton in the singlet peak of coumarin ring at 9.30 ppm. In addition, the  $^{13}\text{C}$ -APT spectrum revealed the presence of  $\delta$  23.52 ( $\text{CH}_3$ ),  $\delta$  88.25 ( $\text{C}\equiv\text{N}$ ), and  $\delta$  173.67 ( $\text{C}=\text{O}$ ), beside the signals for coumarin and the benzene carbons. With respect to these data and the explanation given above, the following structural formula is proposed for compound 2-(1-(3-oxo-3*H*-benzo[*f*]chromen-2-yl)ethylidene)malononitrile (20).

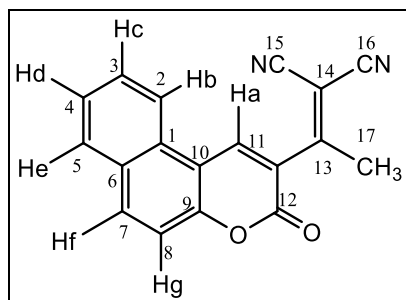


Figure 3.35. Structure of 2-(1-(3-oxo-3*H*-benzo[*f*]chromen-2-yl)ethylidene)malononitrile (20)

### 3.9. The Structural Characterizations and Elucidations of the synthesized 2-Aminothiophenes

#### 3.9.1. Structural elucidation for 2-Amino-4-(2-oxo-2*H*-chromen-3-yl)thiophene-3-carbonitrile (21)

Recrystallization solvent: Ethanol; FT-IR ( $\nu_{\max}$ ,  $\text{cm}^{-1}$ ): 3309, 3361 (Primary amine,  $\text{NH}_2$ ), 3194 (Aromatic C-H), 2211 ( $\text{C}\equiv\text{N}$ ), 1683 ( $\text{C}=\text{O}$ , lactone), 1532 ( $\text{C}=\text{C}$ ), 1249 ( $\text{C}-\text{O}-\text{C}$ ), 578 ( $\text{C}-\text{S}$ );  $^1\text{H}$  NMR ( $\text{DMSO}-d_6/\text{TMS}$ , 300 MHz)  $\delta$ : 6.80 (s, 1H, Ar-H), 7.29 (s, 2H,  $-\text{NH}_2$ ), 7.37-7.78 (complex, m, 4H, Ar-H), 8.20 (s, 1H, Ar-H); HRMS ( $m/e$ ):  $[\text{M}+\text{H}]^+$ :  $\text{C}_{14}\text{H}_9\text{N}_2\text{O}_2\text{S}$ , Calculated: 269.0385; Found: 269.0358.

The chemical structure of (21) was identified and can be explained by using its IR, NMR, and MS spectra as shown in Appendix 3 (Figures 3.1.1-3.1.3).

For the IR spectrum, recorded in KBr pellets, the vibration bands of (21) appear at 3309, 3361, 3194, 2211, 1683, 1639, 1532, 1249, and  $578\text{ cm}^{-1}$ . The band at 3309 and 3361 correspond to the stretching vibrations of the primary amine group. The vibration bands at 3194, 2211, 1683, 1532, 1249, and  $578\text{ cm}^{-1}$  can be related to the aromatic  $\nu(\text{C}-\text{H})$ , nitrile tensile  $\nu(\text{C}\equiv\text{N})$ , lactone  $\nu(\text{C}=\text{O})$ , aromatic  $\nu(\text{C}=\text{C})$ , lactone  $\nu(\text{C}-\text{O}-\text{C})$ , and the carbon-sulfur  $\nu(\text{C}-\text{S})$  stretching vibrations, respectively. The NMR spectrum of (21) was recorded in  $\text{DMSO}-d_6$  using tetramethylsilane (TMS). The singlet proton is easily distinguishable as a singlet linked to the coumarin ring Hf proton at 6.80 ppm in the  $^1\text{H}$ -NMR spectrum. Two singlet protons corresponding to the thiophene ring  $\text{NH}_2$  protons at 7.29 ppm is easily identifiable. The complex multi-peak located at 7.37-7.78 ppm representing the protons; Hb, Hc, Hd, and He, of the coumarin ring. The spectrum also shows a Ha proton in the singlet peak of coumarin ring at 8.20 ppm. With respect to these data and the explanation

given above, the following structural formula is proposed for compound 2-Amino-4-(2-oxo-2*H*-chromen-3-yl)thiophene-3-carbonitrile (21).

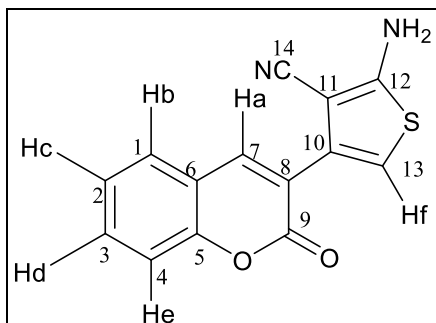


Figure 3.36. Structure of 2-Amino-4-(2-oxo-2*H*-chromen-3-yl)thiophene-3-carbonitrile (21)

### 3.9.2. Structural elucidation for 2-Amino-4-(6-bromo-2-oxo-2*H*-chromen-3-yl)thiophene-3-carbonitrile (22)

Recrystallization solvent: Ethanol; FT-IR ( $\nu_{\max}$ ,  $\text{cm}^{-1}$ ): 3326, 3426 (Primary amine,  $\text{NH}_2$ ), 3206 (Aromatic C-H), 2210 ( $\text{C}\equiv\text{N}$ ), 1742 ( $\text{C}=\text{O}$ , lactone), 1553 ( $\text{C}=\text{C}$ ), 1204 ( $\text{C}-\text{O}-\text{C}$ ), 588 ( $\text{C}-\text{S}$ ), 565 ( $\text{C}-\text{Br}$ );  $^1\text{H}$  NMR ( $\text{DMSO}-d_6$ , 300 MHz)  $\delta$ : 6.82 (s, 1H, Ar-H), 7.32 (s, 2H,  $\text{NH}_2$ ), 7.50 (d,  $J = 8.6$  Hz, 1H, Ar-H), 7.67 (dd,  $J = 8.8, 2.5$  Hz, 1H, Ar-H), 7.91 (d,  $J = 2.5$  Hz, 1H, Ar-H), 8.15 (s, 1H, Ar-H); HRMS ( $m/e$ ):  $[\text{M}+\text{H}]^+$ :  $\text{C}_{14}\text{H}_8\text{N}_2\text{O}_2\text{SBr}$ , Calculated: 346.9490; Found: 346.9489. The chemical structure of (22) was identified and can be explained by using its IR, NMR, and MS spectra as shown in Appendix 3 (Figures 3.2.1-3.2.3).

For the IR spectrum, recorded in KBr pellets, the vibration bands of (22) appear at 3326, 3426, 3206, 2210, 1742, 1676, 1553, 1204, 588, and 565  $\text{cm}^{-1}$ . The band at 3326 and 3426 correspond to the stretching vibrations of the primary amine group. The vibration bands at 3206, 2210, 1742, 1553, 1204, 588, and 565  $\text{cm}^{-1}$  can be related to the aromatic  $\nu(\text{C}-\text{H})$ , nitrile tensile  $\nu(\text{C}\equiv\text{N})$ , lactone  $\nu(\text{C}=\text{O})$ , aromatic  $\nu(\text{C}=\text{C})$ , lactone  $\nu(\text{C}-\text{O}-\text{C})$ , carbon-sulfur  $\nu(\text{C}-\text{S})$ , and the carbon-bromine  $\nu(\text{C}-\text{Br})$ , stretching vibrations, respectively. The NMR spectrum of (22) was recorded in  $\text{DMSO}-d_6$  using tetramethylsilane (TMS). The coumarin He proton is easily distinguishable as a singlet at 6.82 ppm in the  $^1\text{H}$ -NMR spectrum. Two singlet protons corresponding to the thiophene ring  $\text{NH}_2$  protons at 7.32 ppm is easily identifiable. A doublet proton at 7.50 ppm corresponds to Hd (d,  $J = 8.6$  Hz) of an aromatic

proton, and a doublet of doublet at 7.67 ppm can be linked to Hc (dd,  $J = 8.8, 2.5$  Hz), also an aromatic proton. Another doublet proton at 7.91 ppm corresponds to Hb ( $J = 2.5$  Hz), and the Ha proton in the singlet peak of coumarin ring at 8.15 ppm. With respect to these data and the explanation given above, the following structural formula is proposed for compound 2-amino-4-(6-bromo-2-oxo-2H-chromen-3-yl)thiophene-3-carbonitrile (22).

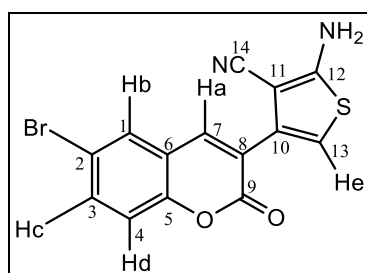


Figure 3.37. Structure of 2-Amino-4-(6-bromo-2-oxo-2H-chromen-3-yl)thiophene-3-carbonitrile (22)

### 3.9.3. Structural elucidation for 2-Amino-4-(6-chloro-2-oxo-2H-chromen-3-yl)thiophene-3-carbonitrile (23)

Recrystallization solvent: Ethanol; FT-IR ( $\nu_{\max}$ ,  $\text{cm}^{-1}$ ): 3326, 3425 (Primary amine,  $\text{NH}_2$ ), 3111 (Aromatic C-H), 2210 ( $\text{C}\equiv\text{N}$ ), 1742 ( $\text{C}=\text{O}$ , lactone), 1566 ( $\text{C}=\text{C}$ ), 1246 ( $\text{C}-\text{O}-\text{C}$ ), 585 ( $\text{C}-\text{S}$ ), 535 ( $\text{C}-\text{Cl}$ );  $^1\text{H}$  NMR ( $\text{DMSO}-d_6$ , 300 MHz)  $\delta$ : 6.82 (s, 1H, Ar-H), 7.32 (s, 2H,  $-\text{NH}_2$ ), 7.49 (d, 1H,  $J = 8.8$  Hz, Ar-H), 7.67 (dd, 1H,  $J = 8.8, 2.5$  Hz, Ar-H), 7.91 (d, 1H,  $J = 2.5$  Hz, Ar-H), 8.15 (s, 1H, Ar-H); HRMS ( $m/e$ ):  $[\text{M}+\text{H}]^+$ :  $\text{C}_{14}\text{H}_8\text{N}_2\text{O}_2\text{SCl}$ , Calculated: 302.9995; Found: 303.0010.

The chemical structure of (23) was identified and can be explained by using its IR, NMR, and MS spectra as shown in Appendix 3 (Figures 3.3.1-3.3.3).

For the IR spectrum, recorded in KBr pellets, the vibration bands of (23) appear at 3326, 3425, 3111, 2210, 1742, 1566, 1246, 585, and 535  $\text{cm}^{-1}$ . The band at 3326 and 3425 correspond to the stretching vibrations of the primary amine group. The vibration bands at 3111, 2210, 1742, 1633, 1566, 1246, 585, and 535  $\text{cm}^{-1}$  can be related to the aromatic  $\nu(\text{C}-\text{H})$ , nitrile tensile  $\nu(\text{C}\equiv\text{N})$ , lactone  $\nu(\text{C}=\text{O})$ , carbonyl  $\nu(\text{C}=\text{O})$ , aromatic  $\nu(\text{C}=\text{C})$ , lactone  $\nu(\text{C}-\text{O}-\text{C})$ , carbon-sulfur  $\nu(\text{C}-\text{S})$ , and the carbon-bromine  $\nu(\text{C}-\text{Cl})$ , stretching vibrations, respectively. The NMR spectrum of (23) was recorded in  $\text{DMSO}-d_6$  using tetramethylsilane (TMS). The singlet proton He belonging to the thiophene is easily

distinguishable at 6.82 ppm in the  $^1\text{H-NMR}$  spectrum. Two singlet protons corresponding to the thiophene ring  $\text{NH}_2$  protons at 7.32 ppm is easily identifiable. A doublet proton at 7.49 ppm corresponds to Hd (d,  $J = 8.8$  Hz, 1H), and a doublet of doublet at 7.67 representing Hc (dd,  $J = 8.8, 2.5$  Hz), both are aromatic protons. There is another doublet at 7.91 ppm which can be linked to Hb (d,  $J = 2.5$  Hz), also an aromatic proton. There is a Ha proton in the singlet peak of coumarin ring at 8.15 ppm. HRMS ( $m/e$ ):  $[\text{M}+\text{H}]^+$ :  $\text{C}_{14}\text{H}_8\text{N}_2\text{O}_2\text{SCl}$ , Calculated: 302.9995; Found: 303.0010. With respect to these data and the explanation given above, the following structural formula is proposed for the compound 2-Amino-4-(6-chloro-2-oxo-2H-chromen-3-yl)thiophene-3-carbonitrile (23).

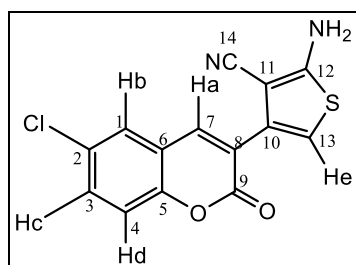


Figure 3.38. Structure of 2-Amino-4-(6-chloro-2-oxo-2H-chromen-3-yl)thiophene-3-carbonitrile (23)

#### 3.9.4. Structural elucidation for 2-Amino-4-(6-hydroxy-2-oxo-2H-chromen-3-yl)thiophene-3-carbonitrile (24)

Recrystallization solvent: Ethanol; FT-IR ( $\nu_{\text{max}}$ ,  $\text{cm}^{-1}$ ): 3338, 3458 (Primary amine,  $\text{NH}_2$ ), 3215 (Phenolic O-H), 3157 (Aromatic C-H), 2197 ( $\text{C}\equiv\text{N}$ ), 1684 ( $\text{C}=\text{O}$ , lactone), 1568 ( $\text{C}=\text{C}$ ), 1284 ( $\text{C}-\text{O}-\text{C}$ ), 575 ( $\text{C}-\text{S}$ );  $^1\text{H NMR}$  ( $\text{DMSO}-d_6$ , 300 MHz  $\delta$ : 6.78(s, 1H, Ar-H), 7.04-7.06 (complex, m, 3H, Ar-H), 7.27 (s, 2H,  $-\text{NH}_2$ ), 8.10 (s, 1H, Ar-H), 9.79 (s, 1H, O-H, exchangeable with  $\text{D}_2\text{O}$ );  $^{13}\text{C-APT}$  ( $\text{DMSO}-d_6$ , 75 MHz)  $\delta$ : 84.91 ( $\text{C}\equiv\text{N}$ ), 110.70, 113.64, 117.24, 118.13, 120.54, 121.30, 122.61, 133.08, 141.82, 147.57, 155.39, 160.45, 166.88 ( $\text{C}=\text{O}$ ); HRMS ( $m/e$ ):  $[\text{M}+\text{H}]^+$ :  $\text{C}_{14}\text{H}_8\text{N}_2\text{O}_3\text{S}$ , Calculated: 285.0334; Found: 285.0340.

The chemical structure of (24) was identified and can be explained by using its IR, NMR, and MS spectra as shown in Appendix 3 (Figures 3.4.1-3.4.4).

For the IR spectrum, recorded in KBr pellets, the vibration bands of (24) appear at 3338, 3458, 3215, 3157, 2197, 1684, 1568, 1284, and  $575\text{cm}^{-1}$ . The band at 3338 and 3458

correspond to the stretching vibrations of the primary amine group. A broad band, characteristic of O-H stretching vibrations is located at  $3215\text{ cm}^{-1}$  in the spectrum of (24). The vibration bands at  $3157$ ,  $2197$ ,  $1684$ ,  $1630$ ,  $1568$ ,  $1284$ , and  $575\text{ cm}^{-1}$  can be related to the aromatic  $\nu(\text{C-H})$ , aliphatic  $\nu(\text{C-H})$ , nitrile tensile  $\nu(\text{C}\equiv\text{N})$ , lactone  $\nu(\text{C}=\text{O})$ , aromatic  $\nu(\text{C}=\text{C})$ , lactone  $\nu(\text{C-O-C})$ , and carbon-sulfur  $\nu(\text{C-S})$ , stretching vibrations, respectively. The NMR spectrum of (24) was recorded in  $\text{DMSO-}d_6$  using tetramethylsilane (TMS). The singlet proton He belonging to the thiophene is easily distinguishable at  $6.78\text{ ppm}$  in the  $^1\text{H-NMR}$  spectrum. The complex multi-peak located at  $7.04\text{--}7.06\text{ ppm}$  representing the 3 protons; Hb, Hc, and Hd, of the coumarin ring. Two singlet protons corresponding to the thiophene ring  $\text{NH}_2$  protons at  $7.27\text{ ppm}$  is easily identifiable. The spectrum also shows a Ha proton in the singlet peak of coumarin ring at  $8.10\text{ ppm}$ . An O-H proton, which is exchangeable with  $\text{D}_2\text{O}$ , is observed at  $9.79\text{ ppm}$ . Moreover, the  $^{13}\text{C-APT}$  spectrum showed the presence of  $\delta\ 84.91(\text{C}\equiv\text{N})$  and  $\delta\ 166.88(\text{C}=\text{O})$  beside the signals for coumarin, benzene and thiophene carbons. HRMS ( $m/e$ ):  $[\text{M}+\text{H}]^+$ :  $\text{C}_{14}\text{H}_8\text{N}_2\text{O}_3\text{S}$ , Calculated:  $285.0334$ ; Found:  $285.0340$ . With respect to these data and the explanation given above, the following structural formula is proposed for the compound 2-Amino-4-(6-hydroxy-2-oxo-2*H*-chromen-3-yl)thiophene-3-carbonitrile (24).

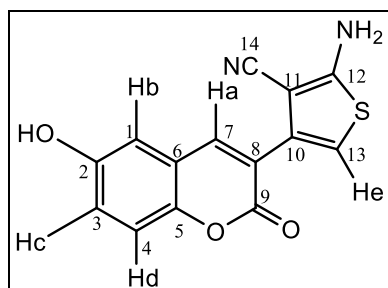


Figure 3.39. Structure of 2-Amino-4-(6-hydroxy-2-oxo-2*H*-chromen-3-yl)thiophene-3-carbonitrile (24)

### 3.9.5. Structural elucidation for 2-Amino-4-(7-(diethylamino)-2-oxo-2*H*-chromen-3-yl) thiophene-3-carbonitrile (25)

Recrystallization solvent: Ethanol; FT-IR ( $\nu_{\text{max}}$ ,  $\text{cm}^{-1}$ ):  $3319$ ,  $3407$  (Primary amine,  $\text{NH}_2$ ),  $3225$  (Aromatic C-H),  $2197$  ( $\text{C}\equiv\text{N}$ ),  $1702$  ( $\text{C}=\text{O}$ , lactone),  $1512$  ( $\text{C}=\text{C}$ ),  $1295$  ( $\text{C-O-C}$ ),  $588$  ( $\text{C-S}$ );  $^1\text{H NMR}$  ( $\text{DMSO-}d_6$ ,  $300\text{ MHz}$ )  $\delta$ :  $1.10$  (t,  $6\text{H}$ ,  $J = 7.58\text{ Hz}$ ),  $3.45$  (q,  $4\text{H}$ ,  $J = 6.9\text{ Hz}$ ),  $6.56$  (d,  $1\text{H}$ ,  $J = 2.2\text{ Hz}$ , Ar-H),  $6.66$  (s,  $1\text{H}$ , Ar-H),  $6.73$  (dd,  $1\text{H}$ ,  $J = 2.4, 2.4\text{ Hz}$ , Ar-

H), 7.20 (s, 2H, NH<sub>2</sub>), 7.48 (d, 1H,  $J = 8.9$  Hz, Ar-H), 7.98 (s, 1H, Ar-H); HRMS ( $m/e$ ): [M+H]<sup>+</sup>: C<sub>18</sub>H<sub>18</sub>N<sub>3</sub>O<sub>2</sub>S, Calculated: 340.1120; Found: 340.1105.

The chemical structure of (25) was identified and can be explained by using its IR, NMR, and MS spectra as shown in Appendix 3 (Figures 3.5.1-3.5.3).

For the IR spectrum, recorded in KBr pellets, the vibration bands of (25) appear at 3319, 3407, 3225, 2197, 1702, 1612, 1512, 1295, and 588 cm<sup>-1</sup>. The band at 3319 and 3407 correspond to the stretching vibrations of the primary amine group. The vibration bands at 3225, 2197, 1702, 1512, 1295, and 588 cm<sup>-1</sup> can be related to the aromatic  $\nu(\text{C-H})$ , nitrile tensile  $\nu(\text{C}\equiv\text{N})$ , lactone  $\nu(\text{C=O})$ , aromatic  $\nu(\text{C=C})$ , lactone  $\nu(\text{C-O-C})$ , and the carbon-sulfur  $\nu(\text{C-S})$ , stretching vibrations, respectively. The NMR spectrum of (25) was recorded in DMSO-*d*<sub>6</sub> using tetramethylsilane (TMS). In the (-N (CH<sub>2</sub>CH<sub>3</sub>)<sub>2</sub>), the two ethyl groups attached to the nitrogen atom have six protons (belonging to 2×CH<sub>3</sub>) at 1.10 ppm (t, 6H,  $J = 7.58$  Hz) in the <sup>1</sup>H-NMR spectrum. The 2 quartet protons at 3.45 ppm (q, 4H,  $J = 6.9$  Hz) correspond to the 2×CH<sub>2</sub> in the (-N (CH<sub>2</sub>CH<sub>3</sub>)<sub>2</sub>). A doublet proton at 6.56 ppm belongs to Hd (d,  $J = 2.2$  Hz) of an aromatic proton, and a singlet proton located at 6.66 ppm, representing the thiophene proton He. The doublet of doublet at 6.73 ppm can be linked to Hc (dd,  $J = 2.4, 2.4$  Hz), also an aromatic proton. Two singlet protons corresponding to the thiophene ring NH<sub>2</sub> protons at 7.20 ppm is easily identifiable. Another doublet proton at 7.48 ppm corresponds to Hb (d, 1H,  $J = 8.9$  Hz), and the Ha proton in the singlet peak of coumarin ring at 7.98 ppm. With respect to these data and the explanation given above, the following structural formula is proposed for the compound 2-amino-4-(7-(diethylamino)-2-oxo-2H-chromen-3-yl) thiophene-3-carbonitrile (25).

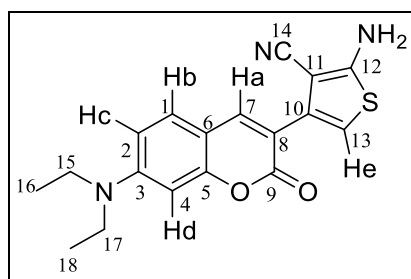


Figure 3.40. Structure of 2-Amino-4-(7-(diethylamino)-2-oxo-2H-chromen-3-yl) thiophene-3-carbonitrile (25)

### 3.9.6. Structural elucidation for 2-Amino-4-(7-methoxy-2-oxo-2H-chromen-3-yl)thiophene-3-carbonitrile (26)

Recrystallization solvent: Ethanol; FT-IR ( $\nu_{\max}$ ,  $\text{cm}^{-1}$ ): 3201, 3298 (Primary amine,  $\text{NH}_2$ ), 3136 (Aromatic C-H), 3080 (Aliphatic C-H), 2213 ( $\text{C}\equiv\text{N}$ ), 1715 ( $\text{C}=\text{O}$ , lactone), 1566 ( $\text{C}=\text{C}$ ), 1299 (C-O-C), 588 (C-S);  $^1\text{H}$  NMR (DMSO- $d_6$ / TMS, 300 MHz):  $\delta$ : 3.90 (s, 3H:  $\text{OCH}_3$ ), 6.75 (s, 1H, Ar-H), 7.00 (dd, 1H,  $J = 2.4, 2.4$  Hz, Ar-H), 7.05 (d, 1H,  $J = 2.3$  Hz, Ar-H), 7.25 (s, 2H,  $-\text{NH}_2$ ), 7.69 (d, 1H,  $J = 8.7$  Hz, Ar-H), 8.14 (s, 1H, Ar-H);  $^{13}\text{C}$ -APT (DMSO- $d_6$ , 75 MHz)  $\delta$ : 56.83 ( $\text{OCH}_3$ ), 84.90 ( $\text{C}\equiv\text{N}$ ), 101.51, 110.08, 114.00, 117.29, 119.03, 131.02, 133.12, 142.03, 156.15, 160.49, 164.12, 166.86 ( $\text{C}=\text{O}$ ); HRMS ( $m/e$ ) :  $[\text{M}+\text{H}]^+$ :  $\text{C}_{15}\text{H}_{11}\text{N}_2\text{O}_3\text{S}$ , Calculated: 299.0490; Found: 299.0481.

The chemical structure of (26) was identified and can be explained by using its IR, NMR, and MS spectra as shown in Appendix 3 (Figures 3.6.1-3.6.4).

For the IR spectrum, recorded in KBr pellets, the vibration bands of (26) appear at 3201, 3298, 3136, 3080, 2213, 1715, 1606, 1566, 1299, and  $588\text{cm}^{-1}$ . The band at 3201 and 3298 correspond to the stretching vibrations of the primary amine group. The vibration bands at 3136, 3080, 2213, 1715, 1555, 1299, and  $588\text{cm}^{-1}$  can be related to the aromatic  $\nu(\text{C-H})$ , aromatic (C-H), nitrile tensile  $\nu(\text{C}\equiv\text{N})$ , lactone  $\nu(\text{C}=\text{O})$ , aromatic  $\nu(\text{C}=\text{C})$ , lactone  $\nu(\text{C-O-C})$ , and carbon-sulfur  $\nu(\text{C-S})$ , stretching vibrations, respectively. The NMR spectrum of (26) was recorded in DMSO- $d_6$  using tetramethylsilane (TMS). The  $\text{OCH}_3$  protons are easily distinguishable as singlets linked to the coumarin ring with 3 protons 3.90 ppm in the  $^1\text{H}$ -NMR spectrum. The singlet proton He belonging to the thiophene is easily distinguishable at 6.75 ppm in the  $^1\text{H}$ -NMR spectrum. The spectrum also shows a doublet of doublet proton at 7.00 ppm which belongs to Hc (dd, 1H,  $J = 2.4$  Hz,  $J = 2.4$  Hz) of an aromatic proton, and a doublet at 7.05 ppm can be linked to Hd (d,  $J = 2.3$  Hz), which is also an aromatic proton. Two singlet protons corresponding to the thiophene ring  $\text{NH}_2$  protons at 7.25 ppm is easily identifiable. Another doublet proton at 7.69 ppm corresponding to Hb ( $J = 8.7$  Hz), and there is the Ha proton in the singlet peak of coumarin ring at 8.14 ppm. Moreover, the  $^{13}\text{C}$ -APT spectrum showed the presence of  $\delta$  56.83 ( $\text{OCH}_3$ ),  $\delta$  84.90 ( $\text{C}\equiv\text{N}$ ), and  $\delta$  166.86 ( $\text{C}=\text{O}$ ) beside the signals for coumarin, benzene and thiophene carbons. HRMS ( $m/e$ ):  $[\text{M}+\text{H}]^+$ :  $\text{C}_{15}\text{H}_{11}\text{N}_2\text{O}_3\text{S}$ , Calculated: 299.0490; Found: 299.0481. With respect to these data and the explanation given above,

the following structural formula is proposed for the compound 2-amino-4-(7-methoxy-2-oxo-2*H*-chromen-3-yl)thiophene-3-carbonitrile (26).

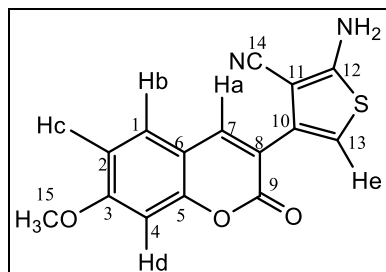


Figure 3.41. Structure of 2-Amino-4-(7-methoxy-2-oxo-2*H*-chromen-3-yl)thiophene-3-carbonitrile (26)

### 3.9.7. Structural elucidation for 2-Amino-4-(7-hydroxy-2-oxo-2*H*-chromen-3-yl)thiophene-3-carbonitrile (27)

Recrystallization solvent: Ethanol; FT-IR ( $\nu_{\max}$ ,  $\text{cm}^{-1}$ ): 3342, 3435 (Primary amine,  $\text{NH}_2$ ), 3309 (Phenolic O-H), 3133 (Aromatic C-H), 2202 ( $\text{C}\equiv\text{N}$ ), 1706 ( $\text{C}=\text{O}$ , lactone), 1598 ( $\text{C}=\text{C}$ ), 1294 (C-O-C), 551 (C-S);  $^1\text{H}$  NMR (DMSO- $d_6$ / TMS, 300 MHz)  $\delta$ : 6.71 (s, 1H, Ar-H), 6.76 (d, 1H,  $J = 2.3$  Hz, Ar-H), 6.83 (dd, 1H,  $J = 2.2, 2.2$  Hz, Ar-H), 7.24 (s, 2H,  $\text{NH}_2$ ), 7.58 (d, 1H,  $J = 8.6$  Hz, Ar-H), 8.08 (s, 1H, Ar-H), 10.70 (s, 1H, O-H, exchangeable with  $\text{D}_2\text{O}$ ); HRMS ( $m/e$ ):  $^{13}\text{C}$ -APT (DMSO- $d_6$ , 75 MHz)  $\delta$ : 84.99 ( $\text{C}\equiv\text{N}$ ), 102.97, 109.78, 112.39, 114.74, 117.33, 118.03, 131.31, 133.31, 142.33, 156.23, 160.62, 162.98, 166.80 ( $\text{C}=\text{O}$ ); HRMS ( $m/e$ ):  $[\text{M}+\text{H}]^+$ :  $\text{C}_{14}\text{H}_9\text{N}_2\text{O}_3\text{S}$ , Calculated: 285.0334; Found: 285.0318.

The chemical structure of (27) was identified and can be explained by using its IR, NMR, and MS spectra as shown in Appendix 3 (Figures 3.7.1-3.7.4).

For the IR spectrum, recorded in KBr pellets, the vibration bands of (27) appear at 3342, 3435, 3309, 3133, 2202, 1706, 1598, 1294, and  $551\text{cm}^{-1}$ . The band at 3342 and 3435 correspond to the stretching vibrations of the primary amine group. A broad band, characteristic of O-H stretching vibrations is located at  $3309\text{cm}^{-1}$  in the spectrum of (26). The vibration bands at 3133, 2202, 1706, 1620, 1598, 1294, 585, and  $551\text{cm}^{-1}$  can be related to the aromatic  $\nu(\text{C}-\text{H})$ , nitrile tensile  $\nu(\text{C}\equiv\text{N})$ , lactone  $\nu(\text{C}=\text{O})$ , aromatic  $\nu(\text{C}=\text{C})$ , lactone  $\nu(\text{C}-\text{O}-\text{C})$ , and carbon-sulfur  $\nu(\text{C}-\text{S})$ , stretching vibrations, respectively. The NMR spectrum of (27) was recorded in DMSO- $d_6$  using tetramethylsilane (TMS). The singlet

proton He belonging to the thiophene is easily distinguishable at 6.71 ppm in the  $^1\text{H-NMR}$  spectrum. A doublet proton at 6.76 ppm belongs to Hd (d, 1H,  $J = 2.3$  Hz) of an aromatic proton, and the doublet of doublet at 6.83 ppm can be linked to Hc (dd, 1H,  $J = 2.2$  Hz and  $J = 2.2$  Hz), also an aromatic proton. Two singlet protons corresponding to the thiophene ring  $\text{NH}_2$  protons at 7.24 ppm is easily identifiable. Another doublet proton at 7.58 ppm corresponds to Hb (d, 1H,  $J = 8.6$  Hz), and the Ha proton in the singlet peak of coumarin ring at 8.08 ppm. An OH proton which can be observed at 10.70 ppm, and is exchangeable with  $\text{D}_2\text{O}$ , is vividly distinguishable as a singlet. Moreover, the  $^{13}\text{C-NMR}$  spectrum showed the presence of  $\delta$  84.99 ( $\text{C}\equiv\text{N}$ ) and  $\delta$  166.80 ( $\text{C}=\text{O}$ ) beside the signals for coumarin, benzene and thiophene carbons. HRMS ( $m/e$ ):  $[\text{M}+\text{H}]^+$ :  $\text{C}_{14}\text{H}_9\text{N}_2\text{O}_3\text{S}$ , Calculated: 285.0334; Found: 285.0318. With respect to these data and the explanation given above, the following structural formula is proposed for the compound 2-amino-4-(7-hydroxy-2-oxo-2H-chromen-3-yl)thiophene-3-carbonitrile (27).

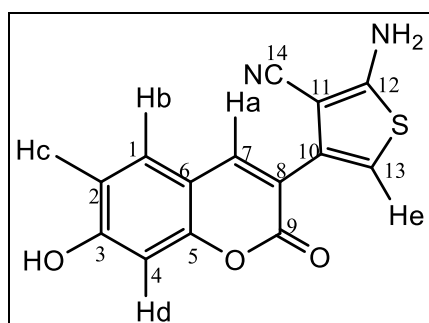


Figure 3.42. Structure of 2-Amino-4-(7-hydroxy-2-oxo-2H-chromen-3-yl)thiophene-3-carbonitrile (27)

### 3.9.8. Structural elucidation for 2-Amino-4-(8-ethoxy-2-oxo-2H-chromen-3-yl)thiophene-3-carbonitrile (28)

Recrystallization solvent: Ethanol; FT-IR ( $\nu_{\text{max}}$ ,  $\text{cm}^{-1}$ ): 3328, 3424 (Primary amine,  $\text{NH}_2$ ), 3138 (Aromatic C-H), 2928 (Aliphatic C-H), 2201 ( $\text{C}\equiv\text{N}$ ), 1717 ( $\text{C}=\text{O}$ , lactone), 1574 ( $\text{C}=\text{C}$ ), 1277 ( $\text{C}-\text{O}-\text{C}$ ), 585 ( $\text{C}-\text{S}$ );  $^1\text{H NMR}$  ( $\text{DMSO-}d_6$ , 300 MHz)  $\delta$ : 1.42 (t, 3H,  $J = 7.0$  Hz,  $\text{OCH}_2\text{CH}_3$ ), 4.19 (q, , 2H,  $J = 6.9$  Hz,  $\text{OCH}_2\text{CH}_3$ ), 6.82 (s, 1H, Ar-H), 7.30 (s, 5H: 3H = Ar-H, 2H =  $\text{NH}_2$ ), 8.17 (s, 1H, Ar-H);  $^{13}\text{C-APT}$  ( $\text{DMSO-}d_6$ , 75 MHz)  $\delta$ : 15.15 ( $\text{OCH}_2\text{CH}_3$ ), 65.29 ( $\text{OCH}_2$ ), 84.73 ( $\text{C}\equiv\text{N}$ ), 110.93, 116.32, 117.24, 120.65, 120.95, 122.64, 125.99, 132.72, 141.93, 143.51, 146.92, 160.02, 166.98 ( $\text{C}=\text{O}$ ); HRMS ( $m/e$ ):  $[\text{M}+\text{H}]^+$ :  $\text{C}_{16}\text{H}_{13}\text{N}_2\text{O}_3\text{S}$ , Calculated: 313.0647; Found: 313.0638.

The chemical structure of (28) was identified and can be explained by using its IR, NMR, and MS spectra as shown in Appendix 3 (Figures 3.8.1-3.8.4).

For the IR spectrum, recorded in KBr pellets, the vibration bands of (28) appear at 3328, 3424, 3138, 2928, 2201, 1717, 1574, 1277, and 585 $\text{cm}^{-1}$ . The band at 3328 and 3424 correspond to the stretching vibrations of the primary amine group. The vibration bands at 3138, 2928, 2201, 1717, 1617, 1574, 1277, and 585 $\text{cm}^{-1}$  can be related to the aromatic  $\nu(\text{C-H})$ , aromatic  $\nu(\text{C-H})$ , nitrile tensile  $\nu(\text{C}\equiv\text{N})$ , lactone  $\nu(\text{C}=\text{O})$ , aromatic  $\nu(\text{C}=\text{C})$ , lactone  $\nu(\text{C-O-C})$ , and carbon-sulfur  $\nu(\text{C-S})$ , stretching vibrations, respectively. The NMR spectrum of (28) was recorded in DMSO- $d_6$  using tetramethylsilane (TMS). In the (-OCH<sub>2</sub>CH<sub>3</sub>), The 3 triplet CH<sub>3</sub> protons at 1.41 ppm (t,  $J = 6.9$  Hz) attached to the OCH<sub>2</sub> group in the <sup>1</sup>H-NMR spectrum. The 2 quartet protons at 4.19 ppm (q,  $J = 6.9$  Hz) correspond to the CH<sub>2</sub> in the (-OCH<sub>2</sub>CH<sub>3</sub>) group. The singlet proton He belonging to the thiophene is easily distinguishable at 6.82 ppm in the <sup>1</sup>H-NMR spectrum. The five protons peak located at 7.28 ppm represents the 3 protons; Hb, Hc, and Hd of the coumarin ring, and the two singlet protons corresponding to the thiophene ring NH<sub>2</sub> protons are easily identifiable. The spectrum also shows a Ha proton in the singlet peak of coumarin ring at 8.17 ppm. Moreover, the <sup>13</sup>C-NMR spectrum showed the presence of  $\delta$  84.73 (C $\equiv$ N) and  $\delta$  166.98 (C=O) beside the signals for coumarin, benzene and thiophene carbons. HRMS ( $m/e$ ): [M+H]<sup>+</sup>: C<sub>16</sub>H<sub>13</sub>N<sub>2</sub>O<sub>3</sub>S, Calculated: 313.0647; Found: 313.0638. With respect to these data and the explanation given above, the following structural formula is proposed for the compound 2-amino-4-(8-ethoxy-2-oxo-2*H*-chromen-3-yl)thiophene-3-carbonitrile (28).

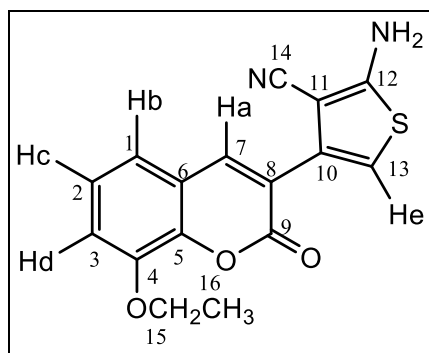


Figure 3.43. Structure of 2-Amino-4-(8-ethoxy-2-oxo-2*H*-chromen-3-yl)thiophene-3-carbonitrile (28)

### 3.9.9. Structural elucidation for 2-Amino-4-(8-methoxy-2-oxo-2H-chromen-3-yl)thiophene-3-carbonitrile (29)

Recrystallization solvent: Ethanol; FT-IR ( $\nu_{\max}$ ,  $\text{cm}^{-1}$ ): 3338, 3431 (Primary amine,  $\text{NH}_2$ ), 3218 (Aromatic C-H), 3136 (Aliphatic C-H), 2191 ( $\text{C}\equiv\text{N}$ ), 1628 ( $\text{C}=\text{O}$ , lactone), 1560 ( $\text{C}=\text{C}$ ), 1351 ( $\text{C}-\text{O}-\text{C}$ ), 585 ( $\text{C}-\text{S}$ );  $^1\text{H}$  NMR ( $\text{DMSO}-d_6/\text{TMS}$ , 300 MHz)  $\delta$ : 3.95 (s, 3H,  $\text{OCH}_3$ ), 6.85 (s, 1H, Ar-H),  $\delta$  7.29-7.38 (complex, 5H: 2H =  $-\text{NH}_2$ , 3H = Ar-H), 8.20 (s, 1H, Ar-H); HRMS ( $m/e$ ):  $[\text{M}+\text{H}]^+$ :  $\text{C}_{15}\text{H}_{11}\text{N}_2\text{O}_3\text{S}$ , Calculated: 299.0490; Found: 299.0493.

The chemical structure of (29) was identified and can be explained by using its IR, NMR, and MS spectra as shown in Appendix 3 (Figures 3.9.1-3.9.4).

For the IR spectrum, recorded in KBr pellets, the vibration bands of (29) appear at 3338, 3431, 3218, 3136, 2191, 1628, 1560, 1351, and 585  $\text{cm}^{-1}$ . The band at 3338 and 3431 correspond to the stretching vibrations of the primary amine group. The vibration bands at 3218, 3136, 2191, 1628, 1560, 1351, and 585  $\text{cm}^{-1}$  can be related to the aromatic  $\nu(\text{C}-\text{H})$ , aliphatic  $\nu(\text{C}-\text{H})$ , nitrile tensile  $\nu(\text{C}\equiv\text{N})$ , lactone  $\nu(\text{C}=\text{O})$ , aromatic  $\nu(\text{C}=\text{C})$ , lactone  $\nu(\text{C}-\text{O}-\text{C})$ , and the carbon-sulfur  $\nu(\text{C}-\text{S})$ , stretching vibrations, respectively. The NMR spectrum of (29) was recorded in  $\text{DMSO}-d_6$  using tetramethylsilane (TMS). The  $\text{OCH}_3$  protons are easily distinguishable as singlets linked to the coumarin with 3 protons at 3.95 ppm in the  $^1\text{H}$ -NMR spectrum. The singlet thiophene proton He is distinguishable at 6.85. Five protons corresponding to the thiophene ring  $\text{NH}_2$  protons is easily identifiable, coumarinyl protons: Hb, Hc, and Hd, all at 7.29-7.38 ppm. The spectrum also shows a Ha proton in the singlet peak of coumarin ring at 8.20 ppm; HRMS ( $m/e$ ):  $[\text{M}+\text{H}]^+$ :  $\text{C}_{15}\text{H}_{11}\text{N}_2\text{O}_3\text{S}$ , Calculated: 299.0490; Found: 299.0493. With respect to these data and the explanation given above, the following structural formula is proposed for the compound 2-amino-4-(8-methoxy-2-oxo-2H-chromen-3-yl)thiophene-3-carbonitrile (29).

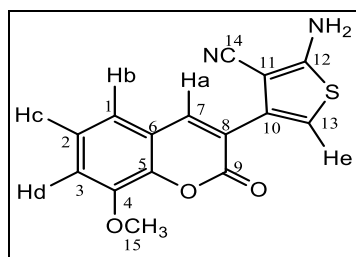


Figure 3.44. Structure of 2-Amino-4-(8-methoxy-2-oxo-2H-chromen-3-yl)thiophene-3-carbonitrile (29)

### 3.9.10. Structural elucidation for 2-Amino-4-(3-oxo-3H-benzo[f]chromen-2-yl)thiophene-3-carbonitrile (30)

Recrystallization solvent: Ethanol; FT-IR ( $\nu_{\max}$ ,  $\text{cm}^{-1}$ ): 3332, 3415 (Primary amine,  $\text{NH}_2$ ), 3222 (Aromatic C-H), 2197 ( $\text{C}\equiv\text{N}$ ), 1698 ( $\text{C}=\text{O}$ , lactone), 1563 ( $\text{C}=\text{C}$ ), 1277 ( $\text{C}-\text{O}-\text{C}$ ), 594 ( $\text{C}-\text{S}$ );  $^1\text{H}$  NMR ( $\text{DMSO}-d_6/\text{TMS}$ , 300 MHz)  $\delta$ : 6.99 (s, 1H, Ar-H), 7.35 (s, 2H,  $-\text{NH}_2$ ), 7.75-7.80 (complex, m, 3H, Ar-H), 8.09 (d, 1H,  $J = 7.7$  Hz, Ar-H), 8.23 (d, 1H,  $J = 9.0$  Hz, Ar-H), 8.53 (d, 1H,  $J = 8.3$  Hz, Ar-H), 9.07 (s, 1H, Ar-H);  $^{13}\text{C}$ -APT ( $\text{DMSO}-d_6$ , 75 MHz)  $\delta$ : 87.72 ( $\text{C}\equiv\text{N}$ ), 113.17 – 112.60, 117.01, 122.67, 123.19, 126.59, 127.13, 129.98 – 129.35, 130.46, 136.31, 142.09, 154.81, 157.25; 172.61 ( $\text{C}=\text{O}$ ); HRMS ( $m/e$ ):  $[\text{M}+\text{H}]^+$ :  $\text{C}_{18}\text{H}_{11}\text{N}_2\text{O}_2\text{S}$ , Calculated: 319.0541; Found: 319.0537.

The chemical structure of (30) was identified and can be explained by using its IR, NMR, and MS spectra as shown in Appendix 3 (Figures 3.10.1-3.10.4).

For the IR spectrum, recorded in KBr pellets, the vibration bands of (30) appear at 3332, 3415, 3222, 2197, 1698, 1563, 1277, and 594  $\text{cm}^{-1}$ . The band at 3332 and 3415 correspond to the stretching vibrations of the primary amine group. The vibration bands at 3222, 2197, 1698, 1622, 1563, 1277, 585, and 594  $\text{cm}^{-1}$  can be related to the aromatic  $\nu(\text{C}-\text{H})$ , aliphatic  $\nu(\text{C}-\text{H})$ , nitrile tensile  $\nu(\text{C}\equiv\text{N})$ , lactone  $\nu(\text{C}=\text{O})$ , aromatic  $\nu(\text{C}=\text{C})$ , lactone  $\nu(\text{C}-\text{O}-\text{C})$ , and carbon-sulfur  $\nu(\text{C}-\text{S})$ , stretching vibrations, respectively. The NMR spectrum of (30) was recorded in  $\text{DMSO}-d_6$  using tetramethylsilane (TMS). The singlet proton Hh belonging to the thiophene is easily distinguishable at 6.99 ppm in the  $^1\text{H}$ -NMR spectrum. Two singlet protons corresponding to the thiophene ring  $\text{NH}_2$  protons at 7.35 ppm is easily identifiable. There is a complex multi-peak located at 7.75-7.80 ppm representing the 3 protons; Hc, He, and Hd of the coumarin ring. A doublet proton at 8.09 ppm which belongs to Hg (d, 1H,  $J = 7.7$  Hz) of an aromatic proton, and the another doublet at 8.23 ppm can be linked to Hb (d, 1H,  $J = 9.0$  Hz), also an aromatic proton. A third and final doublet proton at 8.53 ppm corresponding to Hf (d, 1H,  $J = 8.3$  Hz), can be clearly seen. The Ha proton in the singlet peak of coumarin ring is located at 9.07 ppm. Moreover, the  $^{13}\text{C}$ -APT spectrum showed the presence of  $\delta$  87.72 ( $\text{C}\equiv\text{N}$ ), and  $\delta$  172.61 ( $\text{C}=\text{O}$ ), beside the signals for coumarin, benzene and thiophene carbons. HRMS ( $m/e$ ):  $[\text{M}+\text{H}]^+$ :  $\text{C}_{18}\text{H}_{11}\text{N}_2\text{O}_2\text{S}$ , Calculated: 319.0541; Found: 319.0537. With respect to these data and the

explanation given above, the following structural formula is proposed for the compound 2-amino-4-(3-oxo-3*H*-benzo[*f*]chromen-2-yl)thiophene-3-carbonitrile (30).

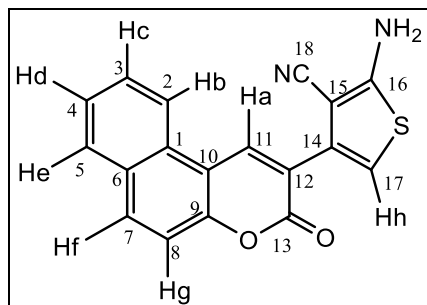


Figure 3.45. Structure of 2-Amino-4-(3-oxo-3*H*-benzo[*f*]chromen-2-yl)thiophene-3-carbonitrile (30)

### 3.10. The Structural Characterizations and Elucidations of the synthesized Amide derivatives

#### 3.10.1. Structural elucidation for N-(3-cyano-4-(3-oxo-3*H*-benzo[*f*]chromen-2-yl)thiophen-2-yl)acetamide (31)

Recrystallization solvent: DCM; FT-IR ( $\nu_{\max}$ ,  $\text{cm}^{-1}$ ): 3289 (NH), 3145 (Aromatic C-H), 3058 (Aliphatic C-H), 2203 ( $\text{C}\equiv\text{N}$ ), 1689 ( $\text{C}=\text{O}$ , lactone), 1538 ( $\text{C}=\text{O}$ , amide), 1511 ( $\text{C}=\text{C}$ ), 1274 ( $\text{C}-\text{O}-\text{C}$ ), 560 ( $\text{C}-\text{S}$ );  $^1\text{H-NMR}$  ( $\text{DMSO-}d_6$ , 300 MHz)  $\delta$ : 2.29 (s, 3H,  $\text{CH}_3$ ), 7.55 (s, 1H, Ar-H), 7.64-7.80 (complex, m, 3H, Ar-H), 8.10 (d, 1H,  $J = 8.1$  Hz, Ar-H), 8.26 (d, 1H,  $J = 9.1$  Hz, Ar-H), 8.60 (d, 1H,  $J = 8.7$  Hz, Ar-H), 9.14 (s, 1H, Ar-H), 11.80 (s, 1H, NH);  $^{13}\text{C-APT}$  ( $\text{DMSO-}d_6$ , 300 MHz)  $\delta$ : 23.16, 84.68, 111.34, 114.09, 117.65, 121.44, 123.42, 127.48, 129.75, 130.07, 130.23, 131.30, 132.80, 134.60, 134.95, 137.35, 153.88, 160.25, 167.07; HRMS ( $m/e$ ) :  $[\text{M}+\text{H}]^+$ :  $\text{C}_{20}\text{H}_{11}\text{N}_2\text{O}_3\text{S}$ , Calculated: 359.0490; Found: 359.0482.

The chemical structure of (31) was identified and can be explained by using its IR, NMR, and MS spectra as shown in Appendix 4 (Figures 4.1.1-4.1.4).

For the IR spectrum, recorded in KBr pellets, the vibration bands of (31) appear at 3289, 3145, 3058, 2203, 1689, 1538, 1511, 1274, and  $560\text{ cm}^{-1}$ . The band at 3332 corresponds to the stretching vibrations of the secondary amine group. The vibration bands at 3145, 3058, 2203, 1689, 1538, 1511, 1274, and  $560\text{ cm}^{-1}$  can be related to the aromatic  $\nu(\text{C}-\text{H})$ , aliphatic  $\nu(\text{C}-\text{H})$ , nitrile tensile  $\nu(\text{C}\equiv\text{N})$ , lactone  $\nu(\text{C}=\text{O})$ , amide  $\nu(\text{N}-\text{C}=\text{O})$ , aromatic  $\nu(\text{C}=\text{C})$ , lactone  $\nu(\text{C}-\text{O}-\text{C})$ , and carbon-sulfur  $\nu(\text{C}-\text{S})$ , stretching vibrations, respectively.

The compound has a peak at  $3272\text{ cm}^{-1}$  in the FT-IR spectrum taken in KBr, the NH stretching vibration due to the 2-position to the thiophene ring; The band at  $3069\text{ cm}^{-1}$  corresponds to aromatic C-H stretching vibrations; The band at  $2980\text{ cm}^{-1}$  corresponds to aliphatic C-H stretching vibrations; The band at  $2218\text{ cm}^{-1}$  corresponds to the  $\text{C}\equiv\text{N}$  tensile vibrations; The violent band  $\text{C}=\text{O}$  at  $1725\text{ cm}^{-1}$ ; The band at  $1559\text{ cm}^{-1}$  corresponds to the  $\text{C}=\text{C}$  tensile vibrations; C-S stretching vibrations at  $1238\text{ cm}^{-1}$  and C-S stretching at  $520\text{ cm}^{-1}$ . The NMR spectrum of (31) was recorded in  $\text{DMSO-}d_6$  using tetramethylsilane (TMS). The  $\text{CH}_3$  protons are easily distinguishable as a singlet linked to the monocyclic carbonyl group of 3 protons at 2.29 ppm in the  $^1\text{H-NMR}$  spectrum. The singlet proton Hh belonging to the thiophene is easily distinguishable at 7.55 ppm in the  $^1\text{H-NMR}$  spectrum. The complex multi-peak located at 7.64-7.80 ppm represents the 3 protons; Hc, Hd, and He, of the coumarin ring. A doublet proton at 8.10 ppm which belongs to Hg (d,  $J = 8.1\text{ Hz}$ ) of an aromatic proton, and another doublet at 8.26 ppm can be linked to Hb (d,  $J = 9.1\text{ Hz}$ ), also an aromatic proton. A third and final doublet proton at 8.60 ppm corresponding to Hf ((d, 1H,  $J = 8.7\text{ Hz}$ ), and the Ha proton in the singlet peak of coumarin ring is located at 9.14 ppm. A singlet proton corresponding to the thiophene ring NH protons at 11.80 ppm is easily identifiable. Moreover, the  $^{13}\text{C-APT}$  spectrum showed the presence of  $\delta 23.16$  ( $\text{CH}_3$ ),  $\delta 84.68$  ( $\text{C}\equiv\text{N}$ ),  $\delta 153.88$  ( $\text{O-C=O}$ ), and  $\delta 167.07$  ( $\text{N-C=O}$ ), beside the signals for coumarin, benzene and thiophene carbons. HRMS ( $m/e$ ):  $[\text{M}+\text{H}]^+$ :  $\text{C}_{20}\text{H}_{11}\text{N}_2\text{O}_3\text{S}$ , Calculated: 359.0490; Found: 359.0482. With respect to these data and the explanation given above, the following structural formula is proposed for the compound *N*-(3-cyano-4-(3-oxo-3*H*-benzo[*f*]chromen-2-yl)thiophen-2-yl)acetamide (31).

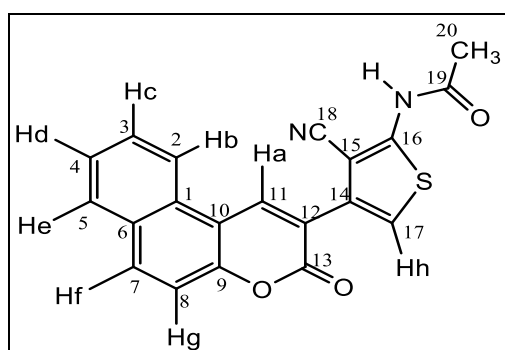


Figure 3.46. Structure of *N*-(3-cyano-4-(3-oxo-3*H*-benzo[*f*]chromen-2-yl)thiophen-2-yl)acetamide (31)

### 3.10.2. Structure elucidation for N-(3-cyano-4-(3-oxo-3H-benzo[f]chromen-2-yl)thiophen-2-yl)benzamide (32)

Recrystallization solvent: DCM; FT-IR ( $\nu_{\max}$ ,  $\text{cm}^{-1}$ ): 3249 (NH), 3058 (Aromatic C-H), 2200 ( $\text{C}\equiv\text{N}$ ), 1711 (C=O, lactone), 1665 (amide C=O), 1532 (C=C), 1274 (C-O-C), 594 (C-S);  $^1\text{H}$  NMR (DMSO- $d_6$ , 300 MHz)  $\delta$ : 7.61-7.79 (complex, m, 5H, Ar-H), 8.01 (d, 1H,  $J = 7.2$  Hz, Ar-H), 8.11 (d, 1H,  $J = 8.2$  Hz, Ar-H), 8.27 (d, 1H,  $J = 9.1$  Hz, Ar-H), 8.62 (d, 1H,  $J = 8.3$  Hz, Ar-H), 9.17 (s, 1H, Ar-H), 12.10 (s, 1H, NH);  $^{13}\text{C}$ -APT (DMSO- $d_6$ , 300 MHz)  $\delta$ : 114.15, 117.75, 121.23, 122.25, 123.66, 124.85, 127.58, 129.82, 130.15, 130.24, 131.32, 133.43, 135.07, 139.72, 151.09, 160.42, 165.94; HRMS ( $m/e$ ) :  $[\text{M}+\text{H}]^+$ :  $\text{C}_{26}\text{H}_{14}\text{N}_2\text{O}_3\text{S}$ , Calculated: 423.0820; Found: 423.0818.

The chemical structure of (32) was identified and can be explained by using its IR, NMR, and MS spectra as shown in Appendix 4 (Figures 4.2.1-4.2.4).

For the IR spectrum, recorded in KBr pellets, the vibration bands of (32) appear at 3249, 3058, 2200, 1711, 1665, 1532, 1274, and 594  $\text{cm}^{-1}$ . The band at 3249 corresponds to the stretching vibrations of the secondary amine group. The vibration bands at 3058, 2200, 1711, 1665, 1532, 1274, and 594  $\text{cm}^{-1}$  can be related to the aromatic  $\nu(\text{C-H})$ , aliphatic  $\nu(\text{C-H})$ , nitrile tensile  $\nu(\text{C}\equiv\text{N})$ , lactone  $\nu(\text{C}=\text{O})$ , amide  $\nu(\text{N}-\text{C}=\text{O})$ , aromatic  $\nu(\text{C}=\text{C})$ , lactone  $\nu(\text{C}-\text{O}-\text{C})$ , and carbon-sulfur  $\nu(\text{C}-\text{S})$ , stretching vibrations, respectively. The NMR spectrum of (32) was recorded in DMSO- $d_6$  using tetramethylsilane (TMS). The complex multi-peak located at 7.61-7.79 ppm representing the 5 protons; Hc, Hf, Hg, Hh, and Hk, of the coumarin ring. A doublet proton at 8.01 ppm which belongs to Hd (d, 1H,  $J = 7.2$  Hz) an aromatic proton, and the another doublet at 8.11 ppm can be linked to Hi (d d, 1H,  $J = 8.2$  Hz), also an aromatic proton. A third doublet proton at 8.27 ppm corresponding to He (d, 1H,  $J = 9.1$  Hz), and finally, a fourth doublet proton at 8.62 ppm corresponding to Hb (d, 1H,  $J = 8.3$  Hz). The Ha proton in the singlet peak of coumarin ring is located at 9.17 ppm. A singlet proton corresponding to the thiophene ring NH proton at 12.10 ppm is easily identifiable. Moreover, the  $^{13}\text{C}$ -APT spectrum showed the presence of  $\delta$  114.15 ( $\text{C}\equiv\text{N}$ ),  $\delta$  160.42 (O-C=O), and  $\delta$  165.94 (N-C=O), beside the signals for coumarin, benzene and thiophene carbons. HRMS ( $m/e$ ):  $[\text{M}+\text{H}]^+$ :  $\text{C}_{26}\text{H}_{14}\text{N}_2\text{O}_3\text{S}$ , Calculated: 423.0820; Found: 423.0818. With respect to these data and the explanation given above,

the following structural formula is proposed for the compound *N*-(3-cyano-4-(3-oxo-3*H*-benzo[*f*]chromen-2-yl)thiophen-2-yl)benzamide (32).

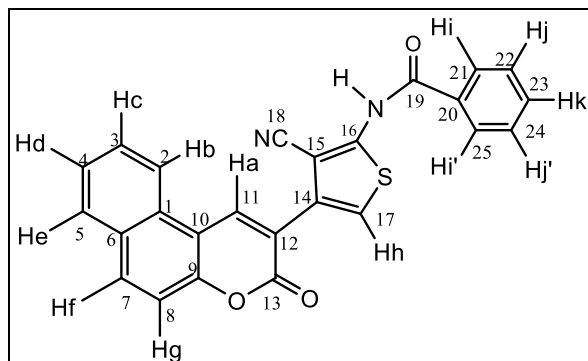


Figure 3.47. Structure of *N*-(3-cyano-4-(3-oxo-3*H*-benzo[*f*]chromen-2-yl)thiophen-2-yl)benzamide (32)

### 3.10.3. Structure elucidation for *N*-(3-cyano-4-(3-oxo-3*H*-benzo[*f*]chromen-2-yl)thiophen-2-yl)-4-nitrobenzamide (33)

Recrystallization solvent: DCM; FT-IR ( $\nu_{\max}$ ,  $\text{cm}^{-1}$ ): 3624 (NH), 3474 (Aromatic C-H), 2209 ( $\text{C}\equiv\text{N}$ ), 1720 ( $\text{C}=\text{O}$ , lactone), 1680 (amide  $\text{C}=\text{O}$ ), 1569 ( $\text{C}=\text{C}$ ), 1280 ( $\text{C}-\text{O}-\text{C}$ ), 594 ( $\text{C}-\text{S}$ );  $^1\text{H}$  NMR (DMSO-*d*<sub>6</sub>/ TMS, 300 MHz)  $\delta$ : 7.65-7.82 (complex, m, 4H, Ar-H), 8.12 (d, 1H,  $J = 7.9$  Hz, Ar-H), 8.18-8.37 (complex, m, 2H, Ar-H), 8.43 (d, 1H,  $J = 8.7$  Hz, Ar-H), 8.63 (d, 1H,  $J = 8.5$  Hz, Ar-H), 9.18 (s, 1H, Ar-H), 12.40 (s, 1H, NH);  $^{13}\text{C}$ -APT (DMSO-*d*<sub>6</sub>, 300 MHz)  $\delta$ : 114.15, 117.74, 121.92, 123.66, 129.69, 129.86, 130.24, 131.33, 134.04, 135.03, 139.60; HRMS ( $m/e$ ) :  $[\text{M}+\text{H}]^+$ :  $\text{C}_{25}\text{H}_{13}\text{N}_3\text{O}_5\text{S}$ , Calculated: 468.0663; Found: 468.0661.

The chemical structure of (33) was identified and can be explained by using its IR, NMR, and MS spectra as shown in Appendix 4 (Figures 4.3.1-4.3.4).

For the IR spectrum, recorded in KBr pellets, the vibration bands of (33) appear at 3624, 3474, 2209, 1720, 1680, 1569, 1280, and 594  $\text{cm}^{-1}$ . The band at 3624 corresponds to the stretching vibrations of the secondary amine group. The vibration bands at 3474, 2209, 1720, 1680, 1569, 1280, and 594  $\text{cm}^{-1}$  can be related to the aromatic  $\nu(\text{C}-\text{H})$ , nitrile tensile  $\nu(\text{C}\equiv\text{N})$ , lactone  $\nu(\text{C}=\text{O})$ , amide  $\nu(\text{N}-\text{C}=\text{O})$ , aromatic  $\nu(\text{C}=\text{C})$ , lactone  $\nu(\text{C}-\text{O}-\text{C})$ , and carbon-sulfur  $\nu(\text{C}-\text{S})$ , stretching vibrations, respectively. The NMR spectrum of (33) was recorded in DMSO-*d*<sub>6</sub> using tetramethylsilane (TMS). The complex multi-peak located at

7.65-7.82 ppm representing the 4 protons; Hc, Hf, Hg, and Hh, of the coumarin ring. A doublet proton at 8.12 ppm which belongs to Hd (d, 1H,  $J = 7.9$  Hz) an aromatic proton. Another complex multi-peak is also located at 8.18-8.37 ppm representing the 2 protons; Hb, and He, of the coumarin ring. Another doublet proton at 8.43 ppm can be linked to Hi (d,  $J = 8.7$  Hz), also an aromatic proton. A third doublet proton at 8.63 ppm corresponding to Hj (d, 1H,  $J = 8.5$  Hz). The Ha proton in the singlet peak of coumarin ring is located at 9.18 ppm. A singlet proton corresponding to the thiophene ring NH proton at 12.40 ppm is easily identifiable. Moreover, the  $^{13}\text{C}$ -APT spectrum showed the presence of  $\delta$  114.15 ( $\text{C}\equiv\text{N}$ ),  $\delta$  135.03 ( $\text{O}-\text{C}=\text{O}$ ), and  $\delta$  139.60 ( $\text{N}-\text{C}=\text{O}$ ), beside the signals for coumarin, benzene and thiophene carbons. HRMS ( $m/e$ ) :  $[\text{M}+\text{H}]^+$ :  $\text{C}_{25}\text{H}_{13}\text{N}_3\text{O}_5\text{S}$ , Calculated: 468.0663; Found: 468.0661. With respect to these data and the explanation given above, the following structural formula is proposed for the compound *N*-(3-cyano-4-(3-oxo-3*H*-benzo[*f*]chromen-2-yl)thiophen-2-yl)-4-nitrobenzamide (33).

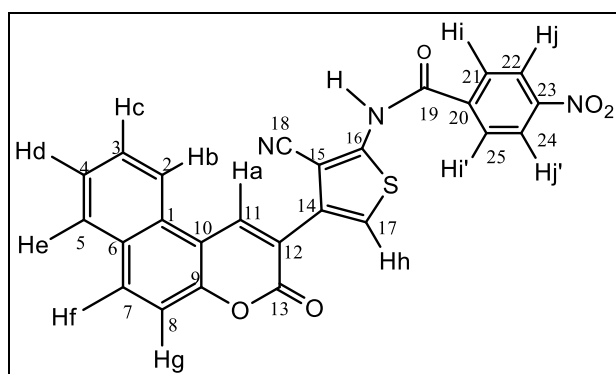


Figure 3.48. Structure of *N*-(3-cyano-4-(3-oxo-3*H*-benzo[*f*]chromen-2-yl)thiophen-2-yl)-4-nitrobenzamide (33)

### 3.11. The Structural Characterization and Elucidation of the synthesized Diulfonamide derivative (34)

#### 3.11.1. Structural elucidation for *N*-(3-cyano-4-(3-oxo-3*H*-benzo[*f*]chromen-2-yl)thiophen-2-yl)-*N*-(methylsulfonyl)methanesulfonamide (34)

Recrystallization solvent: DCM; FT-IR ( $\nu_{\text{max}}$ ,  $\text{cm}^{-1}$ ): 3043 (Aromatic C-H), 2923 (Aliphatic C-H), 2228 ( $\text{C}\equiv\text{N}$ ), 1714 ( $\text{C}=\text{O}$ , lactone), 1569 ( $\text{C}=\text{C}$ ), 1239 ( $\text{C}-\text{O}-\text{C}$ ), 1168 and 1151 ( $\text{O}_2\text{S}-\text{N}$ ), 774 and 753 ( $\text{S}-\text{N}$ ), 556 ( $\text{C}-\text{S}$ );  $^1\text{H}$ -NMR ( $\text{DMSO}-d_6$ , 300 MHz)  $\delta$ : 3.79 (s, 6H,  $\text{SO}_2\text{CH}_3$ ), 7.65-7.70 (complex, m, 3H, Ar-H), 8.12 (d, 1H,  $J = 7.8$  Hz, Ar-H), 8.31 (t, 2H,  $J = 12.6$  Hz, Ar-H), 8.62 (d, 1H,  $J = 8.4$  Hz, Ar-H), 9.36 (s, 1H, Ar-H);  $^{13}\text{C}$ -APT

(DMSO-*d*<sub>6</sub>, 300 MHz)  $\delta$ : 44.18, 114.12, 114.44, 115.66, 117.77, 119.99, 123.59, 127.65, 129.93, 130.28, 131.33, 131.81, 132.35, 134.60, 135.15, 135.39, 140.09, 143.51, 154.60, 160.31; HRMS (m/e): [M+H]<sup>+</sup>: C<sub>20</sub>H<sub>15</sub>N<sub>2</sub>O<sub>6</sub>S<sub>3</sub>, Calculated: 475.0094; Found: 475.0092.

The chemical structure of (34) was identified and can be explained by using its IR, NMR, and MS spectra as shown in Appendix 4 (Figures 4.4.1-4.4.4).

For the IR spectrum, recorded in KBr pellets, the vibration bands of (34) appear at 3043, 2923, 2228, 1714, 1569, 1239, 1168, 1151, 774, 753, and 556 cm<sup>-1</sup>. The vibration bands at 3043, 2923, 2228, 1714, 1569, 1239, 1168, 1151, 774, 753, and 556 cm<sup>-1</sup> can be related to the aromatic  $\nu$ (C-H), aliphatic  $\nu$ (C-H), nitrile tensile  $\nu$ (C $\equiv$ N), lactone  $\nu$ (C=O), aromatic  $\nu$ (C=C), lactone  $\nu$ (C-O-C), sulfur-nitrogen  $\nu$ (O<sub>2</sub>S-N), sulfur-nitrogen  $\nu$ (S-N), and carbon-sulfur  $\nu$ (C-S), stretching vibrations, respectively. The NMR spectrum of (34) was recorded in DMSO-*d*<sub>6</sub> using tetramethylsilane (TMS). The CH<sub>3</sub> protons are easily distinguishable as a singlet linked to the monocyclic sulfonyl group of 6 protons (2 $\times$ O<sub>2</sub>SCH<sub>3</sub>) at 3.79 ppm in the <sup>1</sup>H-NMR spectrum. The complex multi-peak located at 7.65-7.70 ppm representing the 3 protons; Hb, Hd, and He, of the coumarin ring. A doublet proton at 8.12 ppm which belongs to Hc (d, 1H,  $J$  = 7.8 Hz) of an aromatic proton. Two triplet protons at 8.31 ppm which belong to Hg and Hh (t, 2H,  $J$  = 12.6 Hz) are aromatic protons. An aromatic doublet proton located at 8.62 ppm belongs to Hf (d, 1H,  $J$  = 8.4 Hz) of an aromatic proton, and the Ha proton in the singlet peak of coumarin ring is located at 9.36 ppm. Moreover, the <sup>13</sup>C-APT spectrum showed the presence of  $\delta$  44.18 (3 $\times$ SO<sub>2</sub>CH<sub>3</sub>),  $\delta$  114.12 (C $\equiv$ N), and  $\delta$  154.60 (O-C=O), beside the signals for coumarin, benzene and thiophene carbons. HRMS (m/e): [M+H]<sup>+</sup>: C<sub>20</sub>H<sub>15</sub>N<sub>2</sub>O<sub>6</sub>S<sub>3</sub>, Calculated: 475.0094; Found: 475.0092. With respect to these data and the explanation given above, the following structural formula is proposed for the compound *N*-(3-cyano-4-(3-oxo-3*H*-benzo[*f*]chromen-2-yl)thiophen-2-yl)-*N*-(methylsulfonyl)methanesulfonamide (34).

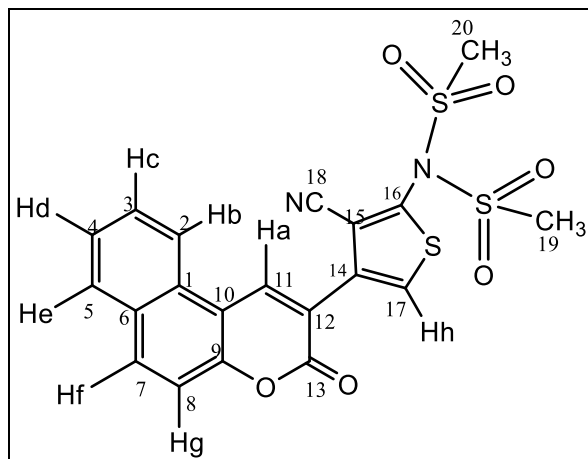


Figure 3.49. Structure of *N*-(3-cyano-4-(3-oxo-3*H*-benzo[*f*]chromen-2-yl)thiophen-2-yl)-*N*-(methylsulfonyl) methanesulfonamide (34)

### 3.12. The Structural Characterization and Elucidation of the synthesized Urea derivative (35)

#### 3.12.1. Structural elucidation for 1-(3-cyano-4-(3-oxo-3*H*-benzo[*f*]chromen-2-yl)thiophen-2-yl)-3-phenylurea (35)

Recrystallization solvent: DCM; FT-IR ( $\nu_{\max}$ ,  $\text{cm}^{-1}$ ): 3354 (2NH), 3040 (Aromatic C-H), 2209 ( $\text{C}\equiv\text{N}$ ), 1723 (C=O, lactone), 1680 (amide C=O), 1597 (C=C), 1280 (C-O-C), 582 (C-S);  $^1\text{H}$  NMR (DMSO- $d_6$ / TMS, 300 MHz)  $\delta$ : 7.08 (t, 1H,  $J = 7.2$  Hz, Ar-H), 7.36 (t, 3H,  $J = 7.8$  Hz, Ar-H), 7.51 (d, 1H,  $J = 8.5$  Hz, Ar-H), 7.68 (t, 1H,  $J = 4.9$  Hz, Ar-H), 7.80 (t, 1H,  $J = 7.2$  Hz, Ar-H), 8.11 (d, 1H,  $J = 7.8$  Hz, Ar-H), 8.26 (d, 1H,  $J = 9.0$  Hz, Ar-H), 8.61 (d, 1H,  $J = 8.7$  Hz, Ar-H), 9.17 (s, 1H, Ar-H), 9.43 (s, 1H, NH), 10.39 (s, 1H, NH);  $^{13}\text{C}$ -APT (DMSO- $d_6$ , 300 MHz)  $\delta$ : 114.16, 116.05, 117.72, 119.55, 119.61, 121.08, 123.60, 124.25, 127.55, 129.81, 130.14, 130.35, 131.33, 131.89, 134.90, 138.77, 139.69, 152.48, 154.08, 154.23; HRMS ( $m/e$ ) :  $[\text{M}+\text{H}]^+$ :  $\text{C}_{25}\text{H}_{16}\text{N}_3\text{O}_3\text{S}$ , Calculated: 438.0912; Found: 438.0909.

The chemical structure of (35) was identified and can be explained by using its IR, NMR, and MS spectra as shown in Appendix 4 (Figures 4.5.1-4.5.4). For the IR spectrum, recorded in KBr pellets, the vibration bands of (35) appear at 3354, 3040, 2209, 1723, 1680, 1597, 1280, and  $582\text{ cm}^{-1}$ . The band at 3354 corresponds to the stretching vibrations of two secondary amine groups. The vibration bands at 3040, 2209, 1723, 1680, 1597, 1280, and  $582\text{ cm}^{-1}$  can be related to the aromatic  $\nu(\text{C-H})$ , nitrile tensile  $\nu(\text{C}\equiv\text{N})$ , lactone

$\nu(\text{C}=\text{O})$ , urea  $\nu(\text{N}-\text{C}=\text{O})$ , aromatic  $\nu(\text{C}=\text{C})$ , lactone  $\nu(\text{C}-\text{O}-\text{C})$ , and carbon-sulfur  $\nu(\text{C}-\text{S})$ , stretching vibrations, respectively. The NMR spectrum of (35) was recorded in  $\text{DMSO}-d_6$  using tetramethylsilane (TMS). The triplet proton located at 7.08 ppm which belongs to Hm (t, 1H,  $J = 7.2$  Hz), is an aromatic proton. Three triplet protons (t, 3H,  $J = 7.8$  Hz, Ar-H) located at 7.36 ppm representing the 3 protons; Hh, Hk, and Hl, all aromatic. A doublet proton at 7.51 ppm can be linked to He (d,  $J = 8.5$  Hz), also an aromatic proton. The triplet proton located at 7.68 ppm which belongs to Hc (t, 1H,  $J = 4.9$  Hz), is an aromatic proton. The third and final triplet proton located at 7.80 ppm which belongs to Hd (t, 1H,  $J = 7.2$  Hz), is an aromatic proton. A doublet proton at 8.11 ppm which belongs to Hg (d, 1H,  $J = 7.8$  Hz) of an aromatic proton. Another doublet proton at 8.26 ppm can be linked to Hb (d, 1H,  $J = 9.0$  Hz), also an aromatic proton. A third doublet proton at 8.61 ppm corresponding to Hf (d, 1H,  $J = 8.7$  Hz). The Ha proton in the singlet peak of coumarin ring is located at 9.17 ppm. Two singlet protons corresponding to the thiophene ring NHi and NHj protons at 9.43 and 10.39 ppm, respectively, are easily identifiable and distinguishable. Moreover, the  $^{13}\text{C}$ -APT spectrum showed the presence of  $\delta$  114.16 ( $\text{C}\equiv\text{N}$ ),  $\delta$  154.08 ( $\text{O}-\text{C}=\text{O}$ ), and  $\delta$  154.23 ( $\text{N}-\text{C}=\text{O}$ ), beside the signals for coumarin, benzene and thiophene carbons. HRMS ( $m/e$ ) :  $[\text{M}+\text{H}]^+$ :  $\text{C}_{25}\text{H}_{16}\text{N}_3\text{O}_3\text{S}$ , Calculated: 438.0912; Found: 438.0909. With respect to these data and the explanation given above, the following structural formula is proposed for the compound 1-(3-cyano-4-(3-oxo-3*H*-benzo[*f*]chromen-2-yl)thiophen-2-yl)-3-phenylurea (35).

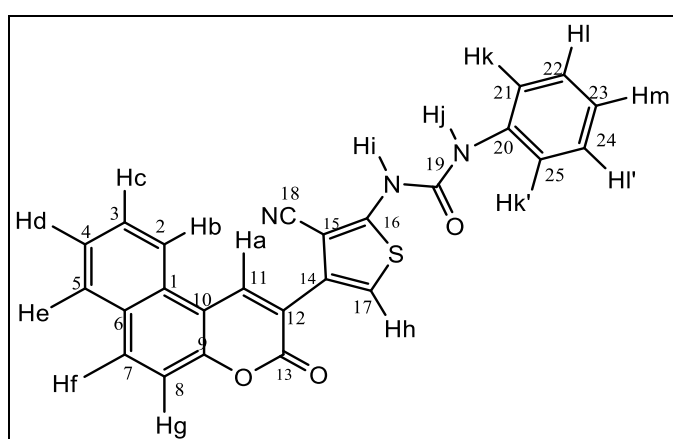


Figure 3.50. Structure of 1-(3-cyano-4-(3-oxo-3*H*-benzo[*f*]chromen-2-yl)thiophen-2-yl)-3-phenylurea (35)



## 4. RESULTS AND DISCUSSION

In the search for the fast, cost-effective, and eco-friendly synthetic protocols for novel molecules with potential biological activities, the synthesis of different 3-acetylcoumarins, malononitrile, and the main target coumarin-thiophene derivatives (in Stepwise and in one-pot three-component) via two procedures; Microwave-assisted Irradiation (MWI) and the Conventional Method (CM) were carried out. Comparisons of the two protocols for the synthesis of all the products have been summarized in Tables 4.9. Table 4.10 contains a comparative analysis between the one-pot three-component and the stepwise procedures for the synthesis of the coumarin-thiophene hybrids.

For the search for optimum condition for the synthesis of the 3-acetylcoumarin derivatives 1-10, it was realized that any of the available solvents (ethanol, methanol, etc.), even water, could lead to the attainment of the products, but the issue had to do with the yields that were desired. For the catalysts, piperidine, pyridine, trimethylamine, diethylamine, etc. were available. The first attempt in the synthesis of derivative 1 using ethanol and piperidine did the trick. So, there was no need to optimize any condition. Therefore, ethanol was used as the solvent, one of the cheapest solvents, and piperidine as the catalyst, also among the cheapest and easily available catalysts, for the synthesis of derivative 1 and later employed in the synthesis of the other 3-acetylcoumarins at different reaction periods.

The synthesis of 3-acetylcoumarins led to the preparation of the products in good to excellent yields (90-100%). Using the Conventional procedure, the yields were found be in 90-98% (Table 5.1) with reaction periods of 5-6 hours. Better yields of 90-100% (Table 5.2) were realized in the case of the microwave-assisted irradiation protocol within the shortest reaction period of 1-2 minutes, which has been adjudged the most convenient for the synthesis of 3-acetylcoumarins in this study. A comparative analysis on the two protocols can be accessed in Table 4.1.

Table 4.1. Comparative analysis of data of 3-acetylcoumarins synthesized via conventional and microwave irradiation procedures

3-Acetylcoumarin Derivative	<sup>a</sup> Conventional Method (CM)		<sup>b</sup> Microwave-assisted Irradiation (MWI)	
	Reaction time (h)	Yield <sup>c</sup> (%)	Reaction time (min)	Yield <sup>c</sup> (%)
1	5	92	1	97
2	5	98	1	100
3	6	90	1	95
4	5	90	1	94
5	5	90	1.5	95
6	6	90	1	90
7	6	90	2	96
8	6	90	2	95
9	5.5	92	1.5	93
10	5	94	1.5	97

<sup>a</sup> Room temperature; <sup>b</sup> 300 W, 80 °C; <sup>c</sup> Yields refer to isolated pure products

In the effort to synthesize the malononitrile derivatives from the reaction of 3-acetylcoumarin and malononitrile, different solvents and catalysts as summarized in Table 4.2 were tried. In the search for optimum conditions, solvents such as ethanol, dichloromethane as well as solvent-free were all tried. The catalysts such as piperidine, pyridine, NH<sub>4</sub>OAc, and NH<sub>4</sub>OAc/AcOH were utilized. Although all the solvents and catalysts tried worked, the solvent-free condition was the preferred and desired one, since it does not require the use of extra fund to purchase any solvent. In the final of several trials, a buffer comprising acetic acid (AcOH) and ammonium acetate (NH<sub>4</sub>OAc) was arrived at. The optimized condition was used in the synthesis of the malononitrile derivative 12 and then applied for the synthesis of the remaining derivatives via the conventional method (CM) and the microwave-assisted irradiation (MWI).

Table 4.2. Optimization of the reaction conditions for synthesis of 11

Trial	Solvent	Catalyst	Reaction time CW, MWI	Temperature CW, MWI	Yield (%) CW, MWI
1	Ethanol	Piperidine	7 h, 5 min	rt, 110 °C	30, 55
2	DCM	Piperidine	7 h, 5 min	rt, 50 °C	15, 40
3	Solvent-free	Piperidine	7 h, 5 min	rt, 110 °C	40, 50
4	Ethanol	Pyridine	7 h, 5 min	rt, 110 °C	20, 25
5	DCM	Pyridine	7 h, 5 min	rt, 50 °C	15, 30
6	Solvent-free	Pyridine	7 h, 5 min	rt, , 110 °C	24, 25
7	Ethanol	NH <sub>4</sub> OAc/AcOH	5 h, 2 min	rt, 110 °C	70, 80
8	DCM	NH <sub>4</sub> OAc/AcOH	7 h, 3 min	rt, 50 °C	60, 77
9	Solvent-free	NH <sub>4</sub> OAc/AcOH	4 h, 1 min	rt, 110 °C	90, 98
10	Ethanol	NH <sub>4</sub> OAc	5 h, 5 min	rt, 110 °C	30, 53
11	DCM	NH <sub>4</sub> OAc	5 h, 5 min	rt, 50 °C	32, 57
12	Solvent-free	NH <sub>4</sub> OAc	5 h, 4 min	rt, 110 °C	35, 62

On the synthesis of the malononitrile derivatives, solvent-free condition was tried and was successful. The yields were found to have followed the same trend as those of the 3-acetylcoumarins. Conventional procedure was realized in good yields of 80-90% (Table 5.3) and reaction times of 4-5 h. As was expected, the microwave-assisted irradiation procedure had the better yields of 90-98% (Table 5.4). It also had the less reaction period of 1-2 minutes with high purity of products. A comparative analysis on the two protocols for the synthesis of the malononitrile derivatives can be accessed in Table 4.3.

Table 4.3. Comparative analysis of data of malononitriles synthesized via conventional and microwave irradiation procedures

Malononitrile derivative	<sup>a</sup> Conventional Method (CM)		<sup>b</sup> Microwave-assisted Irradiation (MWI)	
	Reaction time (h)	Yield <sup>c</sup> (%)	Reaction time (min)	Yield <sup>c</sup> (%)
11	5	89	1	95
12	4	90	1	98
13	5	88	1.5	93
14	4.5	89	1	96
15	5	90	1.25	97
16	4	80	1.5	90
17	4.5	90	2	96
18	5	88	1.5	97
19	4	85	1.5	96
20	4	90	2	93

<sup>a</sup>Room temperature; <sup>b</sup>300W, temperature (90-110 °C); <sup>c</sup>Isolated pure products

As the main desire was to synthesize the target coumarin-thiophene compounds from the reaction of malononitrile derivatives and elemental sulfur, several catalysts and solvents were employed as summarized in Table 4.3. In the search for optimum conditions, solvents such as ethanol, methanol, dimethylformamide, and dichloromethane, and catalysts such diethylamine, triethylamine, piperidine, pyridine, and morpholine) were tried. The combinations of the solvents and the catalysts yielded the good products but not the desired yields. In the final trial, combination of triethylamine (as the catalyst) and ethanol (as the solvent) was propounded as the ideal condition for the synthesis of the title coumarin-thiophenes from the reaction of malononitrile derivatives and elemental sulfur. This condition was employed to synthesize the product 11 and later used to synthesize the other coumari-thiophenes via the conventional method (CM) the microwave-assisted irradiation (MWI) procedure.

Table 4.4. Optimization of the reaction conditions for synthesis of 21

Trial	Solvent	Catalyst	Reaction time CW, MWI	Temperature CW, MWI	Yield (%) CW, MWI
1	Ethanol	Piperidine	3 h, 4 min	rt, 80 °C	30, 40
2	Methanol	Piperidine	4 h, 5 min	rt, 80 °C	25, 40
3	DCM	Piperidine	5 h, 5 min	rt, 80 °C	10, 19
4	DMF	Piperidine	4 h, 6 min	rt, 80 °C	12, 20
5	Ethanol	Pyridine	3 h, 4 min	rt, 80 °C	13, 25
6	Methanol	Pyridine	3 h, 5 min	rt, 80 °C	11, 20
7	DCM	Pyridine	4 h, 3 min	rt, 80 °C	16, 30
8	DMF	Pyridine	3 h, 5 min	rt, 80 °C	10, 26
9	Ethanol	Triethylamine	3 h, 3 min	rt, , 80 °C	90, 96
10	Methanol	Triethylamine	3 h, 3 min	rt, 80 °C	70, 80
11	DCM	Triethylamine	4 h, 4 min	rt, 80 °C	65, 70
12	DMF	Triethylamine	4 h, 3 min	rt, 80 °C	55, 70
13	Ethanol	Morphline	3 h, 6 min	rt, 80 °C	37, 50
14	Methanol	Morphline	3 h, 4 min	rt, 80 °C	30, 50
15	DCM	Morphline	5 h, 5 min	rt, 80 °C	25, 38
16	DMF	Morphline	5 h, 4 min	rt, 80 °C	15, 36
17	Ethanol	Diethylamine	3 h, 3 min	rt, 80 °C	35, 50
18	Methanol	Diethylamine	3 h, 4 min	rt, 80 °C	35, 45
19	DCM	Diethylamine	5 h, 5 min	rt, 80 °C	32, 38
20	DMF	Diethylamine	5 h, 4 min	rt, 80 °C	36, 40

The strategies for the synthesis of the coumarin-thiophene derivatives, the target compounds, in stepwise, were geared towards improving on the yields and purity, as well as reducing the reaction time, in order to make an improvement on the conditions used in our previous study. Employing the newly developed protocols, the compounds were synthesized using the conventional method, in stepwise, but with a decreased reaction time and increased in yield (Table 4.5).

The yields and the reaction duration for the conventional procedure for the synthesis of coumarin-thiophene, in stepwise, were found to be 80-90% (Table 5.5) and within 2-3 hours, respectively. This same reaction was carried out using the designed MWI protocol, in stepwise, and the higher yields (92-96%) (Table 5.6) were obtained with the shorter reaction periods (2-3 minutes) as shown in Table 4.5. A comparative analysis on the three protocols, for the synthesis of the coumarin-thiophene derivatives in stepwise, is summarized in Table 4.5.

Table 4.5. Comparative analysis of data of coumarin-thiophenes synthesized via conventional and microwave irradiation procedures in stepwise

Coumarin-thiophene Derivative	<sup>a</sup> Conventional Method (CM)		<sup>b</sup> Microwave-assisted Irradiation (MWI)	
	Reaction time (h)	Yield <sup>c</sup> (%)	Reaction time (min)	Yield <sup>c</sup> (%)
21	2	90	3	96
22	2	90	2	95
23	3	89	3	94
24	2	83	3	92
25	2	88	3	95
26	3	80	2.5	95
27	3	86	3	92
28	3	87	3	95
29	2.5	90	3	96
30	3	90	3	95

<sup>a</sup>Room temperature; <sup>b</sup>300W, temperature (90-110 °C), time in seconds; <sup>c</sup>Isolated pure products

Optimization of the one-pot three-component reaction conditions for synthesis of target coumarin-thiophene hybrids 21-30 from a reaction of 3-acetylcoumarins 1-10, malononitrile and elemental sulfur (S<sub>8</sub>) was cautiously carried out as it may lead to the synthesis of the malonitrile derivatives instead of the desired coumarin-thiophene derivatives.

As it was the main desire to synthesize the target compounds via the one-pot three-component strategy, varieties of solvents and catalysts were employed as summarized in Table 4.6. Solvents such ethanol, water, and acetic acid, and catalysts such diethylamine, triethylamine, piperidine, L-proline, pyridine, and morpholine, were tried in different combinations. Even though most of the combinations worked, they were either in very low yields or associated with lots of impurities, leading to negligible yield or longer reaction durations. After several trials, diethylamine (as the catalyst) and ethanol (as the solvent) were found to be the ideal combination for the one-pot three-component condition for the synthesis of compound 30. The optimized condition was employed in the syntheses of title coumarin-thiophene hybrids, direct from 3-acetylcoumarins, whether the synthesis was using the conventional method (CM) or microwave-assisted irradiation (MWI).

Table 4.6. Optimization of the one-pot three-component reaction conditions for synthesis of 30

Trial	Solvent	Catalyst	Reaction time	Temperature	Yield (%)
			CW, TH, MWI	CW, TH, MWI	CW, TH, MWI
1	Ethanol	Piperidine	20 h, 5 h, 5 min	rt, 90 °C, 80 °C	15, 37, 40
2	Methanol	Piperidine	20 h, 5 h, 5 min	rt, 90 °C, 80 °C	15, 19, 38
3	DCM	Piperidine	20 h, 5 h, 5 min	rt, 40 °C, 80 °C	18, 20, 28
4	DMF	Piperidine	20 h, 5 h, 5 min	rt, 90 °C, 80 °C	20, 14, 20
5	Ethanol	Pyridine	20 h, 5 h, 5 min	rt, 90 °C, 80 °C	12, 18, 20
6	Methanol	Pyridine	20 h, 5 h, 5 min	rt, 90 °C, 80 °C	10, 13, 18
7	DCM	Pyridine	20 h, 5 h, 5 min	rt, 40 °C, 80 °C	12, 17, 25
8	DMF	Pyridine	20 h, 5 h, 5 min	rt, 90 °C, 80 °C	10, 20, 20
9	Ethanol	Triethylamine	20 h, 5 h, 5 min	rt, 90 °C, 80 °C	35, 43, 55
10	Methanol	Triethylamine	20 h, 5 h, 5 min	rt, 90 °C, 80 °C	37, 43, 50
11	DCM	Triethylamine	20 h, 5 h, 5 min	rt, 40 °C, 80 °C	15, 21, 39
12	DMF	Triethylamine	20 h, 5 h, 5 min	rt, 90 °C, 80 °C	12, 20, 23
13	Ethanol	Morphline	20 h, 5 h, 5 min	rt, 90 °C, 80 °C	42, 44, 48
14	Methanol	Morphline	20 h, 5 h, 5 min	rt, 90 °C, 80 °C	38, 40, 43
15	DCM	Morphline	20 h, 5 h, 5 min	rt, 40 °C, 80 °C	28, 30, 32
16	DMF	Morphline	20 h, 5 h, 5 min	rt, 90 °C, 80 °C	13, 27, 30
17	Ethanol	Diethylamine	20 h, 5 h, 5 min	rt, 90 °C, 80 °C	85, 90, 90
18	Methanol	Diethylamine	20 h, 5 h, 5 min	rt, 90 °C, 80 °C	75, 77, 80
19	DCM	Diethylamine	20 h, 5 h, 5 min	rt, 40 °C, 80 °C	65, 68, 70
20	DMF	Diethylamine	20 h, 5 h, 5 min	rt, 90 °C, 80 °C	63, 66, 68

The optimized conditions were therefore used to synthesize all the target coumarin-thiophene compounds. In this vein, yields and reaction duration for the conventional procedure were found to be 80-85% and 14-20 h, respectively (Table 4.7). The MWI

protocol led to higher yields (82-90%) of the products with the shorter reaction times (3-5 min). A comparative analysis on the two protocols (CM and MWI) for the synthesis of the coumarin-thiophene derivatives in one-pot three-component can be accessed in Table 4.7.

Table 4.7. Comparative analysis of data of coumarin-thiophene synthesized via conventional and microwave-assisted irradiation procedures in one-pot three-component

Coumarin-thiophene hybrid	<sup>a</sup> Conventional Method (CM)		<sup>b</sup> Microwave-assisted Irradiation (MWI)	
	Reaction time (h)	Yield <sup>c</sup> (%)	Reaction time (min)	Yield <sup>c</sup> (%)
21	20	80	5	85
22	18	85	3	90
23	14	84	4.5	90
24	15	83	5	90
25	18	81	5	90
26	20	82	4	90
27	17	80	4.5	82
28	15	85	3.5	90
29	19	84	4	90
30	17	85	5	90

<sup>a</sup>Room temperature; <sup>b</sup>450 W, 80 °C; <sup>c</sup>Isolated pure products

Moreover, in the assessment of the step-wise and the one-pot three-component procedures, as can be seen in Table 4.7, it has been realized that, even though the step-wise conditions led to enhanced yields (80-96%) as compared to that of the one-pot three-component (80-90%), the one-pot three-component conditions were found to be less time consuming. The time talked about here is not related to the reaction duration. This is because, for instance, the synthesis of the derivatives 21-30 follows the trend; CM in stepwise is between 2-3 h but in one-pot three-component it is 14-20 h. For the MWI in stepwise is between 2-3 min. whilst in one-pot three-component the period is between 3-5 min. The reasoning herein is that, if one is to synthesize a coumarin-thiophene derivative, the malononitrile derivative

must be prepared first, which is the intermediate between the 3-acetylcoumarin derivatives and the coumarin-thiophene derivatives, before synthesizing the coumarin-thiophene derivative by reacting it with elemental sulfur. The synthesis of the malononitrile derivatives involves period of filtering, drying, etc. which involves and use of solvents. Moreover, each step, in the stepwise procedure for the synthesis of the coumarin-thiophene hybrids involves washing or purification of the malononitrile intermediate, which also involves extra expenses with respect to the purification solvent(s). However, in the case of the synthesis of the coumarin-thiophene hybrids via the one-pot three-component, the reaction is straight forward from the reaction of 3-acetylcoumarin derivative with malononitrile and elemental sulfur to the coumarin-thiophene hybrid. This did not involve purification as the products were obtained in pure form. Little ethanol, about 10 mL, is enough to wash each of the products. Finally, in the case of the other derivatives (31-35), they were synthesized via both the conventional method (CM) and the microwave-enhanced irradiation (MWI). The compounds were generally prepared in good to excellent yields (90-98%) as can be seen in Table 4.8. The reaction periods were generally found to be good (3 min-18 h) as shown in Table 4.8. For the CM procedure, the reaction time ranges from 16-18h, the yields in 90-94%. In the case of MWI, the reaction durations were even less (3 min-3.5 min) but with enhanced yields (94-98%).

Table 4.8. Comparative analysis of data of compounds synthesized via conventional and microwave-assisted irradiation procedures

Synthesized Compounds	Conventional Procedure		Microwave-Enhanced Irradiation Procedure	
	Reaction time (h)	Yield <sup>a</sup> (%)	Reaction time (min)	Yield <sup>a</sup> (%)
31	18	94	3	98
32	16	90	3.5	95
33	18	90	3	94
34	17	92	3.5	96
35	16	91	3	94

Table 4.9. General comparisons between the two protocols

Protocol	Reaction Period	Isolated Yields
Conventional	2 hours-20 hours	80-98 %
Microwave-Assisted	1 minute-3 minutes	90-100 %

Table 4.10. Comparisons between the stepwise and the one-pot three-component procedures

Protocol	Reaction Period	Isolated Yields
Stepwise Procedure	2 minutes-3 hours	80-96 %
One-Pot Three-Component Procedure	3 minutes-20 hours	80-90 %

#### 4.1. Photophysical activities of dyes 21-35

The UV–vis and fluorescence spectroscopic data of fluorophore 21-30 were determined at 25 °C in different solvents with varying polarities. The extinction coefficients ( $\epsilon$ ) were calculated according to the Beer-Lambert Law. All the chemosensors 21-35 are solids having some degree of fluorescence. The colorimetric and fluorescence changes of 21-30, are shown in Figures 4.1-4.15. Five solvents with varying dielectric constants ( $\epsilon$ ), i.e. DMSO (46.45), DCM (8.93), THF (7.58), MeOH (32.66), and PhMe (2.38), have been employed in this study. Changing the polarity of the solvents led to remarkable solvatochromism and fluorosolvatochromism in all the sensors 21-35 as shown in Figures 4.1-4.15. Fluorophores 22, 23, 25, and 28, are all soluble in all the solvents utilized in this study. The following sensors have been found to have varying solubility in different solvents; 21 (soluble in all the solvents except PhMe), 29 (soluble in all the solvents except DMSO and PhMe), 24 and 27 (soluble in all the solvents except DCM and PhMe), 26 and 30 (soluble in all the solvents except MeOH and PhMe), 31, 34, and 35 (soluble in only DMSO and MeOH), and 32 and 33 (soluble in DMSO only). The molar absorption coefficient for the sensors 21-30 is in the range of 1249-60200  $\text{cm}^{-1}\text{M}^{-1}$ , and the Stokes shift range are in the range of 65-244 nm. The results for the photophysical activities of the dyes 21-30 are shown in Tables 4.9-4.12.

In order to investigate the solvatochromic behavior, the absorption and emission data of the dyes 21-30 were determined in five solvents with different polarities as enlisted above, i.e. DMSO, DCM, MeOH, THF, and PhMe. The analyses were performed using low concentrations of the solutes (10  $\mu\text{M}$  for UV-vis, 0.1  $\mu\text{M}$  for fluorescence). The compounds showed one absorption band in almost all the solvents used and show absorption maxima ( $\lambda_{\text{max}}$ ) ranging from 300 to 409 nm. In addition, the dyes 21-30 have been found to be fluorescent (with emission  $\lambda_{\text{max}}$  413-548 nm in all the solvent used). The probes 21-30 also exhibited one emission band in almost all the solvents used. The dyes bearing as electron-donating groups on the coumarin part such as OH, OCH<sub>3</sub>, OCH<sub>2</sub>CH<sub>3</sub>, N(CH<sub>2</sub>CH<sub>3</sub>)<sub>2</sub>, etc. show the characteristic longer-wavelength of absorption than those bearing electronwithdrawing groups such as Cl and Br, the unsubstituted, and the benzocoumarin ones. This absorption may be due to increasing push-pull character between the electron-donators and the coumarin ring as an acceptor. The absorption and emission maxima for fluorophores 31-35 were not obtained as they are only soluble in either DMSO or THF.

However, we also studied the deprotonation and reverse protonation process of chemosensor 27 in two solvent systems; DMSO alone and DMSO/H<sub>2</sub>O binary mixture. As can be seen vividly in Figure 1.2, most of the coumarin derivatives that have been employed as anticancer or have some biological applications, are appended with the hydroxyl group (OH), the monitoring of the absorption and fluorescence behaviors of probe 27 was therefore decided, which due to the presence of an hydroxyl function is susceptible to deprotonation under alkaline condition, and reverse protonation under acidic condition. Therefore, the investigation of the photophysical behavior of 27 in the presence of different equivalents of tetrabutylammonium hydroxide (TBAOH) and trifluoroacetic acid (TFA) using DMSO as the solvent was inevitable. The electronic transition spectrum of 27 (10  $\mu\text{M}$ ) displayed absorption band at 338 nm ( $\epsilon = 1.72 \times 10^4 \text{ M}^{-1} \text{ cm}^{-1}$ ) as depicted in Figure 4.26.

The titration of probe 27 with TBAOH was studied by adding increasing equivalents of the TBAOH. Upon addition of 1 equiv of TBAOH to solution of 27, as depicted in Figure 4.27, the absorption band at 338 nm showed a decrease in absorption. The addition of 2 equiv of TBAOH leads to a hypochromic shift of the band at 338 nm, which then gradually disappears. The formation of an isosbestic point at 385 nm suggested the existence of

structurally two different forms of 27 in the medium. However, continuous addition of TBAOH up to 5 equiv led to a red shift of the band to 435 nm, and then an exponential increase in the absorption of the band at 435 nm. Further addition of TBAOH (up to 20 equivs) to the solution containing probe 27 did not result in any further absorption change. This therefore indicated that the deprotonation process had been fully completed.

The fluorescence excitation spectra of fluorophore 27 were further examined by adding increasing equivalents of TBAOH. As shown in Figure 4.27, probe 27 shows a weak intensity at 395 nm. Addition of 5 equiv of TBAOH leads to a hypochromic shift of the band, followed by the appearance of an isosbestic point at 455 nm, also indicating the existence of structurally two different forms of 27 in the medium. The curve then red shifted to 493 nm. The band at 493 nm then experienced a hyperchromic shift. As was observed in the case of the absorption spectra, the fluorescence intensity also did not show any change in intensity upon further addition of 20 equiv of TBAOH.

However, as depicted in Figure 4.28 and Figure 4.26, reverse protonation study was conducted by adding 5 equiv of trifluoroacetic acid (TFA) to the solution mixture containing probe 27 and TBAOH. Adding 5 equiv of TFA to the mixture, leads to a hypochromic shift of the band at 434 nm in the UV-vis spectra, which is followed by the occurrence of an isosbestic point at 385 nm. Eventually, the restoration of the absorbance at 332 nm was accomplished, which was associated with change in coloration of the solution from blue to green. The process indicates that, the interaction of probe 27 with  ${}^{-}\text{OH}$  anion can be reversed by adding TFA. With respect to the fluorescence intensity of 27, the strong band located at 488 nm gradually quenched, followed by the development of an isosbestic point at 458 nm, and then blue shifted to 444 nm. The band at 444 nm then eventually diminishes upon addition of 5 equiv of TFA, suggesting that the intended reverse protonation has been achieved.

Again, as shown in Figure 4.29, we also observed a distinct fluorescence coloration change from blue to green with the increase addition of TBAOH (0-5 equiv) to the solution of sensor 27. The coloration change can be attributed to the availability of the phenolic  ${}^{-}\text{OH}$  of the coumarin moiety at C-7, which remains as a deprotonated ion of sensor 27 (Figure 4.26).

However, the reverse protonation of 27, using TFA indicates fluorosolvatochromism as the expected direct reversal of the color change from blue to green was not observed. As shown in Figure 4.28, rather, a light green coloration initially developed, which was then followed by the expected green color. The development of the green color was therefore rationalized by associating it with the nature of the solvent, in this case DMSO. The solvent being a polar aprotic solvent, might have accepted the already available proton, which had been removed in the deprotonation process, to form an H-bond thereafter solvated the olate ion. Upon acid dissociation of the hydroxyl attached to the C-7 of coumarin moiety of sensor 27, the deprotonated ion of sensor 27 is stabilized by solvation through hydrogen bonding between the 'accepted' hydrogen of the DMSO and the negatively charged oxygen of the deprotonated ion of sensor 27. The steric surrounding around the negatively charged oxygen influences the solvation process.

However, the entire procedure was repeated again by replacing DMSO with a solvent mixture containing DMSO/H<sub>2</sub>O, v/v, 9:1. The initial absorption band is located at 338 nm as illustrated in Figure 4.31. In the deprotonation process, in the presence of varying excess of TBAOH, the band at 338 nm gradually quenches, leading to an isosbestic point at 380 nm. Further increments of the equivalents of TBAOH leads to a red shift of the band at 380 nm to 422 nm. The band at 422 nm then shifted hyperchromically. The hyperchromic shift does not continue even upon adding 20 equiv of TBAOH. Due to the fact that receptor 27 is soluble in aqueous medium, its fluorescence spectra just shifted hyperchromically at 493 nm without undergoing any other shifts.

In reverse protonation process, using incremental additions of TFA. As shown in Figure 4.32, an absorption band which is at 420 nm quenches bit by bit until an isosbestic point was reached at 376 nm. A hypsochromic shift occurred leading to the development of a band at 340 nm. The band at 340 nm eventually shifted hyperchromically and did not increase again, even with the addition of 20 equiv of TFA. The fluorescence intensity shows an intense band at 490 nm. The band at 490 nm shows a step by step quenching upon adding 5 equiv of TFA.

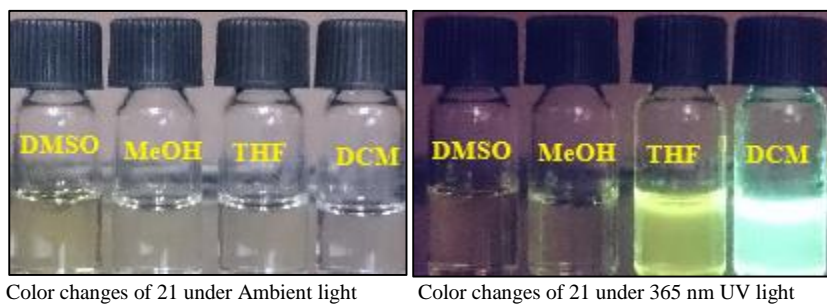


Figure 4.1. Color and emission changes of 21 (10  $\mu$ M) in various solvents

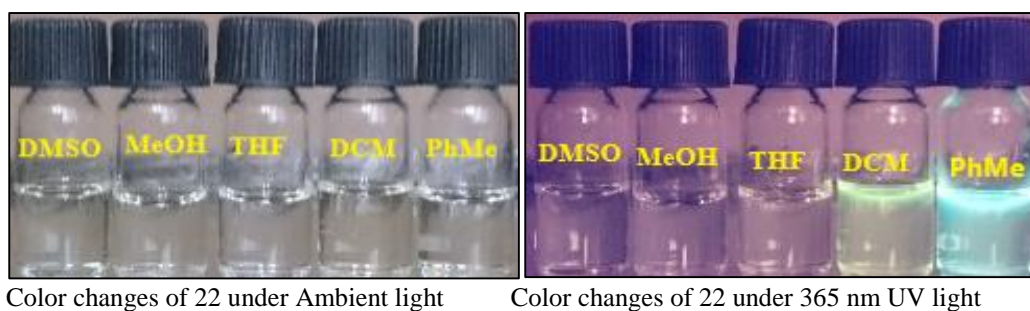


Figure 4.2. Color and emission changes of 22 (10  $\mu$ M) in various solvents



Figure 4.2. Color and emission changes of 23 (10  $\mu$ M) in various solvents

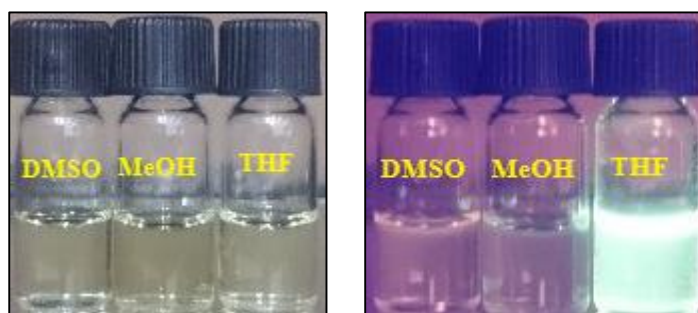
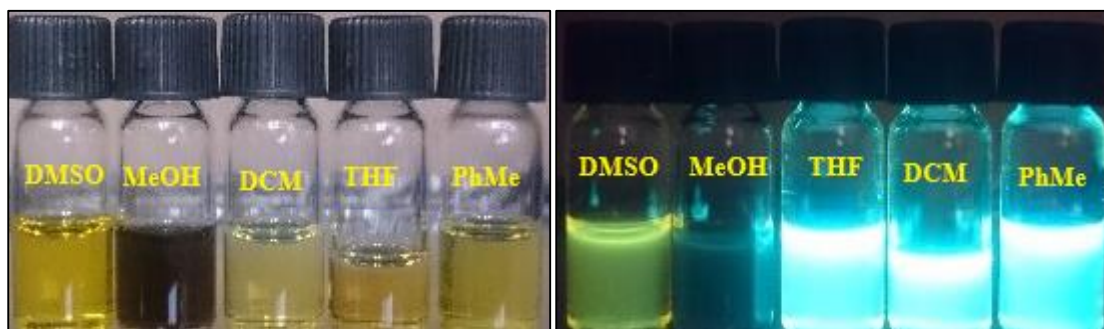


Figure 4.3. Color and emission changes of 24 (10  $\mu$ M) in various solvents



Color changes of 25 under Ambient light

Color changes of 25 under 365 nm UV light

Figure 4.5. Color and emission changes of 25 (10  $\mu$ M) in various solvents

Color changes of 26 under Ambient light

Color changes of 26 under 365 nm UV light

Figure 4.4. Color and emission changes of 26 (10  $\mu$ M) in various solvents

Color changes of 27 under Ambient light

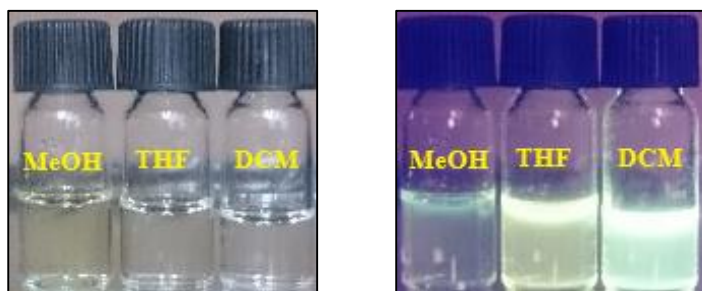
Color changes of 27 under 365 nm UV light

Figure 4.5. Color and emission changes of 27 (10  $\mu$ M) in various solvents

Color changes of 28 under Ambient light

Color changes of 28 under 365 nm UV light

Figure 4.6. Color and emission changes of 28 (10  $\mu$ M) in various solvents



Color changes of 29 under Ambient light    Color changes of 29 under 365 nm UV light

Figure 4.7. Color and emission changes of 29 (10  $\mu$ M) in various solvents



Color changes of 30 under Ambient light    Color changes of 30 under 365 nm UV light

Figure 4.8. Color and emission changes of 30 (10  $\mu$ M) in various solvents



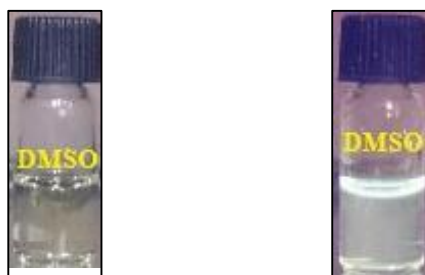
Color changes of 31 under Ambient light    Color changes of 31 under 365 nm UV light

Figure 4.11. Color and emission changes of 31 (10  $\mu$ M) in various solvents



Color changes of 32 under Ambient light    Color changes of 32 under 365 nm UV light

Figure 4.9. Color and emission changes of 32 (10  $\mu$ M) in DMSO



Color changes of 33 under Ambient light    Color changes of 33 under 365 nm UV light

Figure 4.10. Color changes of 33 (10  $\mu$ M) in DMSO

Color changes of 34 under Ambient light    Color changes of 34 under 365 nm UV light

Figure 4.11. Color and emission changes of 34 (10  $\mu$ M) in various solvents

Color changes of 35 under Ambient light    Color changes of 35 under 365 nm UV light

Figure 4.12. Color and emission changes of 35 (10  $\mu$ M) in various solvents

Table 4.9. Photophysical activities of 21-23

Solvent	21				22				23			
	$\lambda_{\text{abs-max}}^a$ (nm)	$\lambda_{\text{fl-max}}^b$ (nm)	Stokes Shift <sup>c</sup> (nm)	$\epsilon^d$ ( $\lambda_{\text{max}}$ )	$\lambda_{\text{abs-max}}^a$ (nm)	$\lambda_{\text{fl-max}}^b$ (nm)	Stokes Shift <sup>c</sup> (nm)	$\epsilon^d$ ( $\lambda_{\text{max}}$ )	$\lambda_{\text{abs-max}}^a$ (nm)	$\lambda_{\text{fl-max}}^b$ (nm)	Stokes Shift <sup>c</sup> (nm)	$\epsilon^d$ ( $\lambda_{\text{max}}$ )
DMSO	364	479	115	5060	348	- <sup>f</sup>	- <sup>f</sup>	7070	333	439	106	10700
DCM	341	504	163	12960	352	523	171	7940	350	509	159	10960
THF	324	526	202	10640	348	508	160	6650	345	537	192	10360
MeOH	320	457	137	9360	345	- <sup>f</sup>	- <sup>f</sup>	6810	340	448	108	7340
PhMe	- <sup>e</sup>	- <sup>e</sup>	- <sup>e</sup>	- <sup>e</sup>	354	499	145	8670	354	491	137	9440

<sup>a</sup>Long wavelength absorption maximum, in nm;  $c = 10 \mu\text{M}$ .<sup>b</sup>Fluorescence maximum, in nm;  $c = 0.1 \mu\text{M}$ .<sup>c</sup>Stokes shift is calculated according to the underlined value.<sup>d</sup> $\epsilon$ = molar absorption coefficient,  $\text{cm}^{-1}\text{M}^{-1}$ .<sup>e</sup>Compound was not soluble in this solvent<sup>f</sup>Not available

Table 4.10. Photophysical activities of 24-26

Solvent	24				25				26			
	$\lambda_{\text{abs-max}}^{\text{a}}$ (nm)	$\lambda_{\text{fl-max}}^{\text{b}}$ (nm)	Stokes Shift <sup>c</sup> (nm)	$\epsilon^{\text{d}}$ ( $\lambda_{\text{max}}$ )	$\lambda_{\text{abs-max}}^{\text{a}}$ (nm)	$\lambda_{\text{fl-max}}^{\text{b}}$ (nm)	Stokes Shift <sup>c</sup> (nm)	$\epsilon^{\text{d}}$ ( $\lambda_{\text{max}}$ )	$\lambda_{\text{abs-max}}^{\text{a}}$ (nm)	$\lambda_{\text{fl-max}}^{\text{b}}$ (nm)	Stokes Shift <sup>c</sup> (nm)	$\epsilon^{\text{d}}$ ( $\lambda_{\text{max}}$ )
DMSO	339	548	209	11830	406	481	75	29220	333	439	106	10700
DCM	- <sup>e</sup>	- <sup>e</sup>	- <sup>e</sup>		- <sup>e</sup>	409	467	58	51560	350	509	159
THF	339	498	159	17630	403	473	70	28810	345	537	192	10360
MeOH	339	443	104	15560	405	478	73	29340	340	448	108	7340
PhMe	- <sup>e</sup>	- <sup>e</sup>	- <sup>e</sup>	- <sup>e</sup>	402	467	65	33170	354	491	137	9440

Table 4.11. Photophysical activities of 27-29

Solvent	27				28				29			
	$\lambda_{\text{abs-max}}^{\text{a}}$ (nm)	$\lambda_{\text{fl-max}}^{\text{b}}$ (nm)	Stokes Shift <sup>c</sup> (nm)	$\epsilon^{\text{d}}$ ( $\lambda_{\text{max}}$ )	$\lambda_{\text{abs-max}}^{\text{a}}$ (nm)	$\lambda_{\text{fl-max}}^{\text{b}}$ (nm)	Stokes Shift <sup>c</sup> (nm)	$\epsilon^{\text{d}}$ ( $\lambda_{\text{max}}$ )	$\lambda_{\text{abs-max}}^{\text{a}}$ (nm)	$\lambda_{\text{fl-max}}^{\text{b}}$ (nm)	Stokes Shift <sup>c</sup> (nm)	$\epsilon^{\text{d}}$ ( $\lambda_{\text{max}}$ )
DMSO	340	413	73	14430	300	544	244	22400	- <sup>e</sup>	- <sup>e</sup>	- <sup>e</sup>	- <sup>e</sup>
DCM	- <sup>e</sup>	- <sup>e</sup>	- <sup>e</sup>	- <sup>e</sup>	300	499	199	7650	347	500	153	11170
THF	340	493	153	18200	300	519	219	16100	351	520	169	9820
MeOH	340	432	92	15350	350	471	121	60200	320	- <sup>f</sup>	- <sup>f</sup>	- <sup>f</sup>
PhMe	- <sup>e</sup>	- <sup>e</sup>	- <sup>e</sup>	- <sup>e</sup>	303	478	175	10650	- <sup>e</sup>	- <sup>e</sup>	- <sup>e</sup>	- <sup>e</sup>

Table 4.12. Photophysical activities of 30

Solvent	$\lambda_{\text{abs-max}}^{\text{a}}$ (nm)	$\lambda_{\text{fl-max}}^{\text{b}}$ (nm)	Stokes Shift <sup>c</sup> (nm)	$\epsilon^{\text{d}}$ ( $\lambda_{\text{max}}$ )
DMSO	367	462	95	12330
DCM	381	474	93	12960
THF	370	467	97	13610
MeOH	- <sup>e</sup>	- <sup>e</sup>	- <sup>e</sup>	- <sup>e</sup>
PhMe	- <sup>e</sup>	- <sup>e</sup>	- <sup>e</sup>	- <sup>e</sup>

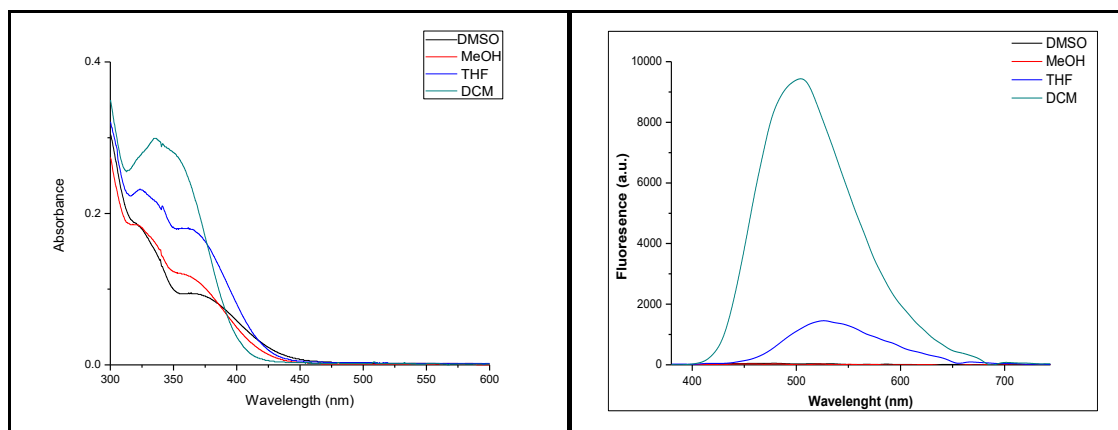


Figure 4.16. UV-vis absorption spectra of 21 (left), Fluorescence emission spectra of 21(right)

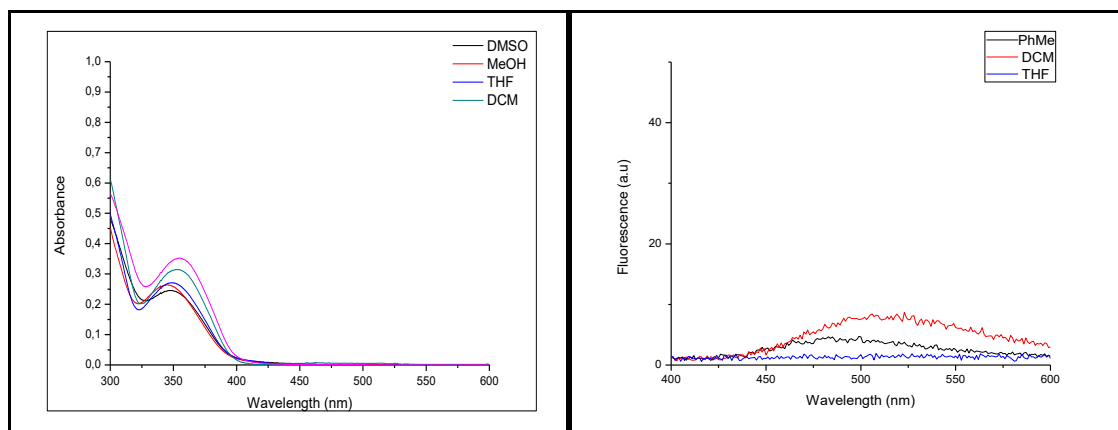


Figure 4.13. UV-vis absorption spectra of 22 (left). Fluorescence emission spectra of 22 (right)

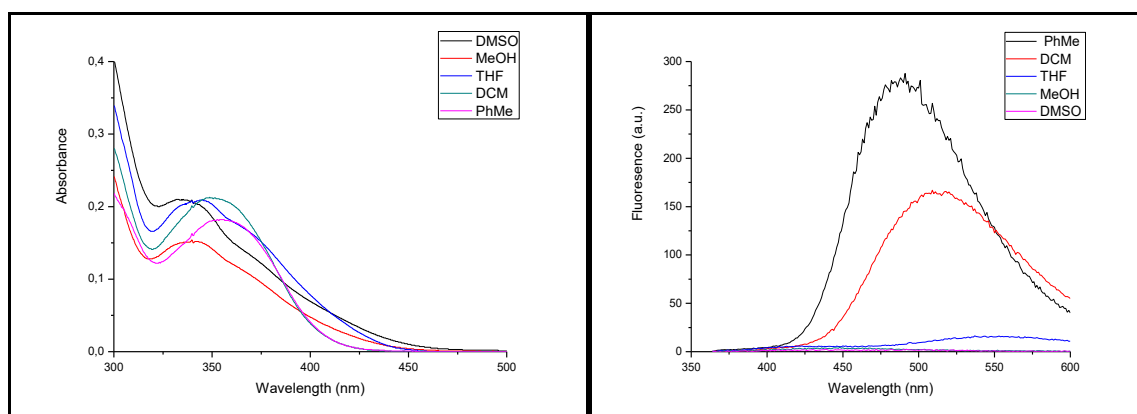


Figure 4.14. UV-vis absorption spectra of 23 (left). Fluorescence emission spectra of 23 (right)

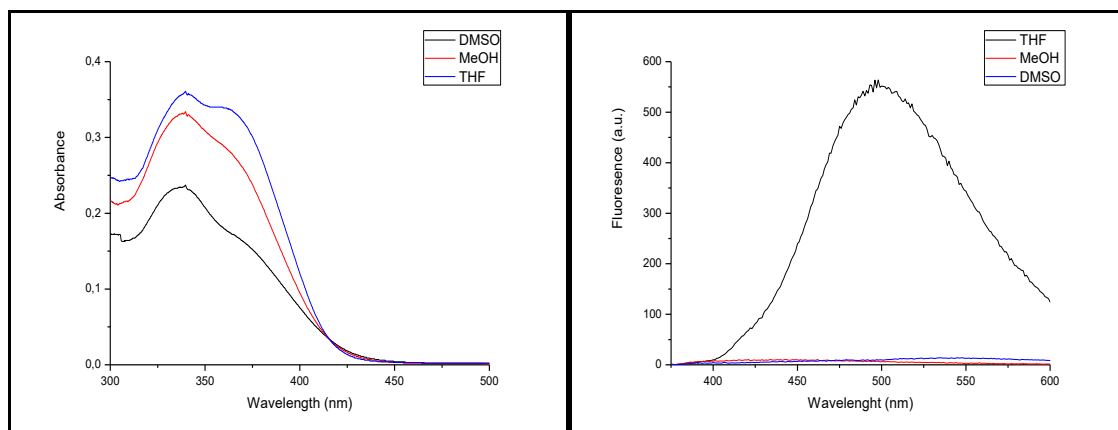


Figure 4.15. UV-vis absorption spectra of 24 (left). Fluorescence emission spectra of 24 (right)

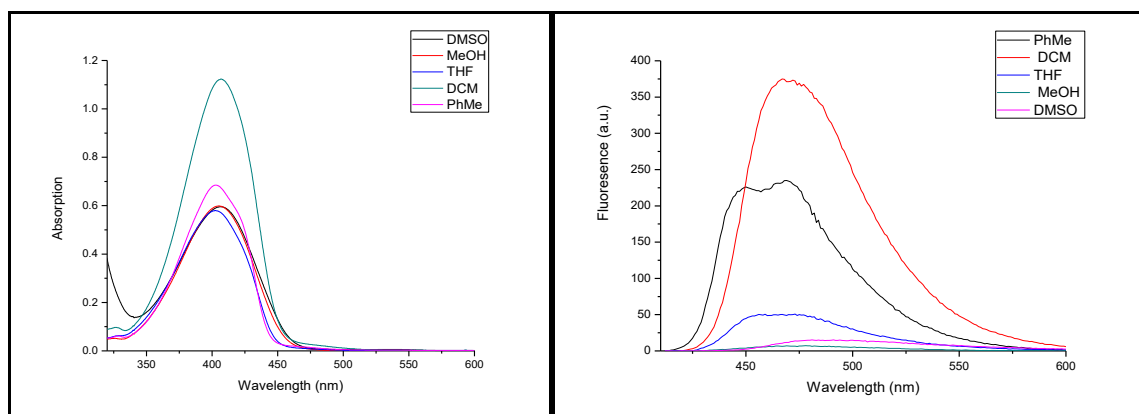


Figure 4.16. UV-vis absorption spectra of 25 (left), Fluorescence emission spectra of 25 (right)

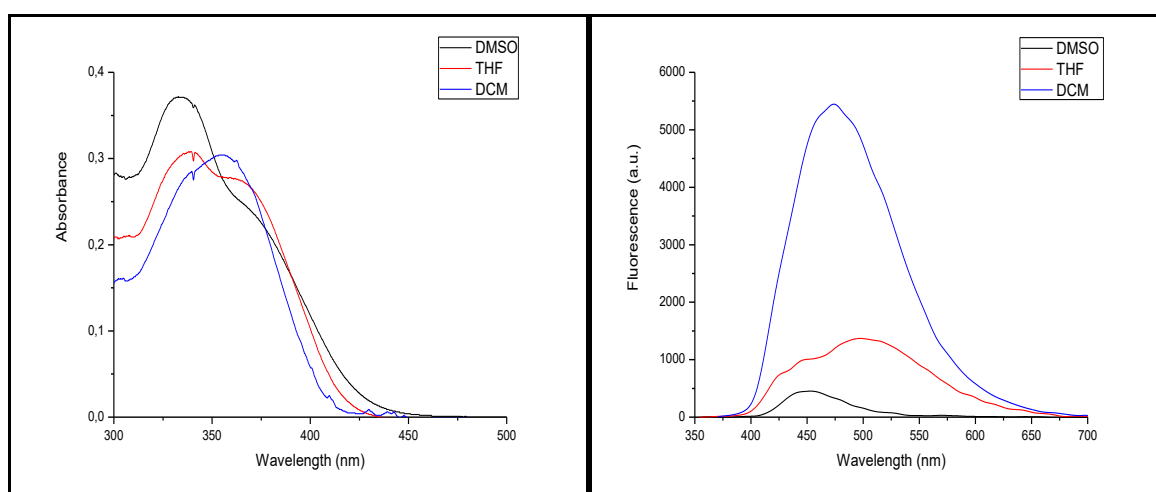


Figure 4.17. UV-vis absorption spectra of 26 (left). Fluorescence emission spectra of 26 (right)

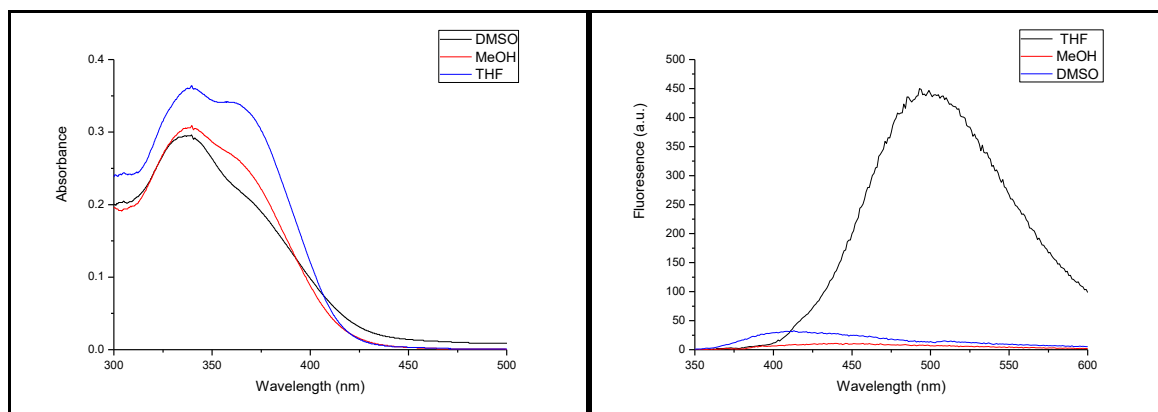


Figure 4.18. UV-vis absorption spectra of 27 (left), Fluorescence emission spectra of 27 (right)

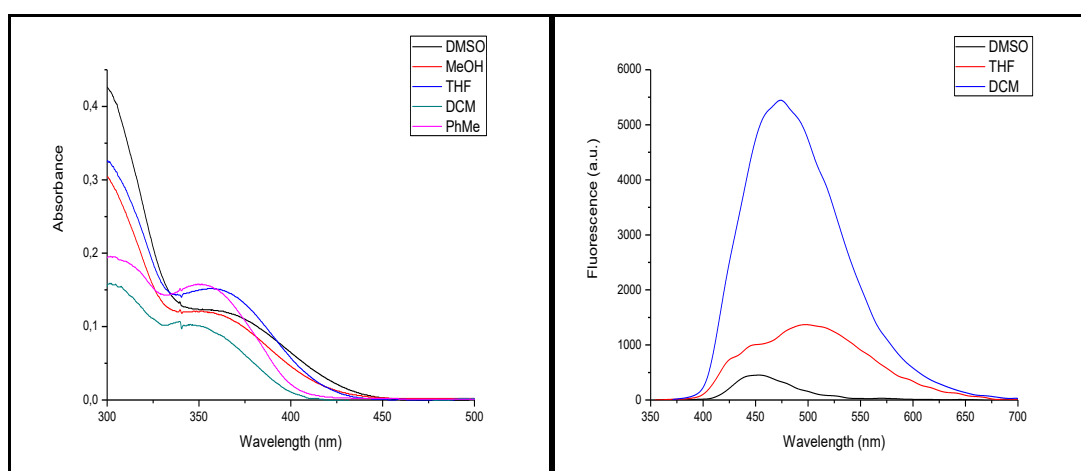


Figure 4.19. UV-vis absorption spectra of 28 (left). Fluorescence emission spectra of 28 (right)

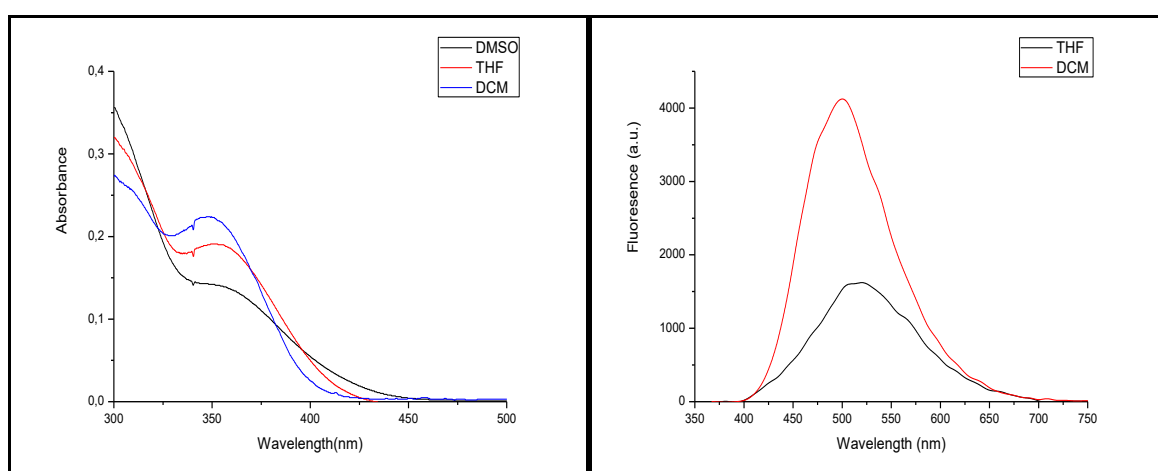


Figure 4.20. UV-vis absorption spectra of 29 (left). Fluorescence emission spectra of 29 (right)

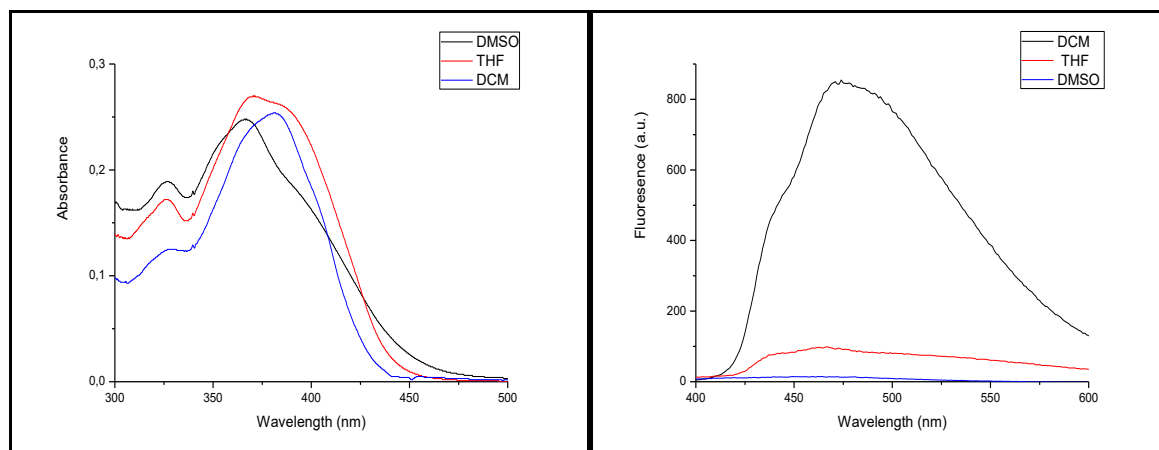


Figure 4.21. UV-vis absorption spectra of 30 (left). Fluorescence emission spectra of 30 (right)

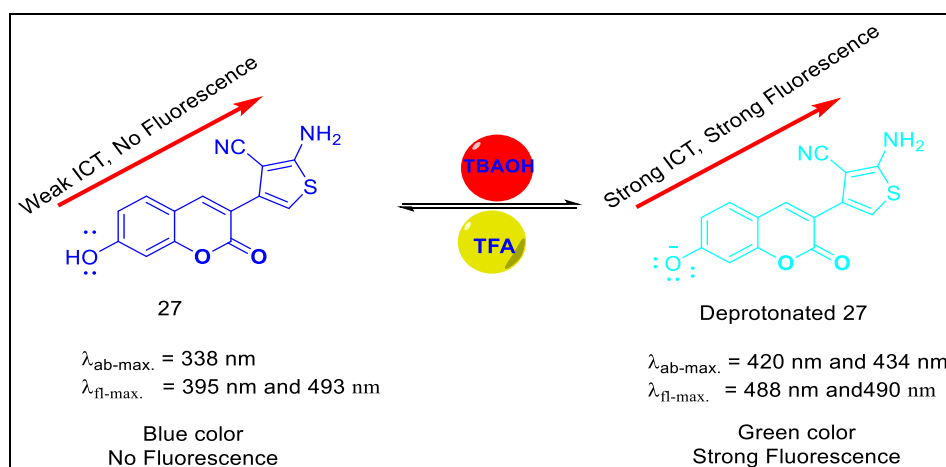


Figure 4.22. Deprotonation and Reverse protonation of 27

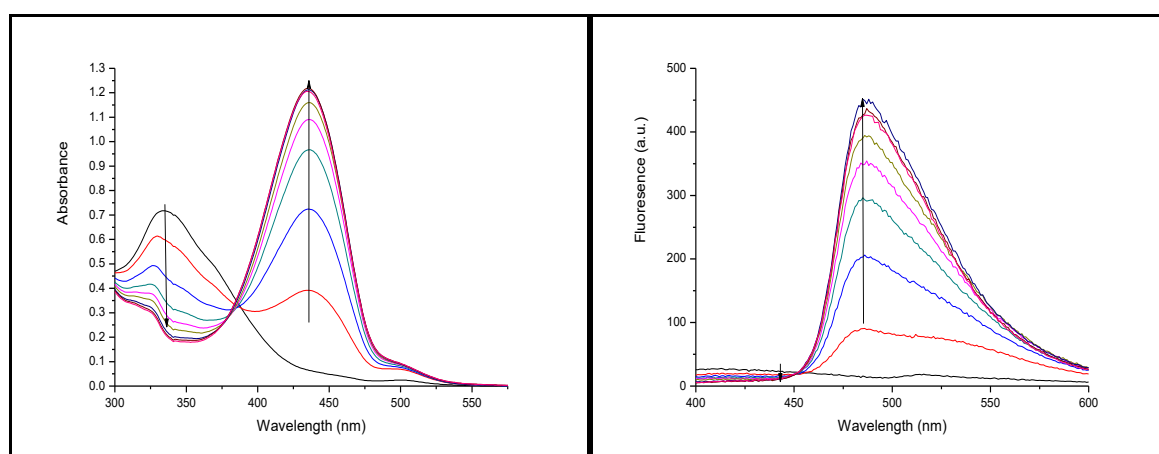


Figure 4.23. Left: UV-vis absorption spectrum of the titration of 27 (10  $\mu\text{M}$ ) in DMSO with incremental addition of TBAOH (0-20 equiv.) in DMSO solution; Right: Fluorescent emission spectra of the titration of 27 (10  $\mu\text{M}$ ) with incremental addition of TBAOH (0-20 equiv.) in DMSO solution

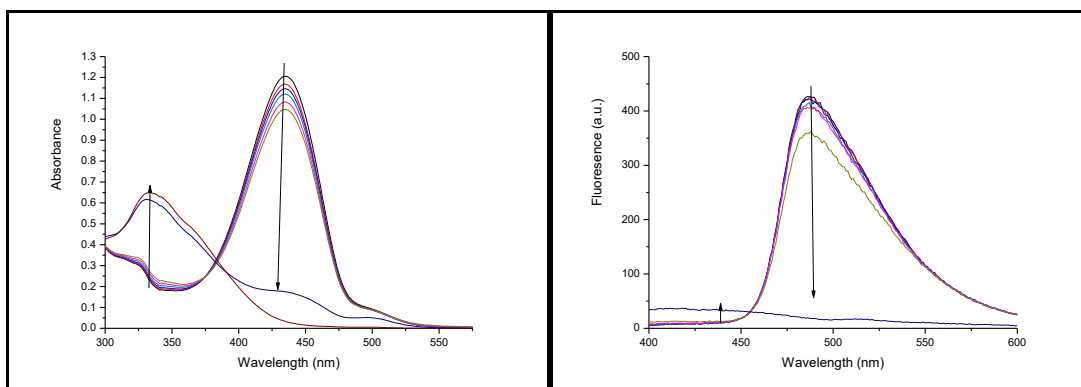


Figure 4.24. Left: UV-vis absorption spectrum of the titration of a mixture containing 27 (10  $\mu\text{M}$ ) in DMSO and TBAOH (0-20 equiv.) in DMSO, with the incremental addition of TFA (0-20 equiv) in DMSO solution; Right: Fluorescent emission spectrum of the titration of a mixture containing 27 (10  $\mu\text{M}$ ) and TBAOH (0-20 equiv.) in DMSO, with the incremental addition of TFA (0-20 equiv) in DMSO solution



Figure 4.25. Left: Color change under Ambient light for the titration of 27 (10  $\mu\text{M}$ ) in DMSO with incremental addition of TBAOH (0-5 equiv) in DMSO solution; Right: Color change under 365 nm UV light for the titration of 27 (10  $\mu\text{M}$ ) with incremental addition of TBAOH (0-5 equiv) in DMSO solution. Description; 1: Host; 2: Host + TBAOH (1 equiv); 3: Host + TBAOH (2 equiv); 4: Host + TBAOH (3 equiv); 5: Host + TBAOH (4 equiv); 6: Host + TBAOH (5 equiv)



Figure 4.26. Left: Color change under Ambient light for the titration of a mixture containing 27 (10  $\mu\text{M}$ ) in DMSO and TBAOH (0-5 equiv.) in DMSO, with the incremental addition of TFA (0-5 equiv) in DMSO solution; Right: Color change under 365 nm UV light for the titration of a mixture containing 3g (10  $\mu\text{M}$ ) and TBAOH (0-5 equiv.) in DMSO, with the incremental addition of TFA (0-5 equiv) in DMSO solution. Description; 1: Host + TBAOH (5 equiv) + TFA (1 equiv); 2: Host + TBAOH (5 equiv) + TFA (2 equiv); 3: Host + TBAOH (5 equiv) + TFA (3 equiv); 4: Host + TBAOH (5 equiv) + TFA (4 equiv); 5: Host + TBAOH (5 equiv) + TFA (5 equiv)

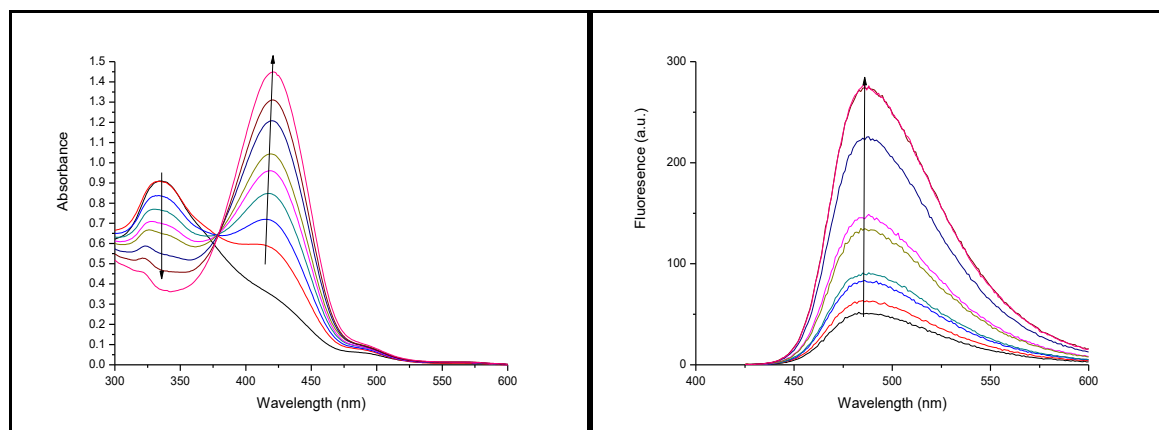


Figure 4.27. Left: UV-vis absorption spectrum of the titration of 27 (10 μM) in DMSO/H<sub>2</sub>O solution with incremental addition of TBAOH (0-20 equiv.) in DMSO solution; Right: Fluorescent emission spectra of the titration of 27 (10 μM) with incremental addition of TBAOH (0-20 equiv) in DMSO solution

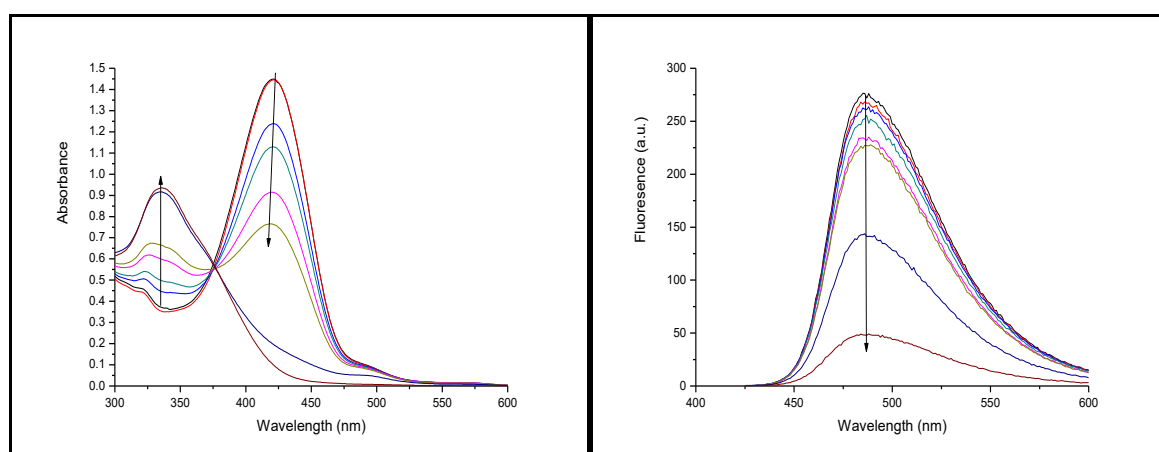


Figure 4.28. Left: UV-vis absorption spectrum of the titration of a mixture containing 27 (10 μM) in DMSO/H<sub>2</sub>O solution, and TBAOH (0-20 equiv.) in DMSO, with the incremental addition of TFA (0-20 equiv) in DMSO solution; Right: Fluorescent emission spectrum of the titration of a mixture containing 27 (10 μM) and TBAOH (0-20 equiv.) in DMSO, with the incremental addition of TFA (0-20 equiv) in DMSO solution

## 4.2. Thermal properties of dyes 21-35

Thermogravimetric analysis is a good method to investigate the thermal stability of a compound, by measuring the change in weight as a function of the temperature. The prepared compounds 21-35 in this study are fluorescently active dyes and have potential for usage as fluorescent emitters. The light emitting potential of these dyes in the solid state is linked to their thermal stability, thus the dyes 21-35 were subjected to

thermogravimetric analysis (TGA). The change in weight of the compounds was measured as a function of temperature. This TGA plot, as depicted in Figure 4.33, shows the decomposition of 21-35 in air. Each measurement curve of the dyes 21-35 was taken between 100 °C and 1000 °C. The decompositions of the dyes 21-29 and 31-35 occur in three mass-loss steps, but that of 30 occurs in two mass-loss steps. The three-step mass-loss decomposition of dyes 21-29 and 31-35 occur as follows; 21 (300 °C, 360 °C, 670 °C), 22 (230 °C, 280 °C, 510 °C), 23 (230 °C, 380 °C, 540 °C), 24 (300 °C, 390 °C, 490 °C), 25 (300 °C, 420 °C, 520 °C), 26 (300 °C, 420 °C, 490 °C), 27 (290 °C, 360 °C, 480 °C), 28 (300 °C, 400 °C, 500 °C), 29 (230 °C, 370 °C, 500 °C), 31 (247 °C, 355 °C, 522 °C), 32 (318 °C, 373 °C, 473 °C), 33(298 °C, 379 °C, 487 °C), 34 (257 °C, 292 °C, 473 °C), and 35 (220 °C, 353 °C, 475 °C), and the two-step mass-loss decomposition of 30 (230 °C, 520 °C). All the compounds show no weight loss up to 80 °C. The absence of weight loss up to 80 °C indicates that no water molecules are present in all the dyes 21-35 in solid state. The least initial decomposition temperature (Td) for all the dyes 21-35 was found to be 220 °C. Therefore, up to 220 °C, all the fluorescent dyes are fairly stable and hence have potential to be employed as optical dyes.

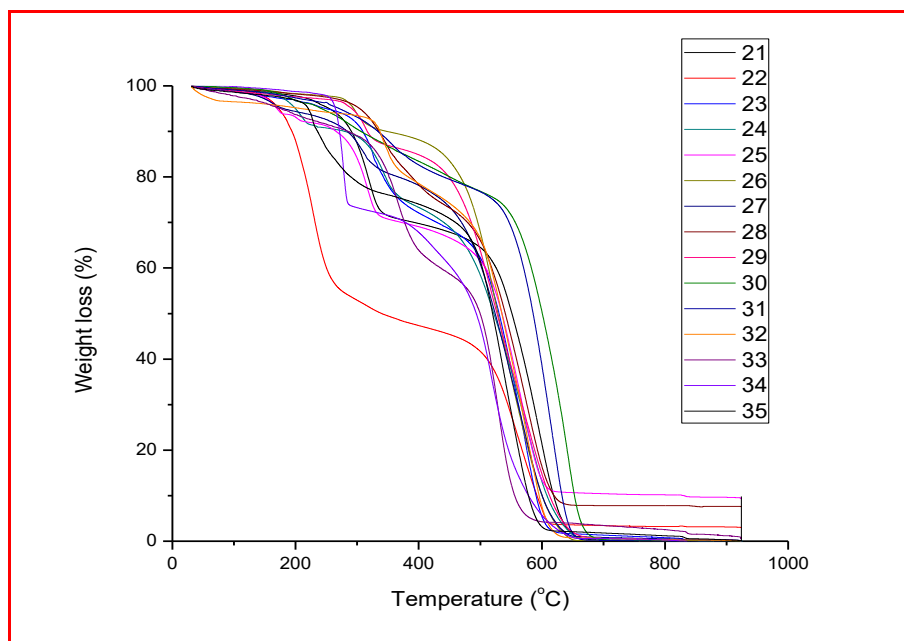


Figure 4.29. TGA curves for the decomposition of 21-35



## 5. CONCLUSION AND RECOMMENDATIONS

In summary, using the protocols for the synthesis of the 3-acetylcoumarins, the malononitriles, and the coumarin-thiophene hybrids (using the step-wise and the one-pot three-component procedure), it has been discovered that, the MWI protocols were more efficient (yields 90-100 %, Table 4.9) than the CM (yields 80-98 %, Table 4.9), in relation to reaction period, enhanced yields, and purity of compounds. These results also indicate that, the MWI procedures are inexpensive and can be used as an alternative in this kind of reaction systems. For the synthesis of the coumarin-thiophene hybrids via the one-pot three-component procedure, the procedure herein has been found to be better (80-90 %, Table 4.10) compared to a similar procedure [70] which reported less yields (77-89 %). The stepwise procedure also better yields of 80-96 % (Table 4.10) than the 2014 literature procedure (78-86 %) [70]. It is therefore clear that the previous procedures have been significantly improved.

It is evident, and can be concluded, that the microwave-assisted reactions are extremely beneficial, in terms of reaction rate, purity of products, yields and energy consumption than the conventional procedures. Most reactions that do not take place under conventional procedure can easily be achieved with high yields and better quality under microwave-assisted irradiation protocols. Finally, the compounds 21-35 were tested for thermal stability and were found to be thermally stable up to at least 220 °C, which means that they can be applied as optical dyes.

It is recommended that future work on the derivatives of the hydroxyl derivatives, should be done for use as fluorescent biothiol probes or for solely detection of low molecular weight aminothiols such as homocysteine (Hcy), cysteine (Cys), and glutathione (GSH), play different important roles in biological systems.



## REFERENCES

1. Lafitte, D., Lamour, V., Tsvetkov, P. O., Makarov, A. A., Klich, M., Deprez, P., and Gilli, R. (2002). DNA gyrase interaction with coumarin-based inhibitors: The role of the hydroxybenzoate isopentenyl moiety and the 5 '-methyl group of the Noviose. *Biochemistry*, 41(23), 7217-7223.
2. Galeotti, F., Barile, E., Lanzotti, V., Dolci, M., and Curir, P. (2008). Quantification of major flavonoids in carnation tissues (*Dianthus caryophyllus*) as a tool for cultivar discrimination. *Zeitschrift für Naturforschung C*, 63(3-4), 161-168.
3. Maucher, A., and Von Angerer, E. (1994). Antitumour activity of coumarin and 7-hydroxycoumarin against 7, 12-dimethylbenz [a] anthracene-induced rat mammary carcinomas. *Journal of cancer research and clinical oncology*, 120(8), 502-504.
4. Hwu, J. R., Singha, R., Hong, S. C., Chang, Y. H., Das, A. R., Vliegen, I., and Neyts, J. (2008). Synthesis of new benzimidazole–coumarin conjugates as anti-hepatitis C virus agents. *Antiviral Research*, 77(2), 157-162.
5. Kirkiacharian, S., Thuy, D. T., Sicsic, S., Bakhchinian, R., Kurkjian, R., and Tonnaire, T. (2002). Structure–activity relationships of some 3-substituted-4-hydroxycoumarins as HIV-1 protease inhibitors. *II Farmaco*, 57(9), 703-708.
6. Lee, Y. Y., Lee, S., Jin, J. L., and Yun-Choi, H. S. (2003). Platelet anti-aggregatory effects of coumarins from the roots of *Angelica genuflexa* and *A. gigas*. *Archives of Pharmacal Research*, 26(9), 723-726.
7. Soyer, A., Özalp, B., Dalmış, Ü., and Bilgin, V. (2010). Effects of freezing temperature and duration of frozen storage on lipid and protein oxidation in chicken meat. *Food Chemistry*, 120(4), 1025-1030.
8. Ducharme, Y., Blouin, M., Brideau, C., Châteauneuf, A., Gareau, Y., Grimm, E. L., and Ouellet, M. (2010). The discovery of setileuton, a potent and selective 5-lipoxygenase inhibitor. *American Chemical Society Medicinal Chemistry Letters*, 1(4), 170-174.
9. Fylaktakidou, K. C., Hadjipavlou-Litina, D. J., Litinas, K. E., and Nicolaidis, D. N. (2004). Natural and synthetic coumarin derivatives with anti-inflammatory/antioxidant activities. *Current Pharmaceutical Design*, 10(30), 3813-3833.
10. Gleye, C., Lewin, G., Laurens, A., Jullian, J. C., Loiseau, P., Bories, C., and Hocquemiller, R. (2003). Acaricidal Activity of Tonka Bean Extracts. Synthesis and Structure– Activity Relationships of Bioactive Derivatives. *Journal of Natural Products*, 66(5), 690-692.
11. Rashamuse, T. J. (2008). *In studies towards the synthesis of novel, coumarin-based HIV-1 protease inhibitors*. Ph. D. Thesi, Rhodes University Department of Chemistry, Grahamstown.

12. Medina, F. G., Marrero, J. G., Macías-Alonso, M., González, M. C., Córdova-Guerrero, I., García, A. G. T., and Osegueda-Robles, S. (2015). Coumarin heterocyclic derivatives: chemical synthesis and biological activity. *Natural Product Reports*, 32(10), 1472-1507.
13. Kwak, J. H., Lee, K. B., and Schmitz, F. J. (2001). Four new coumarin derivatives from artemisia k eiskeana. *Journal of Natural Products*, 64(8), 1081-1083.
14. Hoult, J. R. S., and Paya, M. (1996). Pharmacological and biochemical actions of simple coumarins: natural products with therapeutic potential. *General Pharmacology: The Vascular System*, 27(4), 713-722.
15. Vukovic, N., Sukdolak, S., Solujic, S., and Niciforovic, N. (2010). Substituted imino and amino derivatives of 4-hydroxycoumarins as novel antioxidant, antibacterial and antifungal agents: Synthesis and in vitro assessments. *Food Chemistry*, 120(4), 1011-1018.
16. Fan, H., Peng, J., Hamann, M. T., and Hu, J. F. (2008). Lamellarins and related pyrrole-derived alkaloids from marine organisms. *Chemical Reviews*, 108(1), 264-287.
17. Ridley, C. P., Reddy, M. V. R., Rocha, G., Bushman, F. D., and Faulkner, D. J. (2002). Total synthesis and evaluation of lamellarin  $\alpha$  20-sulfate analogues. *Bioorganic & Medicinal Chemistry*, 10(10), 3285-3290.
18. Reddy, S. M., Srinivasulu, M., Satyanarayana, N., Kondapi, A. K., and Venkateswarlu, Y. (2005). New potent cytotoxic lamellarin alkaloids from Indian ascidian *Didemnum obscurum*. *Tetrahedron*, 61(39), 9242-9247.
19. McKee, T. C., Fuller, R. W., Covington, C. D., Cardellina, J. H., Gulakowski, R. J., Krepps, B. L., and Boyd, M. R. (1996). New pyranocoumarins isolated from *Calophyllum lanigerum* and *Calophyllum teysmannii*. *Journal of Natural Products*, 59(8), 754-758.
20. Flavin, M. T., Rizzo, J. D., Khilevich, A., Kucherenko, A., Sheinkman, A. K., Vilaychack, V., and Pezzuto, J. M. (1996). Synthesis, chromatographic resolution, and anti-human immunodeficiency virus activity of ( $\pm$ )-calanolide A and its enantiomers. *Journal of Medicinal Chemistry*, 39(6), 1303-1313.
21. Patil, A. D., Freyer, A. J., Eggleston, D. S., Haltiwanger, R. C., Bean, M. F., Taylor, P. B., and Bartus, H. R. (1993). The inophyllums, novel inhibitors of HIV-1 reverse transcriptase isolated from the Malaysian tree, *Calophyllum inophyllum* Linn. *Journal of Medicinal Chemistry*, 36(26), 4131-4138.
22. Ranjith, H., Dharmaratne, W., Sotheeswaran, S., Balasubramaniam, S., and Waight, E. S. (1985). Triterpenoids and coumarins from the leaves of *Calophyllum Cordato-Oblongum*. *Phytochemistry*, 24(7), 1553-1556.
23. Al-Amiery, A. A., Musa, A. Y., Kadhun, A. A. H., and Mohamad, A. B. (2011). The use of umbelliferone in the synthesis of new heterocyclic compounds. *Molecules*, 16(8), 6833-6843.

24. Ramesh, B., Viswanathan, P., and Pugalendi, K. V. (2007). Protective effect of Umbelliferone on membranous fatty acid composition in streptozotocin-induced diabetic rats. *European Journal of Pharmacology*, 566(1-3), 231-239.
25. Hafez, O. M. A., Amin, K. M., Abdel-Latif, N. A., Mohamed, T. K., Ahmed, E. Y., and Maher, T. (2009). Synthesis and antitumor activity of some new xanthotoxin derivatives. *European Journal of Medicinal Chemistry*, 44(7), 2967-2974.
26. Wulff, W. D., McCallum, J. S., and Kunng, F. A. (1988). Two regiocomplementary approaches to angular furanocoumarins with chromium carbene complexes: synthesis of sphondin, thiosphondin, heratomin, and angelicin. *Journal of the American Chemical Society*, 110(22), 7419-7434.
27. Magiatis, P., Melliou, E., Skaltsounis, A. L., Mitaku, S., Léonce, S., Renard, P., and Atassi, G. (1998). Synthesis and cytotoxic activity of pyranocoumarins of the seselin and xanthyletin series. *Journal of Natural Products*, 61(8), 982-986.
28. Dong, J., and Du, D. M. (2012). Highly enantioselective synthesis of Warfarin and its analogs catalysed by primary amine–phosphinamide bifunctional catalysts. *Organic and Biomolecular Chemistry*, 10(40), 8125-8131.
29. Tasiar, M., Kim, D., Singha, S., Krzeszewski, M., Ahn, K. H., and Gryko, D. T. (2015).  $\pi$ -Expanded coumarins: synthesis, optical properties and applications. *Journal of Materials Chemistry C*, 3(7), 1421-1446.
30. Lin, Z., Zhang, W., Wang, L., Yu, H., and Wu, C. (2003). Mechanism of the synergistic toxicity of malononitrile and p-nitrobenzaldehyde with photobacterium phosphoreum. *Toxicology Mechanisms and Methods*, 13(4), 241-245.
31. Hussein, A. H. M., Gad-Elkareem, M. A., El-Adasy, A. B. A., Khames, A. A., and Othman, I. M. (2012).  $\beta$ -oxoanilides in heterocyclic synthesis: synthesis and antimicrobial activity of pyridines, pyrans, pyrimidines and azolo, azinopyrimidines incorporating antipyrine moiety. *International Journal of Organic Chemistry*, 2(04), 341.
32. Al-Adiwish, W. M., Yaacob, W. A., Adan, D., and Nazlina, I. (2012). Synthesis and antibacterial activity of thiophenes. *International Journal on Advanced Science, Engineering and Information Technology*, 2(4), 298-301.
33. Mandour, A., El-Sawy, E., Ebaid, M., and Hassan, S. (2012). Synthesis and potential biological activity of some novel 3-[(N-substituted indol-3-yl)methyleneamino]-6-amino-4-aryl-pyrano (2, 3-c) pyrazole-5-carbonitriles and 3, 6-diamino-4-(N-substituted indol-3-yl) pyrano (2, 3-c) pyrazole-5-carbonitriles. *Acta Pharmaceutica*, 62(1), 15-30.
34. Mungra, D. C., Patel, M. P., and Patel, R. G. (2009). An efficient one-pot synthesis and in vitro antimicrobial activity of new pyridine derivatives bearing the tetrazoloquinoline nucleus. *Arkivoc*, 14, 64-74.

35. Velasco, J., Perez-Mayoral, E., Calvino-Casilda, V., Lopez-Peinado, A. J., Banares, M. A., and Soriano, E. (2015). Imidazolium sulfonates as environmental-friendly catalytic systems for the synthesis of biologically active 2-amino-4 h-chromenes: Mechanistic insights. *The Journal of Physical Chemistry B*, 119(36), 12042-12049.
36. El-Shekeil, A., Obeid, A. O., and Al-Aghbari, S. (2012). Anticancer activity studies of some cyclic benzimidazole derivatives. *European Journal of Chemistry*, 3(3), 356-358.
37. Hassaneen, H. M., Abunada, N. M., & Hassaneen, H. M. (2010). Synthesis of some new indeno [1, 2-e] pyrazolo [5, 1-c]-1, 2, 4-triazin-6-one and indeno [2, 1-c] pyridazine-4-carbonitrile derivatives. *Natural Science*, 2(12), 1349.
38. Niranjanea, K., and Kaleb, M. (2011). Synthesis and anti-inflammatory activity of some novel derivatives of 2-amino-3-cyano-14-imino-10-methoxy-4-methylthio pyrimido [2, 1-b] pyrazolo [4, 5-d] pyrimido [2, 1-b] benzothiazole. *Der Pharmacia Lettre*, 3(2), 276-283.
39. Fadda, A. A., Berghot, M. A., Amer, F. A., Badawy, D. S., and Bayoumy, N. M. (2012). Synthesis and antioxidant and antitumor activity of novel pyridine, chromene, thiophene and thiazole derivatives. *Archiv der Pharmazie*, 345(5), 378-385.
40. El-fiky, B. A. (2015). Study the antitumor activity of copper (II) complex of 4-azomalononitrile antipyrine on mice induced with earlich ascites carcinoma cells. *Journal of Environmental Bioremediation and Toxicology*, 2(2), 42-47.
41. Deng, H., Hu, H., He, M., Hu, J., Niu, W., Ferrie, A. M., and Fang, Y. (2011). Discovery of 2-(4-methylfuran-2 (5 H)-ylidene) malononitrile and thieno [3, 2-b] thiophene-2-carboxylic acid derivatives as G protein-coupled receptor 35 (GPR35) agonists. *Journal of Medicinal Chemistry*, 54(20), 7385-7396.
42. Heyde, C., Zug, I., and Hartmann, H. (2000). A simple route to n, n-dialkyl derivatives of 2-amino-5-thiophenecarboxylates. *European Journal of Organic Chemistry*, 2000(19), 3273-3278.
43. Noack, A., and Hartmann, H. (2002). Synthesis and characterisation of N, N-disubstituted 2-amino-5-acylthiophenes and 2-amino-5-acylthiazoles. *Tetrahedron*, 58(11), 2137-2146.
44. Jagodziński, T. S. (2003). Thioamides as useful synthons in the synthesis of heterocycles. *Chemical Reviews*, 103(1), 197-228.
45. Puterová, Z., Krutošiková, A., and Végh, D. (2010). Gewald reaction: synthesis, properties and applications of substituted 2-aminothiophenes. *Archive for Organic Chemistry*, 1(2010), 209-246.
46. Zeika, O., and Hartmann, H. (2004). On the oxidative coupling of N, N-disubstituted 2-aminothiophenes—synthesis of N, N'-persubstituted 5, 5'-diamino-2, 2'-bithiophenes. *Tetrahedron*, 60(37), 8213-8219.

47. Yen, M. S., and Wang, J. (2004). Synthesis and absorption spectra of hetarylazo dyes derived from coupler 4-aryl-3-cyano-2-aminothiophenes. *Dyes and Pigments*, 61(3), 243-250.
48. Bhushan, R. G., Sharma, S. K., Xie, Z., Daniels, D. J., and Portoghese, P. S. (2004). A Bivalent Ligand (KDN-21) Reveals Spinal  $\delta$  and  $\kappa$  Opioid Receptors Are Organized as Heterodimers That Give Rise to  $\delta 1$  and  $\kappa 2$  Phenotypes. Selective Targeting of  $\delta$ - $\kappa$  Heterodimers. *Journal of Medicinal Chemistry*, 47(12), 2969-2972.
49. Doré, K., Dubus, S., Ho, H. A., Lévesque, I., Brunette, M., Corbeil, G., and Leclerc, M. (2004). Fluorescent polymeric transducer for the rapid, simple, and specific detection of nucleic acids at the zeptomole level. *Journal of the American Chemical Society*, 126(13), 4240-4244.
50. Rost, C., Karg, S., Riess, W., Loi, M. A., Murgia, M., and Muccini, M. (2004). Ambipolar light-emitting organic field-effect transistor. *Applied Physics Letters*, 85(9), 1613-1615.
51. Vriezema, D. M., Hoogboom, J., Velonia, K., Takazawa, K., Christianen, P. C., Maan, J. C., and Nolte, R. J. (2003). Vesicles and polymerized vesicles from thiophene-containing rod-coil block copolymers. *Angewandte Chemie International Edition*, 42(7), 772-776.
52. Yu, H. H., Pullen, A. E., Büschel, M. G., and Swager, T. M. (2004). Charge-specific interactions in segmented conducting polymers: an approach to selective ionoresistive responses. *Angewandte Chemie International Edition*, 43(28), 3700-3703.
53. Tranberg, C. E., Zickgraf, A., Giunta, B. N., Luetjens, H., Figler, H., Murphree, L. J., ... and Olsson, R. A. (2002). 2-Amino-3-aryl-4, 5-alkylthiophenes: agonist allosteric enhancers at human A1 adenosine receptors. *Journal of medicinal chemistry*, 45(2), 382-389.
54. Kourounakis, A. P., Van der Klein, P. A., and Ijzerman, A. P. (2000). Elucidation of structure-activity relationships of 2-amino-3-benzoylthiophenes: Study of their allosteric enhancing vs. antagonistic activity on adenosine A1 receptors. *Drug Development Research*, 49(4), 227-237.
55. Duffy, J. L., Kirk, B. A., Konteatis, Z., Campbell, E. L., Liang, R., Brady, E. J., and Qureshi, S. A. (2005). Discovery and investigation of a novel class of thiophene-derived antagonists of the human glucagon receptor. *Bioorganic & Medicinal Chemistry Letters*, 15(5), 1401-1405.
56. Gewald, K. (1961). The reaction of  $\alpha$ -oxo-mercaptans with nitriles. *Angewandte Chemie*, 73(3), 114-114.
57. Tanaka, K., and Toda, F. (2000). Solvent-free organic synthesis. *Chemical Reviews*, 100(3), 1025-1074.

58. Loupy, A., Petit, A., Hamelin, J., Texier-Boullet, F., Jacquault, P., and Mathe, D. (1998). New solvent-free organic synthesis using focused microwaves. *Synthesis*, 1998(09), 1213-1234.
59. Butler, R. N., and Coyne, A. G. (2010). Water: Nature's reaction enforcer comparative effects for organic synthesis "in-water" and "on-water". *Chemical Reviews*, 110(10), 6302-6337.
60. Chanda, A., and Fokin, V. V. (2009). Organic synthesis "on water". *Chemical Reviews*, 109(2), 725-748.
61. Wang, G. W., Jia, C. S., and Dong, Y. W. (2006). Benign and highly efficient synthesis of quinolines from 2-aminoarylketone or 2-aminoarylaldehyde and carbonyl compounds mediated by hydrochloric acid in water. *Tetrahedron Letters*, 47(7), 1059-1063.
62. Anastas, P. T., and Warner, J. C. (2000). *Green chemistry: theory and practice* (Vol. 30). Oxford: Oxford University Press.
63. Loupy, A., Petit, A., Hamelin, J., Texier-Boullet, F., Jacquault, P., and Mathe, D. (1998). New solvent-free organic synthesis using focused microwaves. *Synthesis*, 1998(09), 1213-1234.
64. Ratts, K. W., and Yao, A. N. (1966). Stable Sulfonium Ylids. *The Journal of Organic Chemistry*, 31(4), 1185-1188.
65. Gerssen-Gondelach, S. J., Saygin, D., Wicke, B., Patel, M. K., and Faaij, A. P. C. (2014). Competing uses of biomass: assessment and comparison of the performance of bio-based heat, power, fuels and materials. *Renewable and Sustainable Energy Reviews*, 40, 964-998.
66. Gedye, R., Smith, F., Westaway, K., Ali, H., Baldisera, L., Laberge, L., and Rousell, J. (1986). The use of microwave ovens for rapid organic synthesis. *Tetrahedron Letters*, 27(3), 279-282.
67. Mirzaei, A., and Neri, G. (2016). Microwave-assisted synthesis of metal oxide nanostructures for gas sensing application: A review. *Sensors and Actuators B: Chemical*, 237, 749-775.
68. Kusuma, H. S., and Mahfud, M. (2016). Preliminary study: Kinetics of oil extraction from basil (*Ocimum basilicum*) by microwave-assisted hydrodistillation and solvent-free microwave extraction. *South African Journal of Chemical Engineering*, 21, 49-53.
69. Mubarak, N. M., Sahu, J. N., Abdullah, E. C., and Jayakumar, N. S. (2016). Plam oil empty fruit bunch based magnetic biochar composite comparison for synthesis by microwave-assisted and conventional heating. *Journal of Analytical and Applied Pyrolysis*, 120, 521-528.
70. Srikrishna, D., and Dubey, P. K. (2014). Efficient stepwise and one pot three-component synthesis of 2-amino-4-(2-oxo-2H-chromen-3-yl) thiophene-3-carbonitriles. *Tetrahedron Letters*, 55(48), 6561-6566.

71. Ghasali, E., Yazdani-rad, R., Asadian, K., and Ebadzadeh, T. (2017). Production of Al-SiC-TiC hybrid composites using pure and 1056 aluminum powders prepared through microwave and conventional heating methods. *Journal of Alloys and Compounds*, 690, 512-518.
72. Katritzky, A. R., Ramsden, C. A., Scriven, E. F. V., and Taylor, R. J. K. (2008). *Comprehensive heterocyclic chemistry III* (Vol. 4, p. 1). Amsterdam: Elsevier.
73. Yavari, I., Hekmat-Shoar, R., and Zonouzi, A. (1998). A new and efficient route to 4-carboxymethylcoumarins mediated by vinyltriphenylphosphonium salt. *Tetrahedron Letters*, 39(16), 2391-2392.
74. Singh, J., Kaur, J., Nayyar, S., and Kad, G. L. (1998). Highly efficient and single step synthesis of 4-phenylcoumarins and 3, 4-dihydro-4-phenylcoumarins over montmorillonite k-10 clay, under microwave irradiation. *Journal of Chemical Research, Synopses*, 5, 280-281.
75. Kim, S. Y., Kwon, P. S., Kwon, T. W., Chung, S. K., and Chang, Y. T. (1997). Microwave Enhanced Knoevenagel Condensation of Ethyl Cyanoacetate with Aldehydes. *Synthetic Communications*, 27(4), 533-541.
76. Bose, A. K., Manhas, M. S., Ghosh, M., Raju, V. S., Tabei, K., and Urbanczyk-Lipkowska, Z. (1990). Highly Accelerated Reactions in a Microwave Oven: Synthesis of Heterocycles. *ChemInform*, 21(47), no-no.
77. Milart, P., Wilamowski, J., and Sepiol, J. J. (1998). Synthesis of di-and triamino-1, 1': 3', 1''-terphenyls from arylythyldene-and arylidenemalonodinitriles. *Tetrahedron*, 54(51), 15643-15656.
78. Bassindale, A. R., and Stout, T. (1985). The interaction of electrophilic silanes (Me<sub>3</sub>SiX, X= ClO<sub>4</sub>, I, CF<sub>3</sub>SO<sub>3</sub>, Br, Cl) with nucleophiles. The nature of silylation mixtures in solution. *Tetrahedron Letters*, 26(28), 3403-3406.
79. Yanar, U., Babür, B., Pekyılmaz, D., Yahaya, I., Aydiner, B., Dede, Y., and Seferoğlu, Z. (2016). A fluorescent coumarin-thiophene hybrid as a ratiometric chemosensor for anions: Synthesis, photophysics, anion sensing and orbital interactions. *Journal of Molecular Structure*, 1108, 269-277.
80. Gewald, K. (1976). Methods for the synthesis of 2-aminothiophenes and their reactions. *Chemistry of Heterocyclic Compounds*, 12(10), 1077-1090.
81. Gompper, R., Kutter, E., and Töpfl, W. (1962). Ketenderivate, IV. Neue Thiophene und Thieno [2.3-b] thiophene. *Justus Liebigs Annalen der Chemie*, 659(1), 90-101.
82. Gewald, K., and Schinke, E. (1966). Heterocycles from CH-acidic nitriles. X. Reaction of acetone with cyanoacetic ester and sulfur. *Chemische Berichte*, 99, 271-275.
83. Gewald, K., and Neumann, G. (1968). Heterocyclen aus CH-aciden Nitrilen, XIV. 2-Amino-thionaphthene. *Chemische Berichte*, 101(6), 1933-1939.

84. Gronowitz, S., Fortea-Laguna, J., Ross, S., Sjöberg, B., and Stjernström, N. E. (1968). On thiophene analogues of metaqualone-like compounds. *Acta Pharmaceutica Suecica*, 5(6), 563-578.
85. Chimenti, F., Secci, D., Bolasco, A., Chimenti, P., Granese, A., Carradori, S., and Ortuso, F. (2006). Synthesis, molecular modeling studies, and selective inhibitory activity against monoamine oxidase of N, N'-bis [2-oxo-2H-benzopyran]-3-carboxamides. *Bioorganic & medicinal chemistry letters*, 16(15), 4135-4140.
86. Chimenti, F., Fioravanti, R., Bolasco, A., Chimenti, P., Secci, D., Rossi, F., and Cirilli, R. (2010). A new series of flavones, thioflavones, and flavanones as selective monoamine oxidase-B inhibitors. *Bioorganic & Medicinal Chemistry*, 18(3), 1273-1279.
87. Dar, A., Khan, K. M., Ateeq, H. S., Khan, S., Rahat, S., Perveen, S., and Supuran, C. T. (2005). Inhibition of monoamine oxidase-A activity in rat brain by synthetic hydrazines: Structure-activity relationship (SAR). *Journal of Enzyme Inhibition and Medicinal Chemistry*, 20(3), 269-274.
88. Madziga, H. A., Sanni, S., and Sandabe, U. K. (2010). Phytochemical and elemental analysis of *Acalypha wilkesiana* leaf. *Journal of American Science*, 6(11), 510-514.
89. Singh, H. P., Gupta, N., and Sharma, R. K. (2014). Ethnopharmacological damdei plant extract assisted synthesis of copper nanoparticles and evaluation in non-enzymatic kinetics of o-dianisidine oxidation. *Journal of Biomedical and Therapeutic Sciences*, 1(1), 34-40.
90. Cho, J. Y., Chang, H. J., Lee, S. K., Kim, H. J., Hwang, J. K., and Chun, H. S. (2007). Amelioration of dextran sulfate sodium-induced colitis in mice by oral administration of  $\beta$ -caryophyllene, a sesquiterpene. *Life Sciences*, 80(10), 932-939.
91. Li, N., Harrison, R. G., and Lamb, J. D. (2014). Application of resorcinarene derivatives in chemical separations. *Journal of Inclusion Phenomena and Macrocyclic Chemistry*, 78(1-4), 39-60.
92. Ennis, C. P., and Kaiser, R. I. (2010). Mechanistical studies on the electron-induced degradation of polymethylmethacrylate and Kapton. *Physical Chemistry Chemical Physics*, 12(45), 14902-14915.
93. Koleva, B. B., Kolev, T., Nikolova, R., Zagraniansky, Y., and Spitteller, M. (2008). Novel organic material with potential NLO application-electronic and spectroscopic properties. *Central European Journal of Chemistry*, 6(4), 592-599.
94. Hu, Q. S., Li, L. C., and Wang, X. (2008). Theoretical study on the mechanism of reaction between 3-hydroxy-3-methyl-2-butanone and malononitrile catalyzed by lithium ethoxide. *Central European Journal of Chemistry*, 6(2), 304-309.

95. Elinson, M. N., Fedukovich, S. K., Vereshchagin, A. N., Dorofeev, A. S., Dmitriev, D. E., and Nikishin, G. I. (2003). Electrocatalytic transformation of malononitrile and cycloalkylidenemalononitriles into spirobicyclic and spirotricyclic compounds containing 1, 1, 2, 2-tetracyanocyclopropane fragment. *Russian Chemical Bulletin*, 52(10), 2235-2240.
96. Chen, T. A., Jen, A. K., and Cai, Y. (1996). Two-step synthesis of side-chain aromatic polyimides for second-order nonlinear optics. *Macromolecules*, 29(2), 535-539.
97. MacNevin, C. J., Gremyachinskiy, D., Hsu, C. W., Li, L., Rougie, M., Davis, T. T., and Hahn, K. M. (2013). Environment-sensing merocyanine dyes for live cell imaging applications. *Bioconjugate Chemistry*, 24(2), 215-223.
98. Reichardt, C. (2007). Solvents and solvent effects: an introduction. *Organic Process Research & Development*, 11(1), 105-113.
99. Chen, J. R., Wong, J. B., Kuo, P. Y., and Yang, D. Y. (2008). Synthesis and characterization of coumarin-based spiropyran photochromic colorants. *Organic Letters*, 10(21), 4823-4826.
100. Davidenko, N. A., Dehtarenko, S. V., Getmanchuk, Y. P., Ishchenko, A. A., Kozinetz, A. V., Kostenko, L. I., and Tretyak, O. V. (2009). Photoconducting properties of holographic media based on ferrocenyl-containing cooligomers of glycidyl carbazole with these oligomers sensitized by organic dye. *Semiconductors*, 43(11), 1473.
101. Sabnis, R. W., Rangnekar, D. W., and Sonawane, N. D. (1999). 2-Aminothiophenes by the Gewald reaction. *Journal of Heterocyclic Chemistry*, 36(2), 333-345.
102. Nikolakopoulos, G., Figler, H., Linden, J., and Scammells, P. J. (2006). 2-Aminothiophene-3-carboxylates and carboxamides as adenosine A1 receptor allosteric enhancers. *Bioorganic & Medicinal Chemistry*, 14(7), 2358-2365.
103. Ferguson, G. N., Valant, C., Horne, J., Figler, H., Flynn, B. L., Linden, J., and Scammells, P. J. (2008). 2-Aminothiopyridazines as novel adenosine A1 receptor allosteric modulators and antagonists. *Journal of Medicinal Chemistry*, 51(19), 6165-6172.
104. McKay, G. A., Reddy, R., Arhin, F., Belley, A., Lehoux, D., Moeck, G., and Far, A. R. (2006). Triaminotriazine DNA helicase inhibitors with antibacterial activity. *Bioorganic & Medicinal Chemistry Letters*, 16(5), 1286-1290.
105. Hegab, M. I., Abdel-Fattah, A. S. M., Yousef, N. M., Nour, H. F., Mostafa, A. M., and Ellithy, M. (2007). Synthesis, X-ray Structure, and Pharmacological Activity of Some 6, 6-Disubstituted Chromeno [4, 3-b]-and Chromeno-[3, 4-c]-quinolines. *Archiv der Pharmazie: An International Journal Pharmaceutical and Medicinal Chemistry*, 340(8), 396-403.

106. Siddiqui, N., Alam, M., and Ahsan, W. (2008). Synthesis, anticonvulsant and toxicity evaluation of 2-(1H-indol-3-yl) acetyl-N-(substituted phenyl) hydrazine carbothioamides and their related heterocyclic derivatives. *Acta Pharmaceutica*, 58(4), 445-454.
107. Galewicz-Walesa, K., and Pachuta-Stec, A. (2003). The synthesis and properties of N-substituted amides of 1-(5-methylthio-1, 2, 4-triazol-3-yl)-cyclohexane--2-carboxylic acid. *Synthesis*, 58(9), 118-123.
108. Graybill, T. L., Ross, M. J., Gauvin, B. R., Gregory, J. S., Harris, A. L., Ator, M. A., and Dolle, R. E. (1992). Synthesis and evaluation of azapeptide-derived inhibitors of serine and cysteine proteases. *Bioorganic & Medicinal Chemistry Letters*, 2(11), 1375-1380.
109. Moise, M., Sunel, V., Profire, L., Popa, M. and Lionte, C. (2008). Synthesis and antimicrobial activity of some new (sulfon-amidophenyl)-amide derivatives of N-(4-nitrobenzoyl)-phenylglycine and N-(4-nitrobenzoyl)-phenylalanine. *Farmacia-Bucuresti-*, 56(3), 283.
110. Warnecke, A., Fichtner, I., Saß, G., and Kratz, F. (2007). Synthesis, cleavage profile, and antitumor efficacy of an albumin-binding prodrug of methotrexate that is cleaved by plasmin and cathepsin B. *Archiv der Pharmazie: An International Journal Pharmaceutical and Medicinal Chemistry*, 340(8), 389-395.
111. Naik, T. A., and Chikhalia, K. H. (2007). Studies on synthesis of pyrimidine derivatives and their pharmacological evaluation. *Journal of Chemistry*, 4(1), 60-66.
112. Rehse, K., Kotthaus, J., and Khadembashi, L. (2009). New 1H-Pyrazole-4-Carboxamides with Antiplatelet Activity. *Archiv der Pharmazie: An International Journal Pharmaceutical and Medicinal Chemistry*, 342(1), 27-33.
113. Strupi—Ska, M., Rostafi—Ska-Suchar, G., Stables, J. P. and Paruszewski, R. (2009). New derivatives of benzylamide with anticonvulsant activity. *Acta Poloniae Pharmaceutica*, 66(2), 155-159.
114. Ronad, P. M., Hunashal, R. D., Darbhamalla, S., and Maddi, V. S. (2008). Synthesis and Evaluation of Antiinflammatory and Analgesic Activities of a Novel Series of Substituted-N-(4-methyl-2-oxo-2H-chromen-7-yl) benzamides. *Arzneimittelforschung*, 58(12), 641-646.
115. Xu, Q. Q., Qin, T. Y., Wang, T. T., Wang, T. J., & Liao, W. W. (2015). Diastereoselective allylic rearrangement of Morita–Baylis–Hillman C-adducts: a facile access to functionalized 1, 2-dihydroisoquinolines. *Tetrahedron*, 71(6), 941-948.
116. Kanda, Y., Kawanishi, Y., Oda, K., Sakata, T., Mihara, S. I., Asakura, K., and Konoike, T. (2001). Synthesis and structure–activity relationships of potent and orally active sulfonamide ETB selective antagonists. *Bioorganic & Medicinal Chemistry*, 9(4), 897-907.

117. Stokes, S. S., Albert, R., Buurman, E. T., Andrews, B., Shapiro, A. B., Green, O. M., and Otterbein, L. R. (2012). Inhibitors of the acetyltransferase domain of N-acetylglucosamine-1-phosphate-uridylyltransferase/glucosamine-1-phosphate-acetyltransferase (GlmU). Part 2: optimization of physical properties leading to antibacterial aryl sulfonamides. *Bioorganic & Medicinal Chemistry Letters*, 22(23), 7019-7023.
118. Chibale, K., Haupt, H., Kendrick, H., Yardley, V., Saravanamuthu, A., Fairlamb, A. H., and Croft, S. L. (2001). Antiprotozoal and cytotoxicity evaluation of sulfonamide and urea analogues of quinacrine. *Bioorganic & Medicinal Chemistry Letters*, 11(19), 2655-2657.
119. Ezabadi, I. R., Camoutsis, C., Zoumpoulakis, P., Geronikaki, A., Soković, M., Glamočilija, J., and Ćirić, A. (2008). Sulfonamide-1, 2, 4-triazole derivatives as antifungal and antibacterial agents: Synthesis, biological evaluation, lipophilicity, and conformational studies. *Bioorganic & Medicinal Chemistry*, 16(3), 1150-1161.
120. Kennedy, J. F., & Thorley, M. (1999). Pharmaceutical substances. *Bioseparation*, 8(6), 336-336.
121. Gal, C. S. L. (2001). An overview of SR121463, a selective non-peptide vasopressin V2 receptor antagonist. *Cardiovascular Drug Reviews*, 19(3), 201-214.
122. Natarajan, A., Guo, Y., Harbinski, F., Fan, Y. H., Chen, H., Luus, L., and Halperin, J. A. (2004). Novel arylsulfoanilide-oxindole hybrid as an anticancer agent that inhibits translation initiation. *Journal of Medicinal Chemistry*, 47(21), 4979-4982.
123. Vullo, D., De Luca, V., Scozzafava, A., Carginale, V., Rossi, M., Supuran, C. T., and Capasso, C. (2013). The extremophilic  $\alpha$ -carbonic anhydrase from the thermophilic bacterium *Sulfurihydrogenibium azorense* is highly inhibited by sulfonamides. *Bioorganic & Medicinal Chemistry*, 21(15), 4521-4525.
124. Beale, J. M., Block, J., and Hill, R. (2010). *Organic medicinal and pharmaceutical chemistry*. Philadelphia: Lippincott Williams & Wilkins, 744-754.
125. Levin, J. I., Chen, J. M., Du, M. T., Nelson, F. C., Killar, L. M., Skala, S., and March, C. J. (2002). Anthranilate sulfonamide hydroxamate TACE inhibitors. Part 2: SAR of the acetylenic P1' group. *Bioorganic & Medicinal Chemistry Letters*, 12(8), 1199-1202.
126. Kim, D. K., Lee, J. Y., Lee, N., Kim, J. S., Lee, S., Choi, J. Y., and Kim, T. K. (2001). Synthesis and phosphodiesterase inhibitory activity of new sildenafil analogues containing a carboxylic acid group in the 5'-sulfonamide moiety of a phenyl ring. *Bioorganic & Medicinal Chemistry*, 9(11), 3013-3021.
127. Hu, B., Ellingboe, J., Han, S., Largis, E., Lim, K., Malamas, M., and Singanallore, T. (2001). Novel (4-piperidin-1-yl)-phenyl sulfonamides as potent and selective human  $\beta_3$  agonists. *Bioorganic & Medicinal Chemistry*, 9(8), 2045-2059.

128. Ma, T., Fuld, A. D., Rigas, J. R., Hagey, A. E., Gordon, G. B., Dmitrovsky, E., and Dragnev, K. H. (2012). A phase I trial and in vitro studies combining ABT-751 with carboplatin in previously treated non-small cell lung cancer patients. *Chemotherapy*, 58(4), 321-329.
129. Ma, T., Fuld, A. D., Rigas, J. R., Hagey, A. E., Gordon, G. B., Dmitrovsky, E., and Dragnev, K. H. (2012). A phase I trial and in vitro studies combining ABT-751 with carboplatin in previously treated non-small cell lung cancer patients. *Chemotherapy*, 58(4), 321-329.
130. Roush, W. R., Gwaltney, S. L., Cheng, J., Scheidt, K. A., McKerrow, J. H., and Hansell, E. (1998). Vinyl sulfonate esters and vinyl sulfonamides: potent, irreversible inhibitors of cysteine proteases. *Journal of the American Chemical Society*, 120(42), 10994-10995.
131. Lawrence, H. R., Kazi, A., Luo, Y., Kendig, R., Ge, Y., Jain, S., and Sebti, S. M. (2010). Synthesis and biological evaluation of naphthoquinone analogs as a novel class of proteasome inhibitors. *Bioorganic & Medicinal Chemistry*, 18(15), 5576-5592.
132. Fujita, T., and Hansch, C. (1967). Analysis of the structure-activity relationship of the sulfonamide drugs using substituent constants. *Journal of Medicinal Chemistry*, 10(6), 991-1000.
133. Abbasi, M. A., Masood, M., Siddiqui, S. Z., Fatima, A., Shahid, M., Fatima, H., and Khan, K. M. (2017). Synthesis of Some 1, 4-Benzodioxane Containing Methanesulfonamides and Their Hemolytic Study on Human Blood. *Journal of the Chemical Society of Pakistan*, 39(6), 999-1005 .
134. Alsughayer, A., Elassar, A. Z. A., Mustafa, S., and Al Sagheer, F. (2011). Synthesis, structure analysis and antibacterial activity of new potent sulfonamide derivatives. *Journal of Biomaterials and Nanobiotechnology*, 2(02), 143.
135. Özbek, N., Katircioğlu, H., Karacan, N., and Baykal, T. (2007). Synthesis, characterization and antimicrobial activity of new aliphatic sulfonamide. *Bioorganic & Medicinal Chemistry*, 15(15), 5105-5109.
136. Eshghi, H., Rahimizadeh, M., Zokaei, M., Eshghi, S., Eshghi, S., Faghihi, Z., and Kihanyan, M. (2011). Synthesis and antimicrobial activity of some new macrocyclic bis-sulfonamide and disulfides. *European Journal of Chemistry*, 2(1), 47-50.
137. Kołaczek, A., Fusiarcz, I., Ławecka, J., and Branowska, D. (2014). Biological activity and synthesis of sulfonamide derivatives: a brief review. *Chemik*, 68(7), 620-628.
138. Kim, Y. J., Kwak, H., Lee, S. J., Lee, J. S., Kwon, H. J., Nam, S. H., and Kim, C. (2006). Urea/thiourea-based colorimetric chemosensors for the biologically important ions: efficient and simple sensors. *Tetrahedron*, 62(41), 9635-9640.
139. Kapuscinska, A., and Nowak, I. (2014). The use of urea and its derivatives in the cosmetics industry. *Chemik*, 68(2), 91-96.

140. Borelli, C., Bielfeldt, S., Borelli, S., Schaller, M., and Korting, H. C. (2011). Cream or foam in pedal skin care: towards the ideal vehicle for urea used against dry skin. *International Journal of Cosmetic Science*, 33(1), 37-43.
141. Fluhr, J. W., Cavallotti, C., and Berardesca, E. (2008). Emollients, moisturizers, and keratolytic agents in psoriasis. *Clinics in Dermatology*, 26(4), 380-386.
142. Mishra, B. B., and Tiwari, V. K. (2011). Natural products: An evolving role in future drug discovery. *European Journal of Medicinal Chemistry*, 46(10), 4769-4807.
143. Jose, D. A., Kumar, D. K., Ganguly, B., and Das, A. (2004). Efficient and simple colorimetric fluoride ion sensor based on receptors having urea and thiourea binding sites. *Organic Letters*, 6(20), 3445-3448.
144. Cho, E. J., Moon, J. W., Ko, S. W., Lee, J. Y., Kim, S. K., Yoon, J., and Nam, K. C. (2003). A new fluoride selective fluorescent as well as chromogenic chemosensor containing a naphthalene urea derivative. *Journal of the American Chemical Society*, 125(41), 12376-12377.
145. Padmesh, T. V. N., Vijayaraghavan, K., Sekaran, G., and Velan, M. (2005). Batch and column studies on biosorption of acid dyes on fresh water macro alga *Azolla filiculoides*. *Journal of Hazardous Materials*, 125(1-3), 121-129.
146. Pivonka, D. E., and Empfield, J. R. (2004). Real-time in situ Raman analysis of microwave-assisted organic reactions. *Applied Spectroscopy*, 58(1), 41-46.
147. Horikoshi, S., Sakai, F., Kajitani, M., Abe, M., and Serpone, N. (2009). Microwave frequency effects on the photoactivity of TiO<sub>2</sub>: Dielectric properties and the degradation of 4-chlorophenol, bisphenol A and methylene blue. *Chemical Physics Letters*, 470(4-6), 304-307.
148. Kappe, C. O. (2004). Controlled microwave heating in modern organic synthesis. *Angewandte Chemie International Edition*, 43(46), 6250-6284.
149. Kappe, C. O., and Dallinger, D. (2006). The impact of microwave synthesis on drug discovery. *Nature Reviews Drug Discovery*, 5(1), 51.
150. Alcazar, J., and Oehrich, D. (2010). Recent applications of microwave irradiation to medicinal chemistry. *Future Medicinal Chemistry*, 2(2), 169-176.
151. Collins, J. M., and Leadbeater, N. E. (2007). Microwave energy: a versatile tool for the biosciences. *Organic & Biomolecular Chemistry*, 5(8), 1141-1150.
152. Merritt, E. A., and Bagley, M. C. (2007). Holzappel-Meyers-Nicolaou modification of the Hantzsch thiazole synthesis. *Synthesis*, 2007(22), 3535-3541.
153. Merritt, E. A., and Bagley, M. C. (2007). Convergent synthesis of the central heterocyclic domain of micrococin P1. *Synlett*, 2007(06), 0954-0958.
154. Bogdał, D. (1998). Coumarins: fast synthesis by Knoevenagel condensation under microwave irradiation. *Journal of Chemical Research, Synopses*, 8, 468-469.

155. Ajani, O. O., and Nwinyi, O. C. (2010). Microwave-assisted synthesis and evaluation of antimicrobial activity of 3-{3-(s-aryl and s-heteroaromatic) acryloyl}-2H-chromen-2-one derivatives. *Journal of Heterocyclic Chemistry*, 47(1), 179-187.
156. Bowman, M. D., Schmink, J. R., McGowan, C. M., Kormos, C. M., and Leadbeater, N. E. (2008). Scale-up of microwave-promoted reactions to the multigram level using a sealed-vessel microwave apparatus. *Organic Process Research & Development*, 12(6), 1078-1088.
157. Schmink, J. R., Kormos, C. M., Devine, W. G., and Leadbeater, N. E. (2010). Exploring the scope for scale-up of organic chemistry using a large batch microwave reactor. *Organic Process Research & Development*, 14(1), 205-214.
158. Venugopala, K. N., and Jayashree, B. S. (2008). Microwave-induced synthesis of Schiff bases of aminothiazolyl bromocoumarins as antibacterials. *Indian Journal of Pharmaceutical Sciences*, 70(1), 88.
159. Kempf, D. J., Flentge, C. A., Wideburg, N. E., Saldivar, A., Vasavanonda, S., and Norbeck, D. W. (1995). Evaluation of substituted benzamides as P2 ligands for symmetry-based inhibitors of HIV protease. *Bioorganic & Medicinal Chemistry Letters*, 5(22), 2725-2728.
160. Boons, G. J. (2008). Protecting groups. *Organic Synthesis with Carbohydrates*, 1, 26.
161. Gedye, R., Smith, F., Westaway, K., Ali, H., Baldisera, L., Laberge, L., and Rousell, J. (1986). The use of microwave ovens for rapid organic synthesis. *Tetrahedron Letters*, 27(3), 279-282.
162. Verma, R. S. (2001). Solvent free accelerated organic synthesis using microwave. *Pure and Applied Chemistry*, 73-193.
163. Ahluwalia, V. K., and Kidwai, M. (2004). Basic principles of green chemistry. In *New Trends in Green Chemistry* (pp. 5-14). Springer, Dordrecht.
164. Kappe, C. O., Dallinger, D., and Murphree, S. S. (2008). *Practical microwave synthesis for organic chemists*. Weinheim: John Wiley & Sons.
165. Panetta, J. A., and Rapoport, H. (1982). New syntheses of coumarins. *The Journal of Organic Chemistry*, 47(6), 946-950.
166. Miyano, M., and Dorn, C. R. (1972). Mirestrol. I. Preparation of the tricyclic intermediate. *The Journal of Organic Chemistry*, 37(2), 259-268.
167. Woods, L. L., and Sapp, J. (1962). A new one-step synthesis of substituted coumarins. *The Journal of Organic Chemistry*, 27(10), 3703-3705.
168. Shah, V., Bose, J., and Shah, R. (1960). Communication-New Synthesis of 4-Hydroxycoumarins. *The Journal of Organic Chemistry*, 25(4), 677-678.

169. Gribble, G. W. (2000). Recent developments in indole ring synthesis—methodology and applications. *Journal of the Chemical Society, Perkin Transactions 1*, 7, 1045-1075.
170. Hoefnagel, A. J., Gunnewegh, E. A., Downing, R. S., and van Bekkum, H. (1995). Synthesis of 7-hydroxycoumarins catalysed by solid acid catalysts. *Journal of the Chemical Society, Chemical Communications*, 2, 225-226.
171. Wang, J. X., Wu, X., Hu, Y., Zhao, K., and Liu, Z. (1999). Synthesis of substituted glycerol selenide ethers under microwave irradiation. *Journal of Chemical Research, Synopses*, 12, 688-689.
172. Li, T. S., Zhang, Z. H., Yang, F., and Fu, C. G. (1998). Montmorillonite clay catalysis. Part 7. 1 an environmentally friendly procedure for the synthesis of coumarins via pechmann condensation of phenols with ethyl acetoacetate. *Journal of Chemical Research, Synopses*, 1, 38-39.
173. John, E., and Israelstam, S. (1961). Use of Cation Exchange Resins in Organic Reactions. I. The Von Pechmann Reaction. *The Journal of Organic Chemistry*, 26(1), 240-242.
174. Musa, M. A., Cooperwood, J. S., and Khan, M. O. F. (2008). A review of coumarin derivatives in pharmacotherapy of breast cancer. *Current Medicinal Chemistry*, 15(26), 2664-2679.
175. Hussien, F. A. H., Keshe, M., Alzobar, K., Merza, J., and Karam, A. (2016). Synthesis and nitration of 7-Hydroxy-4-Methyl coumarin via pechmann condensation using eco-friendly medias. *International Letters of Chemistry, Physics and Astronomy*, 69, 66-73.
176. Sunitha, K., Balasubramanian, K. K., and Rajagopalan, K. (1984). A new route to the synthesis of 3-methylenecoumarins-via Lewis acid catalyzed rearrangement of methyl  $\alpha$ -aryloxymethylacrylates. *Tetrahedron Letters*, 25(29), 3125-3126.
177. Johnson, J. R. (2004). The perkin reaction and related reactions. *Organic Reactions*, 1, 210-265.
178. Staunton, J., and Sutkowski, A. C. (1991). The polyketide synthase (PKS) of aspyrone biosynthesis: evidence for the enzyme bound intermediates from incorporation studies with N-acetylcysteamine thioesters in intact cells of *Aspergillus melleus*. *Journal of the Chemical Society, Chemical Communications*, 16, 1110-1112.
179. Balakrishna, M. S., and Kaboudin, B. (2001). A simple and new method for the synthesis of 1, 5-benzodiazepine derivatives on a solid surface. *Tetrahedron Letters*, 42(6), 1127-1129.
180. Greber, G. (1991). Vogel's textbook of practical organic chemistry. *Journal of Polymer Science Part A: Polymer Chemistry*, 29(8), 1223-1223.

181. Mali, R. S., and Yadav, V. J. (1977). Convenient synthesis of naturally occurring coumarins,(2-oxo-2H-benzopyrans) and 4-methylcoumarins(4-methyl-2-oxo-2H-benzopyrans). *Synthesis*, 1977(07), 464-465.
182. Narasimhan, N. S., Mali, F. S., and Barve, M. V. (1979). Synthetic application of lithiation reactions; Part XIII. Synthesis of 3-phenylcoumarins and their benzo derivatives. *Synthesis*, 1979(11), 906-909.
183. Cartwright, G. A., and McNab, H. (1997). Synthesis of Coumarins by Flash Vacuum Pyrolysis of 3-(2-Hydroxyaryl) propenoic Esters, 1. *Journal of Chemical Research, Synopses*, 8, 296-297.
184. Black, M., Cadogan, J. I. G., Cartwright, G. A., McNab, H., and MacPherson, A. D. (1993). Carboxylic esters radical leaving groups: a new and efficient gas-phase synthesis of benzofurans. *Journal of the Chemical Society, Chemical Communications*, 11, 959-960.
185. Abdel-Rahman, R. M., Salem, M. A., Ali, T. E., and Ibrahim, M. A. (2015). Utility of 4, 6-diacetylresorcinol in heterocyclic synthesis. *Chemistry of Heterocyclic Compounds*, 51(4), 299-309.
186. Fall, Y., Teran, C., Teijeira, M., Santana, L., and Uriarte, E. (2000). Synthesis of new 4-cyclohexylcoumarin derivatives. *Synthesis*, 2000(05), 643-645.
187. Jones, G. (2004). The Knoevenagel Condensation. *Organic reactions*, 15, 204-599.
188. Bogdał, D. (1998). Coumarins: fast synthesis by Knoevenagel condensation under microwave irradiation. *Journal of Chemical Research, Synopses*, 8, 468-469.
189. Yalçın, E., Alkış, M., Seferoğlu, N., and Seferoğlu, Z. (2018). A novel coumarin-pyrazole-triazine based fluorescence chemosensor for fluoride detection via deprotonation process: Experimental and theoretical studies. *Journal of Molecular Structure*, 1155, 573-581.
190. Gouda, M. A., Berghot, M. A., El-Ghani, G. E. A., Elattar, K. M., and Khalil, A. E. G. M. (2011). Chemistry of 2-aminothiophene-3-carboxamide and related compounds. *Turkish Journal of Chemistry*, 35(6), 815-837.
191. Fondjo, E. S., and Döpp, D. (2006). Reactions of three [c] annelated 2-aminothiophenes with electron poor olefins. *Arkivoc*, 10, 90-101.
192. Zhao, D. D., Li, L., Xu, F., Wu, Q., and Lin, X. F. (2013). Bovine serum albumin-catalyzed one-pot synthesis of 2-aminothiophenes via Gewald reaction. *Journal of Molecular Catalysis B: Enzymatic*, 95, 29-35.
193. Dell'Erba, C., Spinelli, D., and Leandri, G. (1969). Ring-opening reaction in the thiophen series: reaction between 3, 4-dinitrothiophen and secondary amines. *Journal of the Chemical Society D: Chemical Communications*, 10, 549-549.

194. Blackwood, J. E., and Giles, P. M. (1975). Chemical abstracts stereochemical nomenclature of organic substances in the ninth collective period (1972-1976). *Journal of Chemical Information and Computer Sciences*, 15(2), 67-72.
195. Tinney, F. J., Sanchez, J. P., and Nogas, J. A. (1974). Synthesis and pharmacological evaluation of 2, 3-dihydro-1H-thieno [2, 3-e][1, 4] diazepines. *Journal of Medicinal Chemistry*, 17(6), 624-630.
196. Fabis, F., Jolivet-Fouchet, S., Robba, M., Landelle, H., and Rault, S. (1998). Thiaisatoic anhydrides: Efficient synthesis under microwave heating conditions and study of their reactivity. *Tetrahedron*, 54(36), 10789-10800.
197. De Mello, M. B., Clososki, G. C., Piovan, L., and de Oliveira, A. R. (2015). An alternative approach to differentially substituted 2-oxazoline chalcogen derivatives. *Journal of Organometallic Chemistry*, 794, 11-16.
198. Terfassa, B., Holzer, C., Schachner, J. A., Cias, P., Krenn, H., Belaj, F., and Mösch-Zanetti, N. C. (2016). A tetranuclear nickel (II) heterocubane complex of a bidentate N, O-hydroxymethyl-oxazoline ligand. Synthesis, characterization, magnetic measurements and DFT investigations. *Journal of Coordination Chemistry*, 69(3), 433-446.
199. Brouillette, Y., Lisowski, V., Fulcrand, P., and Martinez, J. (2007). Reactivity Study of 1 H-Thieno [3, 2-d][1, 3] oxazine-2, 4-dione toward the Synthesis of Bicyclic 3, 4-Dihydro-1 H-thieno [3, 2-e][1, 4] diazepine-2, 5-dione Analogues. *The Journal of Organic Chemistry*, 72(7), 2662-2665.
200. C. W. Young, R. B. DuVall, and Norman Wright, Characterization of Benzene Ring Substitution by Infrared Spectra. *Analytical Chemistry*, 1951, 23 (5), pp 709–714.
201. Cotterill, W. D., Iqbal, M., and Livingstone, R. (1998). Preparation of Some 6-Substituted 2, 2-Dimethyl-and 2, 2-and 2, 4-Diphenyl-naphtho [1, 2-b] pyrans. *Journal of Chemical Research, Synopses*, 1, 2-3.
202. Sabnis, R. W., Rangnekar, D. W., and Sonawane, N. D. (1999). 2-Aminothiophenes by the Gewald reaction. *Journal of Heterocyclic Chemistry*, 36(2), 333-345.
203. Binder, D., Hromatka, O., Noe, CR, Hillebrand, F., Veit, W., and Blum, JE (1980). Thiophene as a structural element of physiologically active substances; 4. Mitt. O-Substituted 5-phenylthieno [2,3-e] [1,4] diazepines. *Pharmacy Archives*, 313(7), 587-602.
204. Binder, D., Hromatka, O., Noe, C. R., Bara, Y. A., Feifel, M., Habison, G., and Blum, J. E. (1980). Thiophene as a structural element of physiologically active compounds, V: 5 (o-Nitrophenyl) thieno (2, 3-e)[1, 4] diazepines (author's transl)]. *Archiv der Pharmazie*, 313(7), 636.
205. Zaki, M. E. A. (1998). Synthesis of novel fused heterocycles based on pyrano [2, 3-c] pyrazole. *Molecules*, 3(3), 71-79.

206. Knobloch, E. (1961). Studies on anticoagulants. XXXII. Isomeric mono-O-alkylethers of di (4-hydroxycumarinyl-3) acetic acid ethyl ether. *Collection of Czechoslovak Chemical Communications*, 26(3), 710-716.
207. Schroeder, C. H., Titus, E. D., and Link, K. P. (1957). A new synthetic approach to some 3-aralkyl-4-hydroxycoumarins. *Journal of the American Chemical Society*, 79(12), 3291-3292.
208. Traven, V. F., Negrebetsky, V. V., Vorobjeva, L. I., and Carberry, E. A. (1997). Keto-enol tautomerism, NMR spectra, and H-D exchange of 4-hydroxycoumarins. *Canadian Journal of Chemistry*, 75(4), 377-383.
209. Abramovitch, R. A., and Gear, J. R. (1958). Unsymmetrically substituted 3, 3'-methylene bridged 2, 2'-dihydroxychromones. *Canadian Journal of Chemistry*, 36(11), 1501-1510.
210. Farmer, V. C. (1959). Spectra and structure of 4-hydroxycoumarins. *Spectrochimica Acta*, 15, 870-882.
211. Perel'son, M. E., Sheinker, Y. N., Zaitsev, B. E., and Pozdyshev, V. A. (1964). Integral intensities of the carbonyl bands of a number of pyrones and quinones. *Russian Chemical Bulletin*, 13(5), 754-757.
212. Perel'Son, M. E., and Sheinker, Y. N. (1966). Spectra and structure of hydroxycoumarin and hydroxyfurocoumarin salts. *Journal of Applied Spectroscopy*, 5(1), 78-82.
213. Albuquerque, F. B., Fo, R. B., Gottlieb, O. R., Magalhães, M. T., Maia, J. G. S., de Oliveira, A. B., and Wilberg, V. C. (1981). Isoflavone evolution in *Monopteryx*. *Phytochemistry*, 20(2), 235-236.
214. Mattoo, B. N. (1956). Absorption and fluorescence spectra of coumarins. *Transactions of the Faraday Society*, 52, 1184-1194.
215. Bogdał, D. (1998). Coumarins: fast synthesis by Knoevenagel condensation under microwave irradiation. *Journal of Chemical Research, Synopses*, 8, 468-469.
216. Mohamed, H. M., El-Wahab, A. H., Ahmed, K. A., El-Agrody, A. M., Bedair, A. H., Eid, F. A., and Khafagy, M. M. (2012). Synthesis, reactions and antimicrobial activities of 8-ethoxycoumarin derivatives. *Molecules*, 17(1), 971-988.
217. Kumar, B. V., Naik, H. S. B., Giriya, D., and Kumar, B. V. (2011). ZnO nanoparticle as catalyst for efficient green one-pot synthesis of coumarins through Knoevenagel condensation. *Journal of Chemical Sciences*, 123(5), 615-621.
218. Liu, X. H., Fan, J. C., Liu, Y., and Shang, Z. C. (2008). L-Proline as an efficient and reusable promoter for the synthesis of coumarins in ionic liquid. *Journal of Zhejiang University Science B*, 9(12), 990-995.

219. Barrientos, C., Navarrete-Encina, P., Carbajo, J., and Squella, J. A. (2018). New voltammetric method useful for water insoluble or weakly soluble compounds: application to pKa determination of hydroxyl coumarin derivatives. *Journal of Solid State Electrochemistry*, 22(5), 1423–1429.



**APPENDICES**

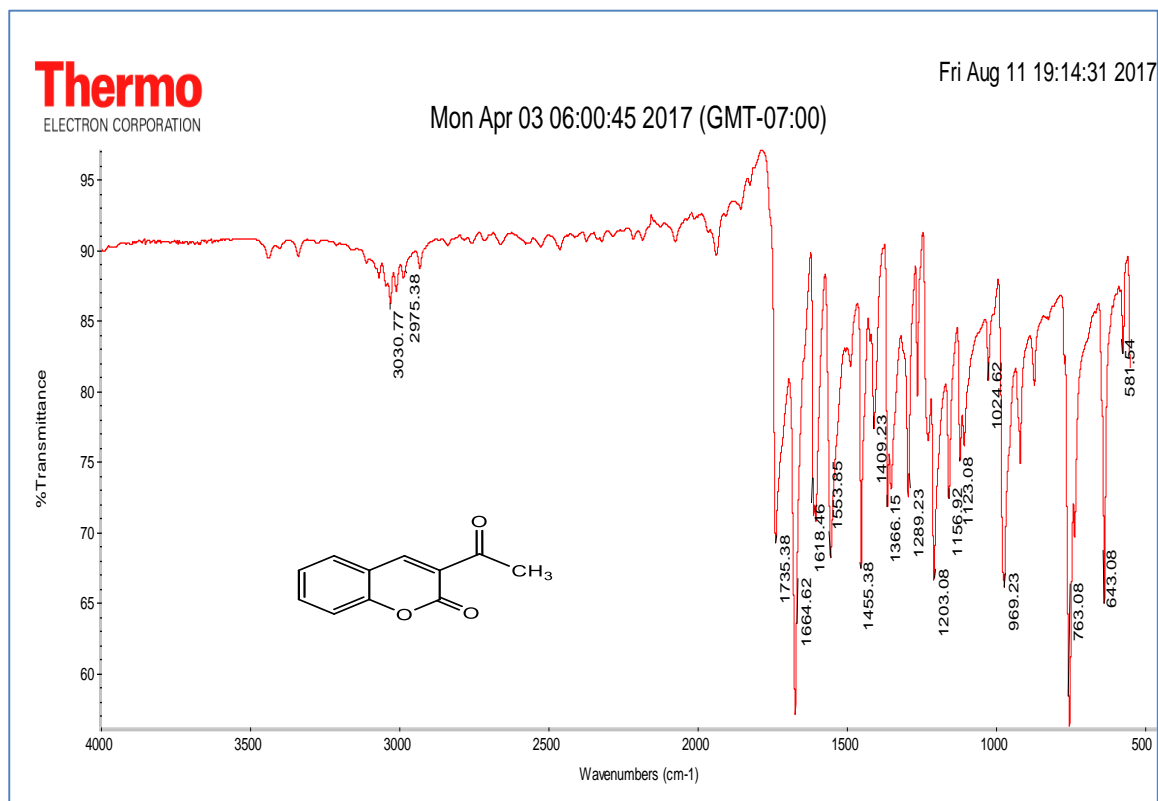
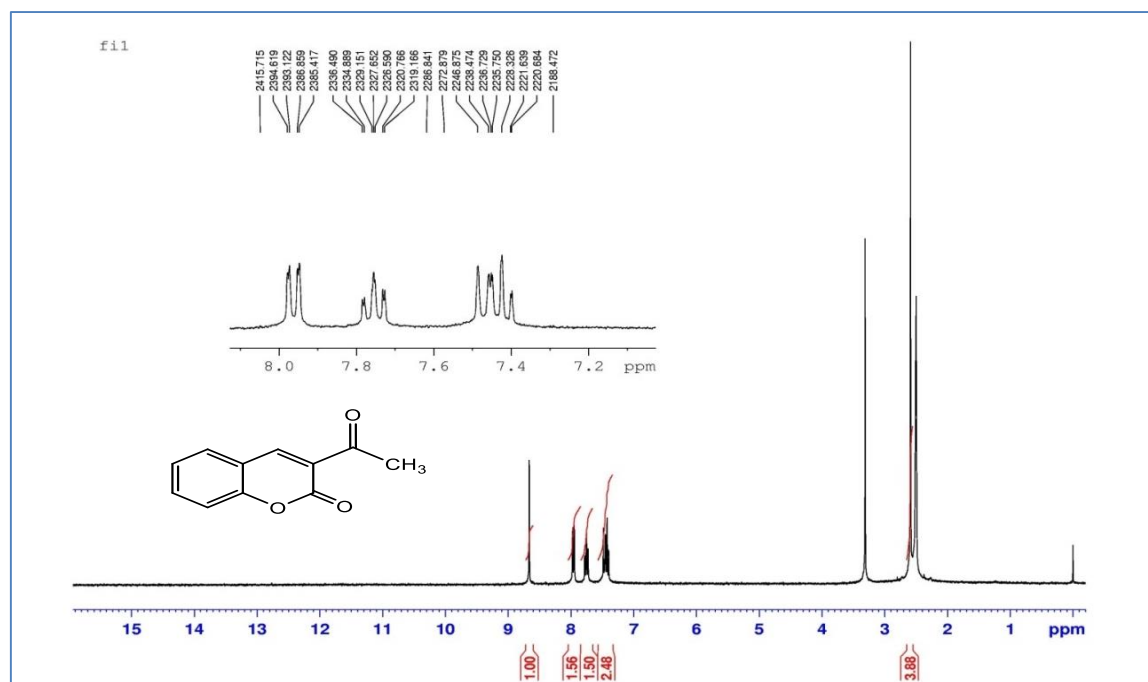
Appendix-1. FT-IR,  $^1\text{H-NMR}$ ,  $^{13}\text{C-NMR}$ , HR-MS of the 3-Acetylcoumarins (1)-(10)

Figure 1.1.1. FT-IR Spectrum of 1

Figure 1.1.2.  $^1\text{H-NMR}$  (DMSO- $d_6$ ) Spectrum of 1

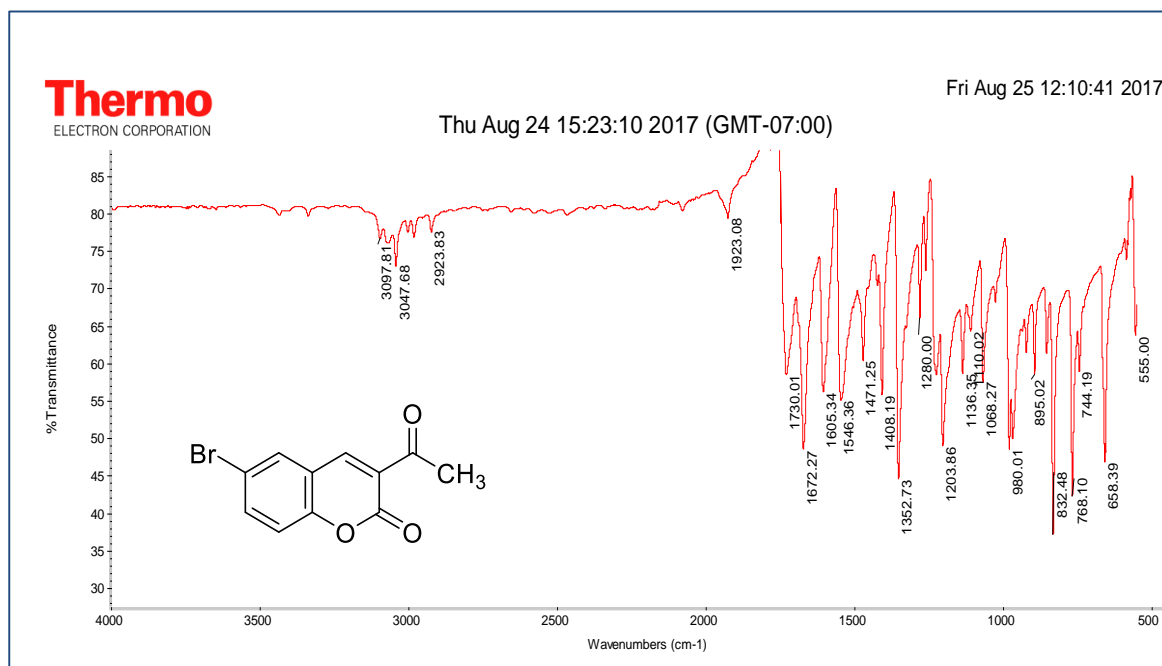
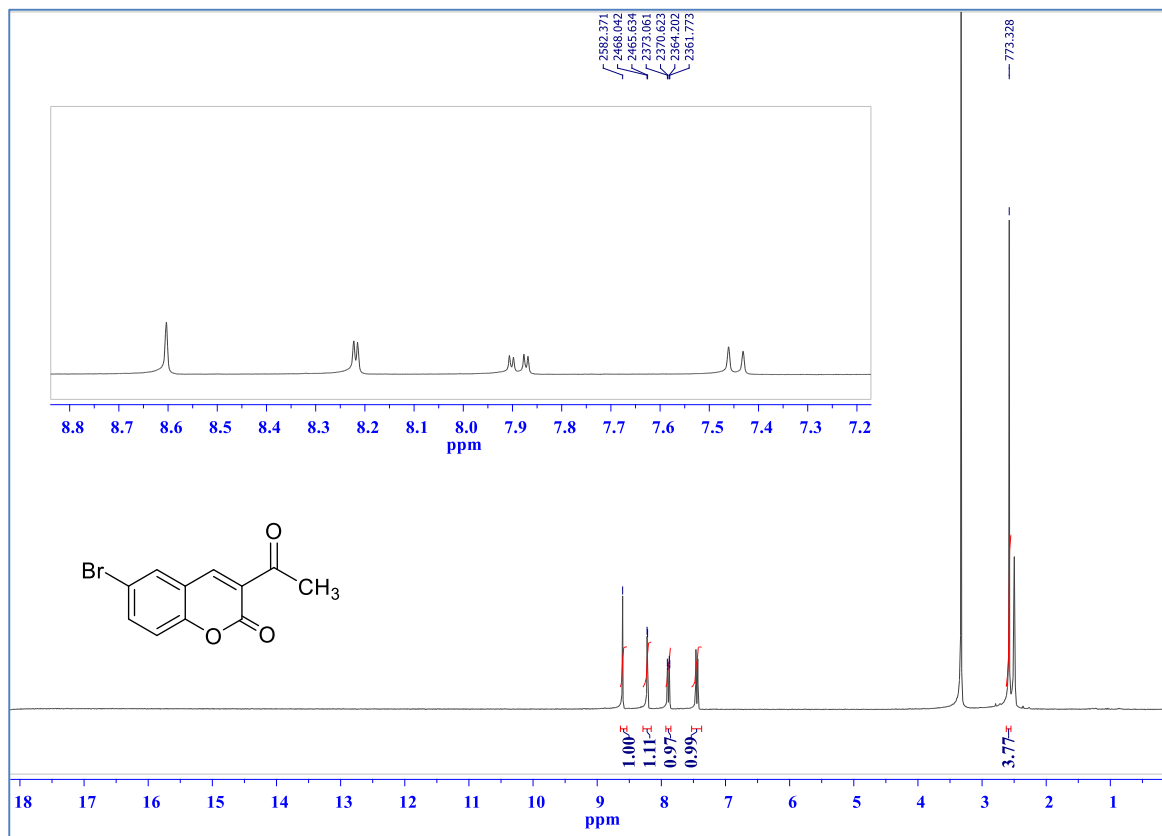
Appendix-1. (Continues) FT-IR,  $^1\text{H-NMR}$ ,  $^{13}\text{C-NMR}$ , HR-MS of the 3-Acetylcoumarins (1)-(10)

Figure 1.2.1. FT-IR Spectrum of 2

Figure 1.2.2.  $^1\text{H-NMR}$  (DMSO- $d_6$ ) Spectrum of 2

Appendix-1. (Continues) FT-IR,  $^1\text{H-NMR}$ ,  $^{13}\text{C-NMR}$ , HR-MS of the 3-Acetylcoumarins (1)-(10)

Figure 1.3.1. FT-IR Spectrum of 3

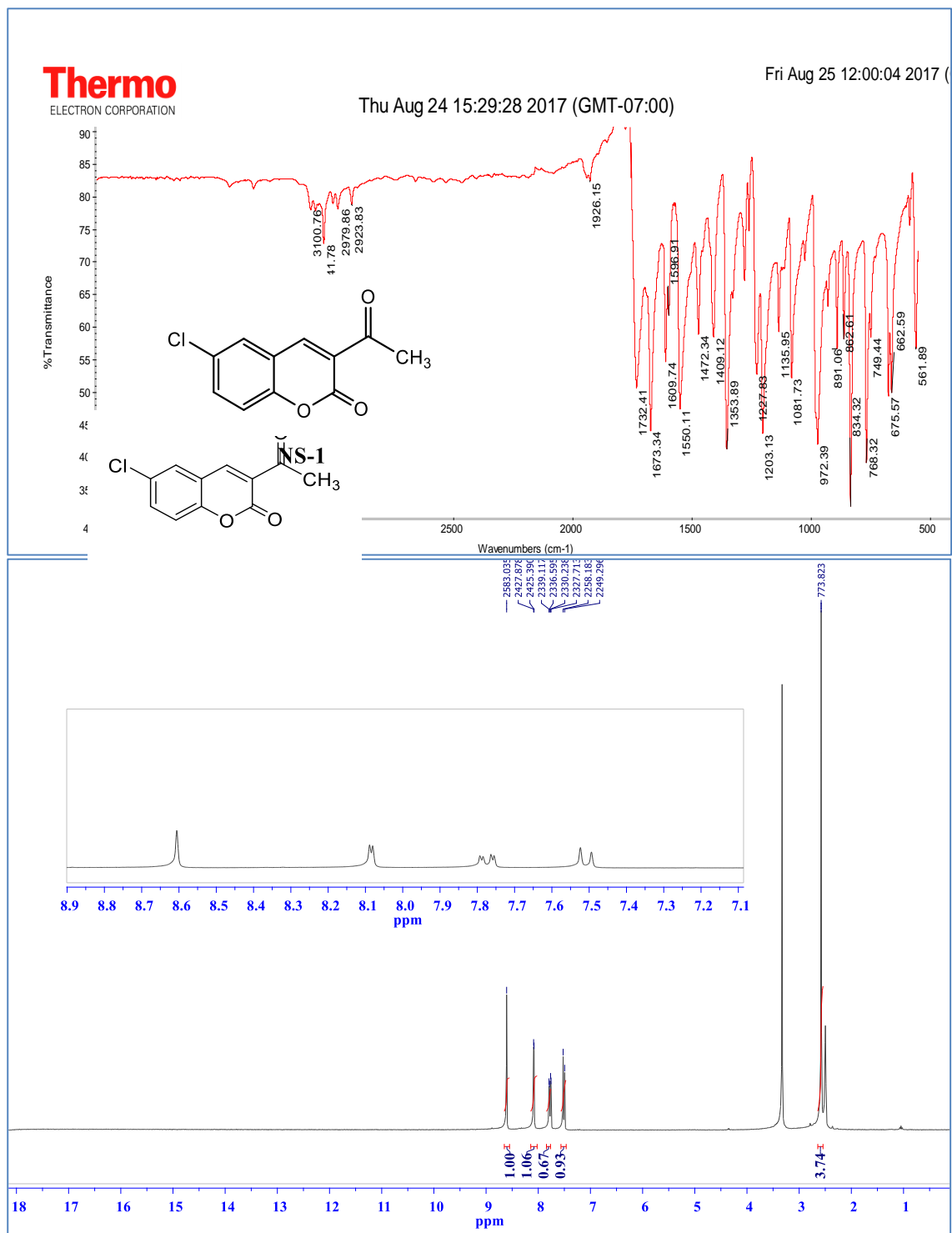


Figure 1.3.2.  $^1\text{H-NMR}$  (DMSO- $d_6$ ) Spectrum of 3

Appendix-1. (Continues) FT-IR,  $^1\text{H-NMR}$ ,  $^{13}\text{C-NMR}$ , HR-MS of the 3-Acetylcoumarins (1)-(10)

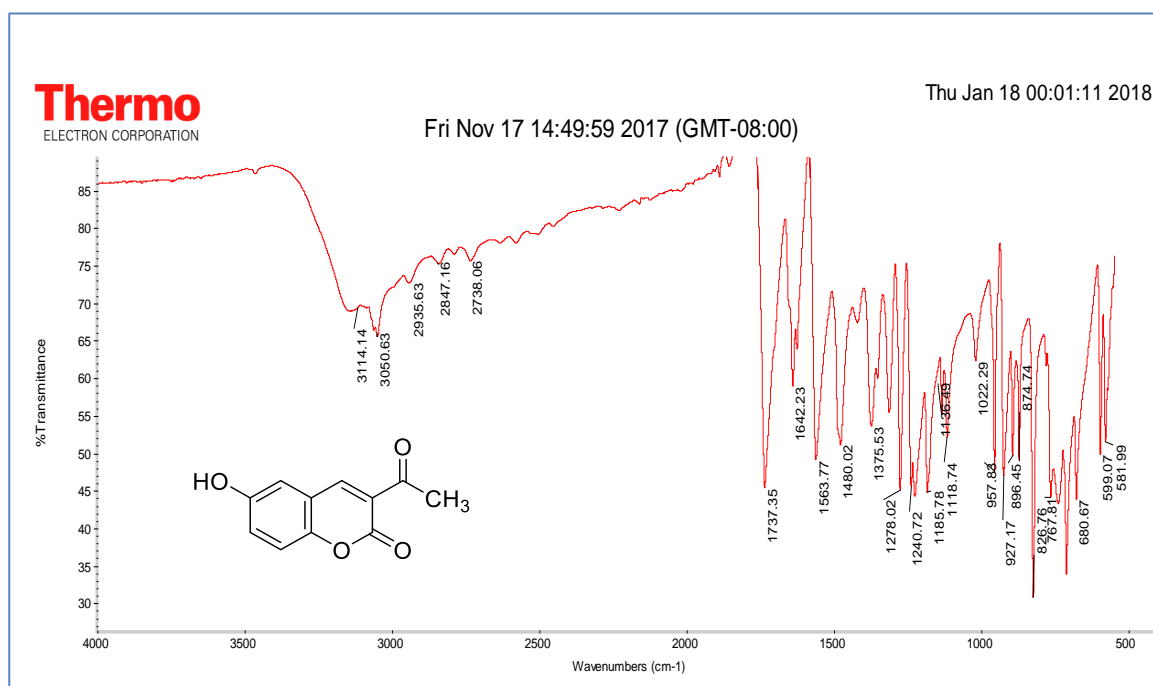


Figure 1.4.1. FT-IR Spectrum of 4

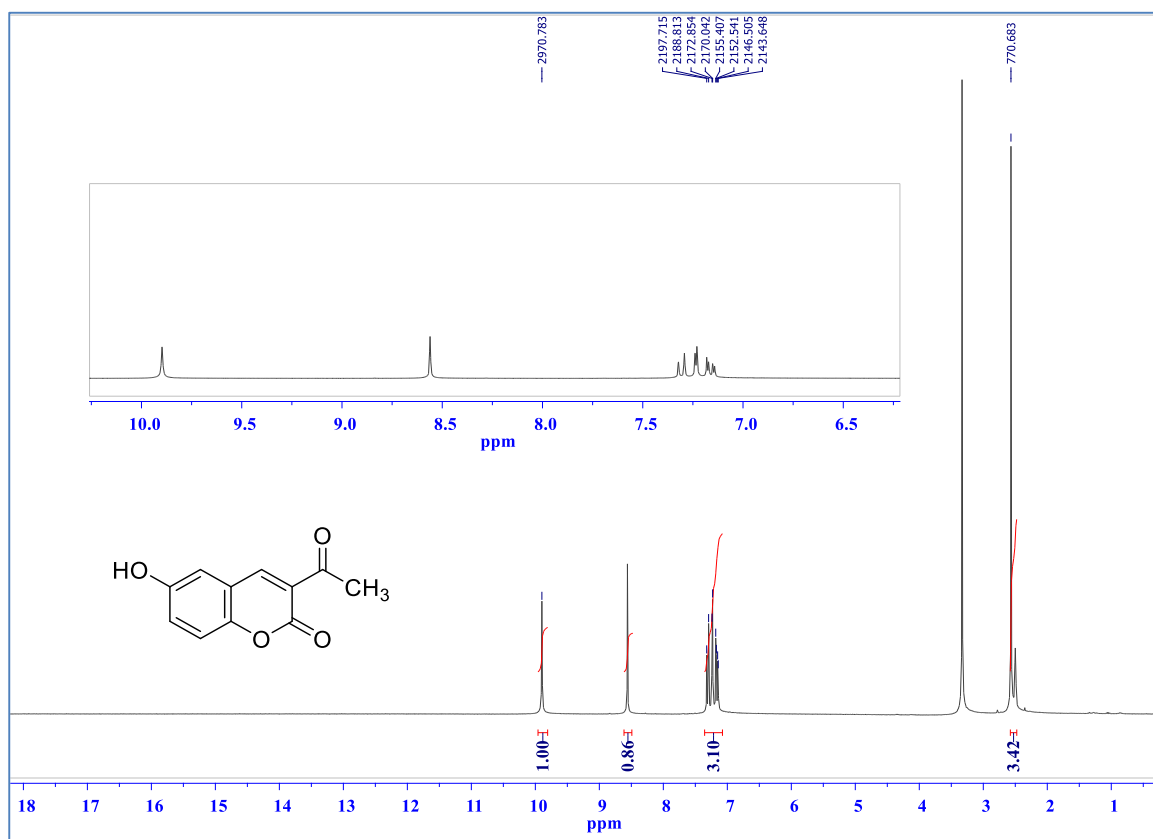


Figure 1.4.2.  $^1\text{H-NMR}$  ( $\text{DMSO-}d_6$ ) Spectrum of 4

Appendix-1. (Continues) FT-IR,  $^1\text{H-NMR}$ ,  $^{13}\text{C-NMR}$ , HR-MS of the 3-Acetylcoumarins (1)-(10)

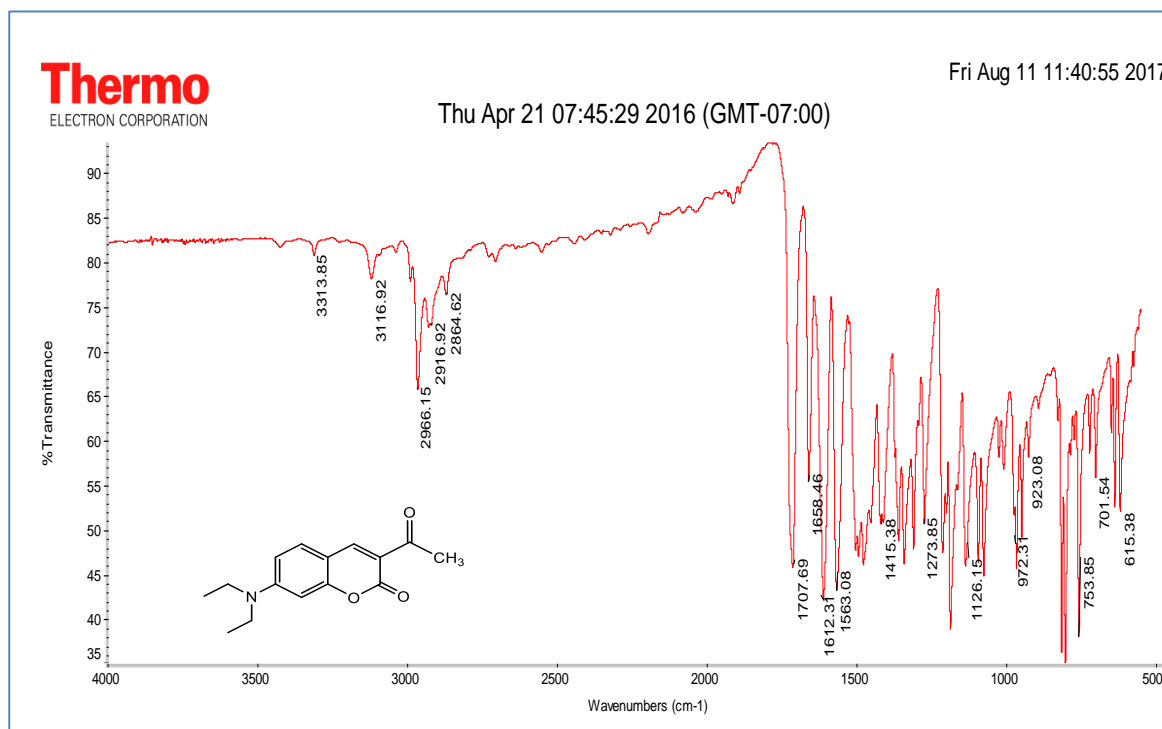


Figure 1.5.1. FT-IR Spectrum of 5

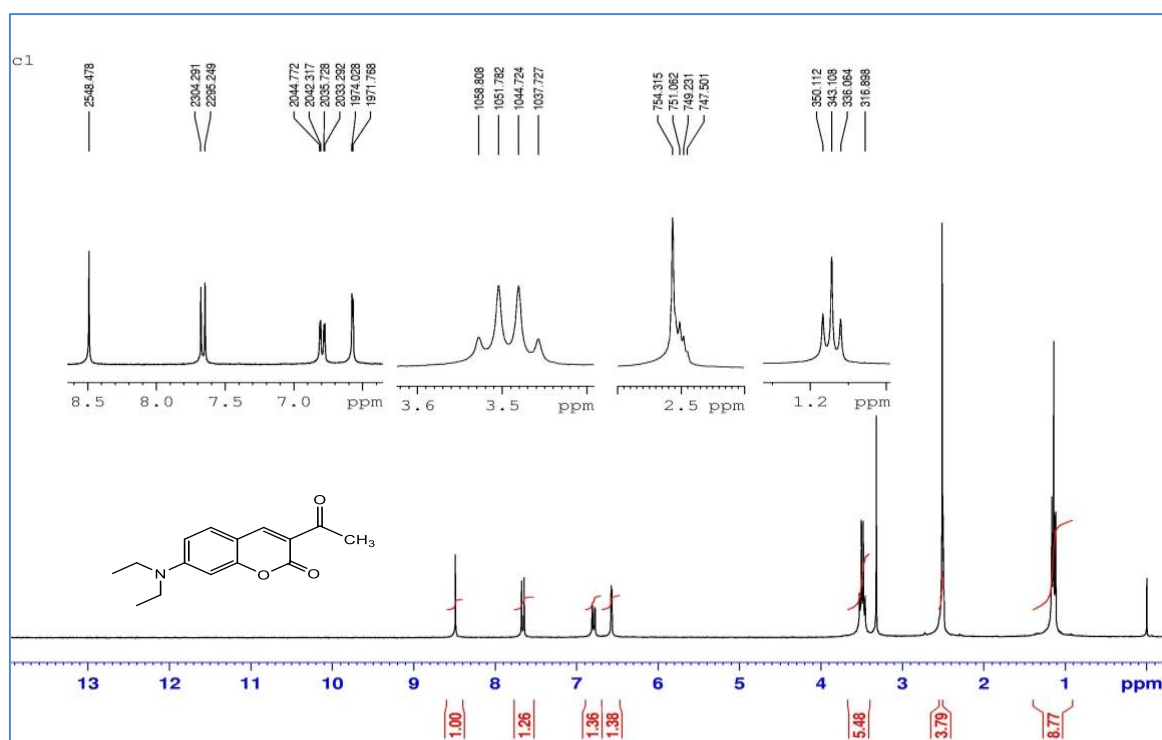


Figure 1.5.2.  $^1\text{H-NMR}$  ( $\text{DMSO-}d_6$ ) Spectrum of 5

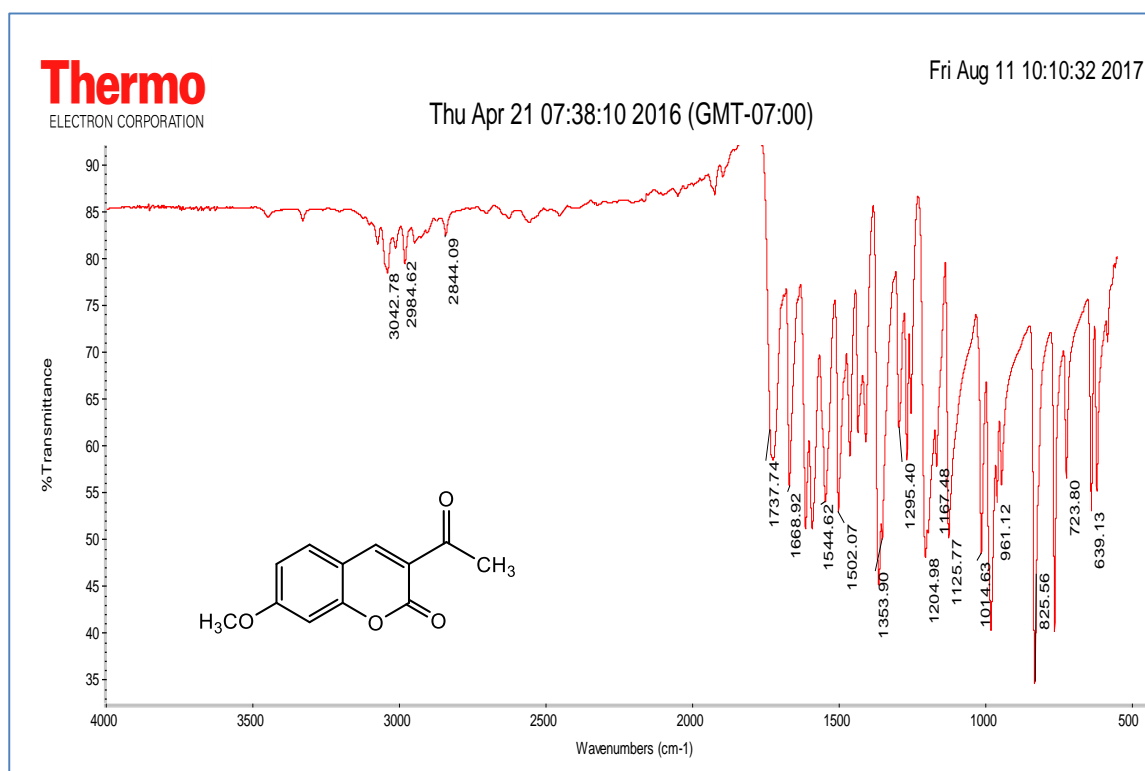
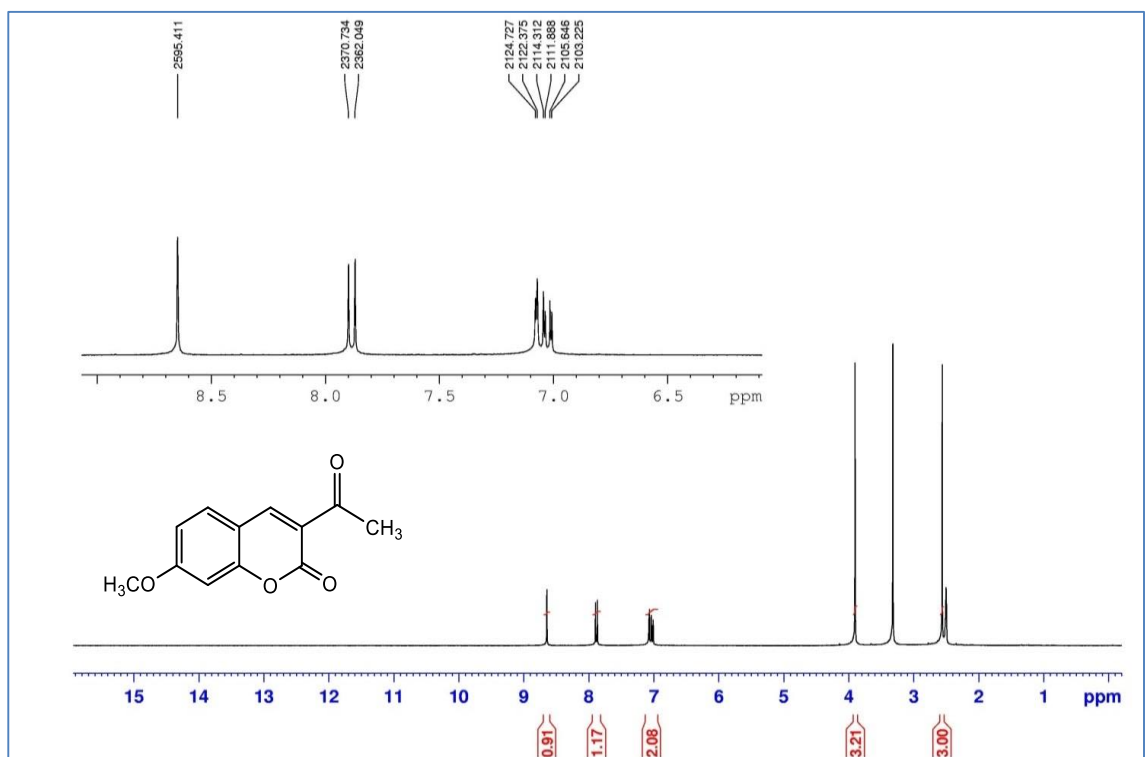
Appendix-1. (Continues) FT-IR,  $^1\text{H-NMR}$ ,  $^{13}\text{C-NMR}$ , HR-MS of the 3-Acetylcoumarins (1)-(10)

Figure 1.6.1. FT-IR Spectrum of 6

Figure 1.6.2.  $^1\text{H-NMR}$  (DMSO- $d_6$ ) Spectrum of 6

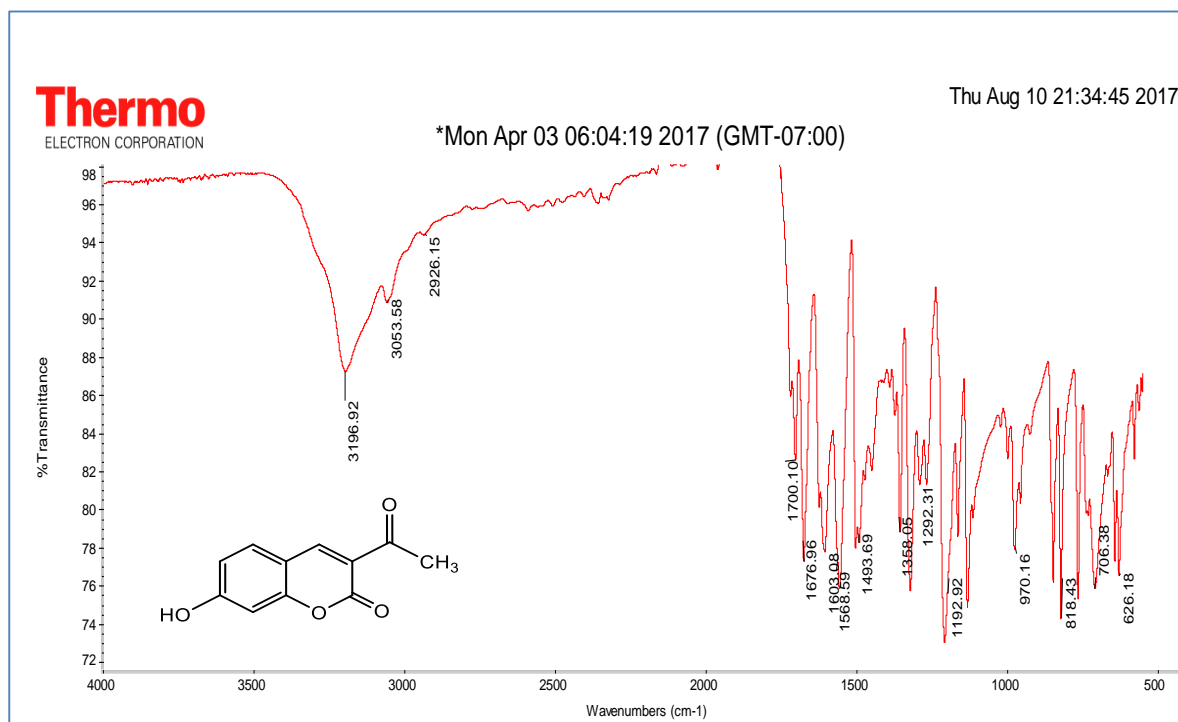
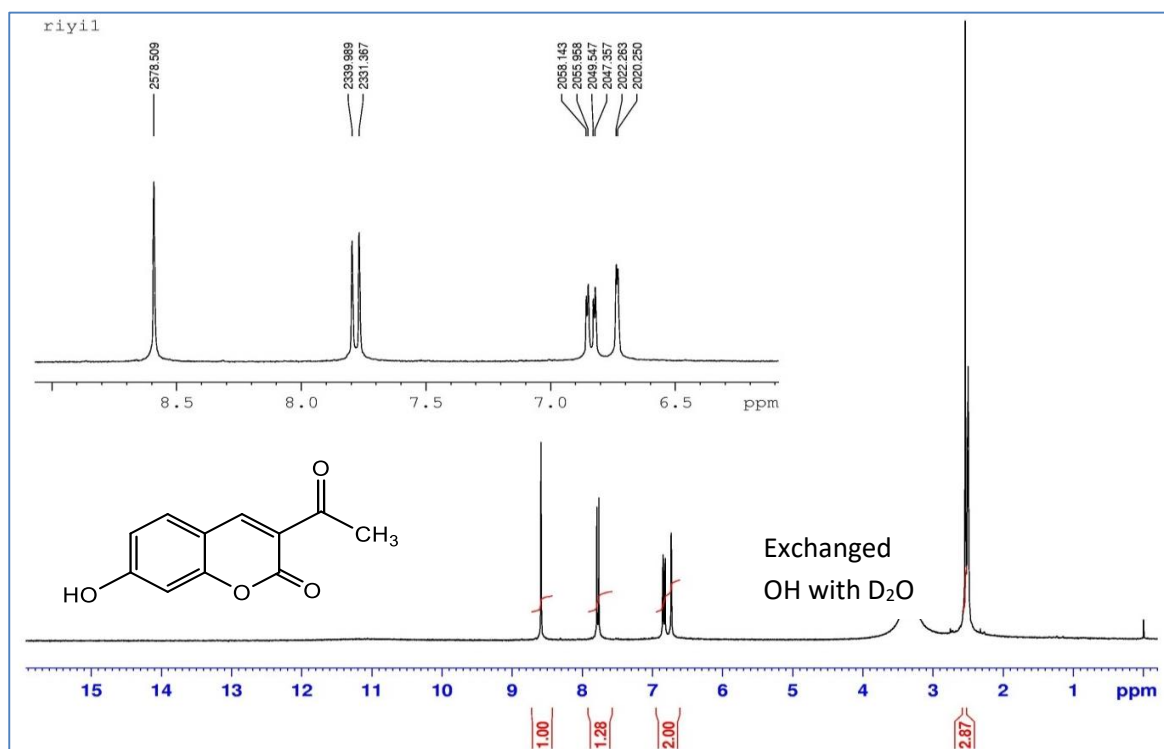
Appendix-1. (Continues) FT-IR,  $^1\text{H-NMR}$ ,  $^{13}\text{C-NMR}$ , HR-MS of the 3-Acetylcoumarins (1)-(10)

Figure 1.7.1. FT-IR Spectrum of 7

Figure 1.7.2.  $^1\text{H-NMR}$  (DMSO- $d_6$ ) Spectrum of 7



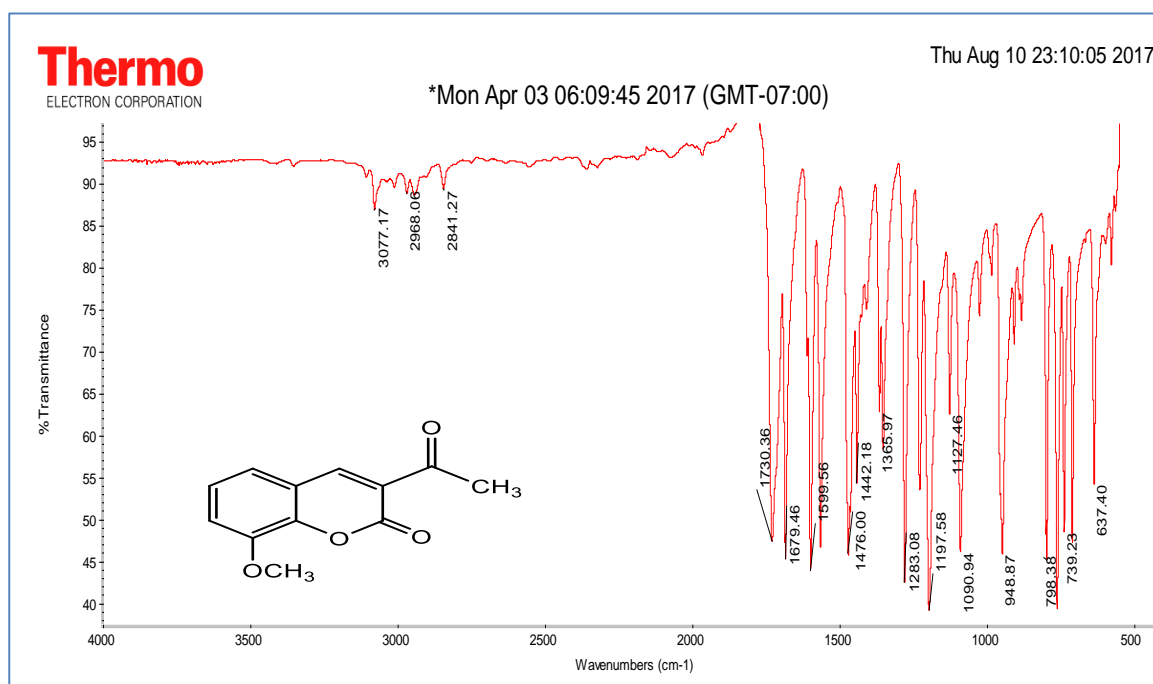
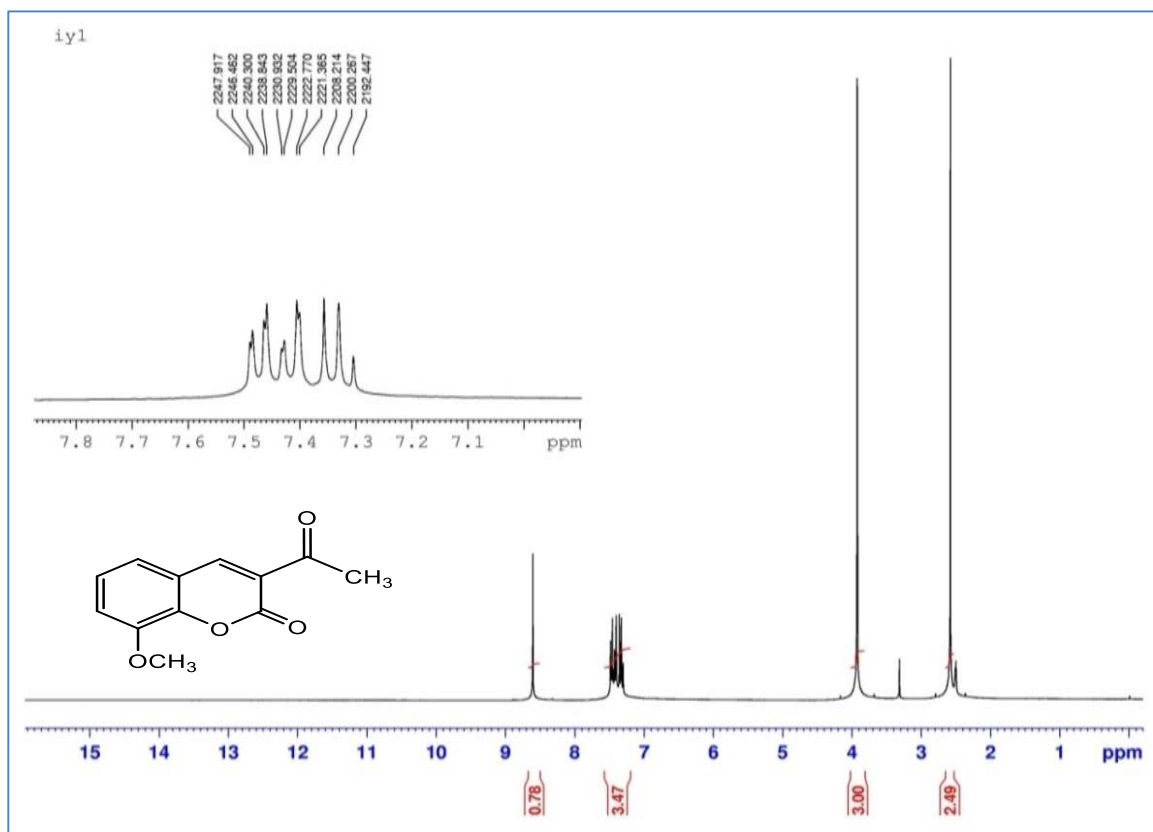
Appendix-1. (Continues) FT-IR,  $^1\text{H-NMR}$ ,  $^{13}\text{C-NMR}$ , HR-MS of the 3-Acetylcoumarins (1)-(10)

Figure 1.9.1. FT-IR Spectrum of 9

Figure 1.9.2.  $^1\text{H-NMR}$  ( $\text{DMSO-}d_6$ ) Spectrum of 9

Appendix-1. (Continues) FT-IR,  $^1\text{H-NMR}$ ,  $^{13}\text{C-NMR}$ , HR-MS of the 3-Acetylcoumarins (1)-(10)

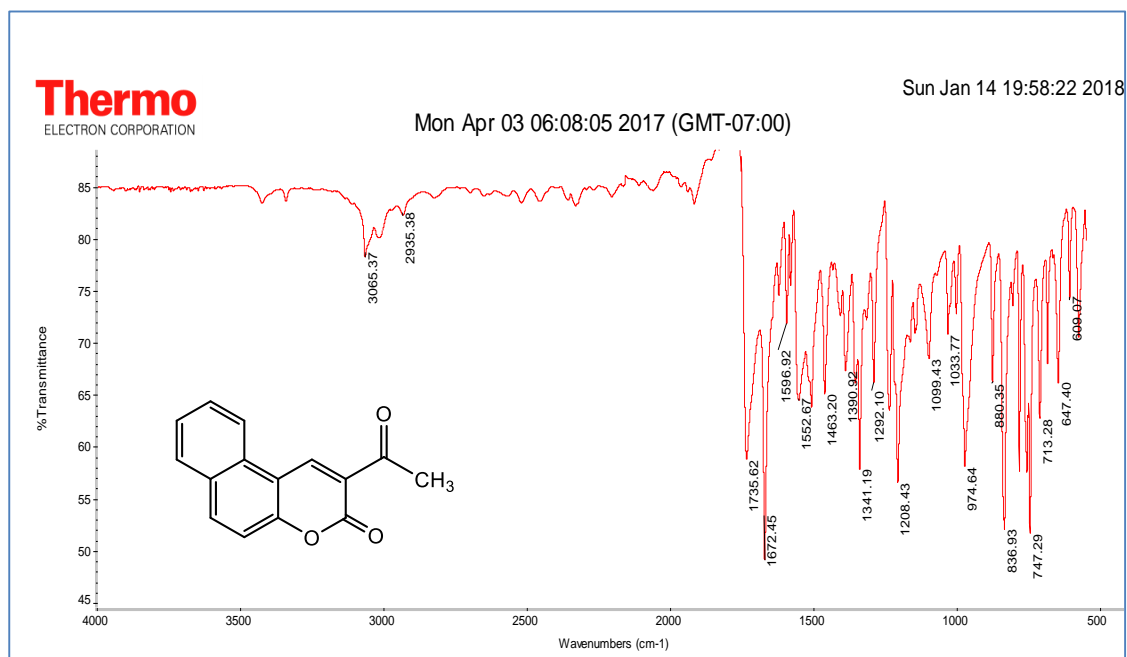


Figure 1.10.1 FT-IR Spectrum of 10

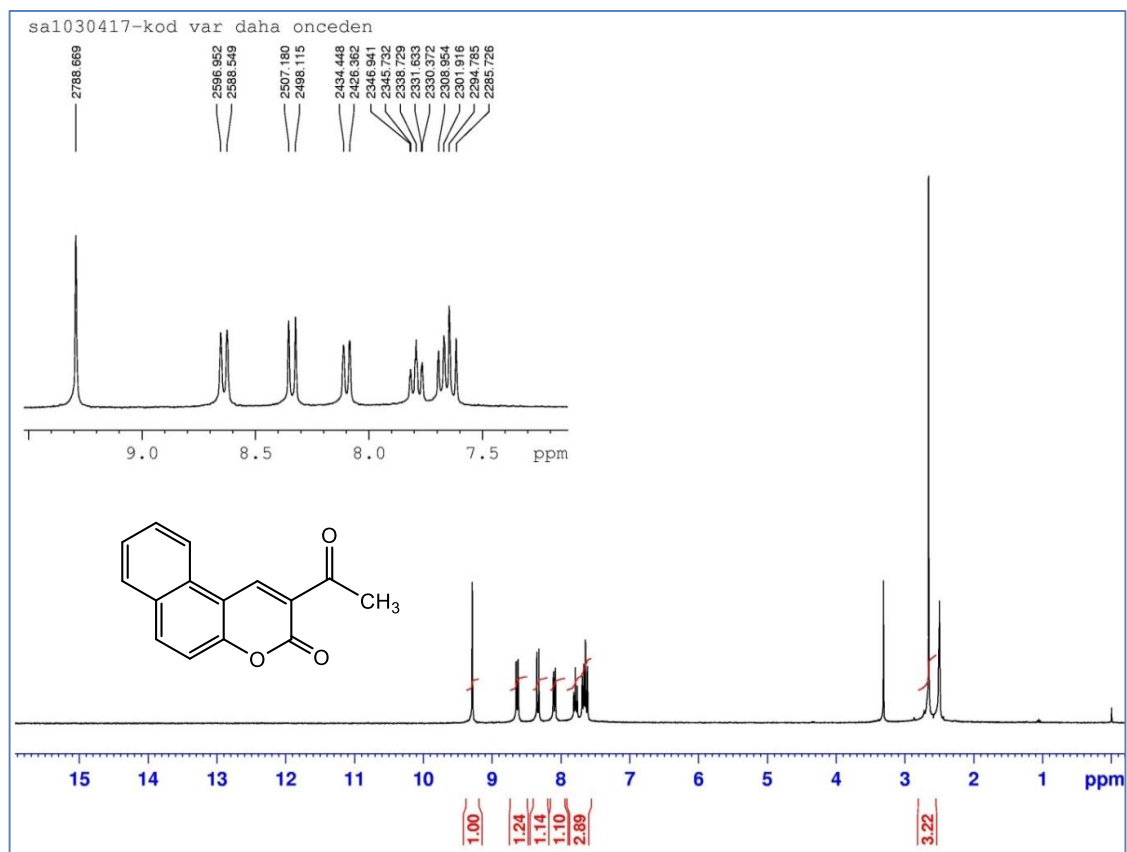


Figure 1.10.2.  $^1\text{H-NMR}$  (DMSO- $d_6$ ) Spectrum of 10

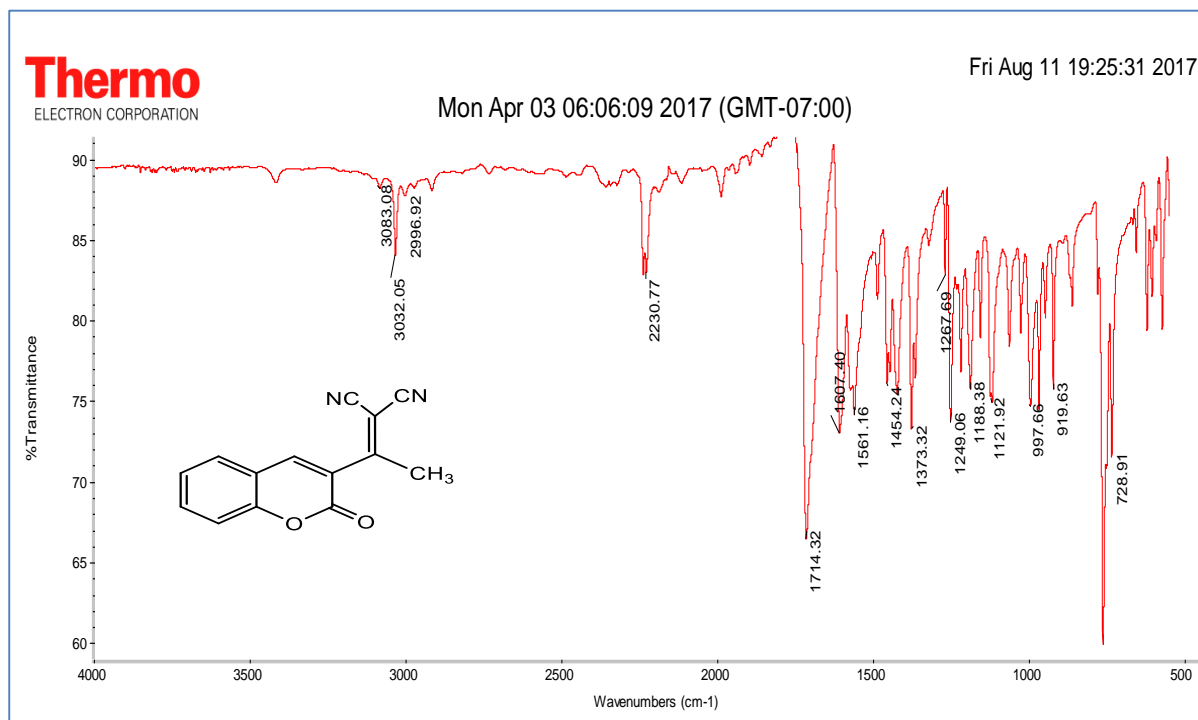
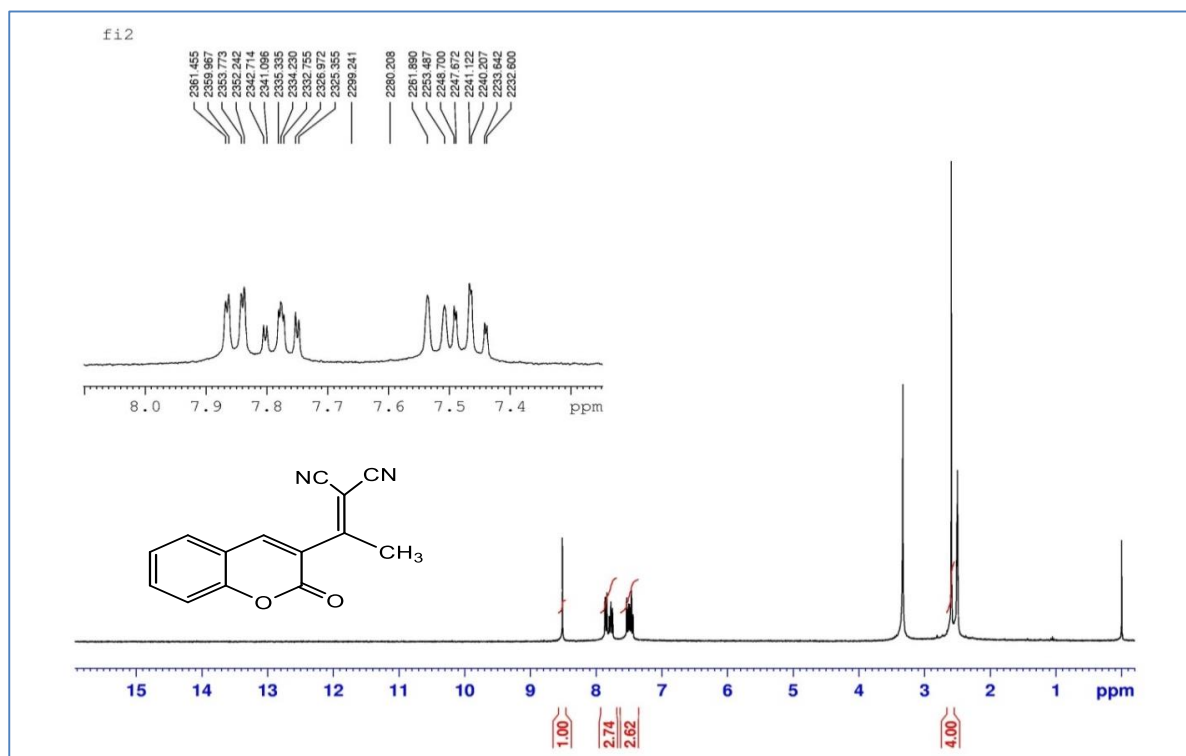
Appendix-2. FT-IR,  $^1\text{H-NMR}$ ,  $^{13}\text{C-APT}$ , HRMS of the Malononitriles 11-20

Figure 2.1.1. FT-IR Spectrum of 11

Figure 2.1.2.  $^1\text{H-NMR}$  ( $\text{DMSO-}d_6$ ) Spectrum of 11

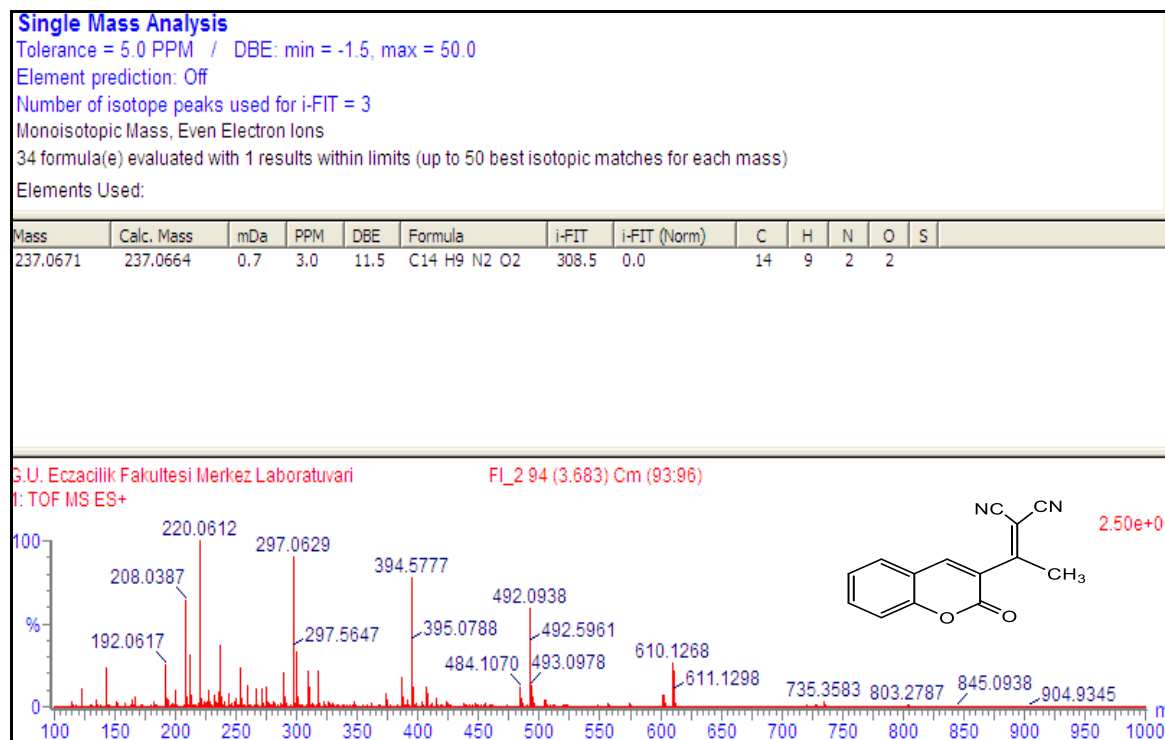
Appendix-2. (Continues) FT-IR, <sup>1</sup>H-NMR, <sup>13</sup>C-APT, HRMS of the Malononitriles 11-20

Figure 2.1.3. HRMS spectrum of 11

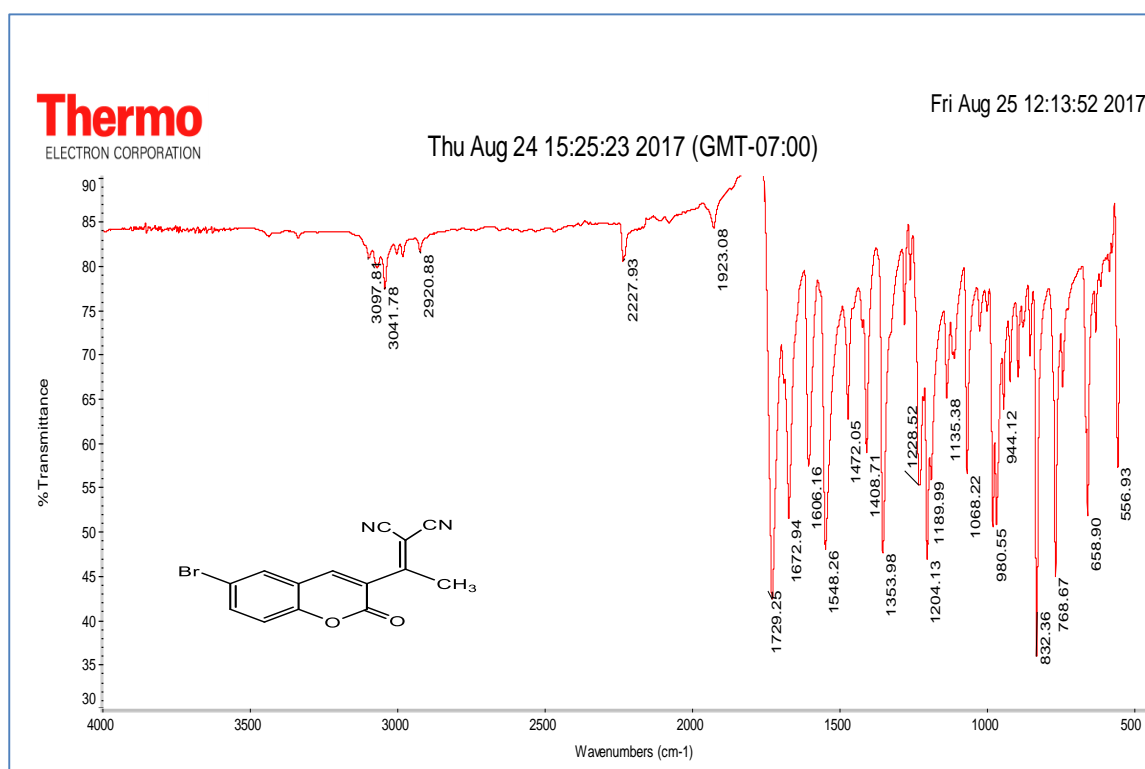


Figure 2.2.1. FT-IR Spectrum of 12

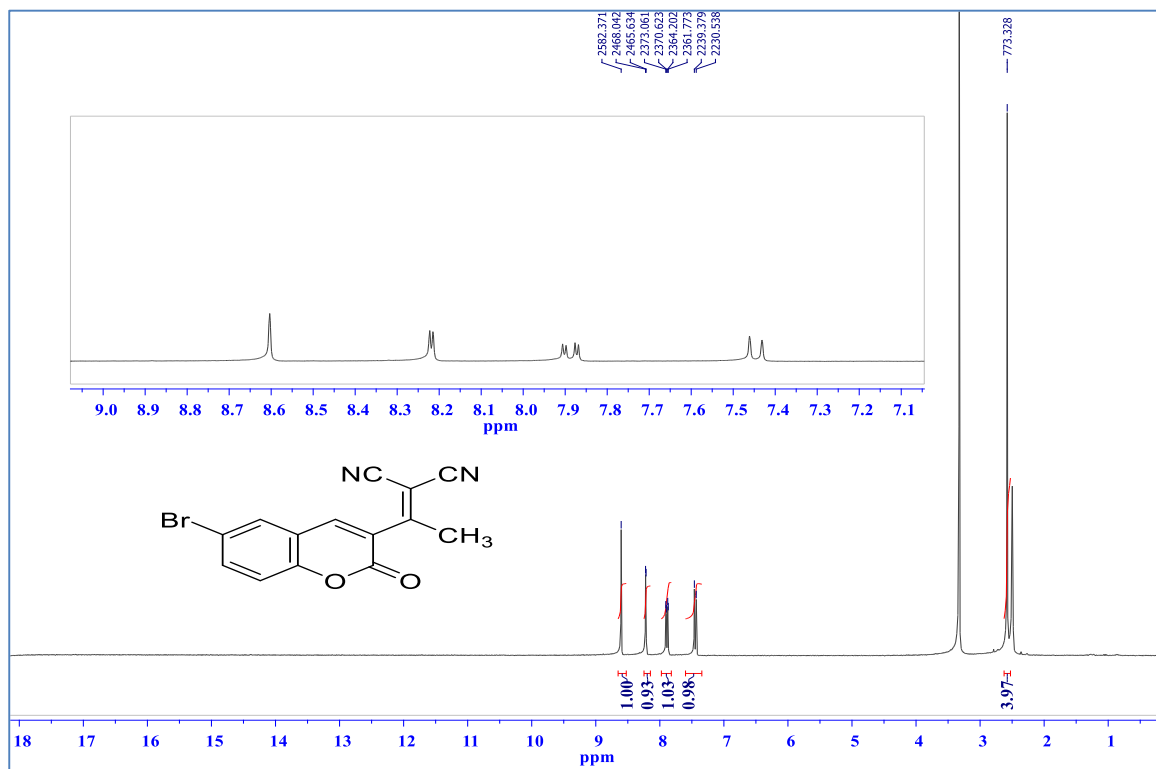
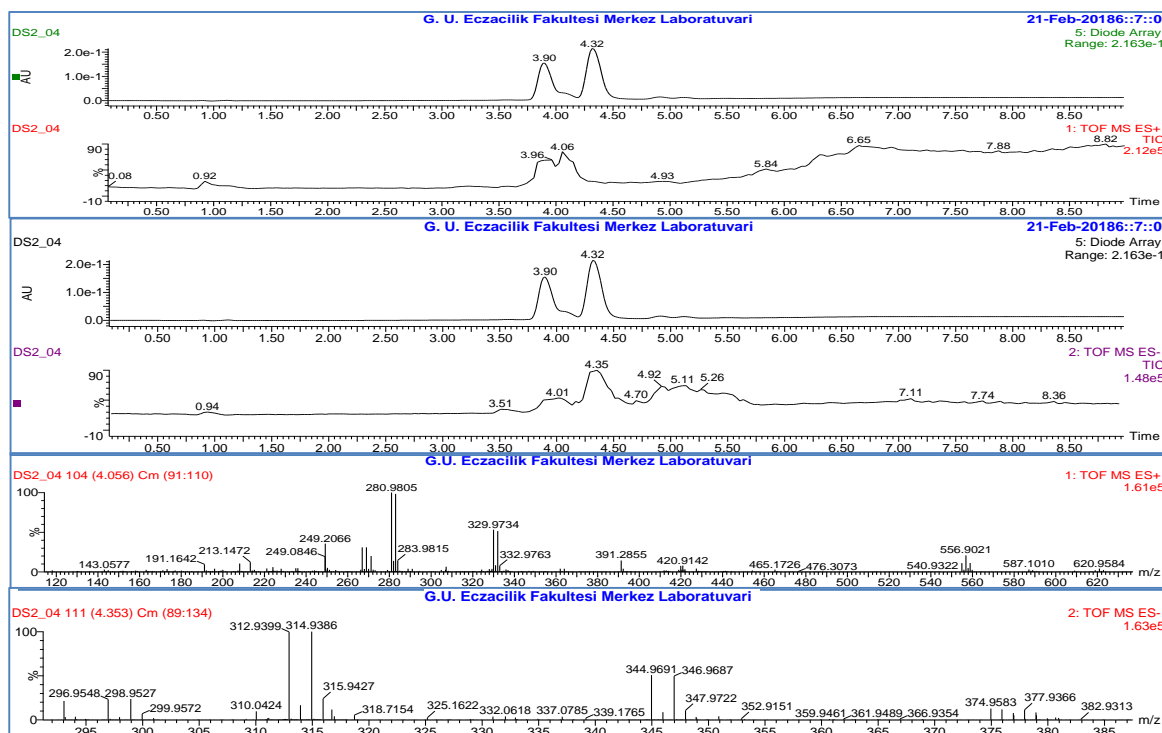
Appendix-2. (Continues) FT-IR,  $^1\text{H-NMR}$ ,  $^{13}\text{C-APT}$ , HRMS of the Malononitriles 11-20Figure 2.2.2.  $^1\text{H-NMR}$  (DMSO- $d_6$ ) Spectrum of 12

Figure 2.2.3. HRMS spectrum of 12

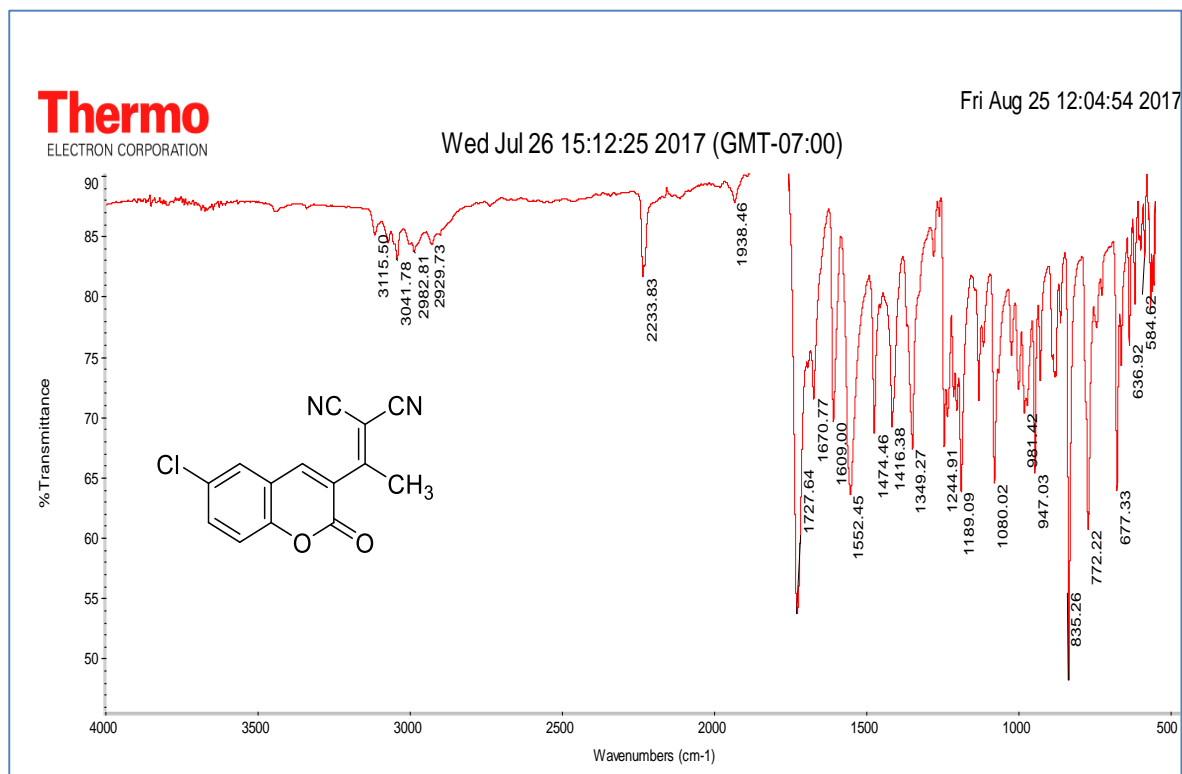
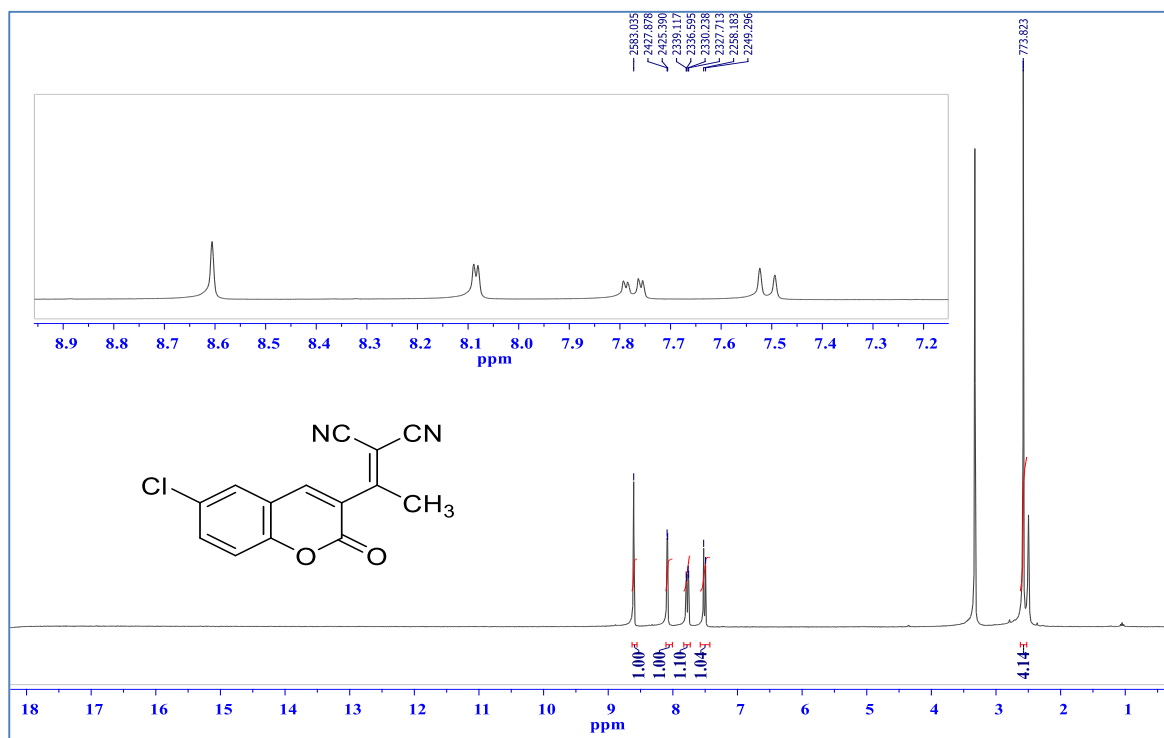
Appendix-2. (Continues) FT-IR,  $^1\text{H-NMR}$ ,  $^{13}\text{C-APT}$ , HRMS of the Malononitriles 11-20

Figure 2.3.1. FT-IR Spectrum of 13

Figure 2.3.2.  $^1\text{H-NMR}$  ( $\text{DMSO-}d_6$ ) Spectrum of 13

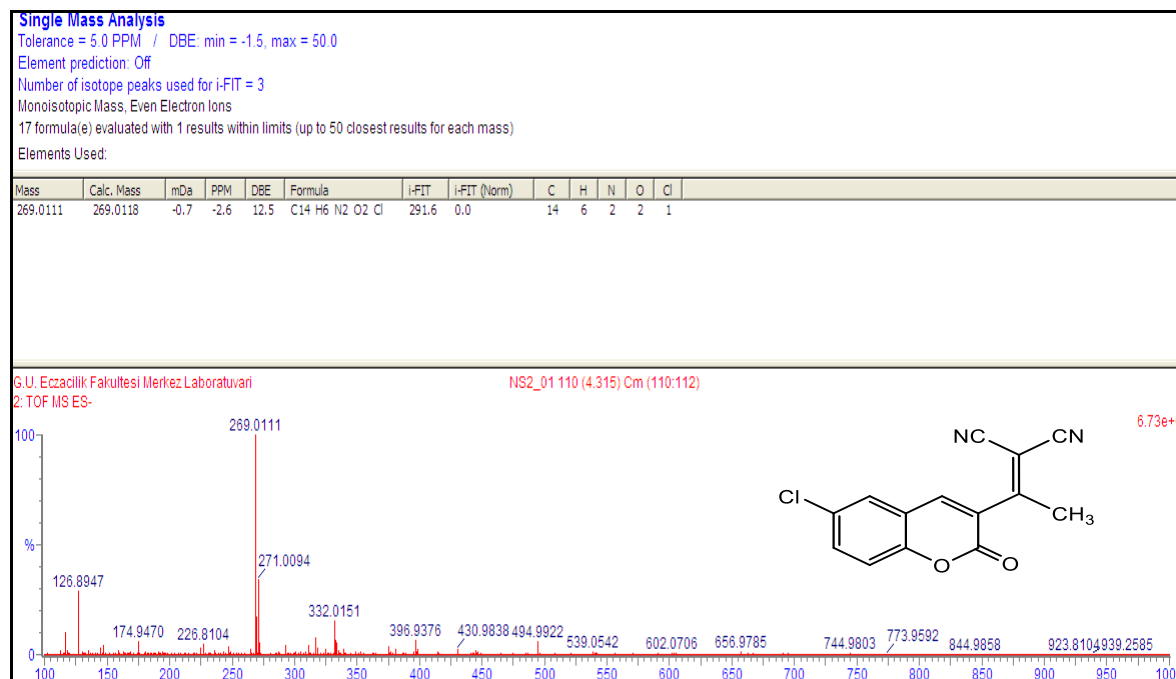
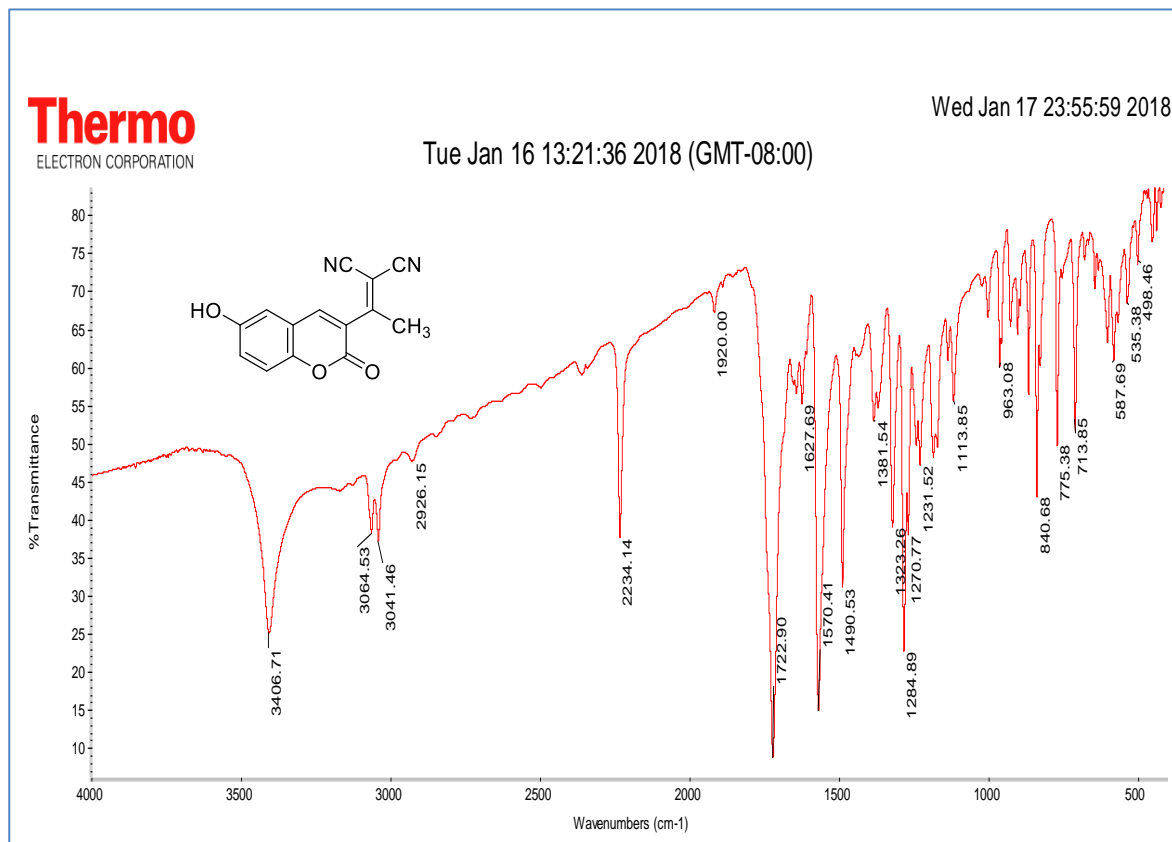
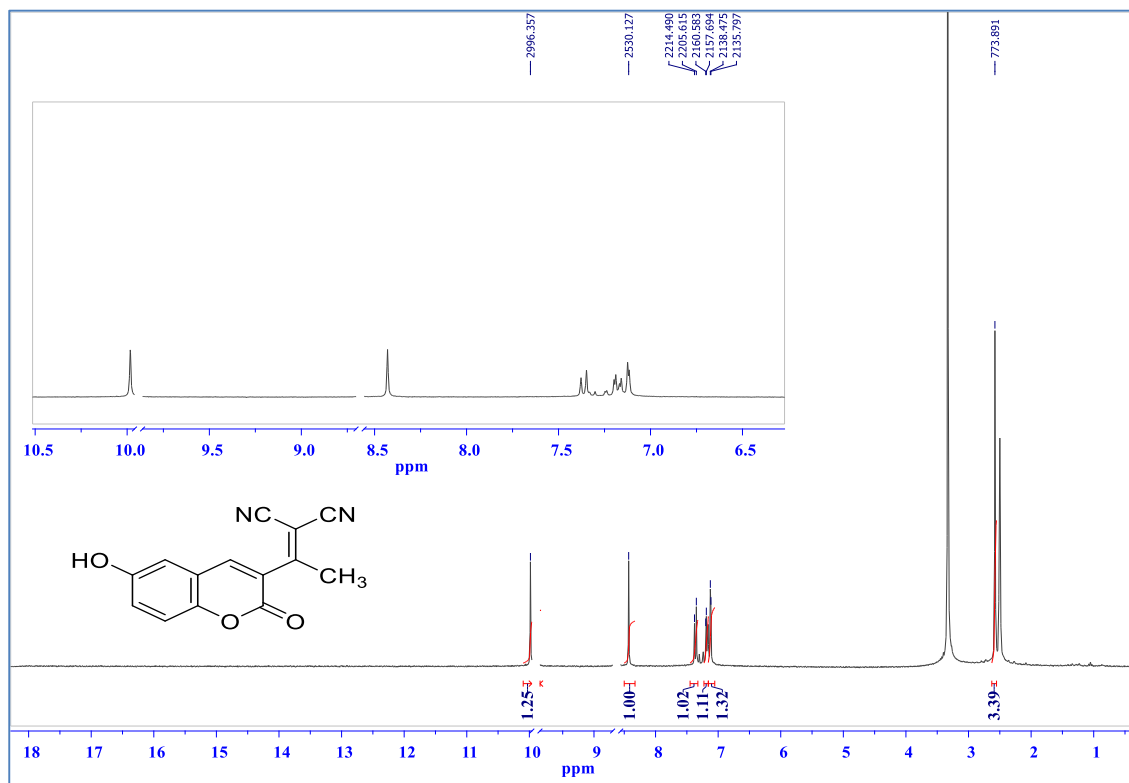
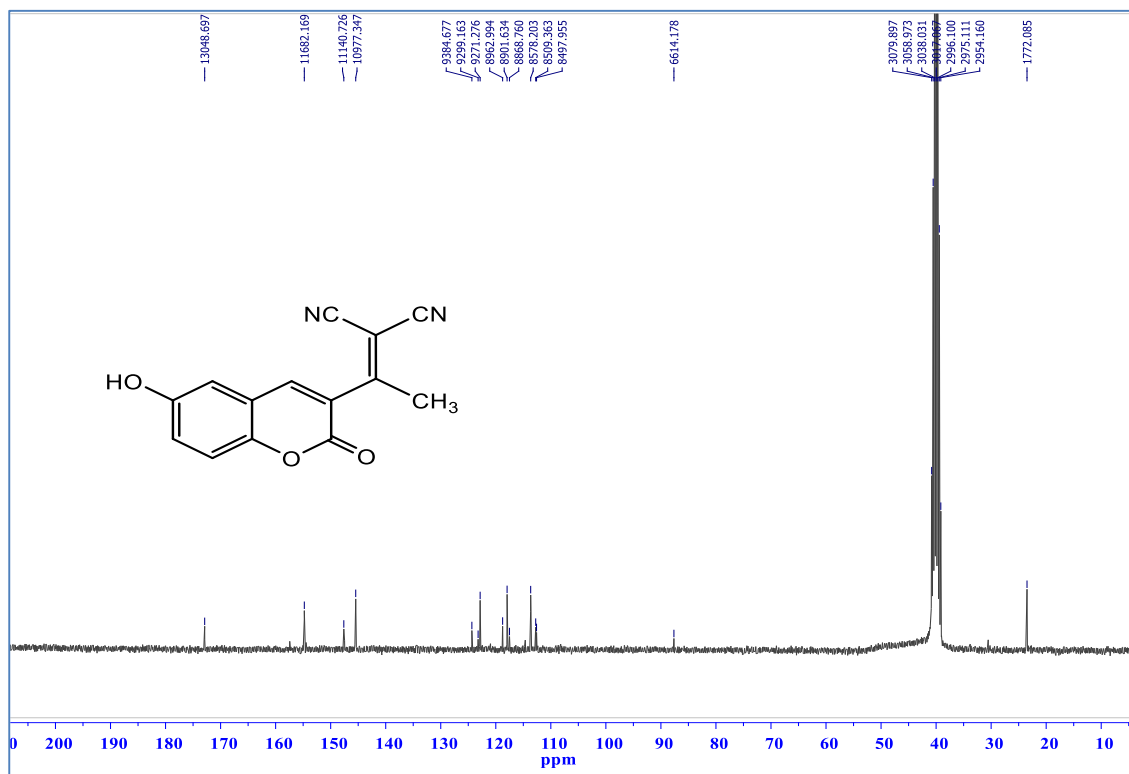
Appendix-2. (Continues) FT-IR, <sup>1</sup>H-NMR, <sup>13</sup>C-APT, HRMS of the Malononitriles 11-20

Figure 2.3.3. HRMS spectrum of 13

Figure 2.4.1. FT-IR (DMSO-*d*<sub>6</sub>) Spectrum of 14

Appendix-2. (Continues) FT-IR,  $^1\text{H-NMR}$ ,  $^{13}\text{C-APT}$ , HRMS of the Malononitriles 11-20Figure 2.4.2.  $^1\text{H-NMR}$  (DMSO- $d_6$ ) Spectrum of 14Figure 2.4.3.  $^{13}\text{C-APT}$  (DMSO- $d_6$ ) Spectrum of 14

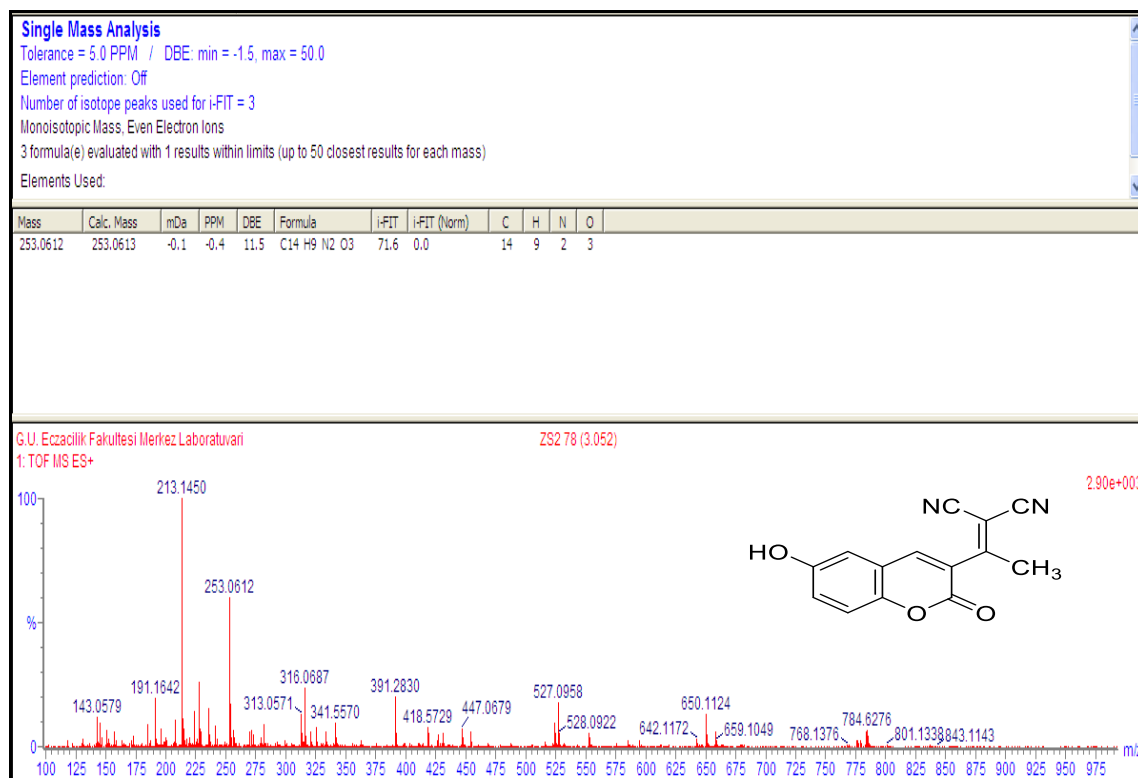
Appendix-2. (Continues) FT-IR, <sup>1</sup>H-NMR, <sup>13</sup>C-APT, HRMS of the Malononitriles 11-20

Figure 2.4.4. HRMS Spectrum of 14

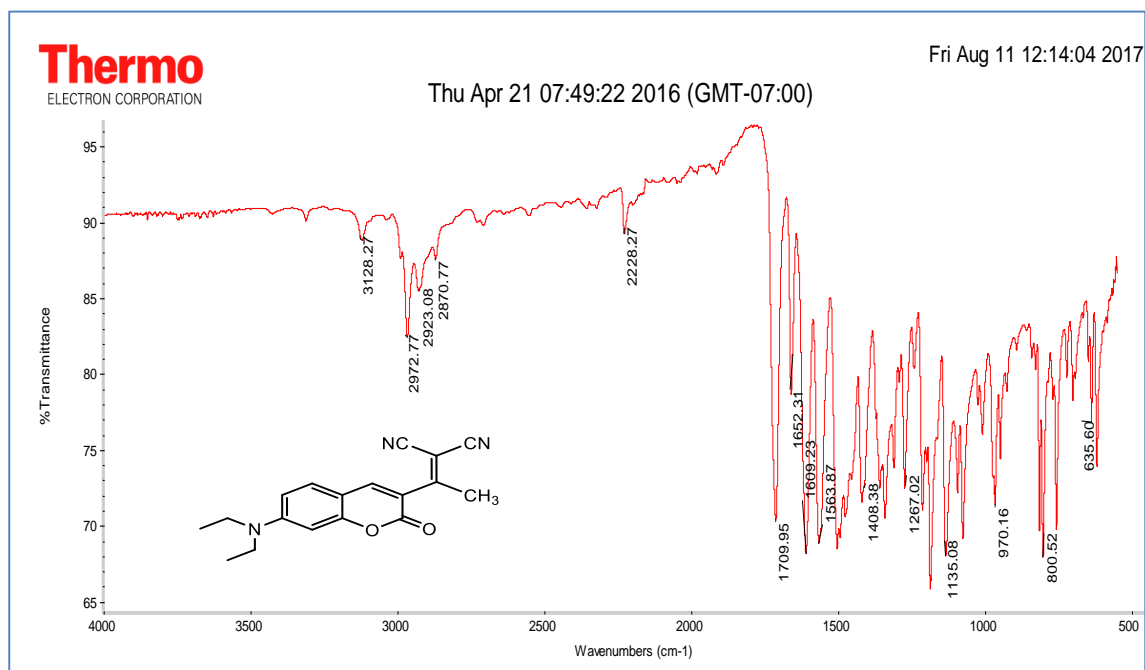


Figure 2.5.1. FT-IR spectrum of 15

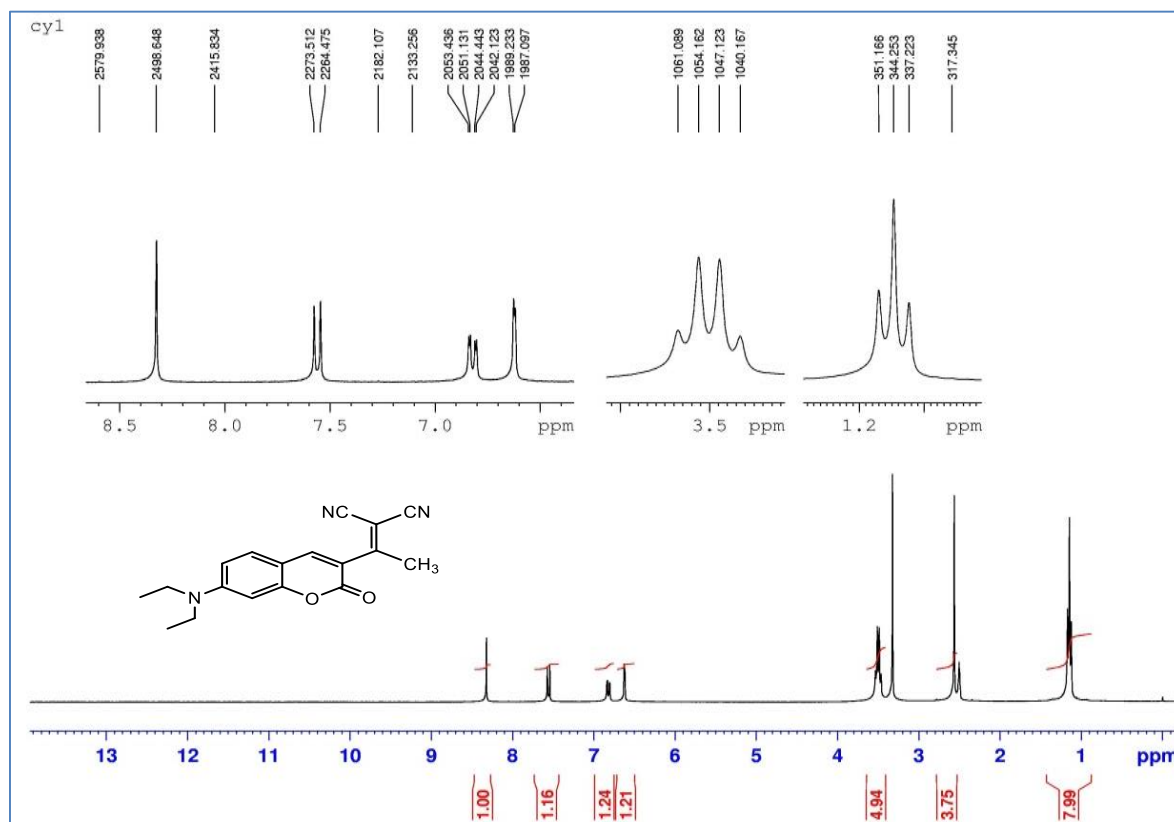
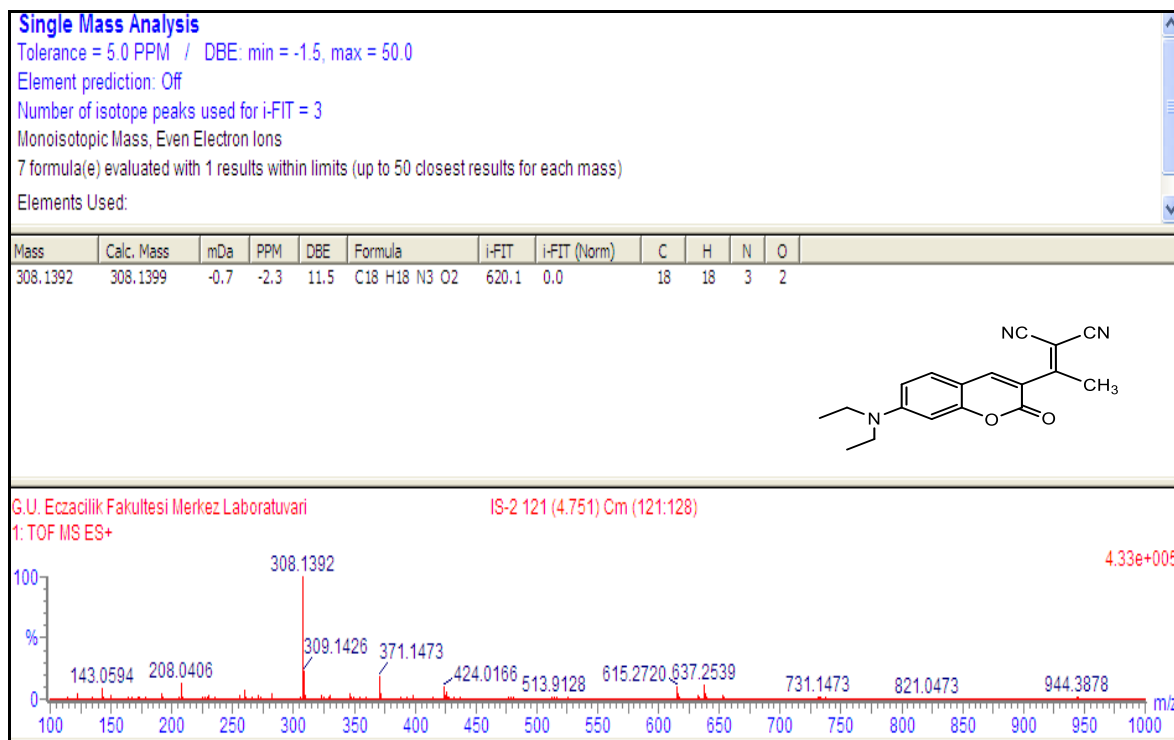
Appendix-2. (Continues) FT-IR,  $^1\text{H-NMR}$ ,  $^{13}\text{C-APT}$ , HRMS of the Malononitriles 11-20Figure 2.5.2.  $^1\text{H-NMR}$  ( $\text{DMSO-}d_6$ ) Spectrum of 15

Figure 2.5.3. HRMS Spectrum of 15

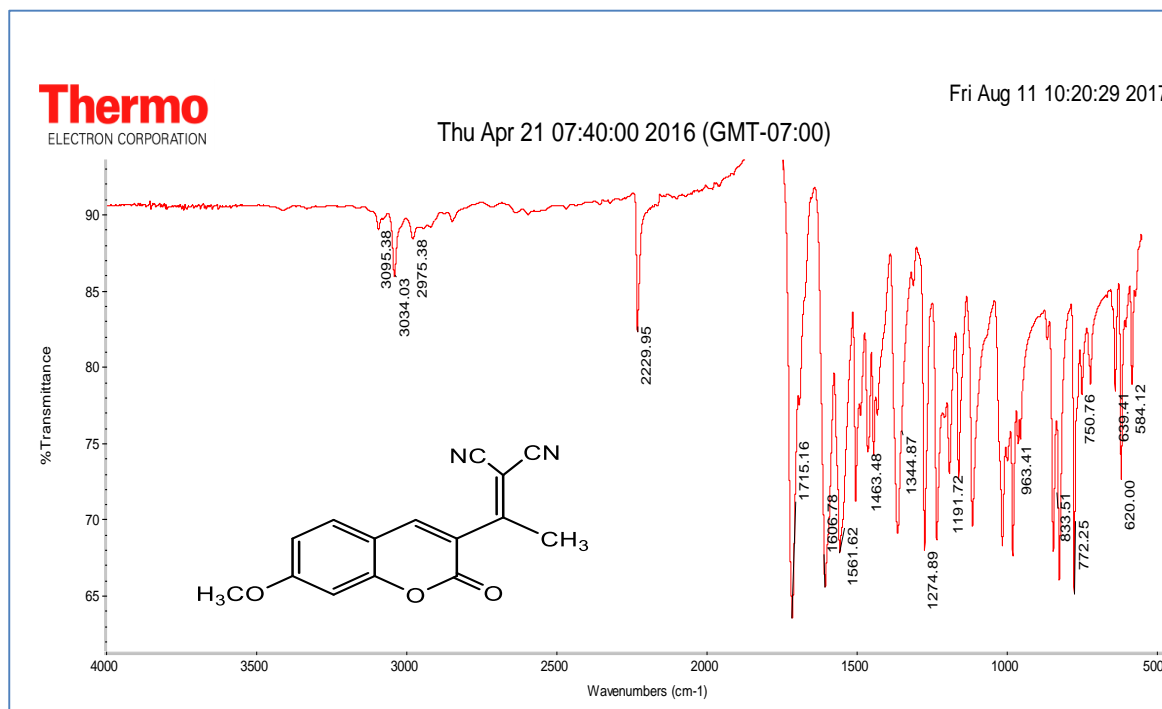
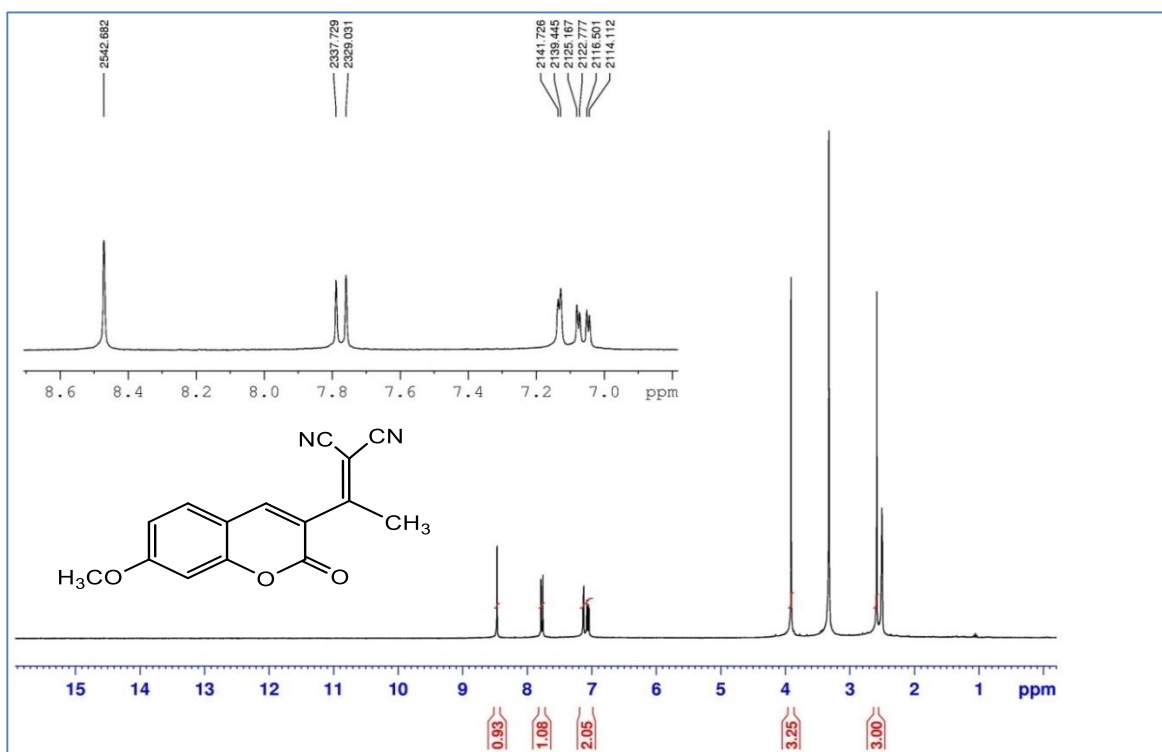
Appendix-2. (Continuous) FT-IR,  $^1\text{H-NMR}$ ,  $^{13}\text{C-NMR}$ , HRMS of the Malononitriles 11-20

Figure 2.6.1. FT-IR Spectrum of 16

Figure 2.6.2.  $^1\text{H-NMR}$  ( $\text{DMSO-}d_6$ ) Spectrum of 16

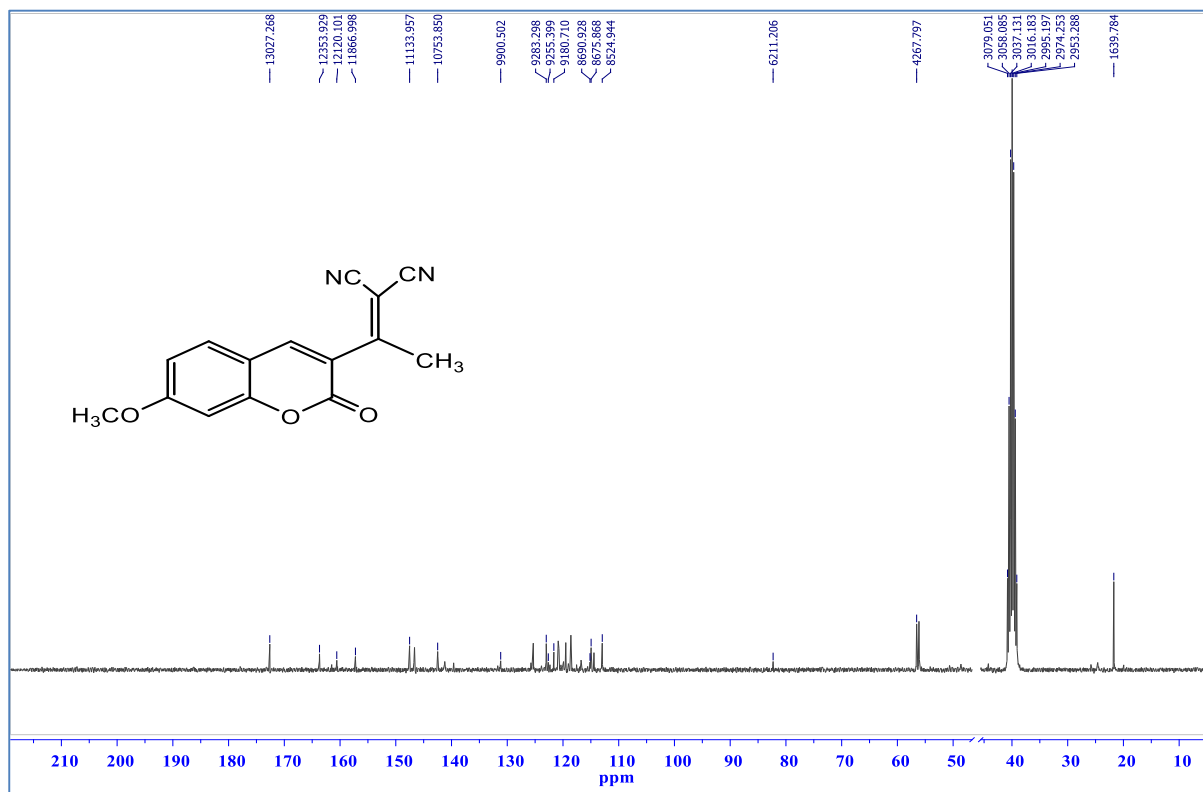
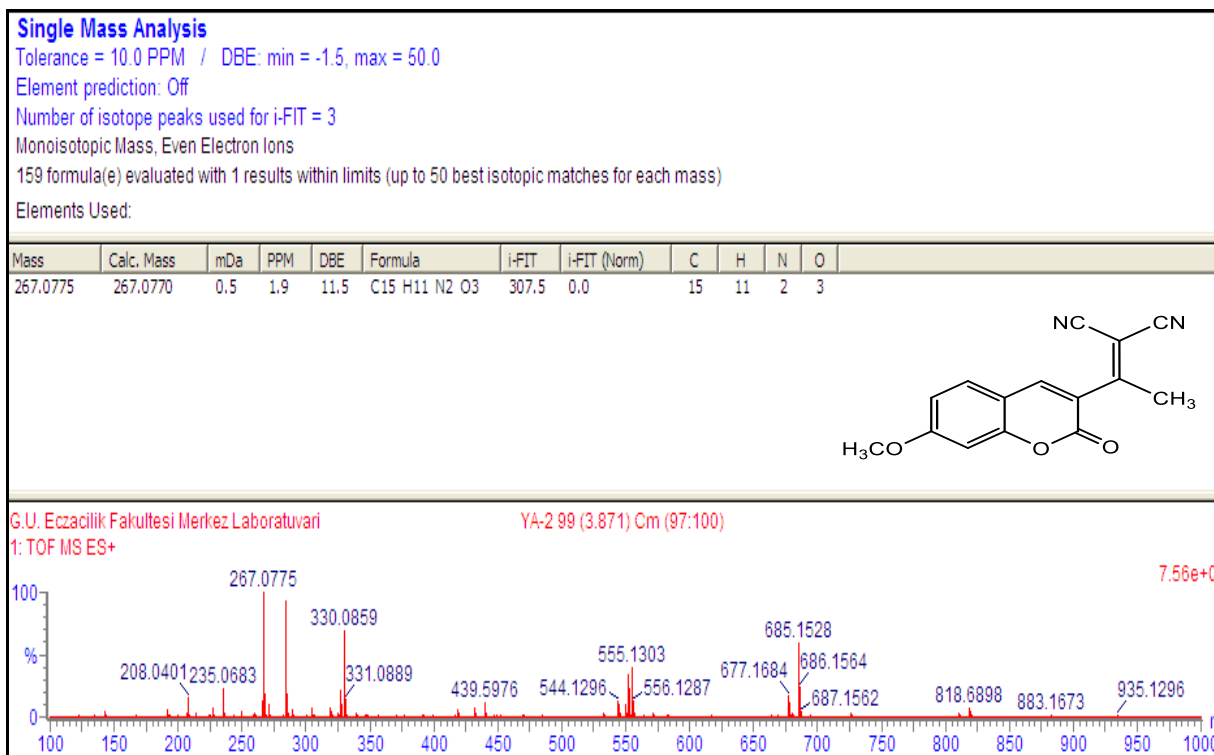
Appendix-2. (Continues) FT-IR, <sup>1</sup>H-NMR, <sup>13</sup>C-APT, HRMS of the Malononitriles 11-20Figure 2.6.3. <sup>13</sup>C-APT (DMSO-*d*<sub>6</sub>) Spectrum of 16

Figure 2.6.4. HRMS spectrum of 16

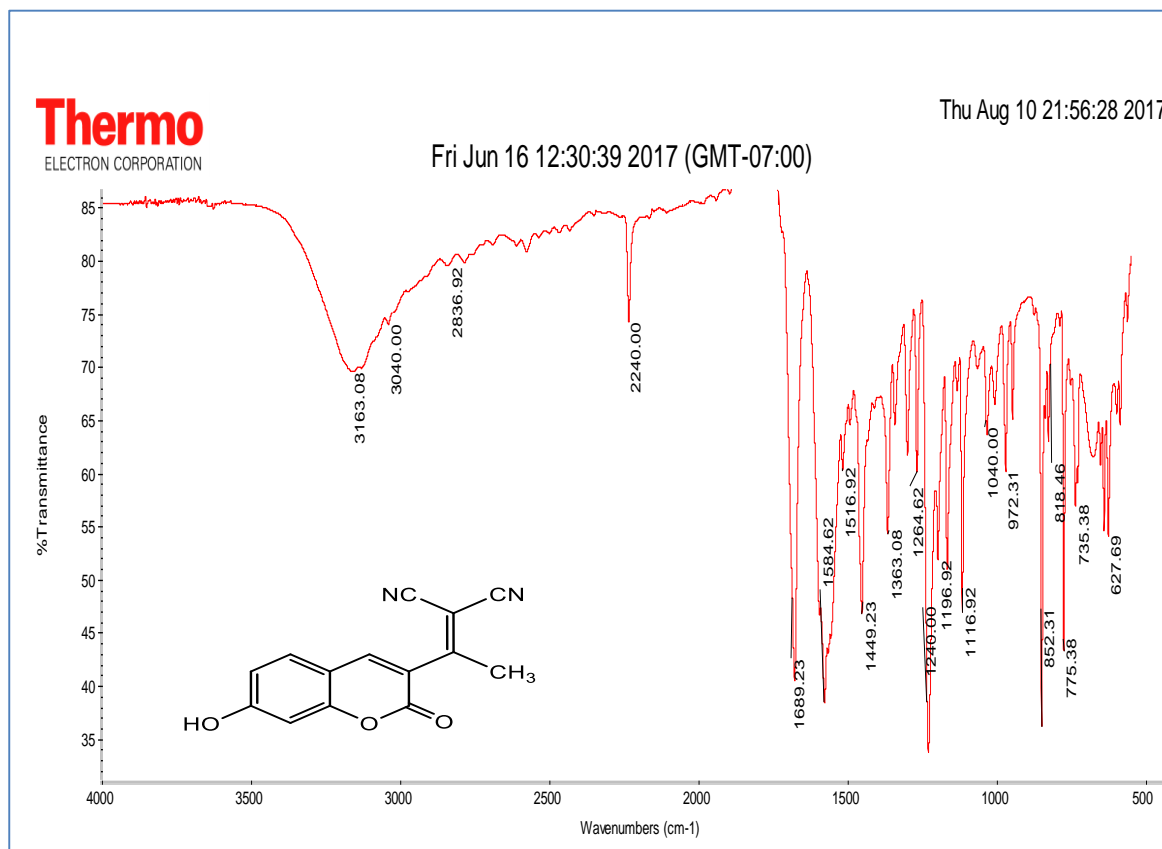
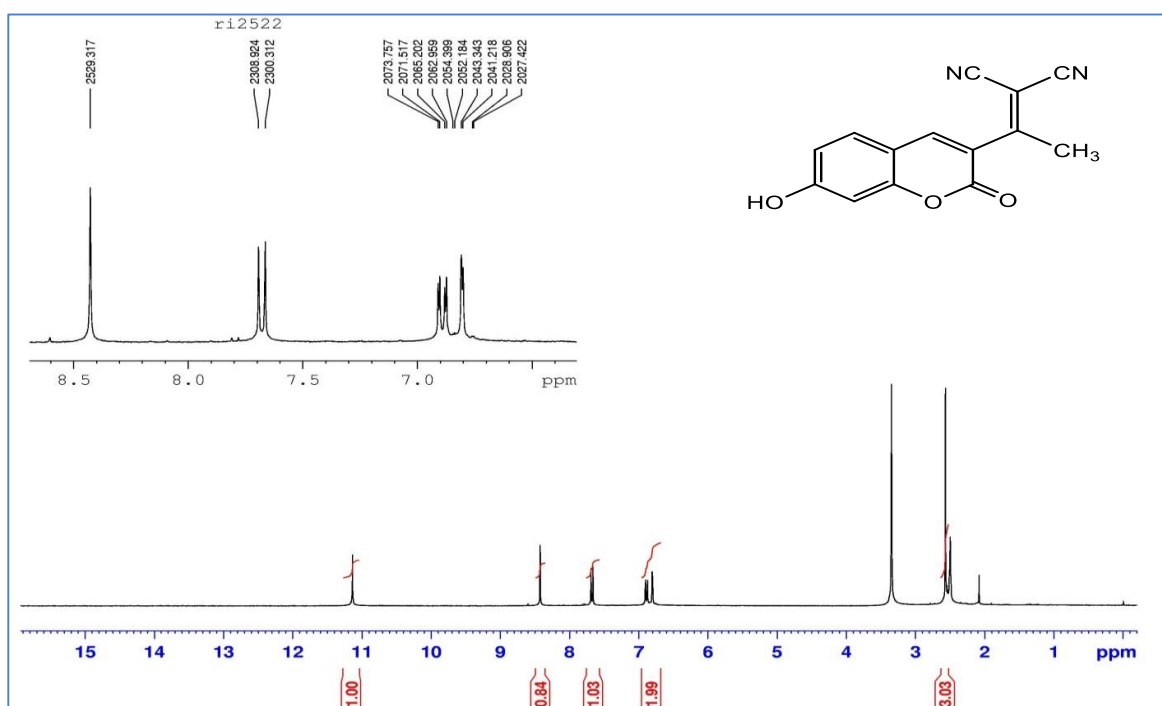
Appendix-2. (Continuous) FT-IR,  $^1\text{H-NMR}$ ,  $^{13}\text{C-NMR}$ , HRMS of the Malononitriles 11-20

Figure 2.7.1. FT-IR Spectrum of 17

Figure 2.7.2.  $^1\text{H-NMR}$  ( $\text{DMSO-}d_6$ ) Spectrum of 17

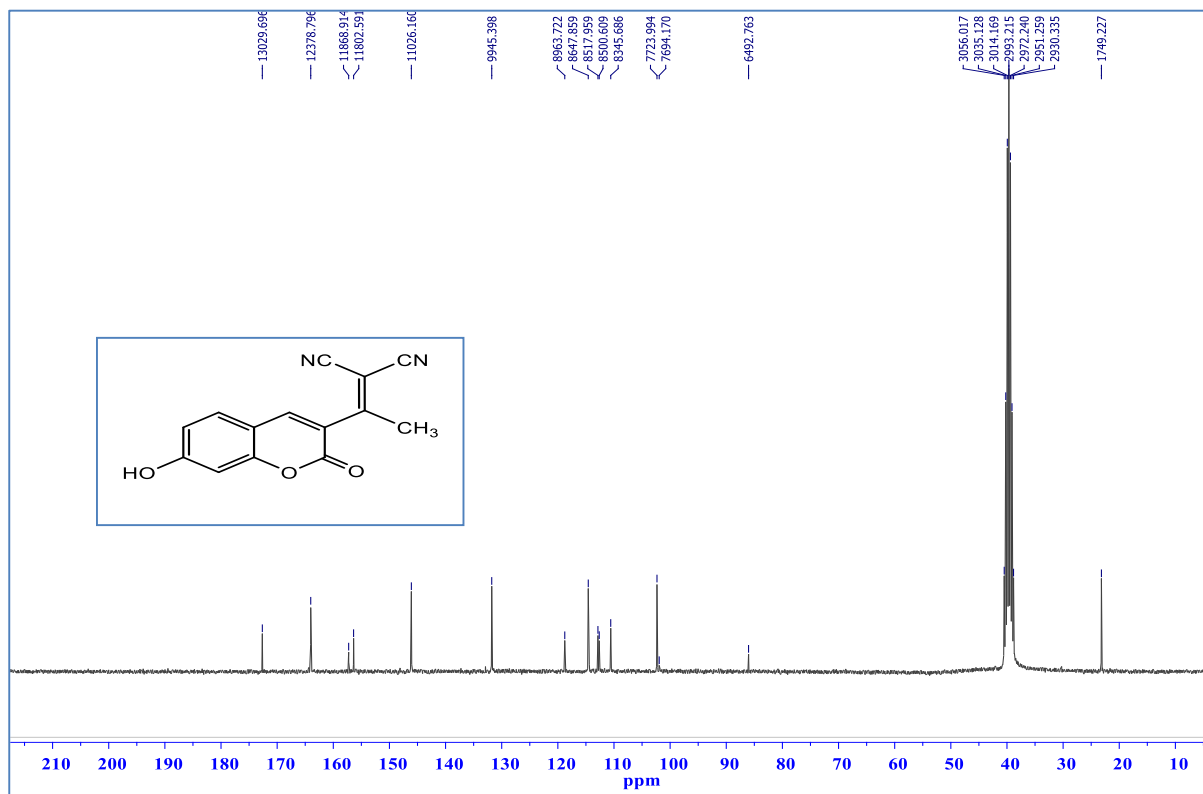
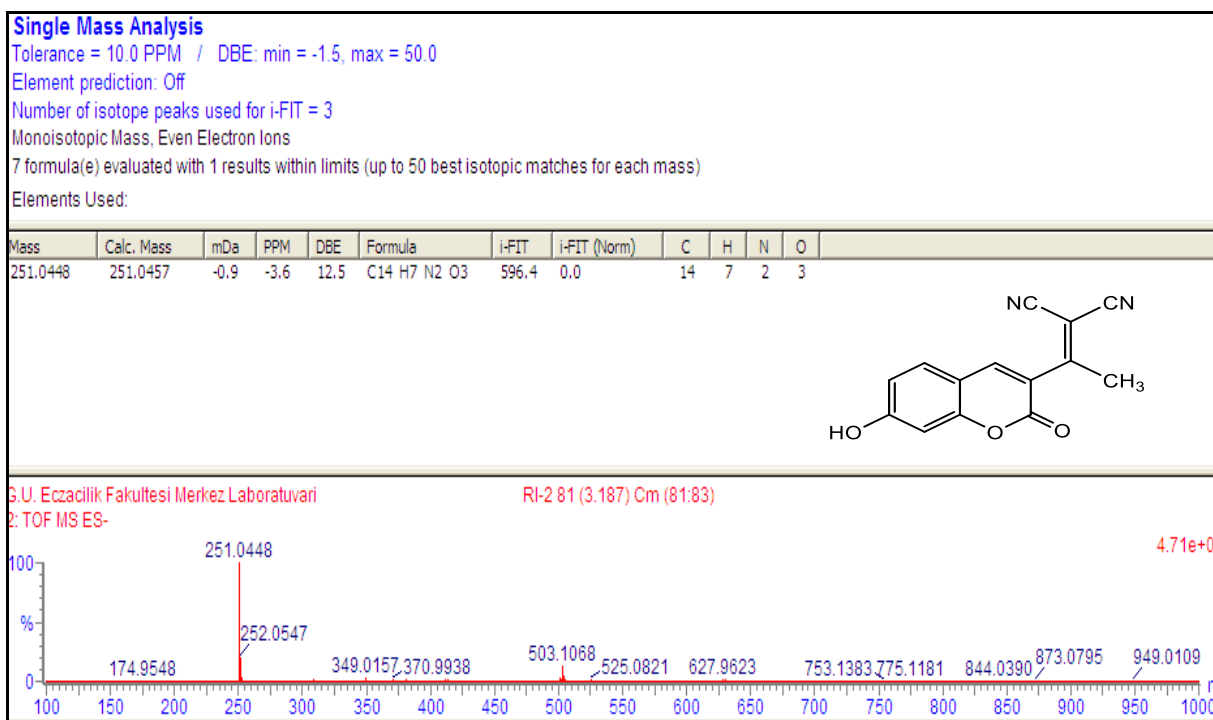
Appendix-2. (Continues) FT-IR, <sup>1</sup>H-NMR, <sup>13</sup>C-APT, HRMS of the Malononitriles 11-20Figure 2.7.3. <sup>13</sup>C-APT (DMSO-*d*<sub>6</sub>) Spectrum of 17

Figure 2.7.4. HRMS spectrum of 17

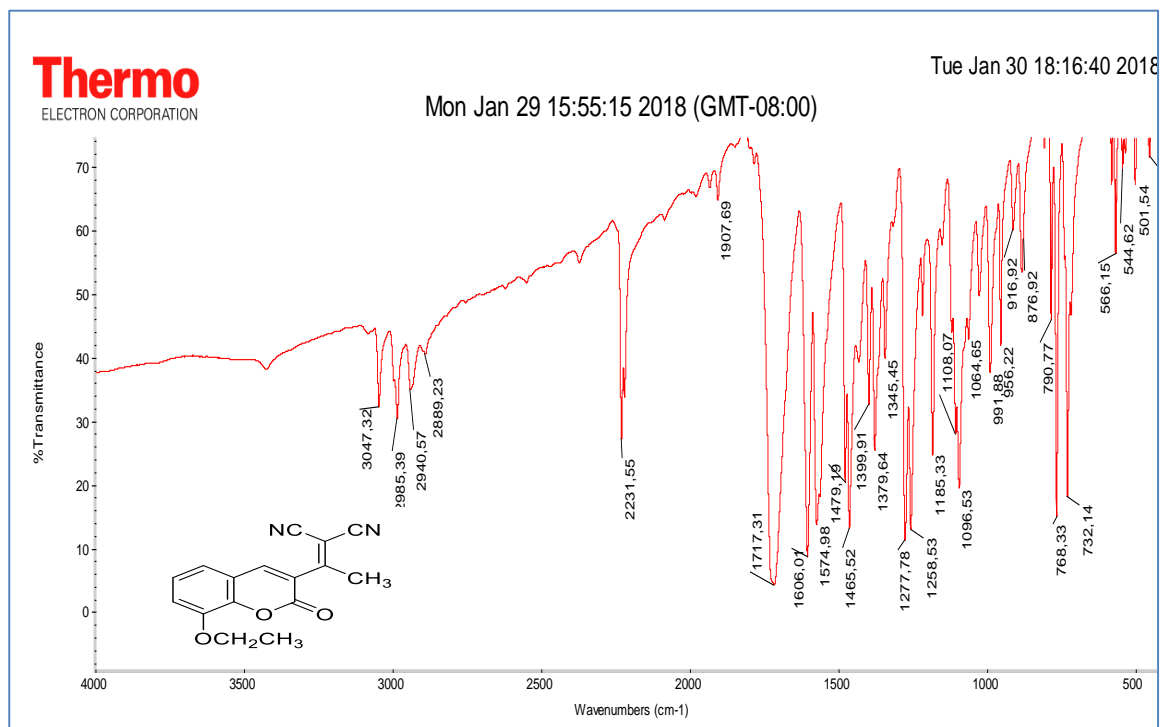
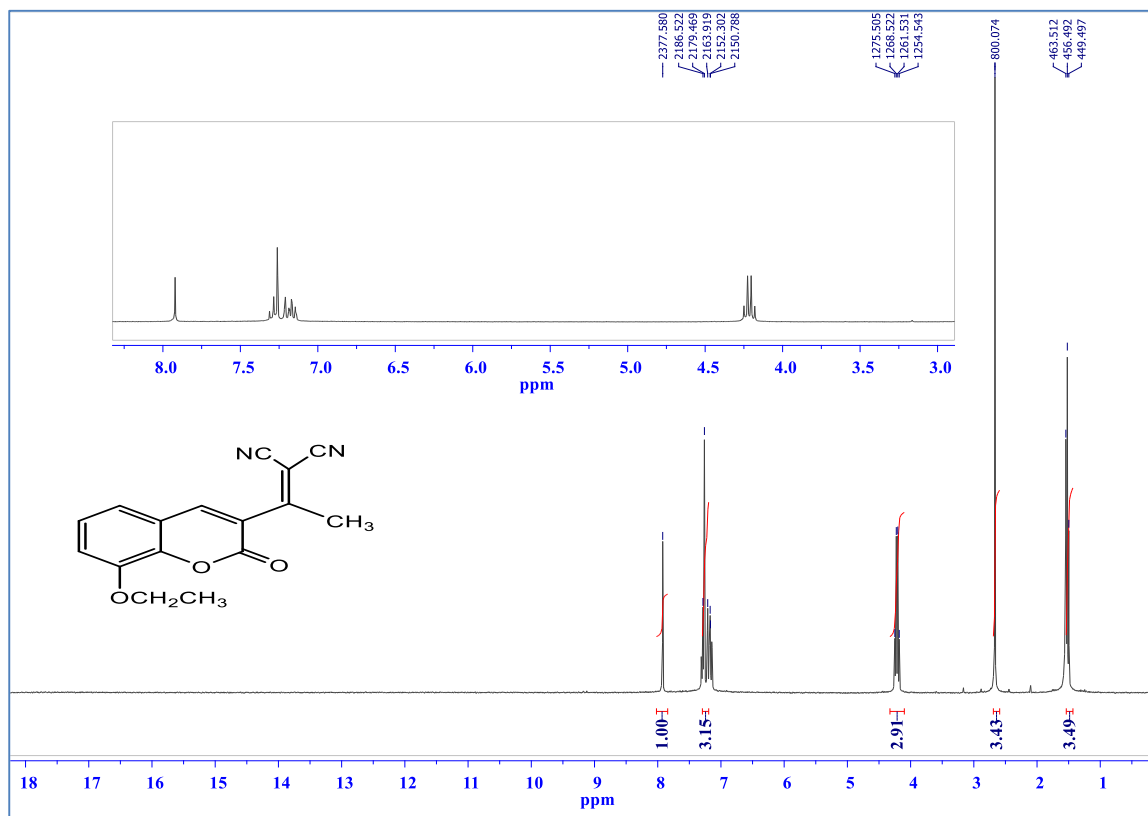
Appendix-2. (Continuous) FT-IR, <sup>1</sup>H-NMR, <sup>13</sup>C-APT, HRMS of the Malononitriles 11-20

Figure 2.8.1. FT-IR Spectrum of 18

Figure 2.8.2. <sup>1</sup>H-NMR (CDCl<sub>3</sub>) Spectrum of 18

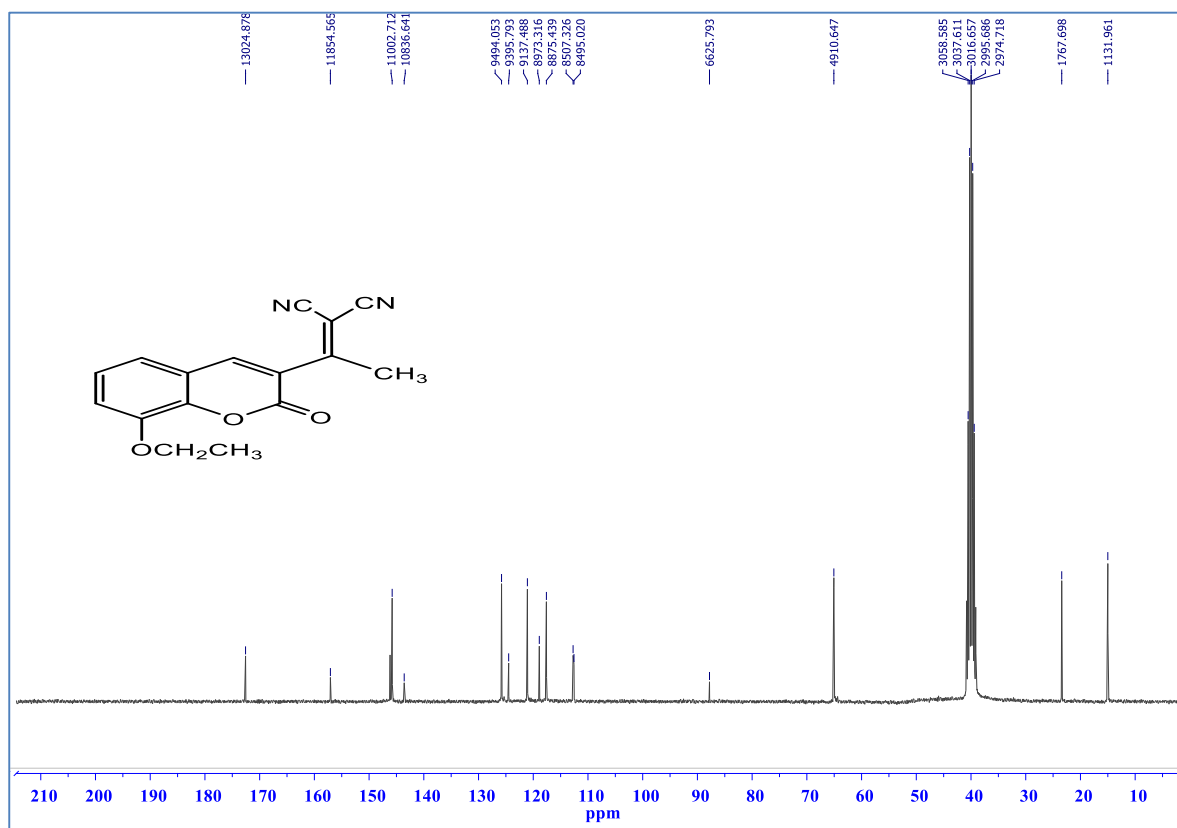
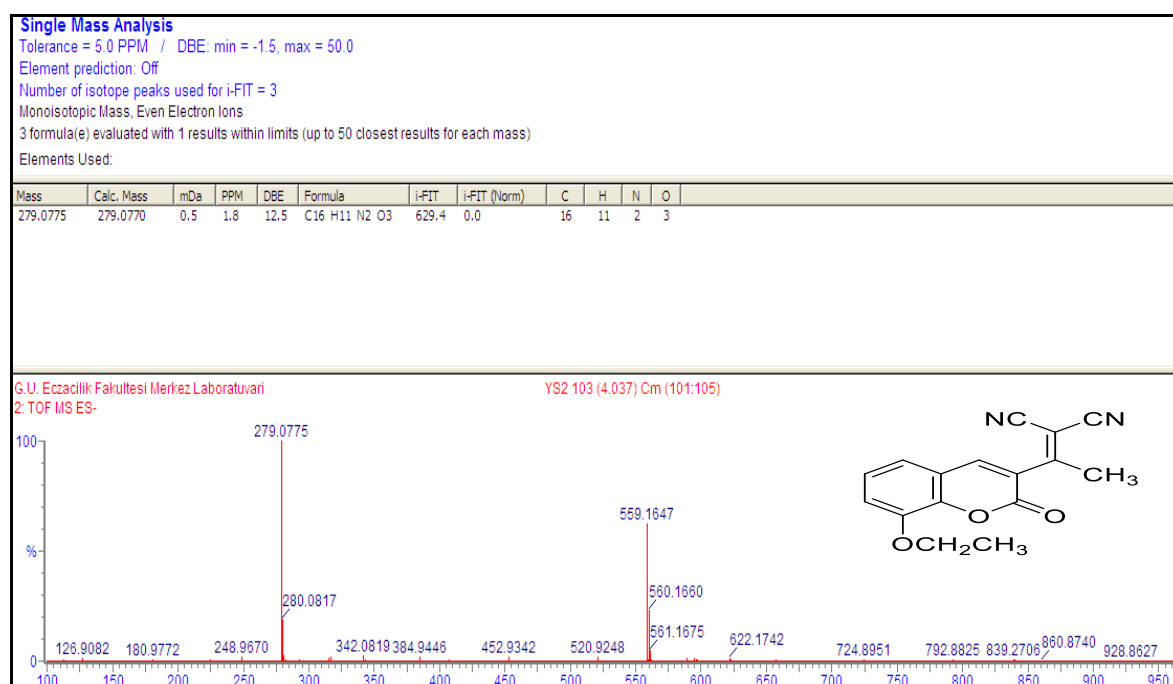
Appendix-2. (Continues) FT-IR, <sup>1</sup>H-NMR, <sup>13</sup>C-APT, HRMS of the Malononitriles 11-20Figure 2.8.3. <sup>13</sup>C-APT (DMSO-*d*<sub>6</sub>) Spectrum of 18

Figure 2.8.4. HRMS Spectrum of 18

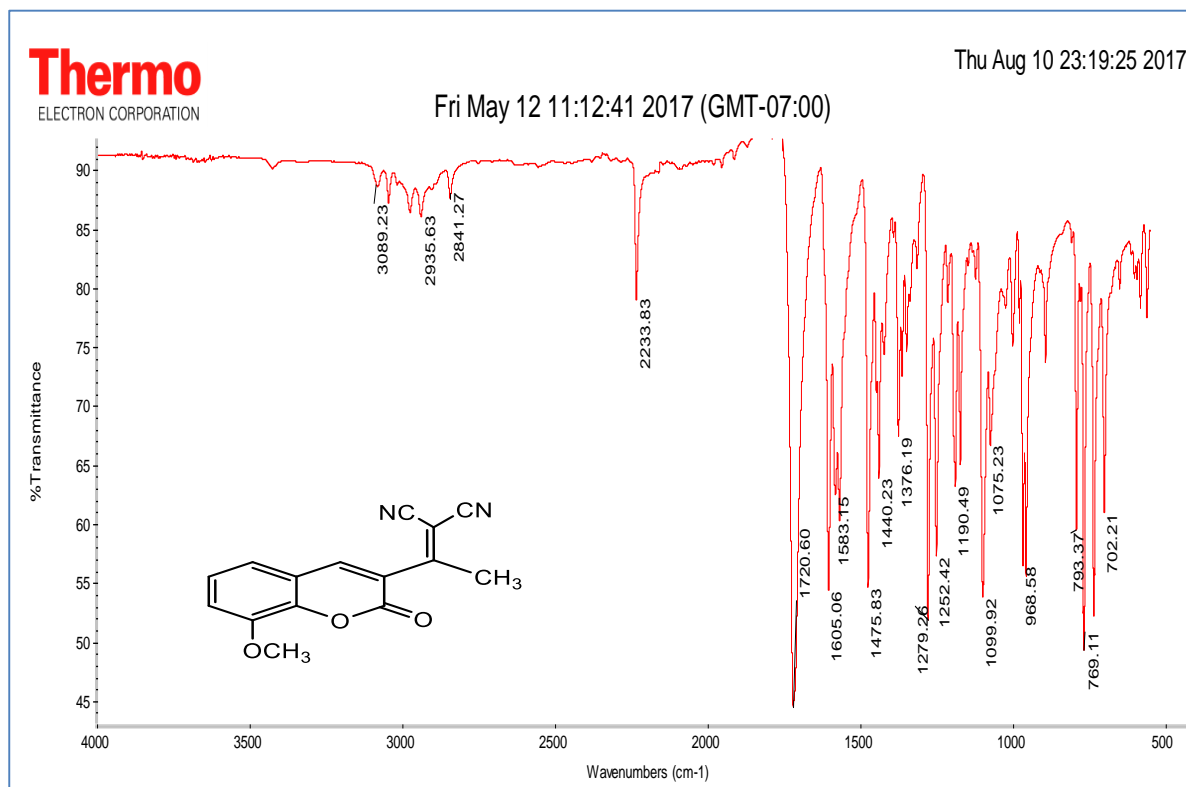
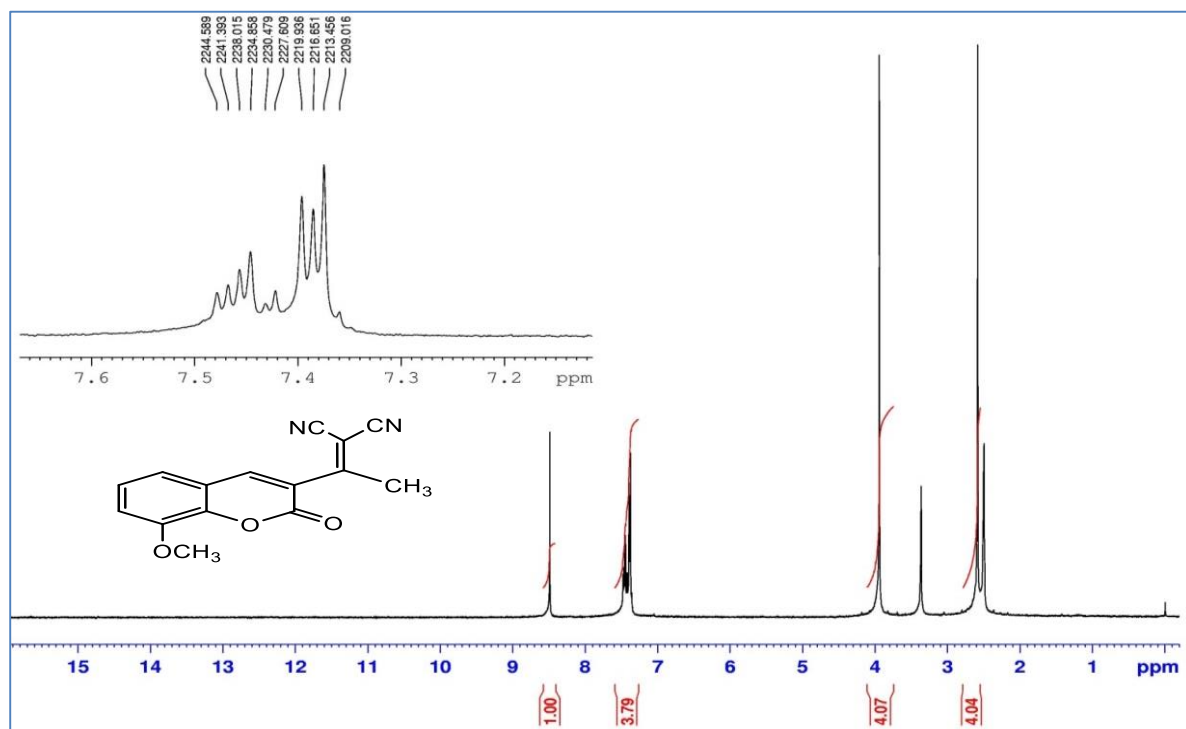
Appendix-2. (Continuous) FT-IR,  $^1\text{H-NMR}$ ,  $^{13}\text{C-NMR}$ , HRMS of the Malononitriles 11-20

Figure 2.9.1. FT-IR Spectrum of 19

Figure 2.9.2.  $^1\text{H-NMR}$  (DMSO- $d_6$ ) Spectrum of 19

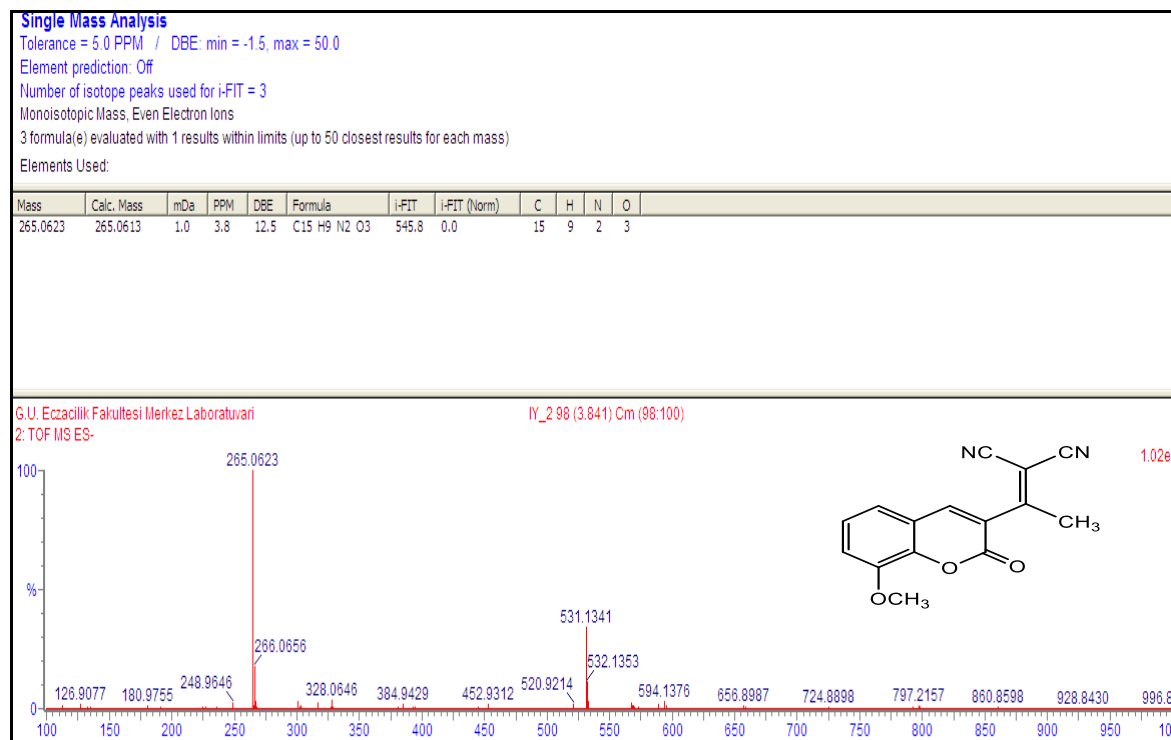
Appendix-2. (Continues) FT-IR, <sup>1</sup>H-NMR, <sup>13</sup>C-APT, HRMS of the Malononitriles 11-20

Figure 2.9.3. HRMS spectrum of 19

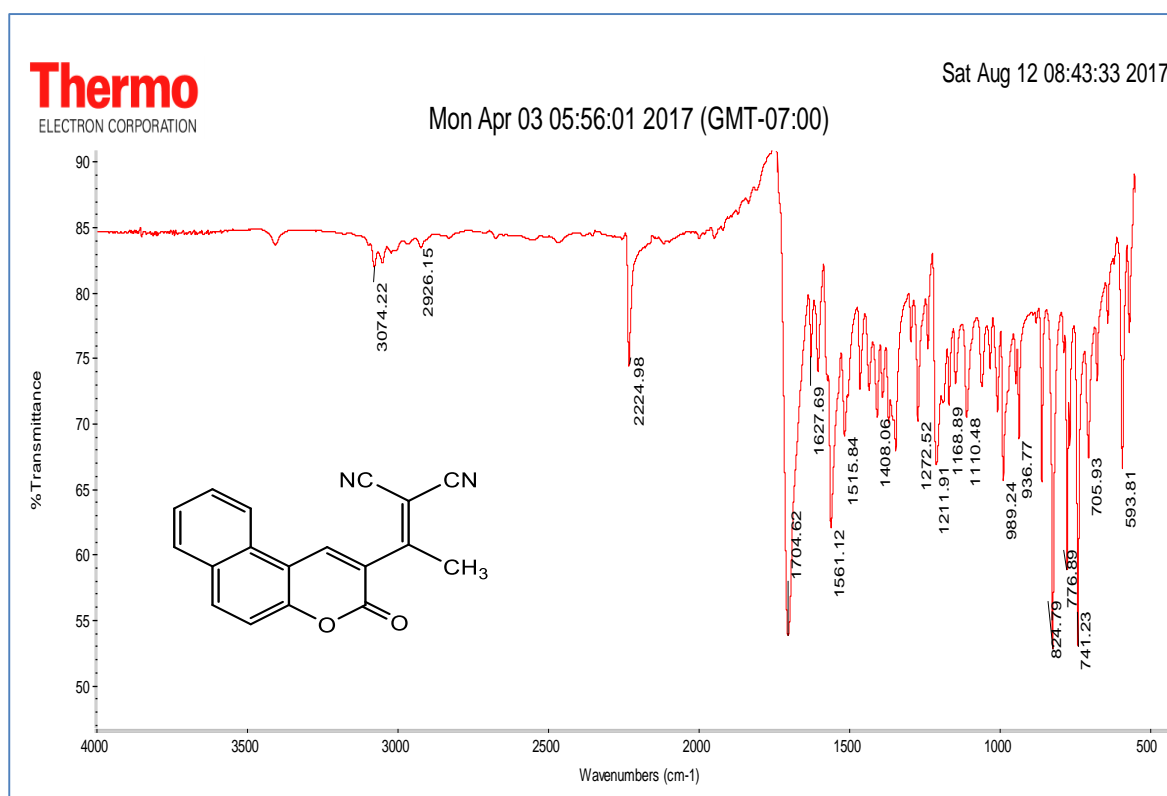
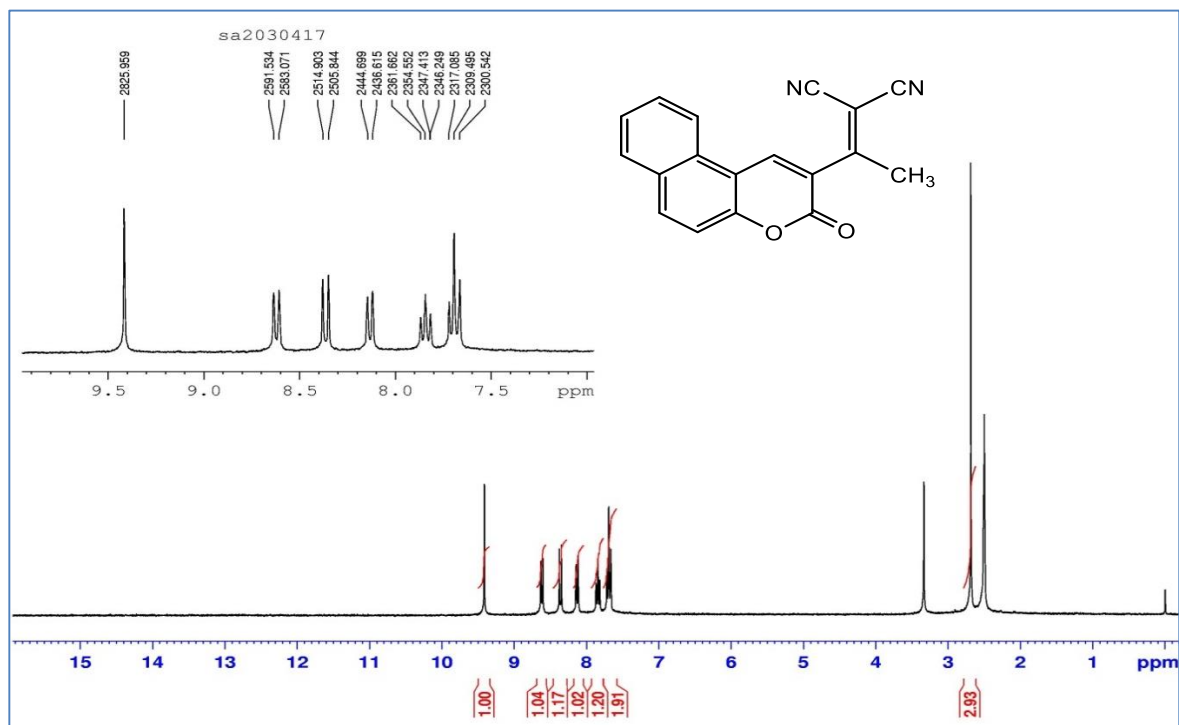
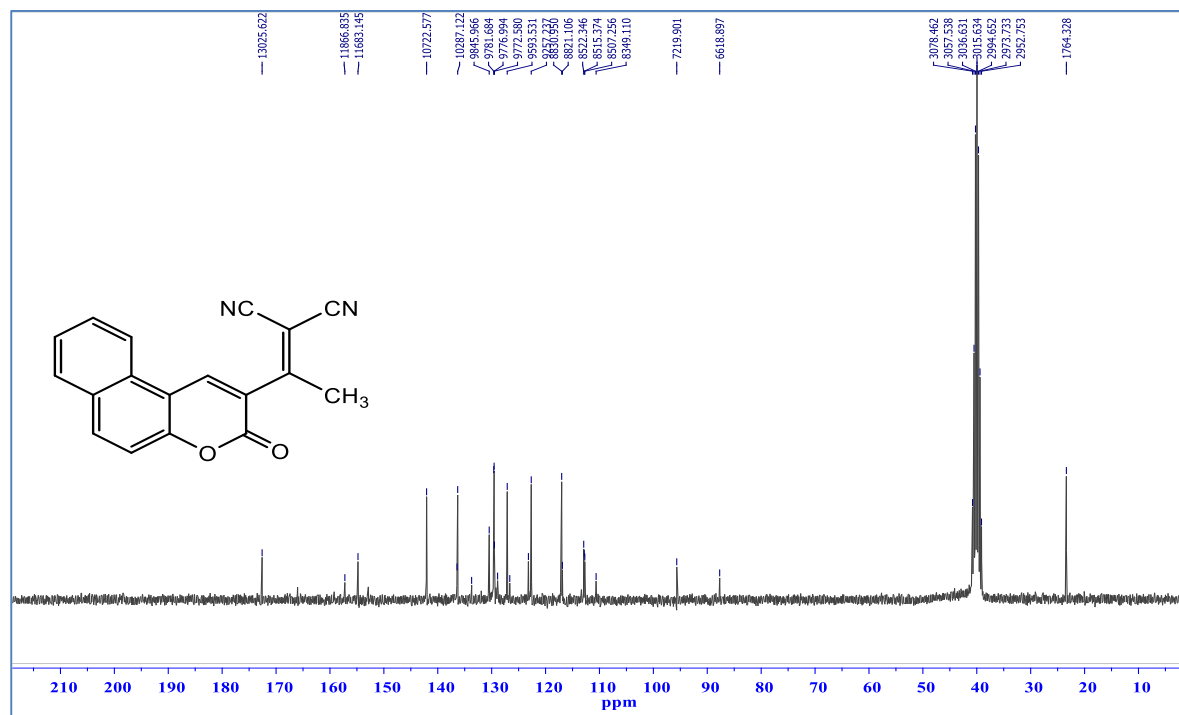


Figure 2.10.1. FT-IR Spectrum of 20

Appendix-2. (Continues) FT-IR,  $^1\text{H-NMR}$ ,  $^{13}\text{C-APT}$ , HRMS of the Malononitriles 11-20Figure 2.10.2.  $^1\text{H-NMR}$  (DMSO- $d_6$ ) Spectrum of 20Figure 2.10.3.  $^{13}\text{C-APT}$  (DMSO- $d_6$ ) Spectrum of 20

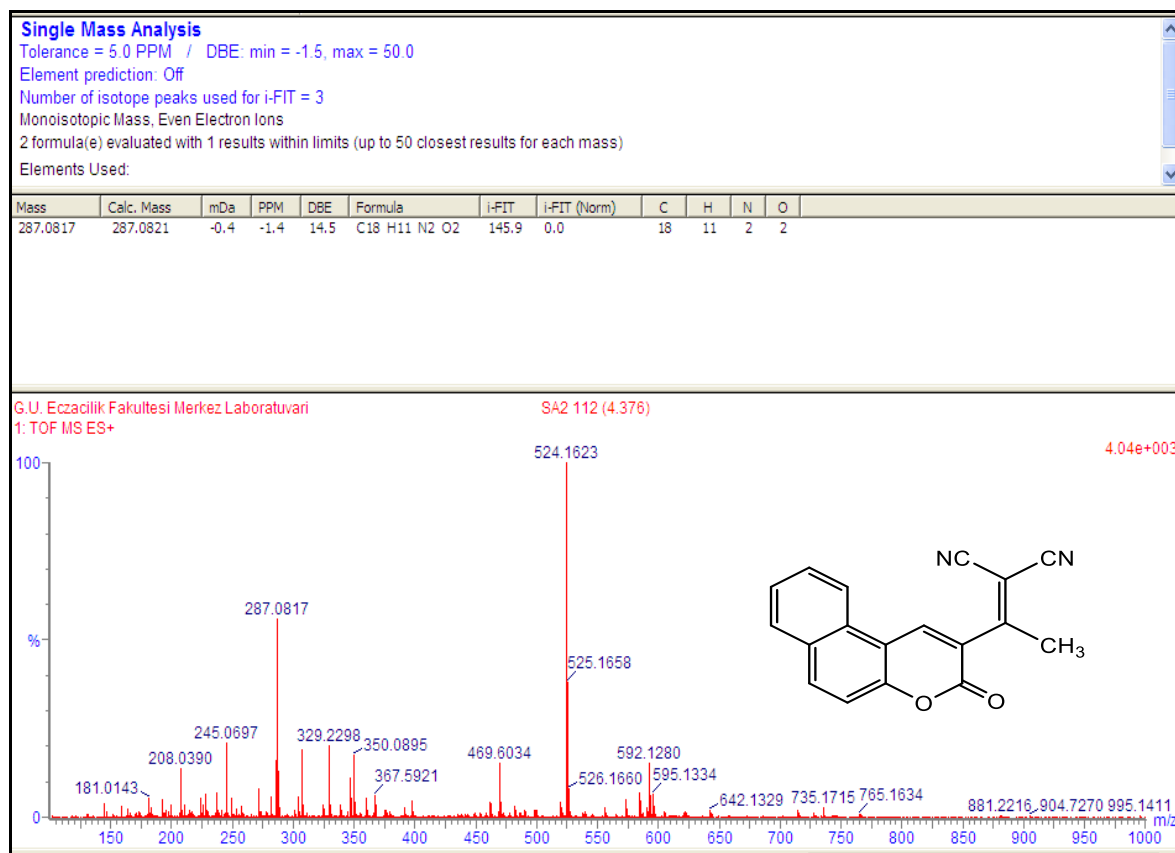
Appendix-2. (Continues) FT-IR, <sup>1</sup>H-NMR, <sup>13</sup>C-APT, HRMS of the Malononitriles 11-20

Figure 2.10.4. HRMS Spectrum of 20

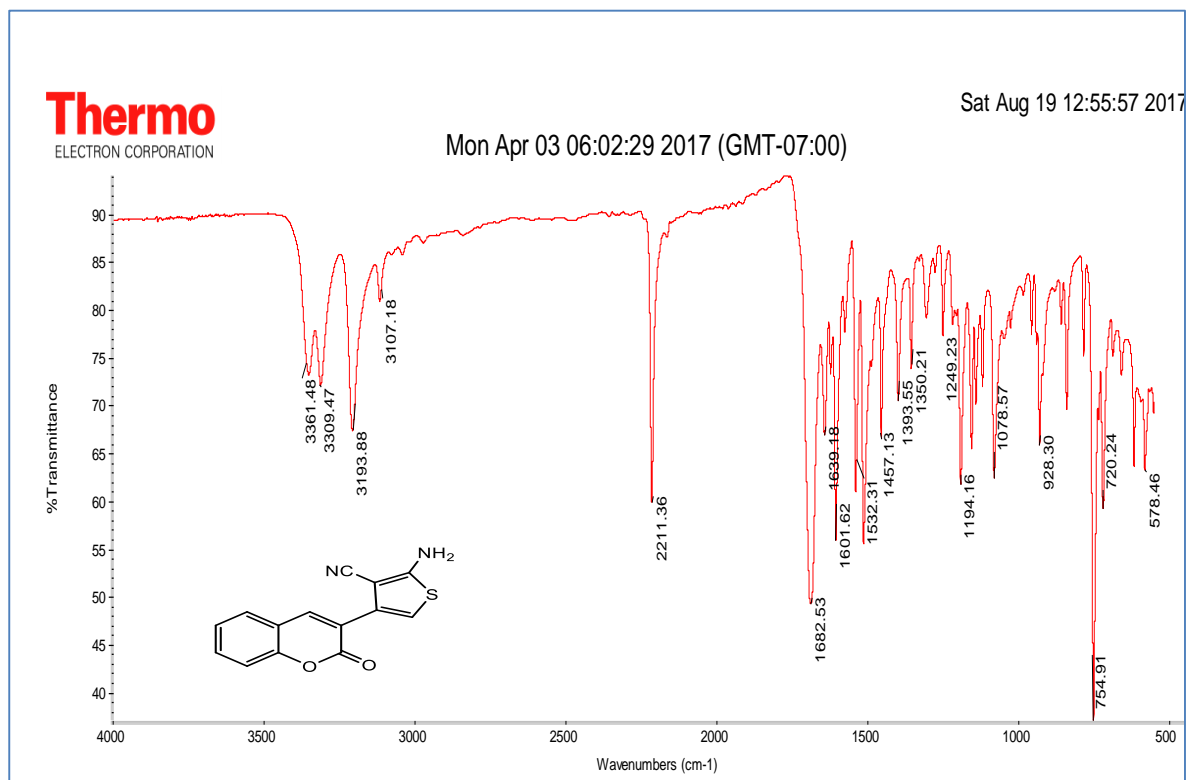
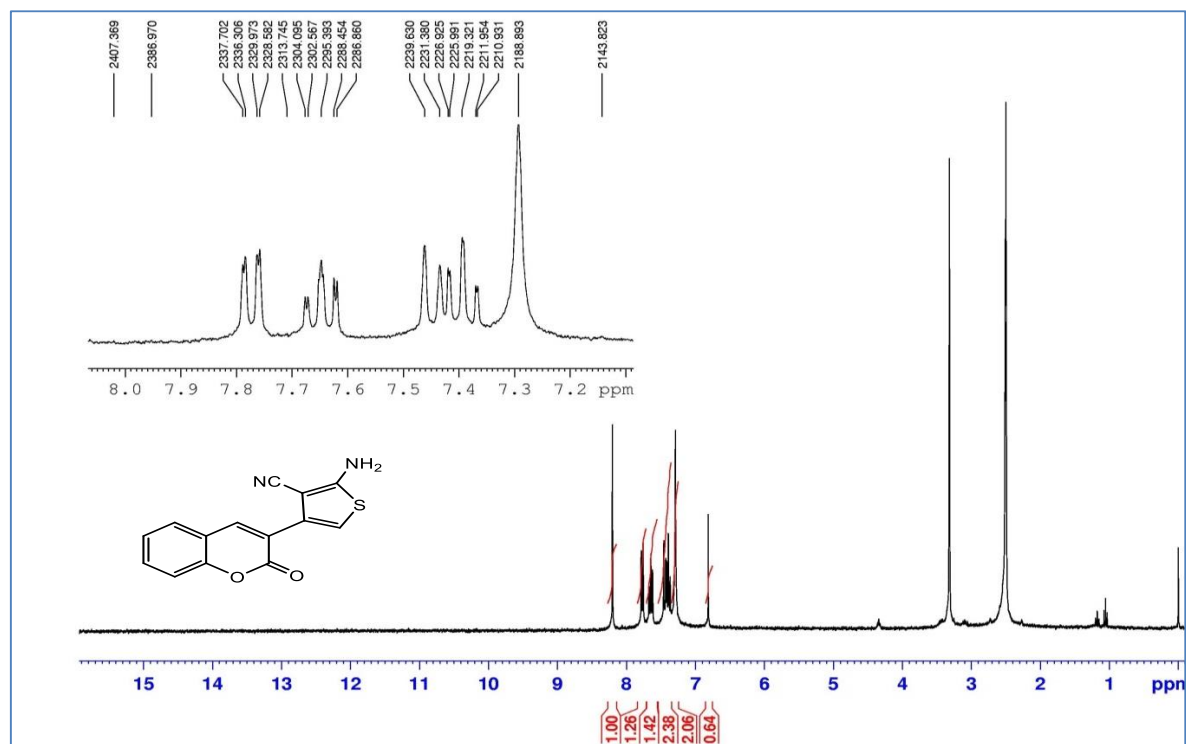
Appendix-3. FT-IR,  $^1\text{H-NMR}$ ,  $^{13}\text{C-APT}$ , HRMS of the 2-Aminothiophenes 21-30

Figure 3.1.1. FT-IR Spectrum of 21

Figure 3.1.2.  $^1\text{H-NMR}$  ( $\text{DMSO-}d_6$ ) Spectrum of 21

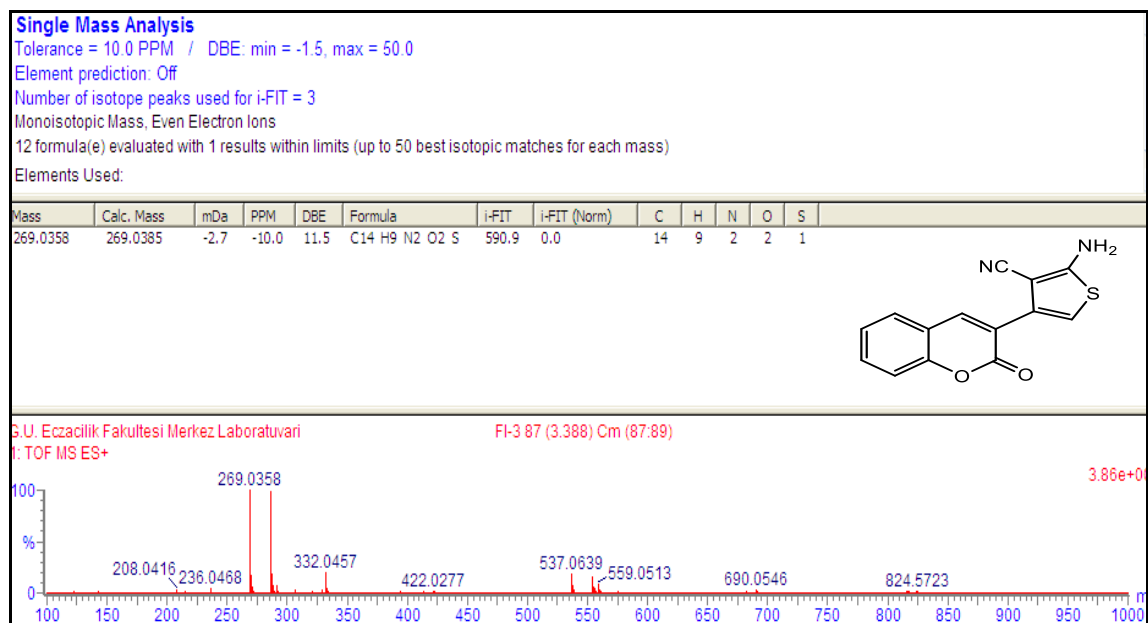
Appendix-3. (Continues) FT-IR,  $^1\text{H-NMR}$ ,  $^{13}\text{C-APT}$ , HRMS of the 2-Aminothiophenes 21-30

Figure 3.1.3. HRMS spectrum of 21

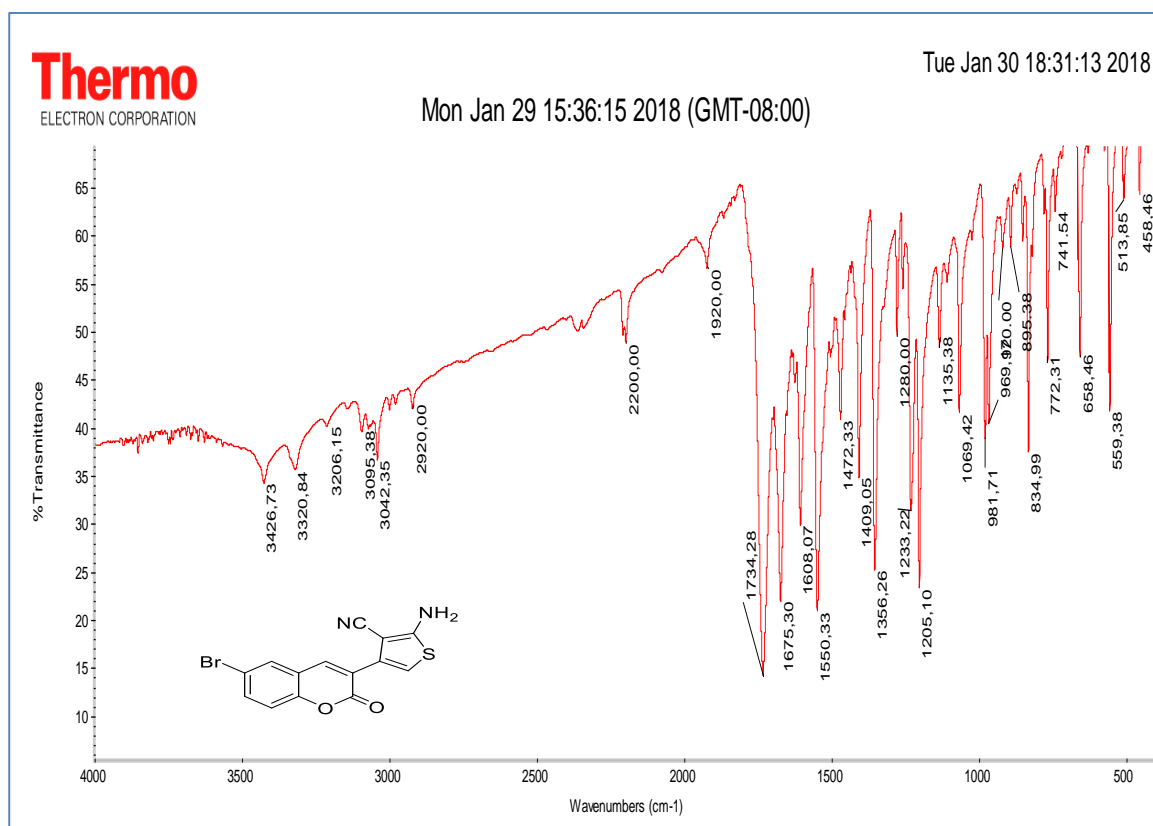


Figure 3.2.1. FT-IR Spectrum of 22

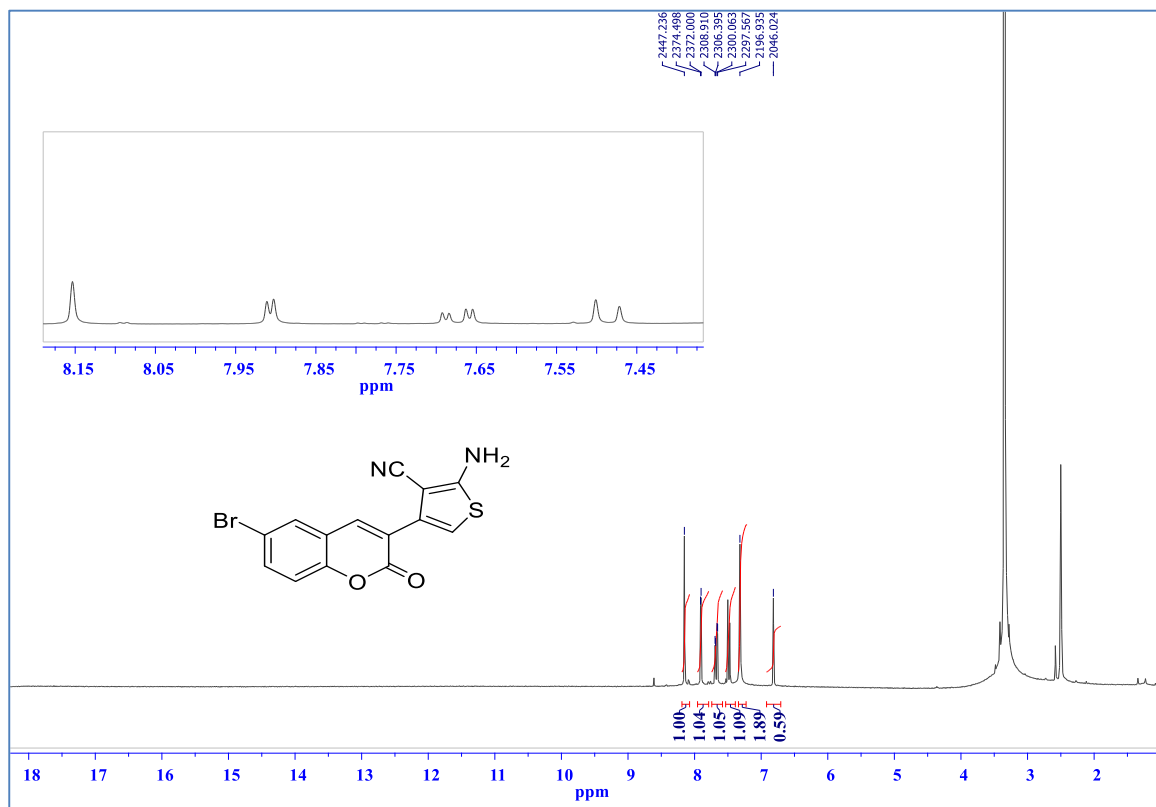
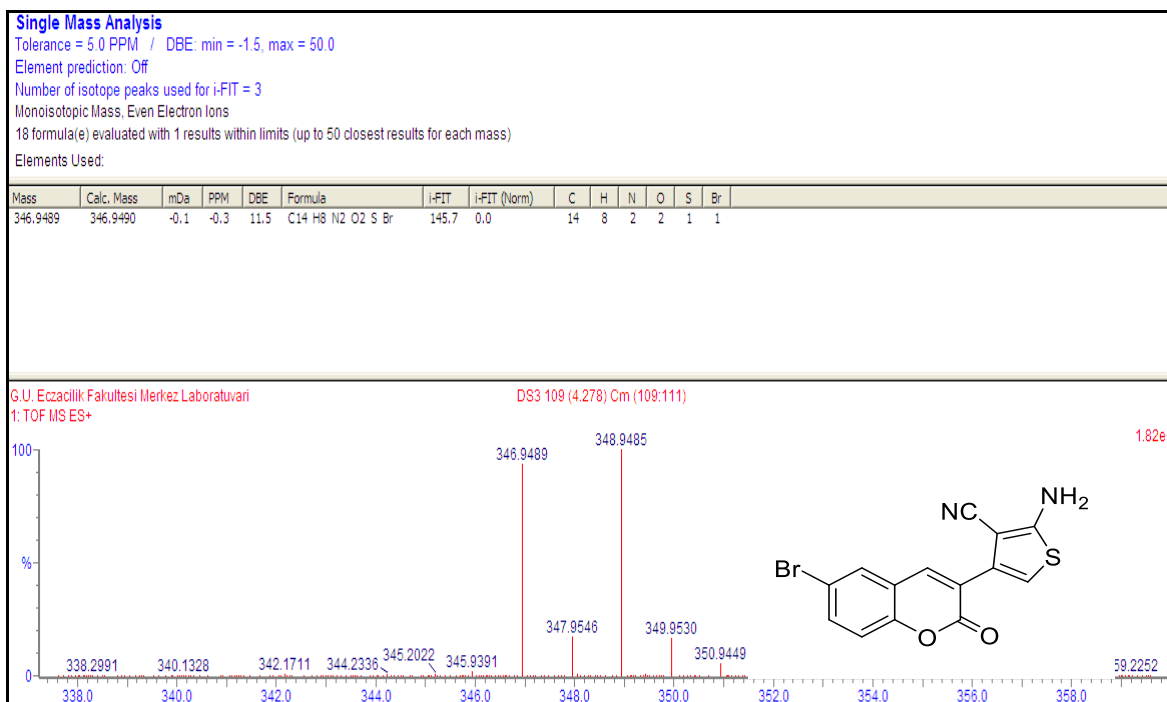
Appendix-3. (Continues) FT-IR,  $^1\text{H-NMR}$ ,  $^{13}\text{C-APT}$ , HRMS of the 2-Aminothiophenes 21-30Figure 3.2.2.  $^1\text{H-NMR}$  (DMSO- $d_6$ ) Spectrum of 22

Figure 3.2.3. HRMS Spectrum of 22

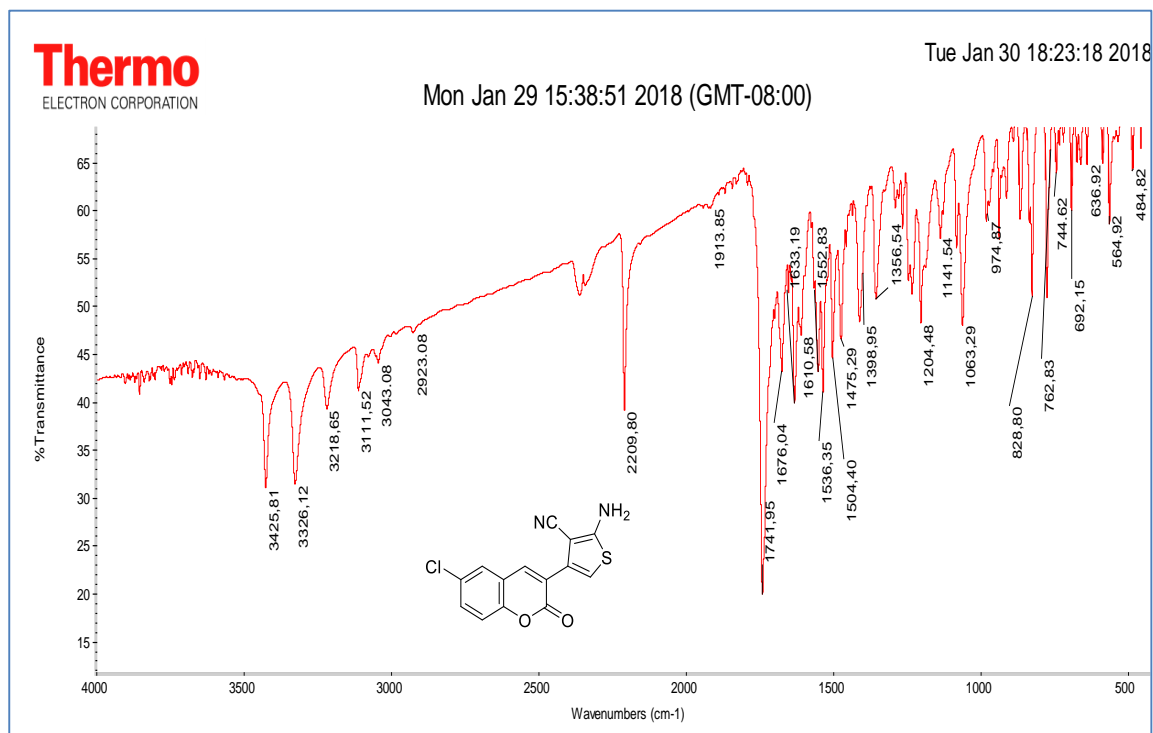
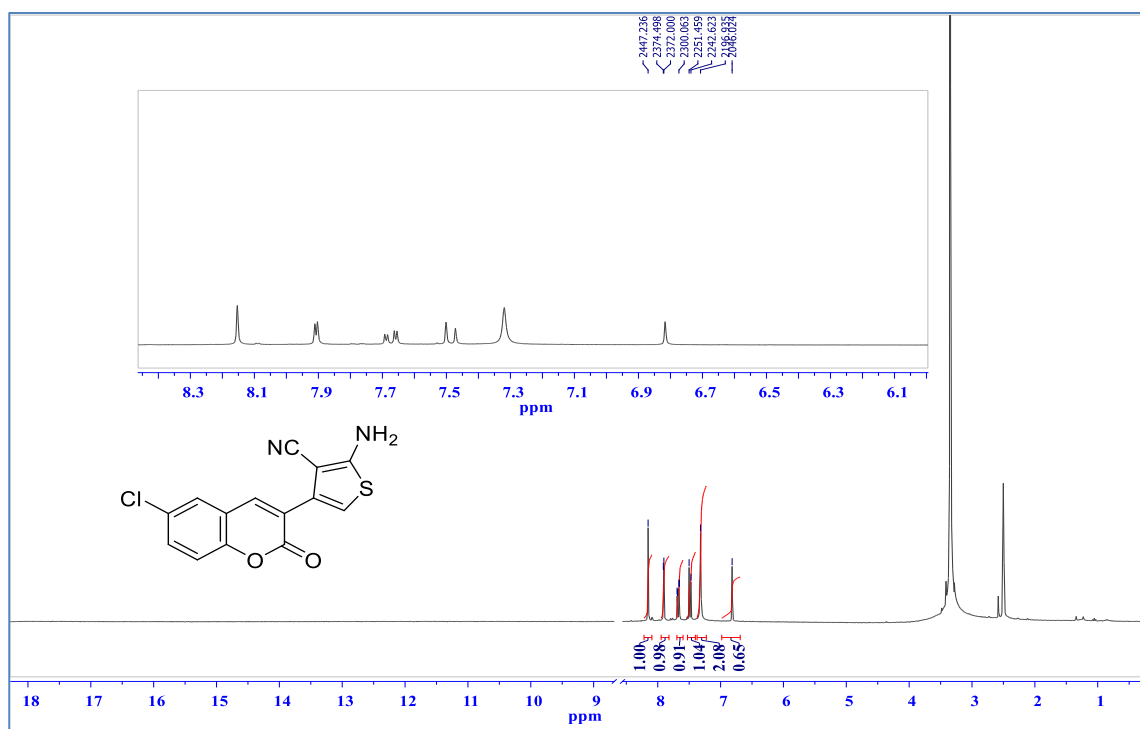
Appendix-3. (Continues) FT-IR,  $^1\text{H-NMR}$ ,  $^{13}\text{C-APT}$ , HRMS of the 2-Aminothiophenes 21-30

Figure 3.3.1. FT-IR Spectrum of 23

Figure 3.3.2.  $^1\text{H-NMR}$  ( $\text{DMSO-}d_6$ ) Spectrum of 23

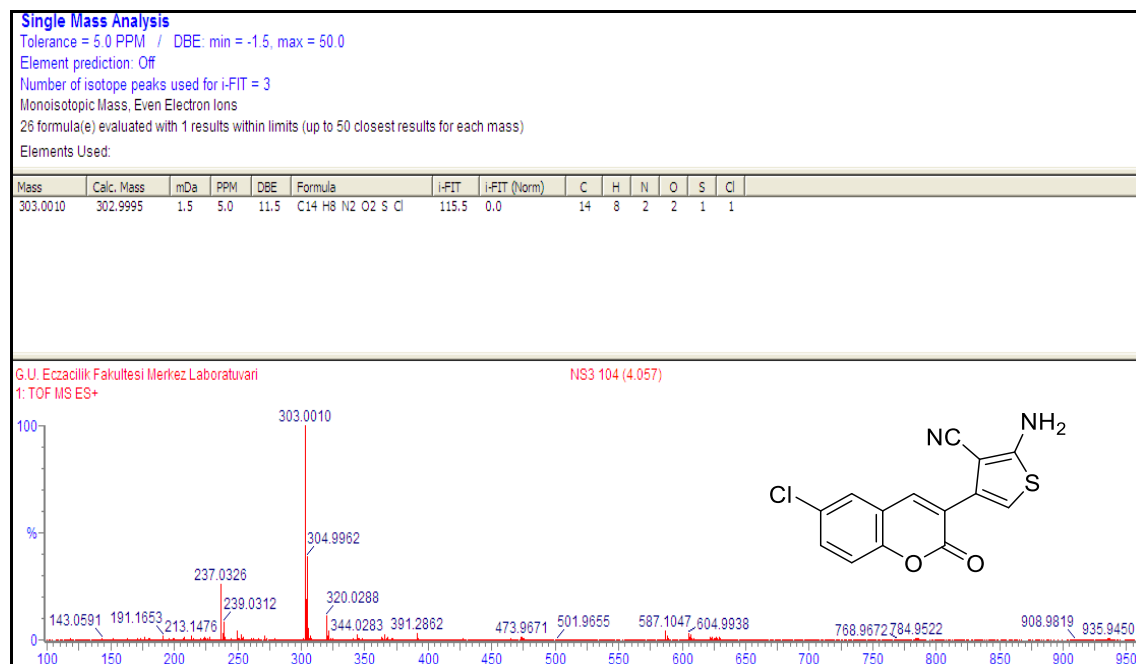
Appendix-3. (Continues) FT-IR, <sup>1</sup>H-NMR, <sup>13</sup>C-APT, HRMS of the 2-Aminothiophenes 21-30

Figure 3.3.3. HRMS Spectrum of 23

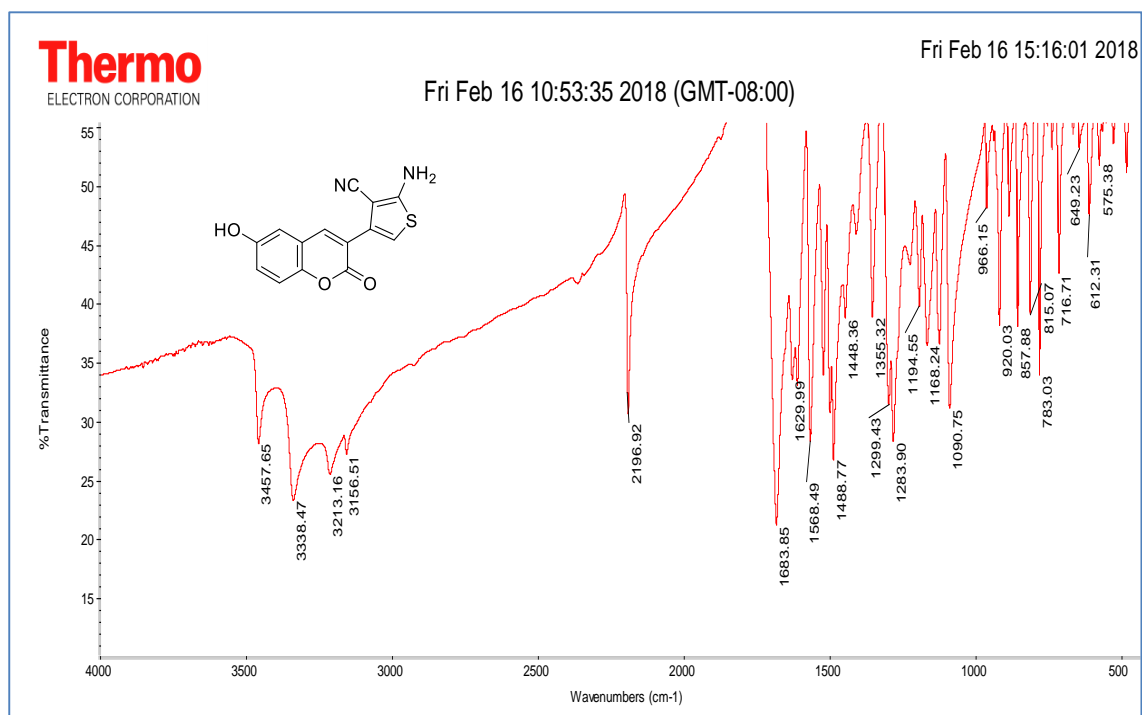
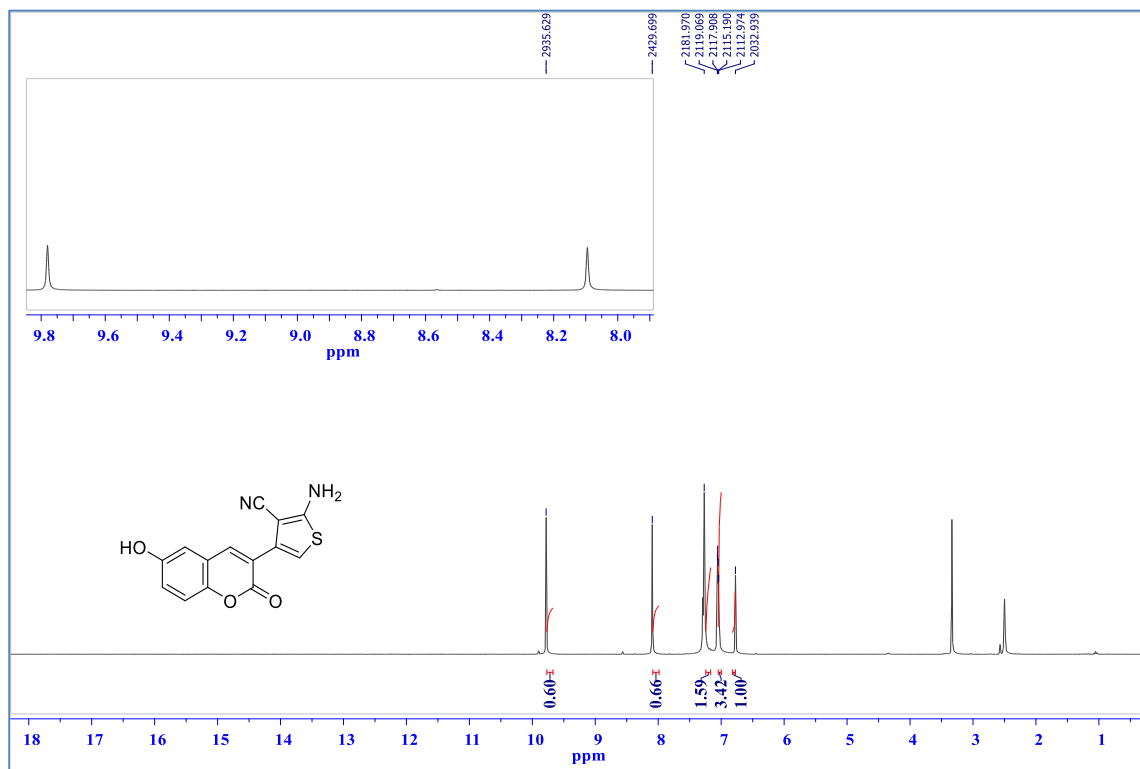
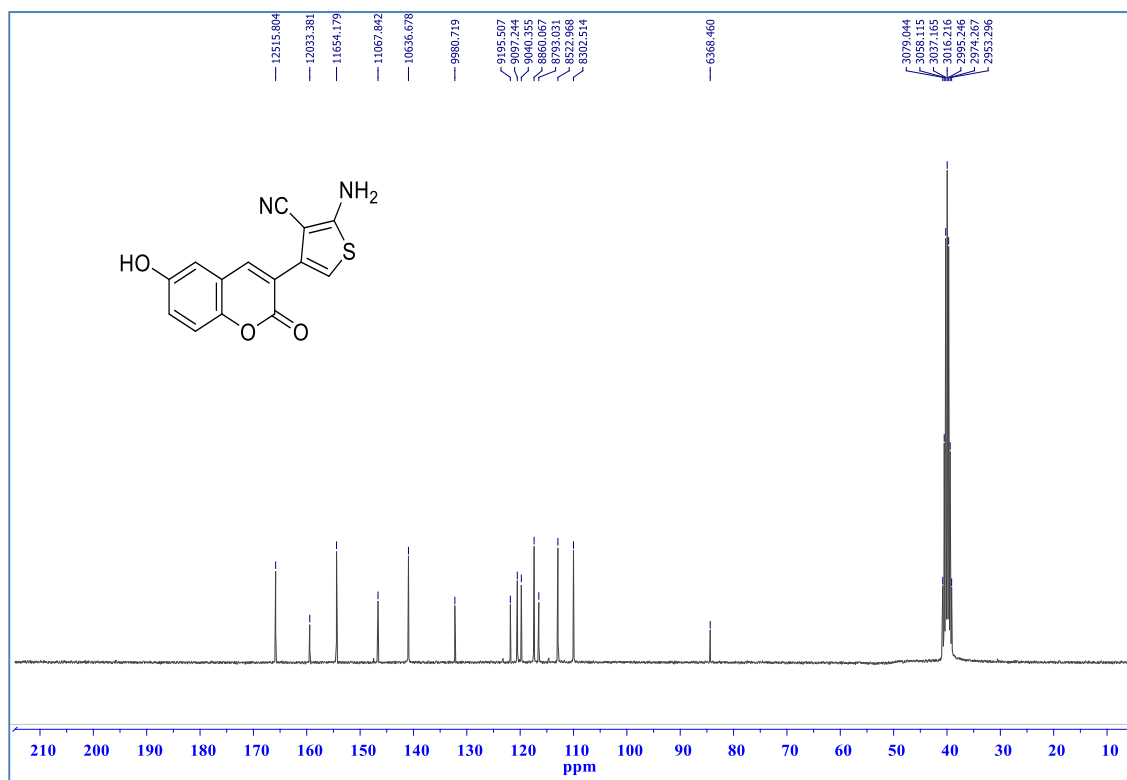


Figure 3.4.1. FT-IR Spectrum of 24

Appendix-3. (Continues) FT-IR,  $^1\text{H-NMR}$ ,  $^{13}\text{C-APT}$ , HRMS of the 2-Aminothiophenes 21-30Figure 3.4.2.  $^1\text{H-NMR}$  (DMSO- $d_6$ ) Spectrum of 24Figure 3.4.3.  $^{13}\text{C-APT}$  (DMSO- $d_6$ ) Spectrum of 24

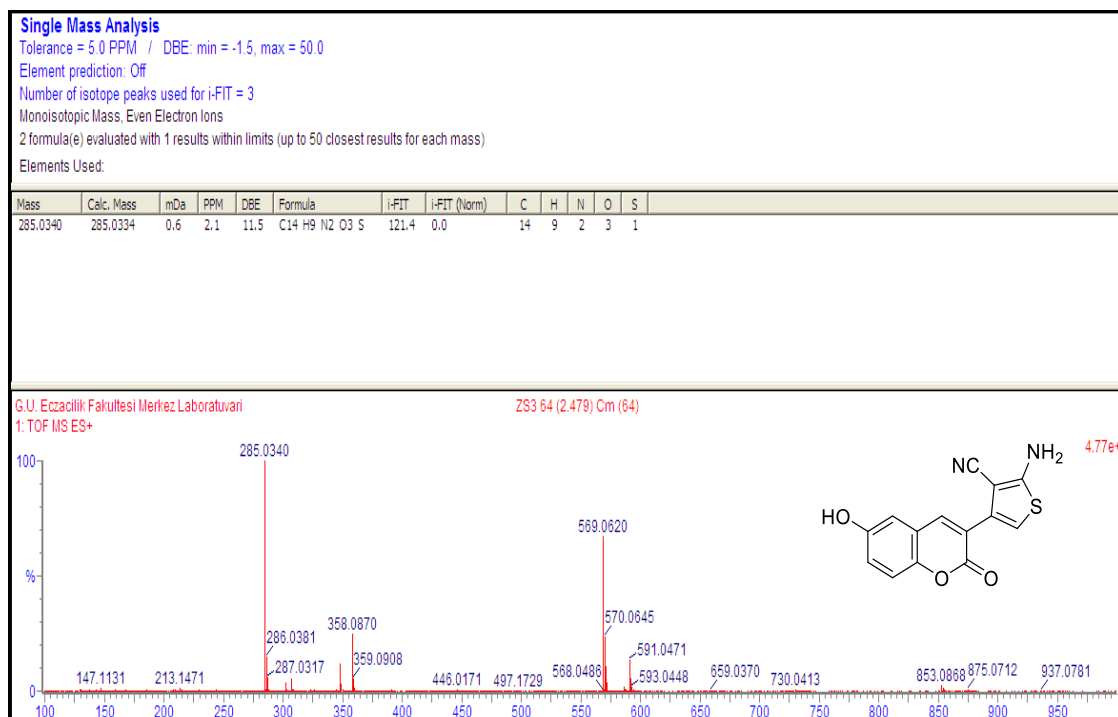
Appendix-3. (Continues) FT-IR, <sup>1</sup>H-NMR, <sup>13</sup>C-APT, HRMS of the 2-Aminothiophenes 21-30

Figure 3.4.4. HRMS spectrum of 24

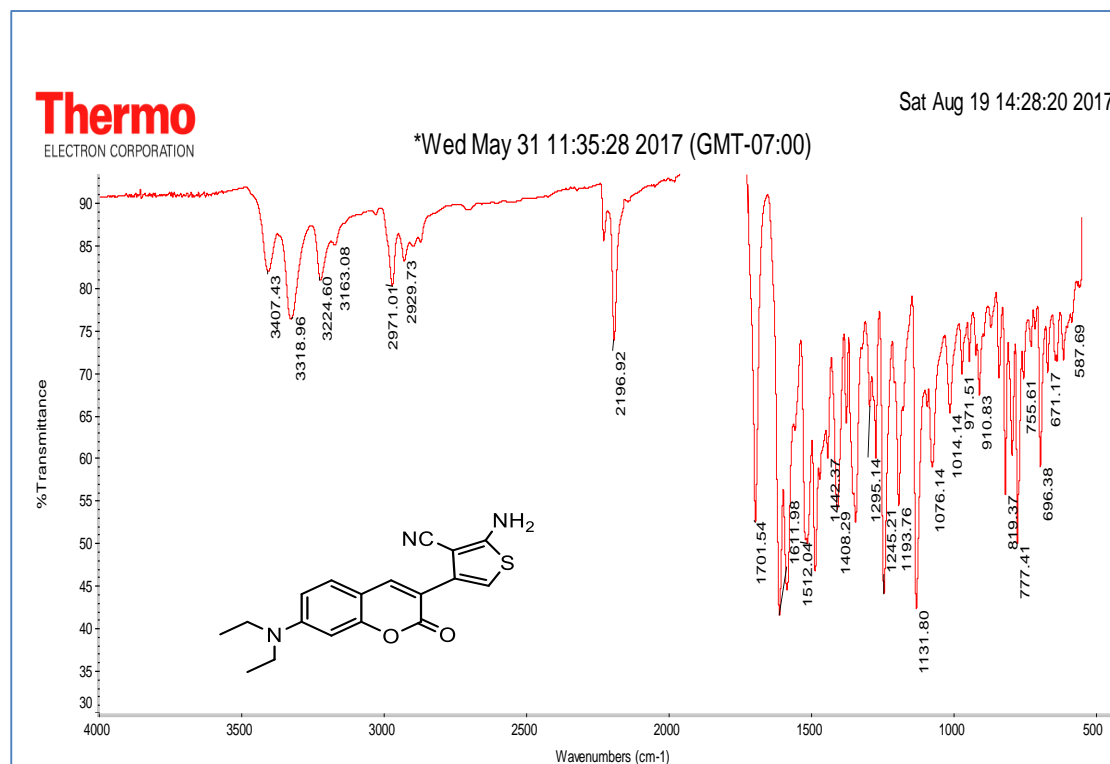


Figure 3.5.1. FT-IR Spectrum of 25

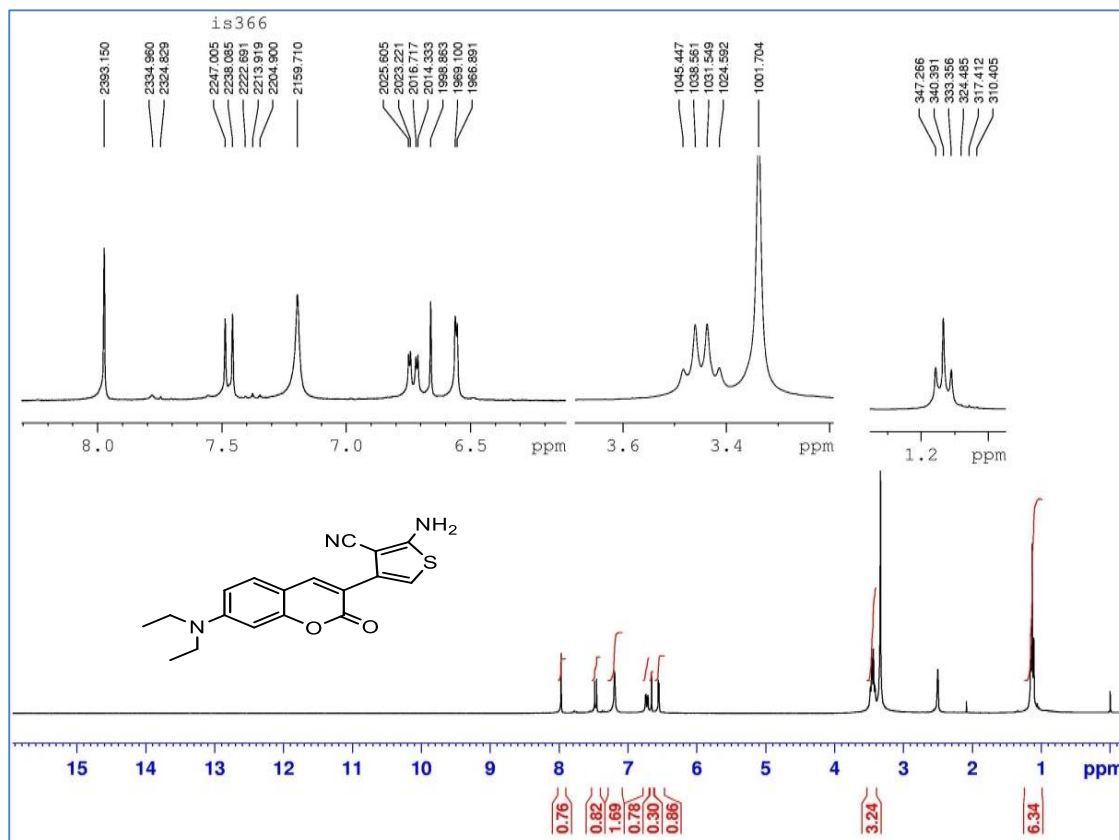
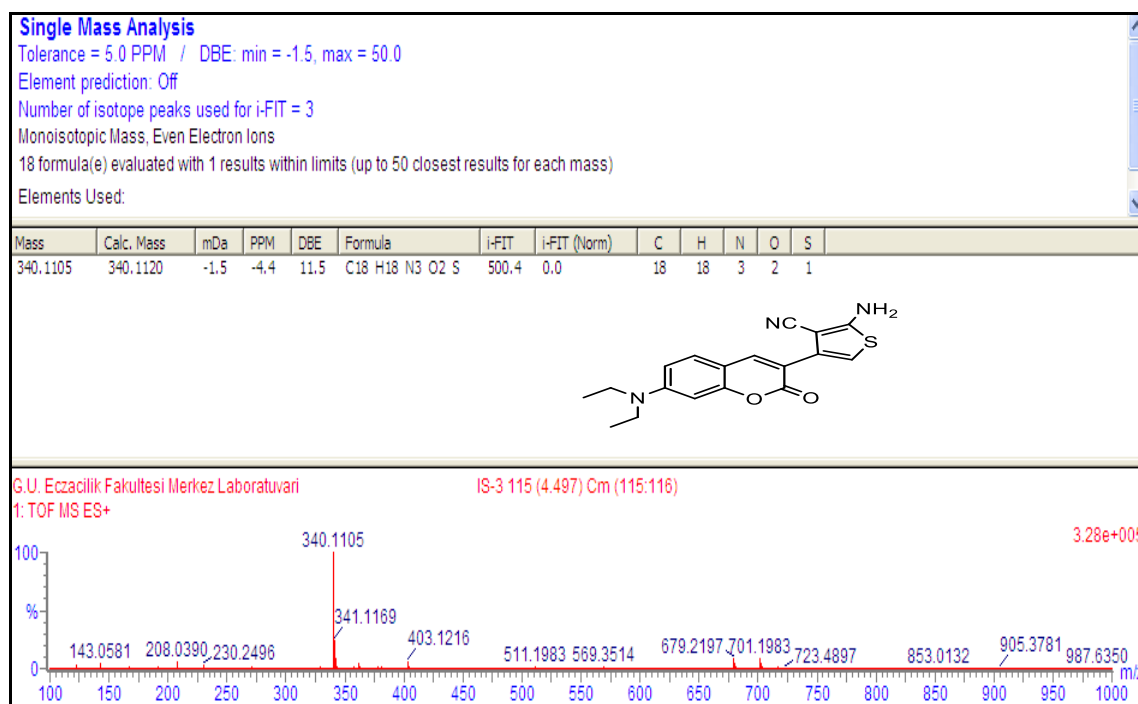
Appendix-3. (Continues) FT-IR,  $^1\text{H-NMR}$ ,  $^{13}\text{C-APT}$ , HRMS of the 2-Aminothiophenes 21-30Figure 3.5.2.  $^1\text{H-NMR}$  (DMSO- $d_6$ ) Spectrum of 25

Figure 3.5.3. HRMS spectrum of 25

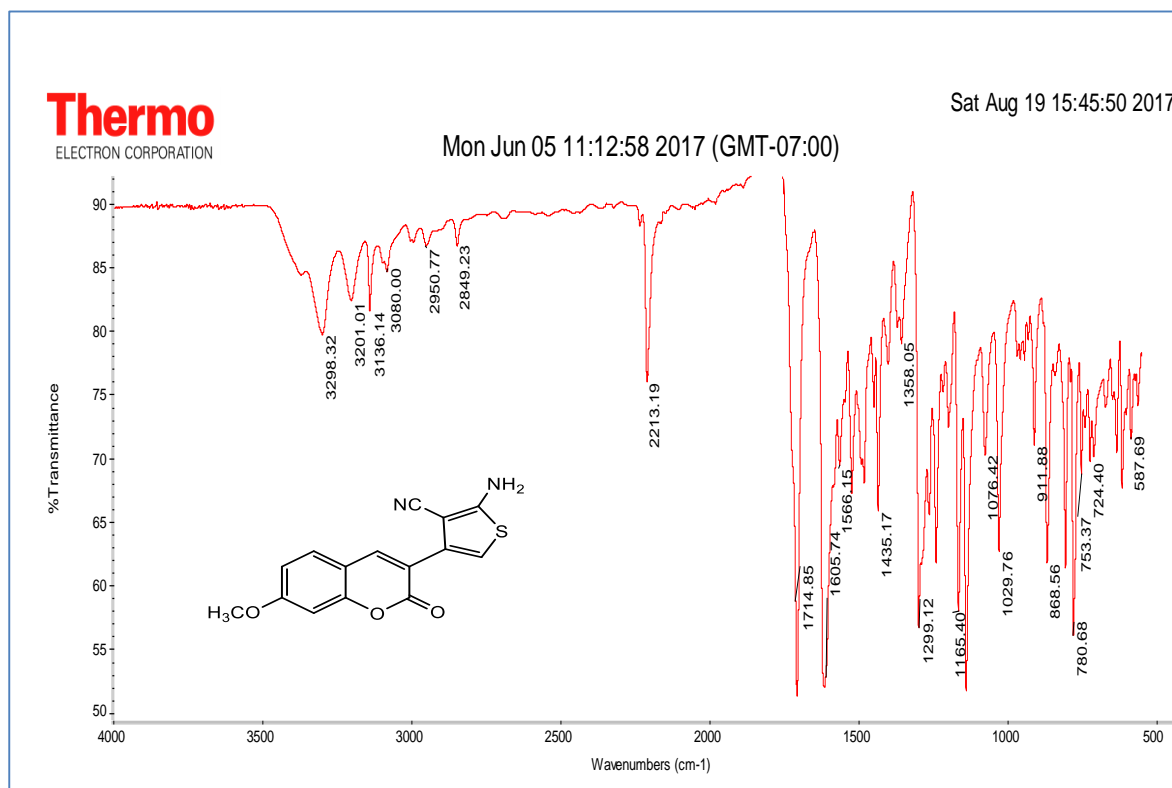
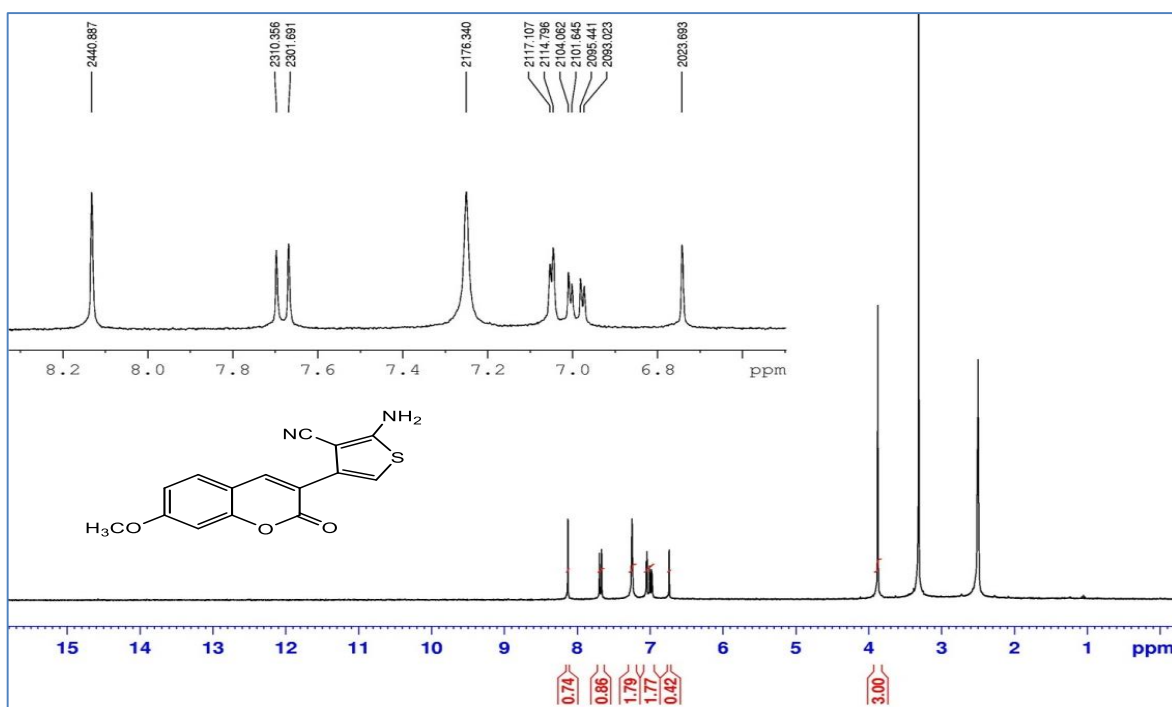
Appendix-3. (Continuous) FT-IR,  $^1\text{H-NMR}$ ,  $^{13}\text{C-APT}$ , HRMS of the 2-Aminothiophenes 21-30

Figure 3.6.1. FT-IR Spectrum of 26

Figure 3.6.2.  $^1\text{H-NMR}$  (DMSO- $d_6$ ) Spectrum of 26

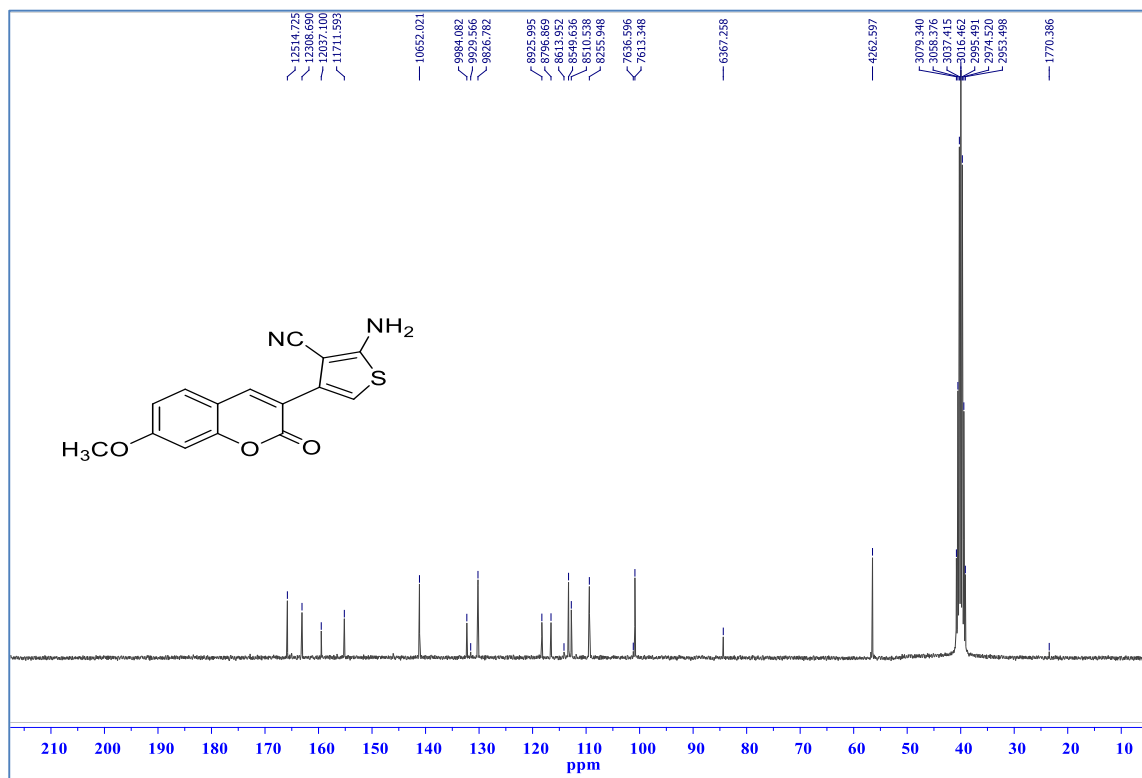
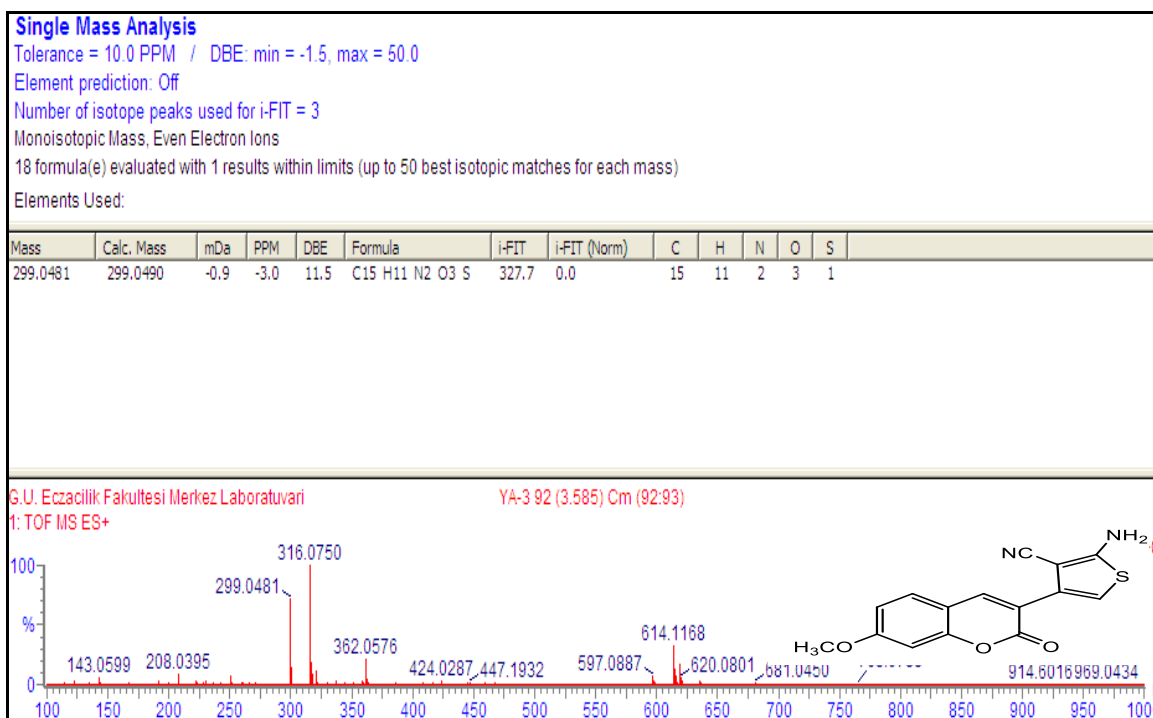
Appendix-3. (Continues) FT-IR, <sup>1</sup>H-NMR, <sup>13</sup>C-APT, HRMS of the 2-Aminothiophenes 21-30Figure 3.6.3. <sup>13</sup>C-APT (DMSO-*d*<sub>6</sub>) Spectrum of 26

Figure 3.6.4. HRMS Spectrum of 26

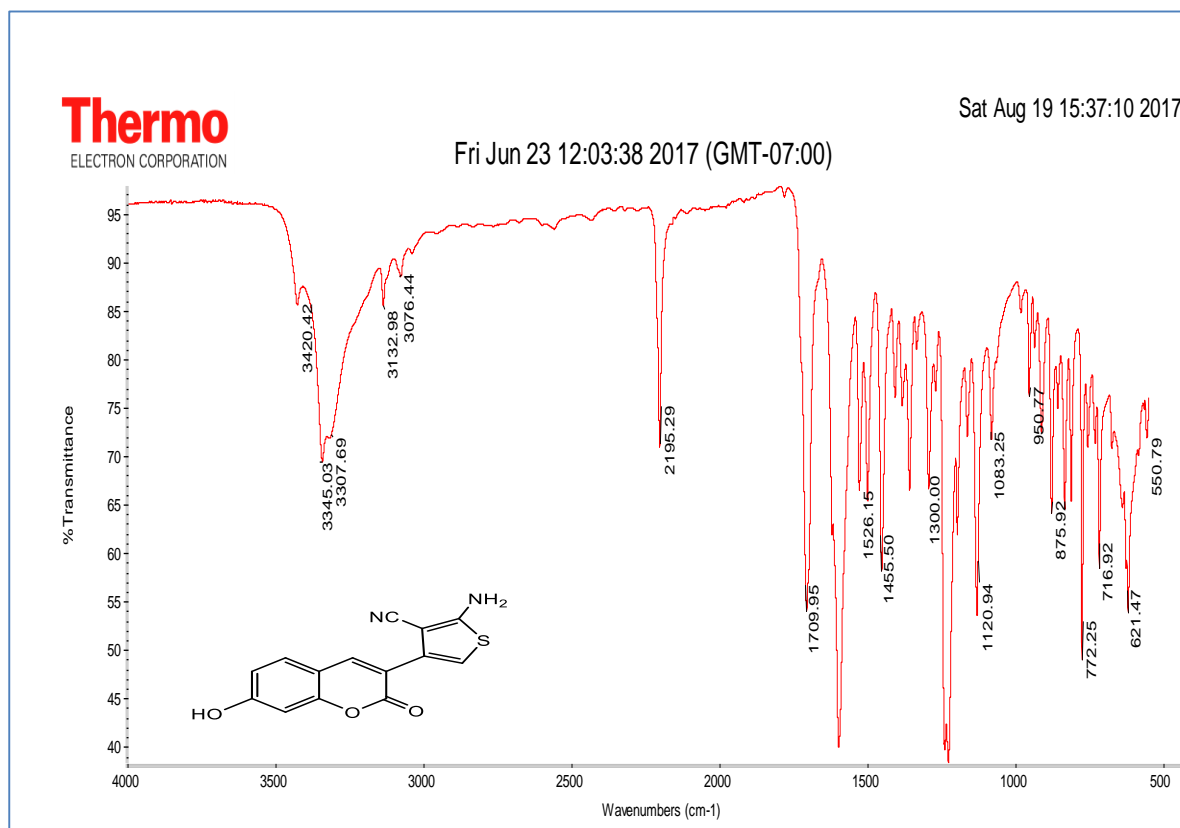
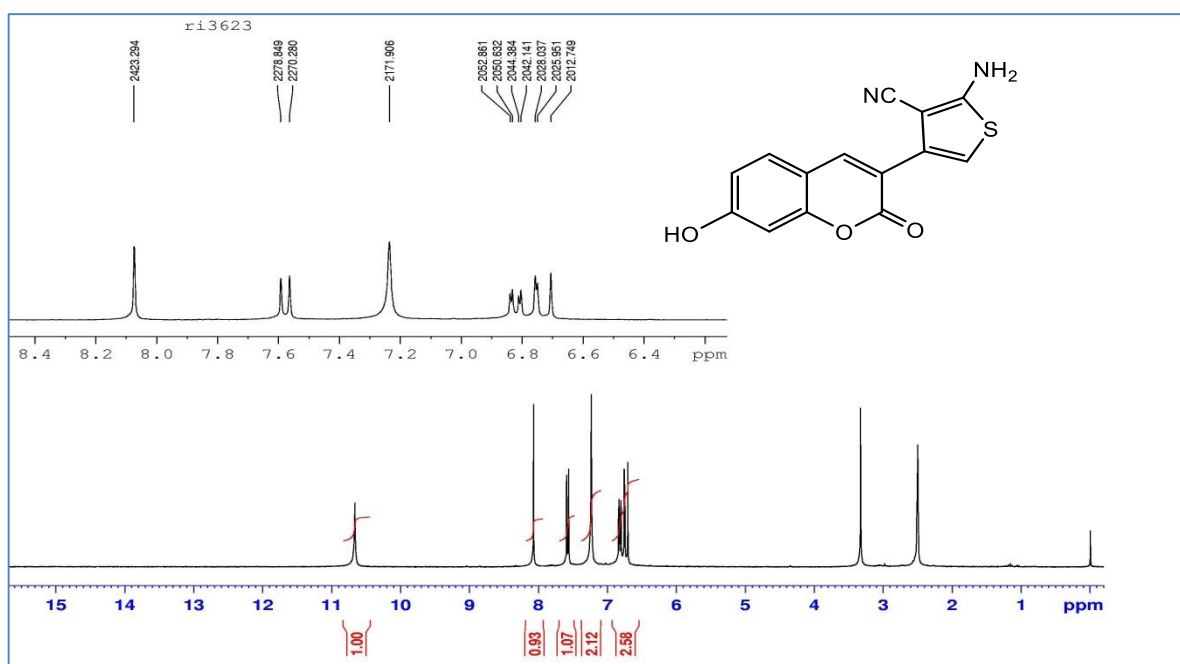
Appendix-3. (Continuous) FT-IR,  $^1\text{H-NMR}$ ,  $^{13}\text{C-APT}$ , HRMS of the 2-Aminothiophenes 21-30

Figure 3.7.1. FT-IR Spectrum of 27

Figure 3.7.2.  $^1\text{H-NMR}$  (DMSO- $d_6$ ) Spectrum of 27

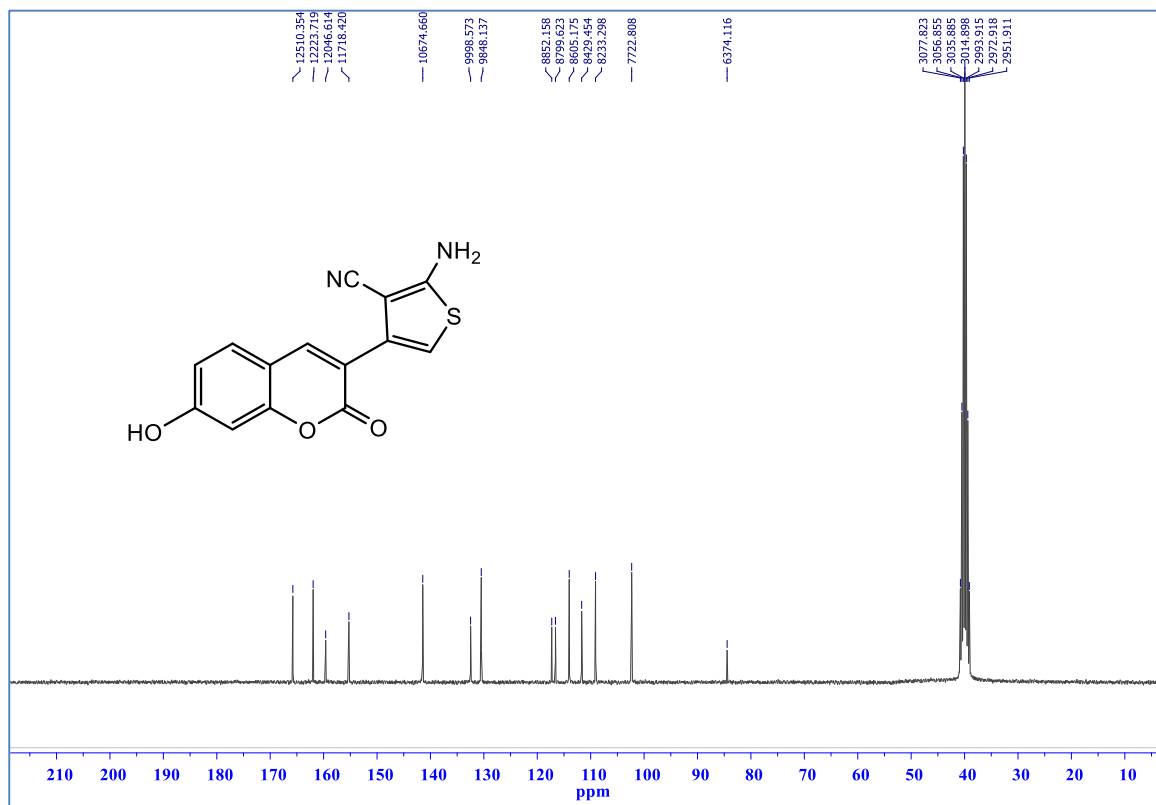
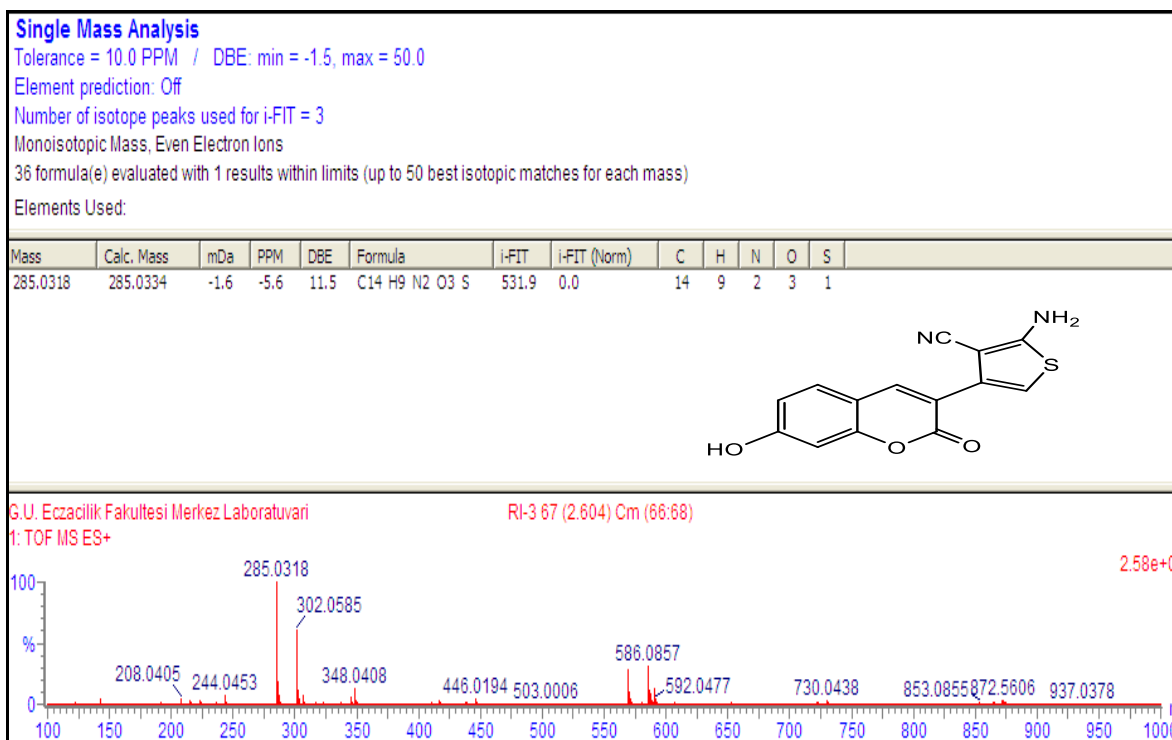
Appendix-3. (Continues) FT-IR,  $^1\text{H-NMR}$ ,  $^{13}\text{C-APT}$ , HRMS of the 2-Aminothiophenes 21-30Figure 3.7.3.  $^{13}\text{C-APT}$  (DMSO- $d_6$ ) Spectrum of 27

Figure 3.7.4. HRMS Spectrum of 27

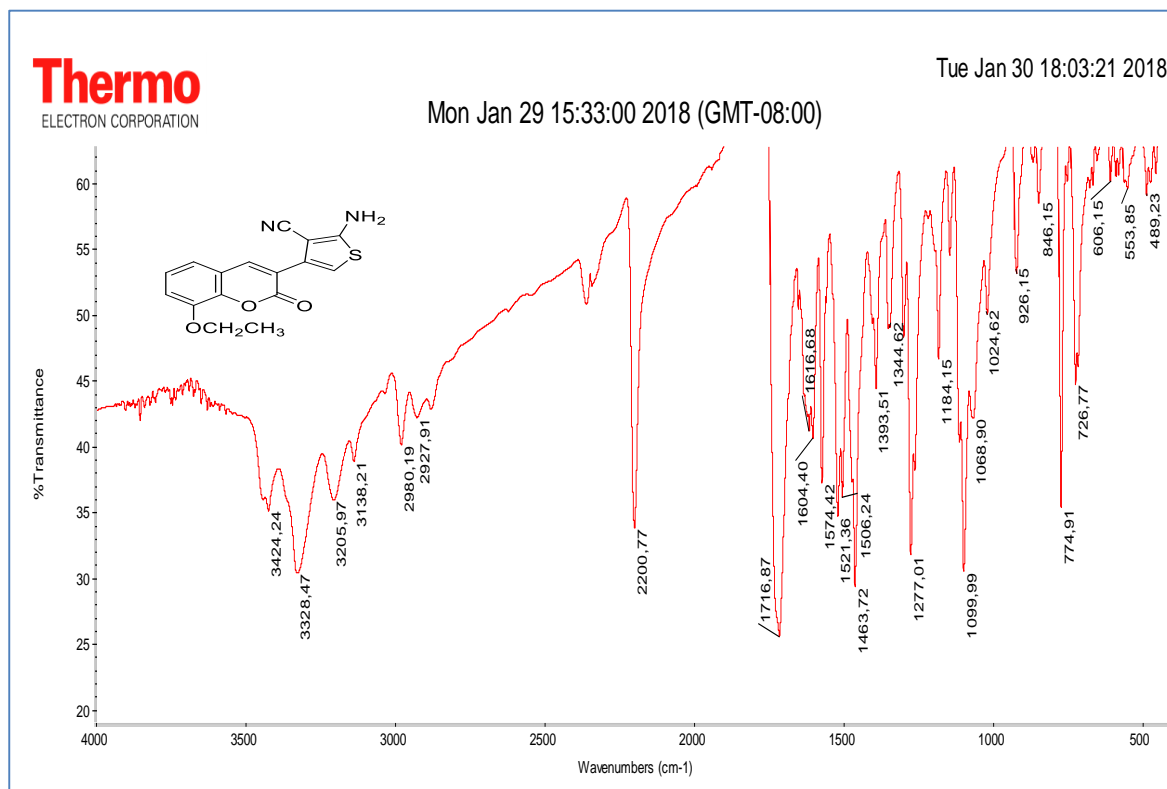
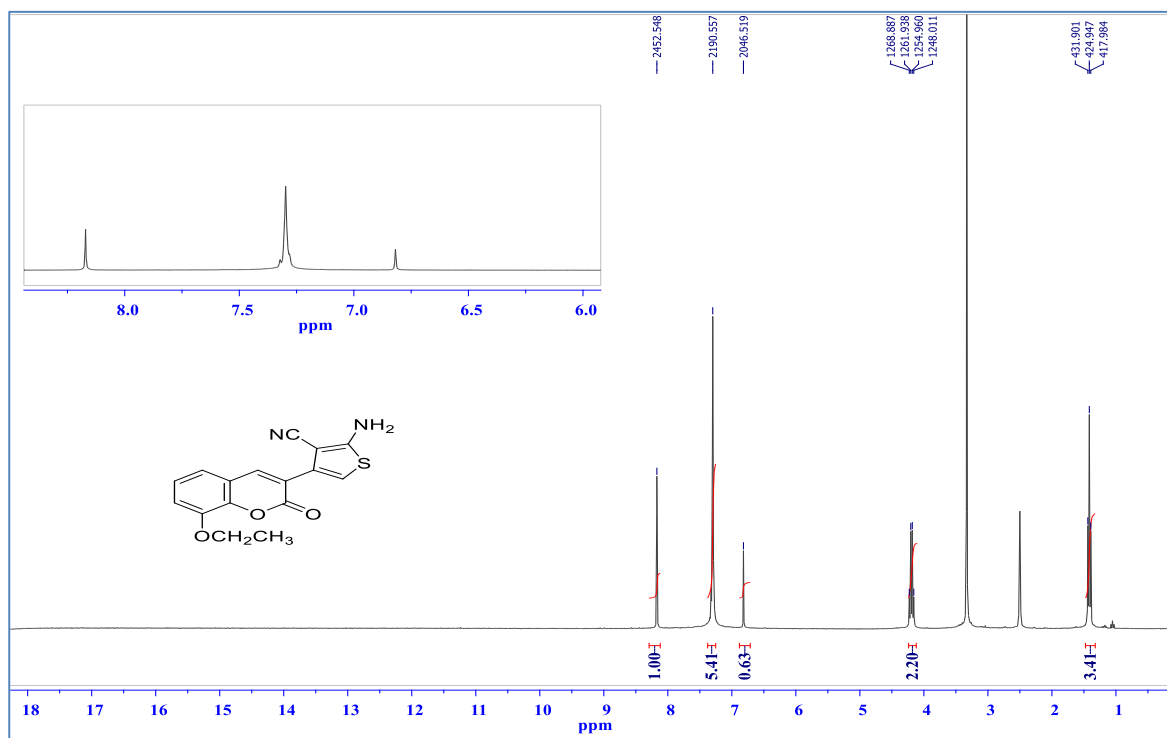
Appendix-3. (Continues) FT-IR,  $^1\text{H-NMR}$ ,  $^{13}\text{C-APT}$ , HRMS of the 2-Aminothiophenes 21-30

Figure 3.8.1. FT-IR Spectrum of 28

Figure 3.8.2.  $^1\text{H-NMR}$  ( $\text{DMSO-}d_6$ ) Spectrum of 28

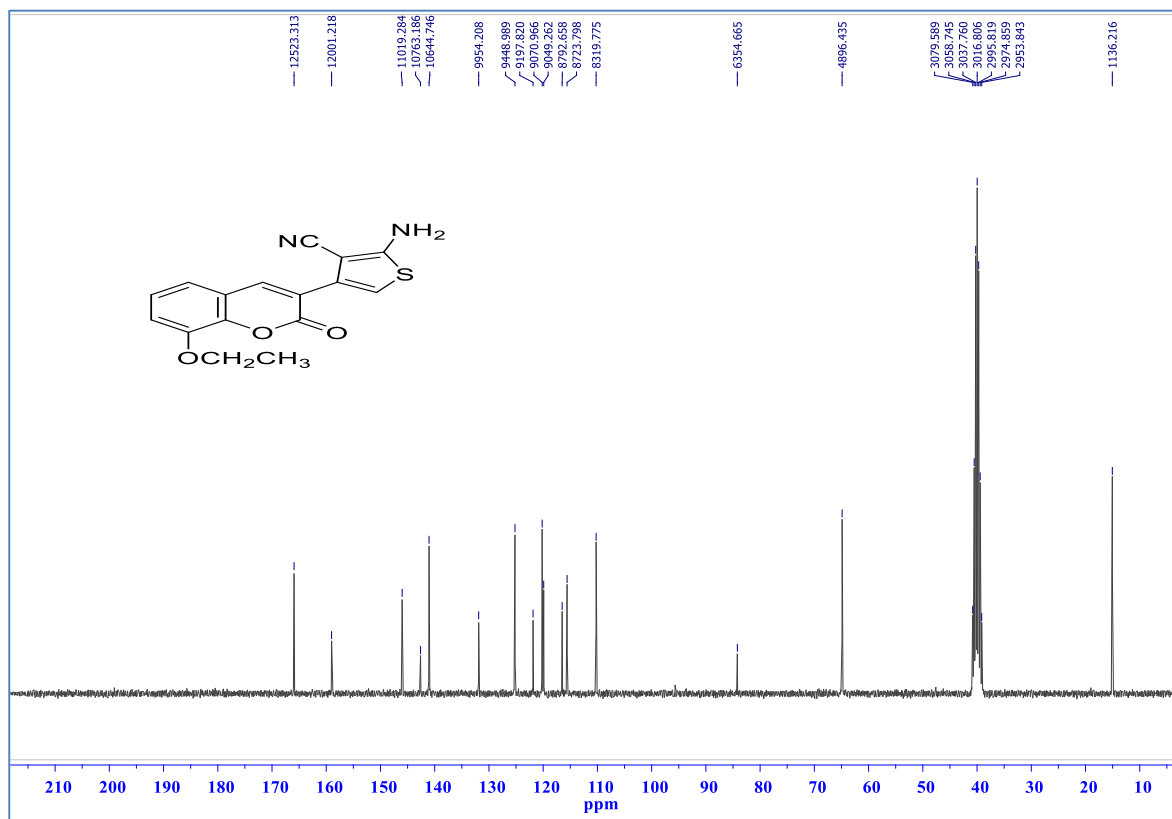
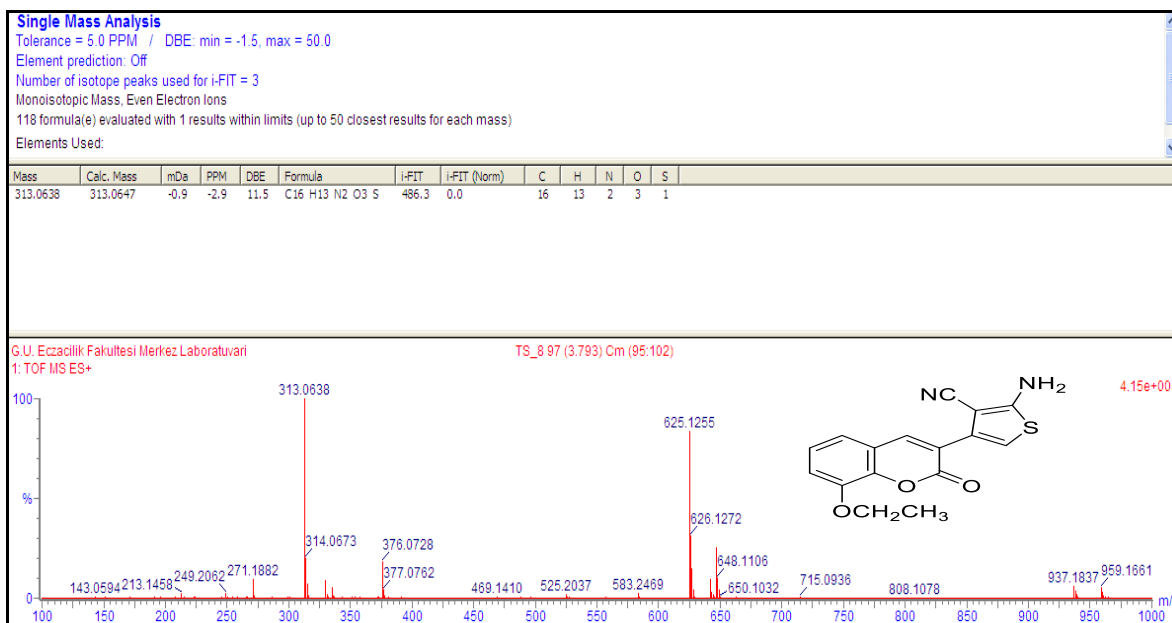
Appendix-3. (Continues) FT-IR, <sup>1</sup>H-NMR, <sup>13</sup>C-APT, HRMS of the 2-Aminothiophenes 21-30Figure 3.8.3. <sup>13</sup>C-APT (DMSO-d<sub>6</sub>) Spectrum of 28

Figure 3.8.4. HRMS Spectrum of 28

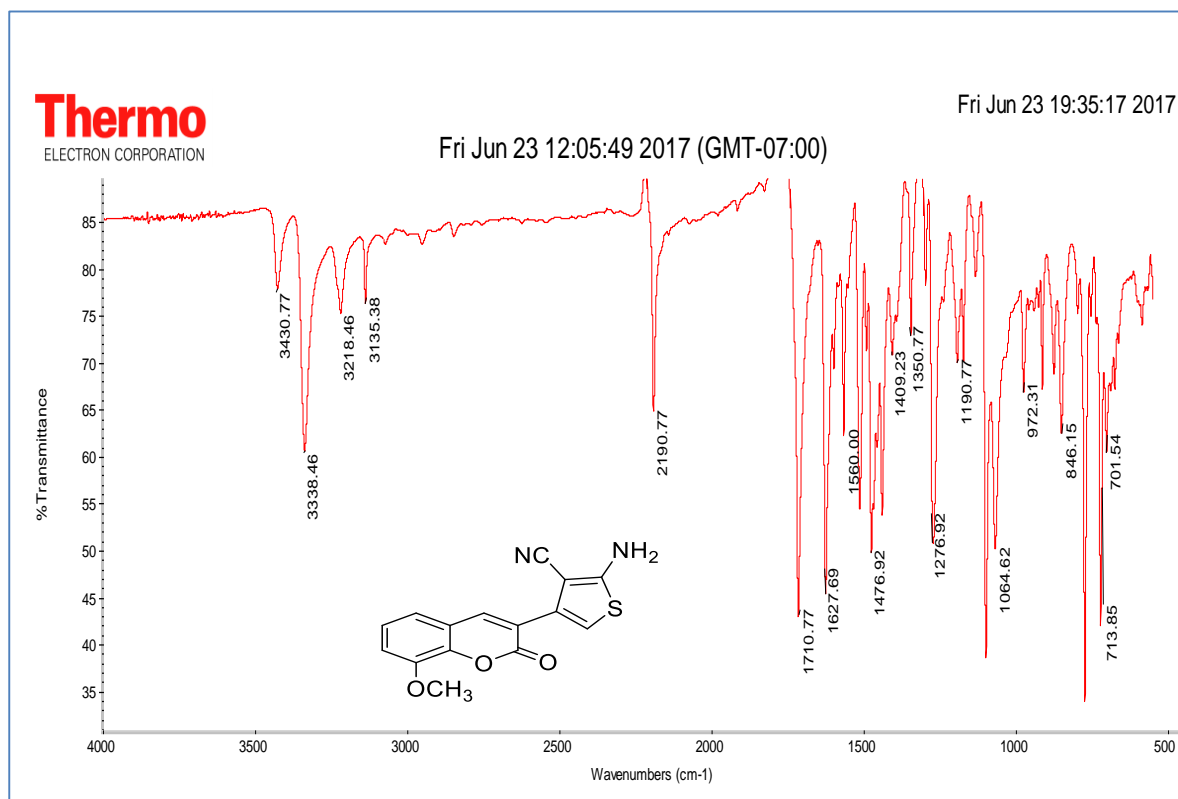
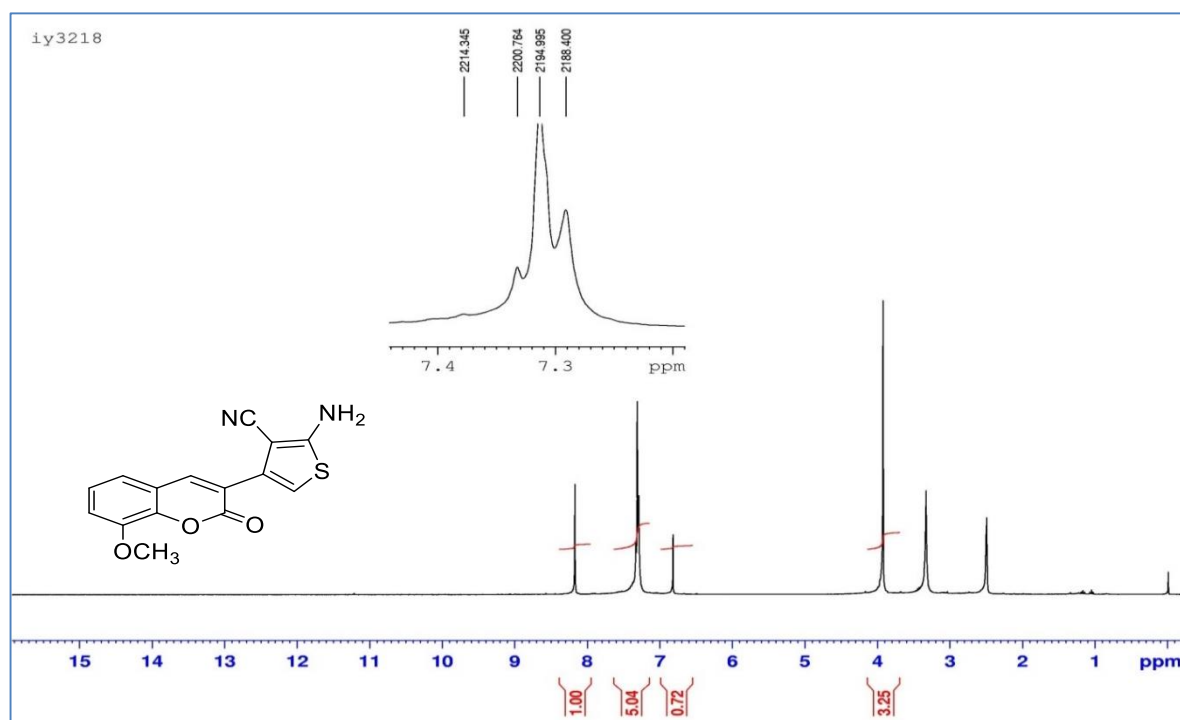
Appendix-3. (Continuous) FT-IR,  $^1\text{H-NMR}$ ,  $^{13}\text{C-NMR}$ , HRMS of the 2-Aminothiophenes 21-30

Figure 3.9.1. FT-IR Spectrum of 29

Figure 3.9.2.  $^1\text{H-NMR}$  (DMSO-*d*<sub>6</sub>) Spectrum of 29

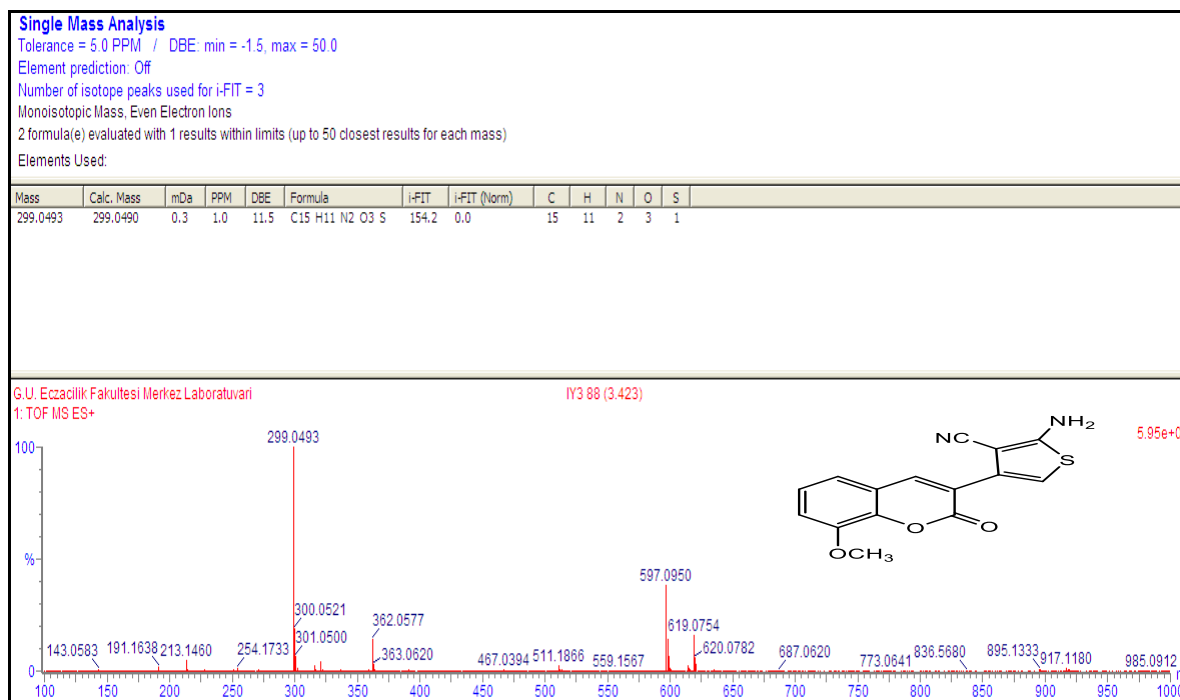
Appendix-3. (Continues) FT-IR, <sup>1</sup>H-NMR, <sup>13</sup>C-APT, HRMS of the 2-Aminothiophenes 21-30

Figure 3.9.4. HRMS spectrum of 29

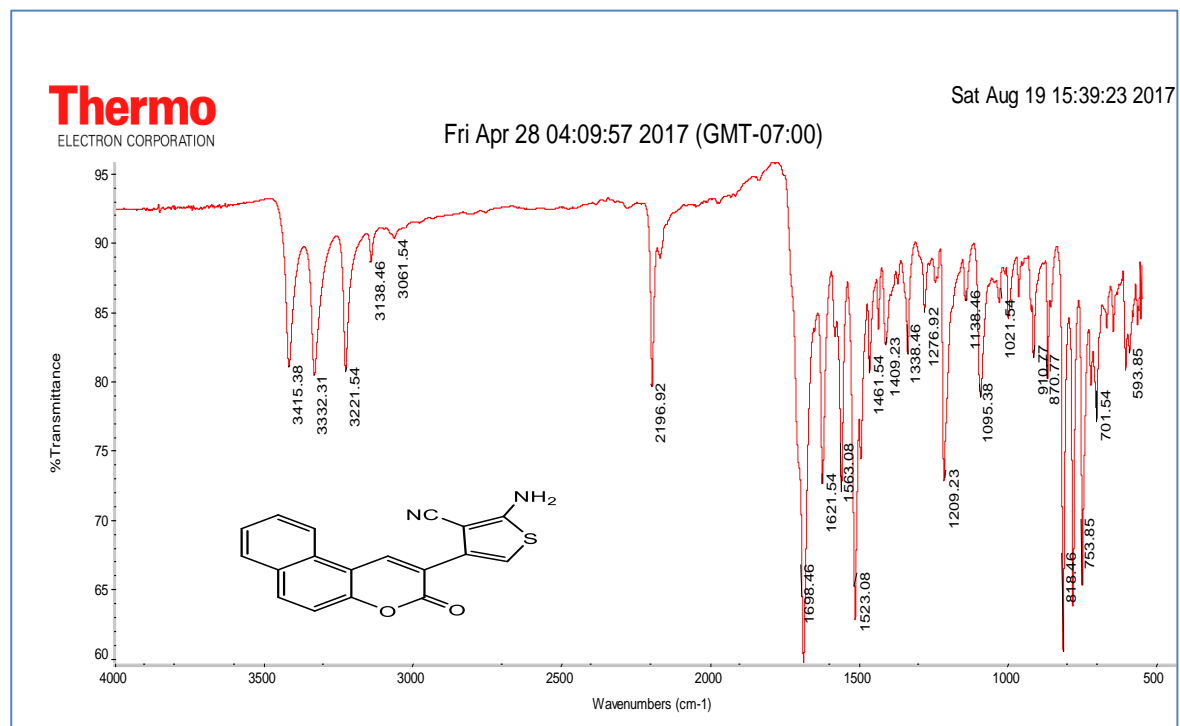
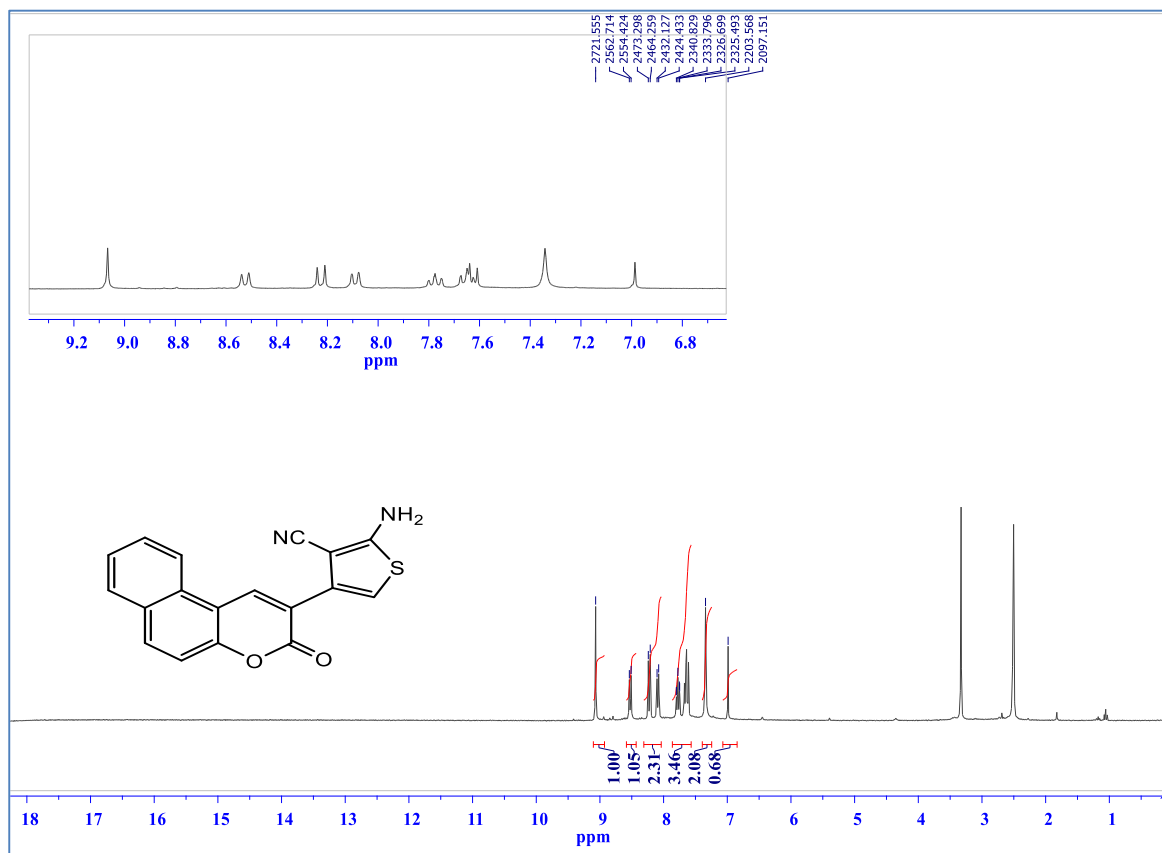
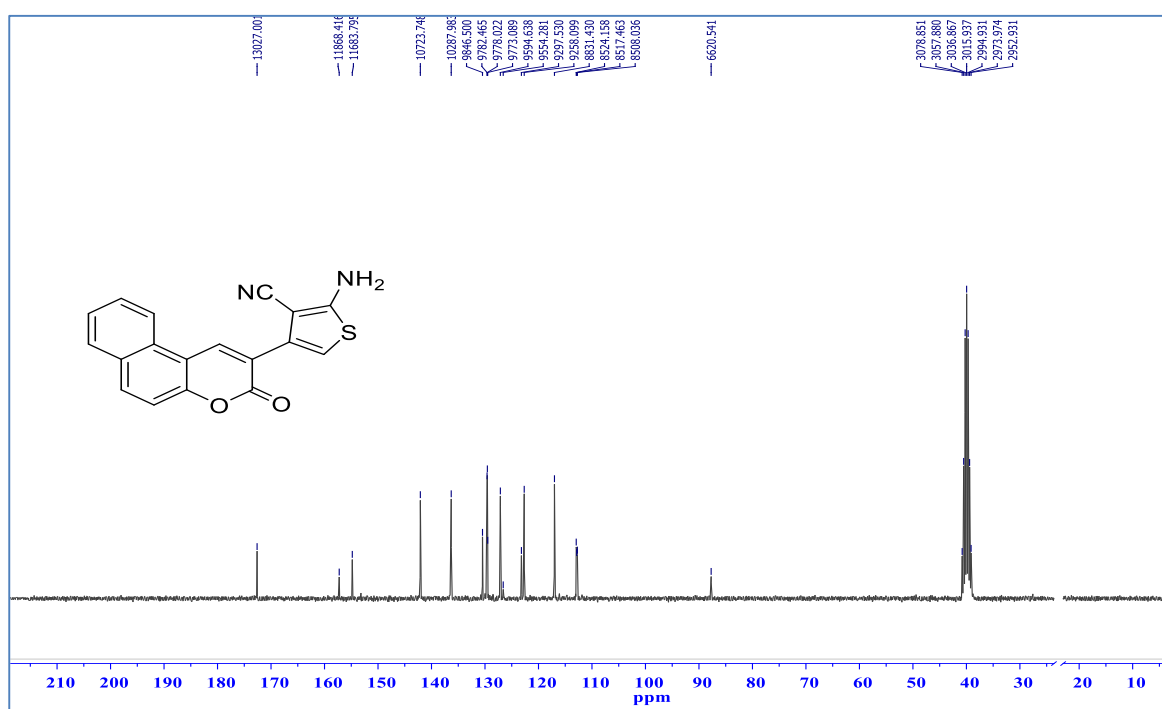


Figure 3.10.1. FT-IR Spectrum of 30

Appendix-3. (Continues) FT-IR,  $^1\text{H-NMR}$ ,  $^{13}\text{C-APT}$ , HRMS of the 2-Aminothiophenes 21-30Figure 3.10.2.  $^1\text{H-NMR}$  ( $\text{DMSO-}d_6$ ) Spectrum of 30Figure 3.10.3.  $^{13}\text{C-APT}$  ( $\text{DMSO-}d_6$ ) Spectrum of 30

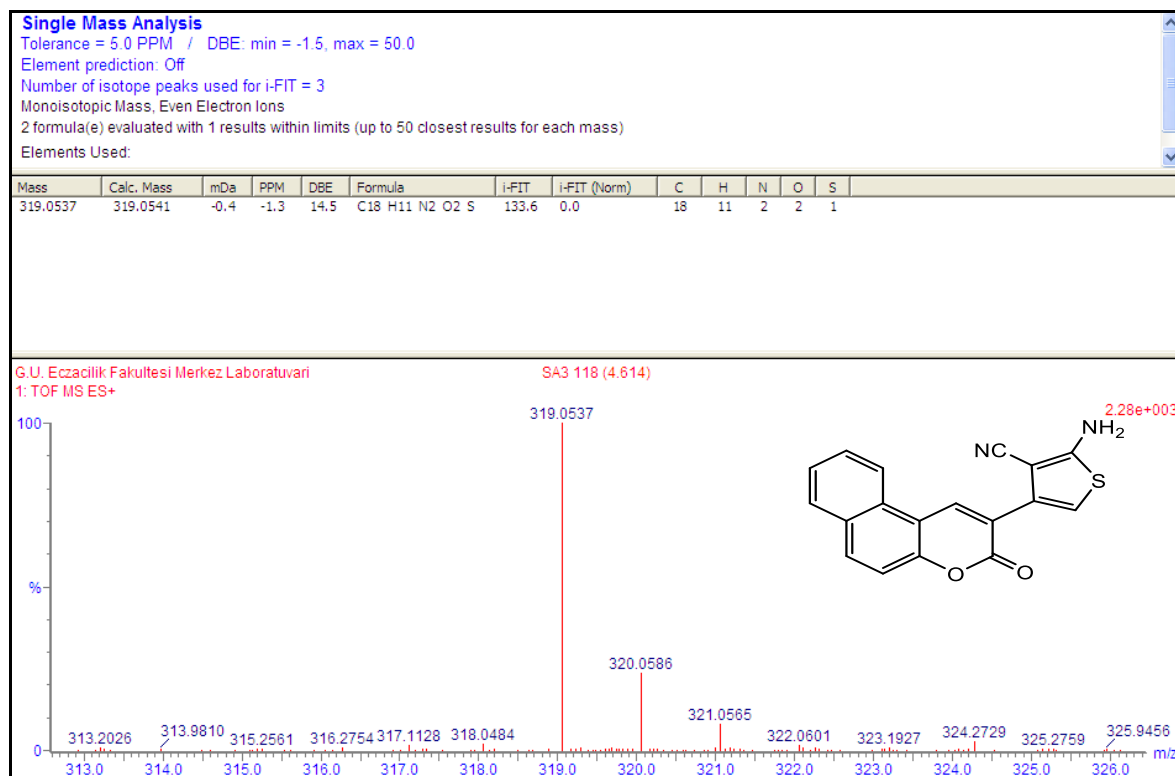
Appendix-3. (Continues) FT-IR, <sup>1</sup>H-NMR, <sup>13</sup>C-APT, HRMS of the 2-Aminothiophenes 21-30

Figure 3.10.4. HRMS Spectrum of 30

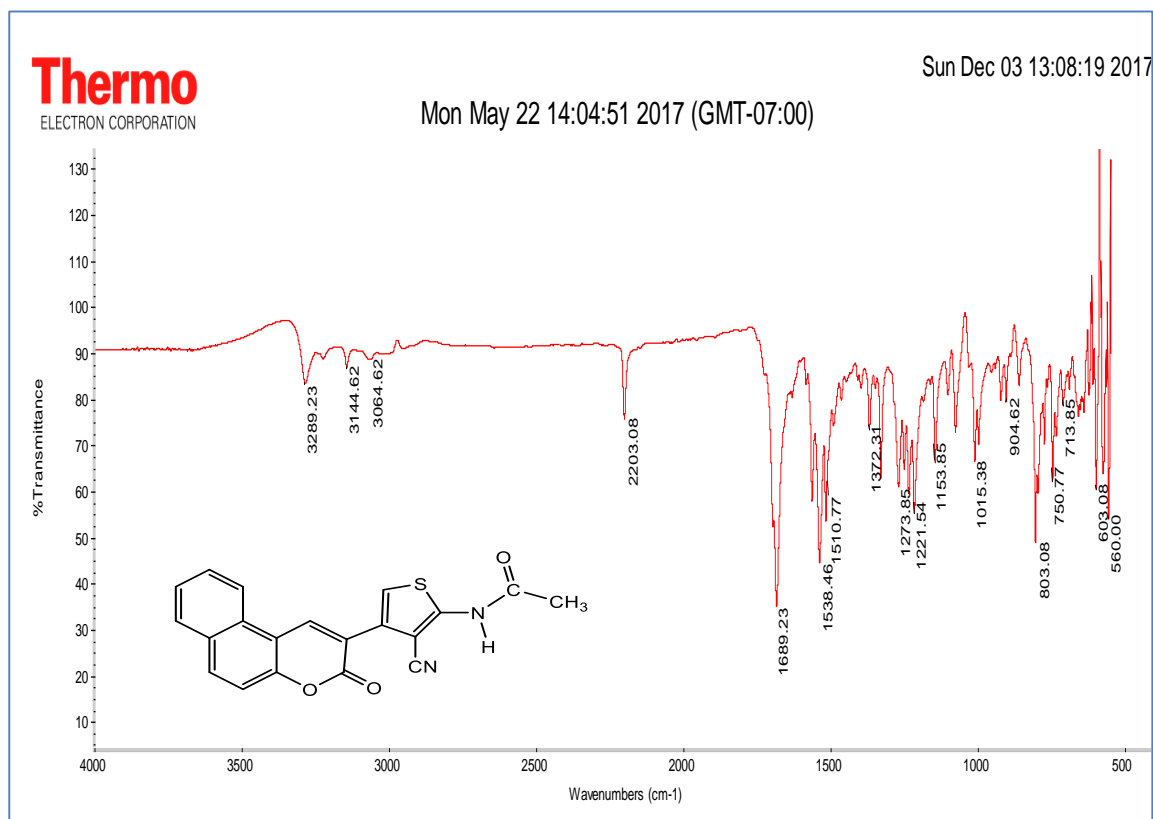
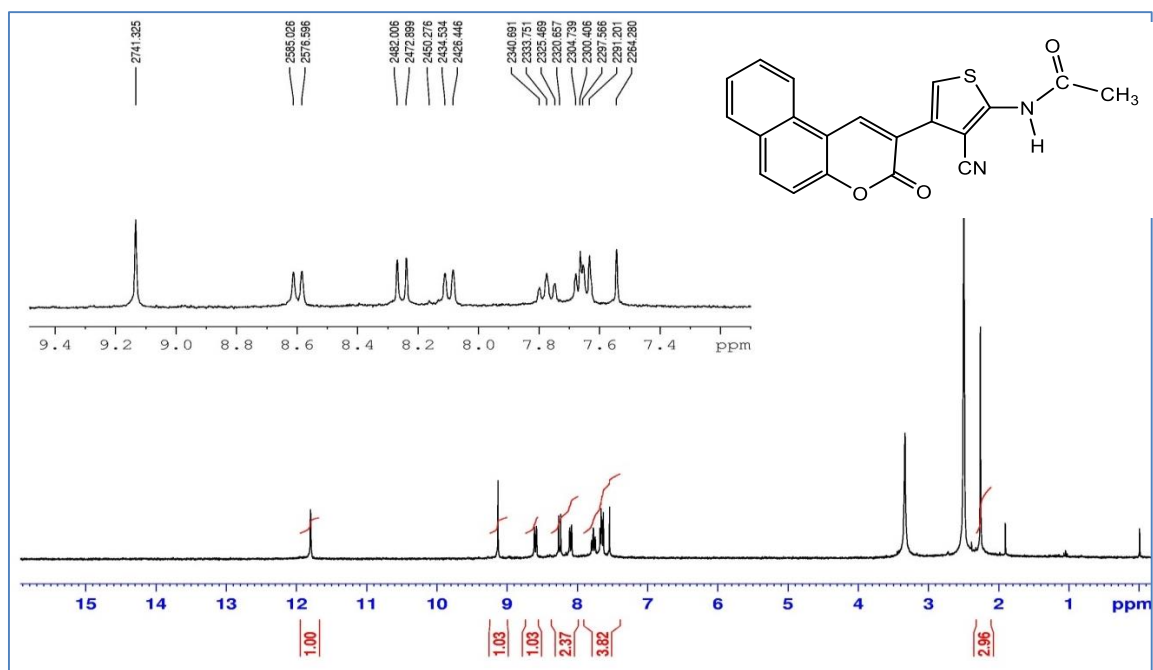
Appendix-4. FT-IR,  $^1\text{H-NMR}$ ,  $^{13}\text{C-APT}$ , HRMS for the Amides, the Sulfonamide, and the Urea 31-35

Figure 4.1.1. FT-IR Spectrum of 31

Figure 4.1.2.  $^1\text{H-NMR}$  (DMSO-*d*<sub>6</sub>) Spectrum of 31

Appendix-4. (Continues) FT-IR,  $^1\text{H-NMR}$ ,  $^{13}\text{C-APT}$ , HRMS for the Amides, the Sulfonamide, and the Urea 31-35

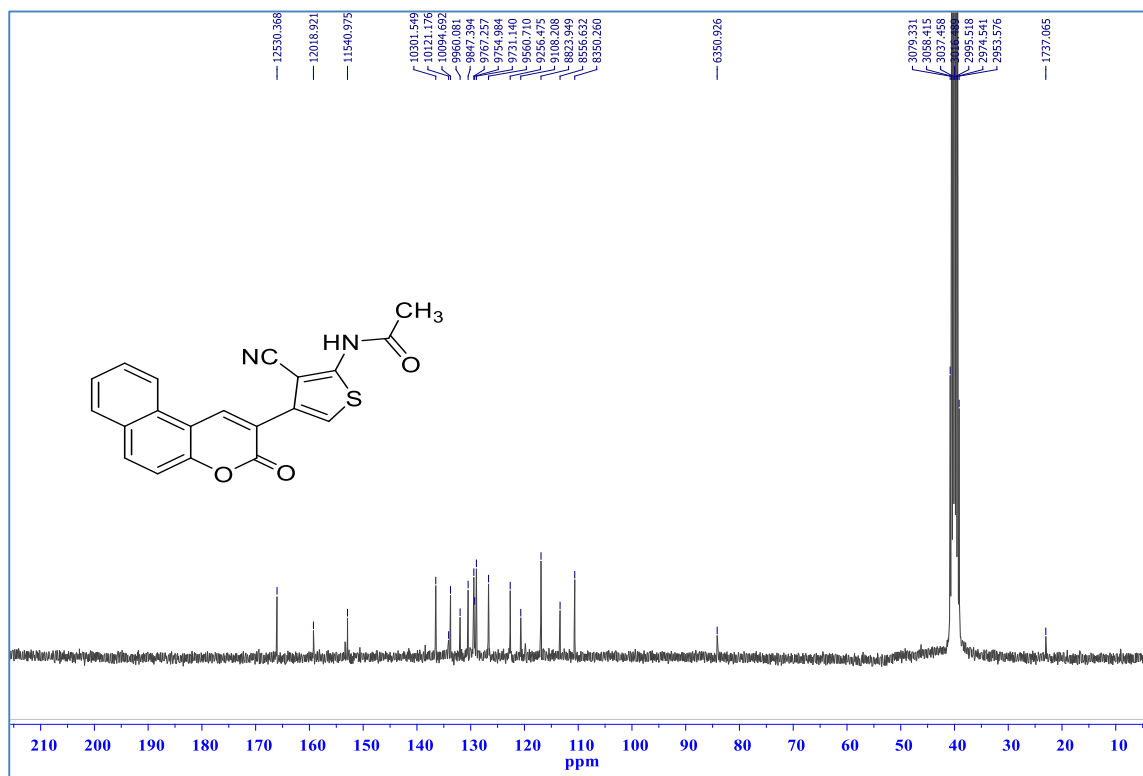


Figure 4.1.3.  $^{13}\text{C-APT}$  (DMSO- $d_6$ ) Spectrum of 31

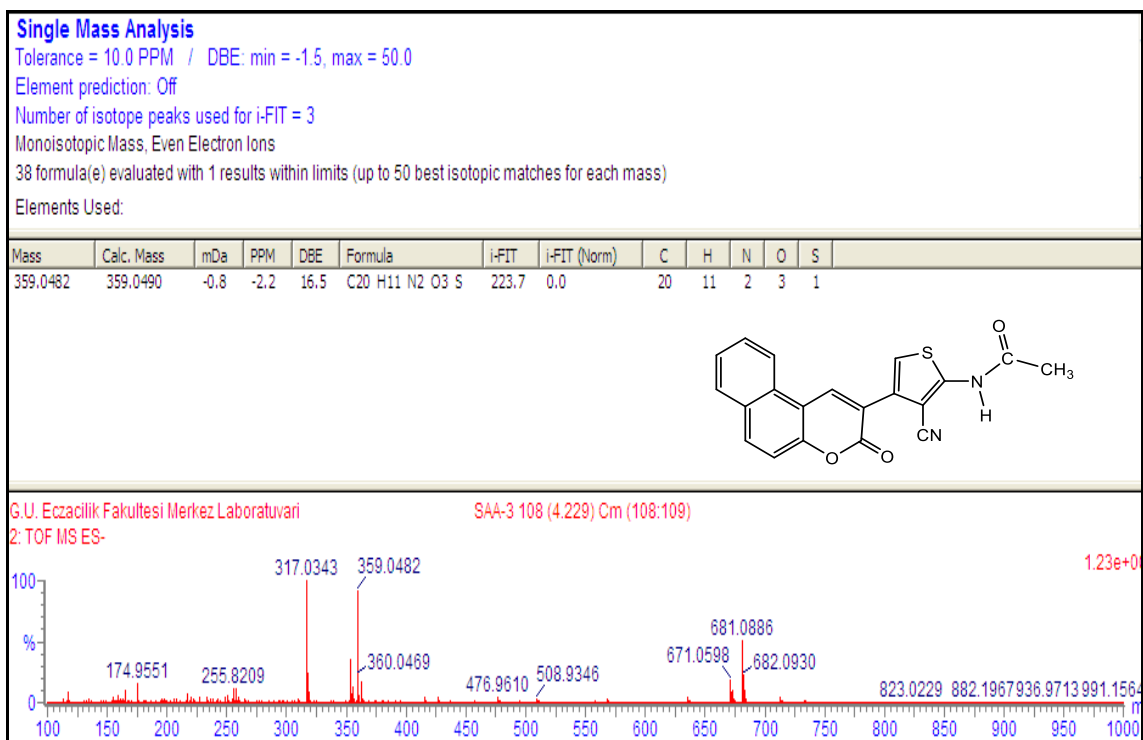


Figure 4.1.4. HRMS spectrum of 31

Appendix-4. (Continues) FT-IR,  $^1\text{H-NMR}$ ,  $^{13}\text{C-APT}$ , HRMS for the Amides, the Sulfonamide, and the Urea 31-35

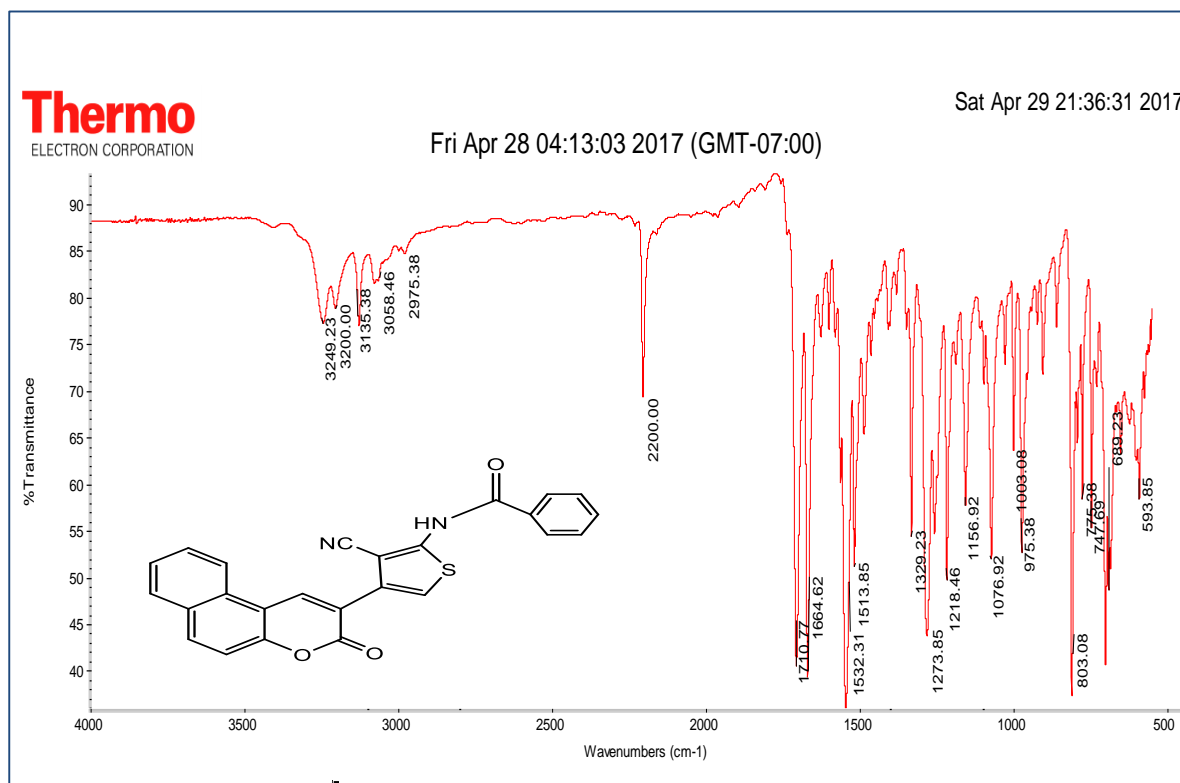


Figure 4.2.1. FT-IR Spectrum of 32

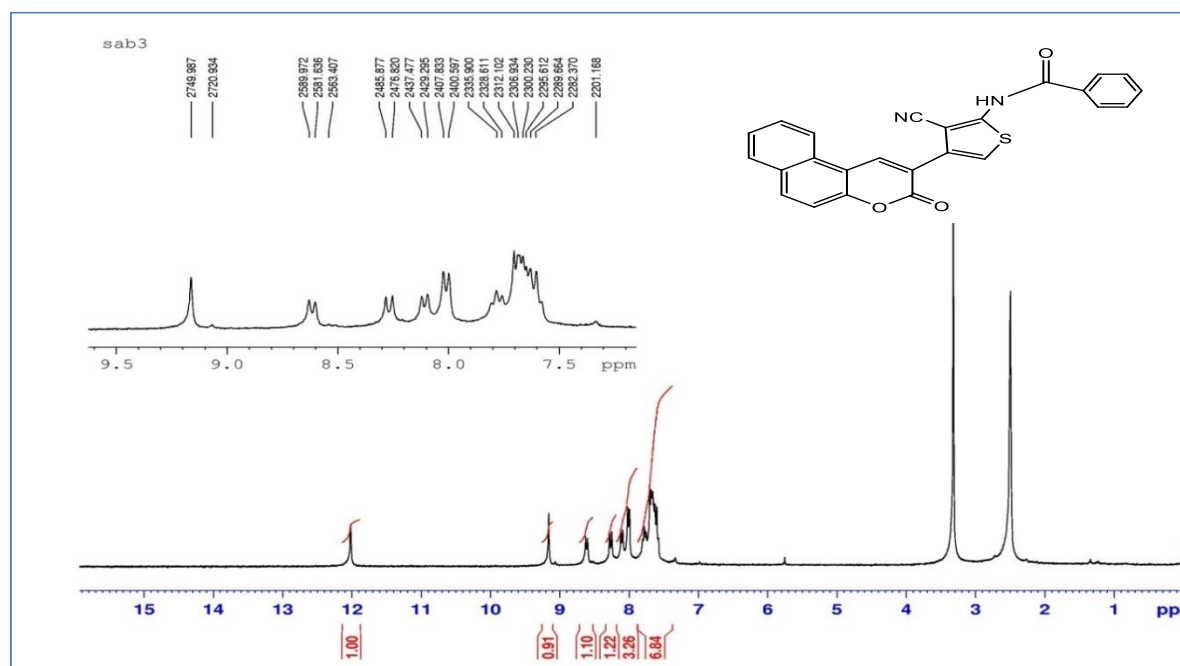


Figure 4.2.2.  $^1\text{H-NMR}$  ( $\text{DMSO-}d_6$ ) Spectrum of 32

Appendix-4. (Continues) FT-IR,  $^1\text{H-NMR}$ ,  $^{13}\text{C-APT}$ , HRMS for the Amides, the Sulfonamide, and the Urea 31-35

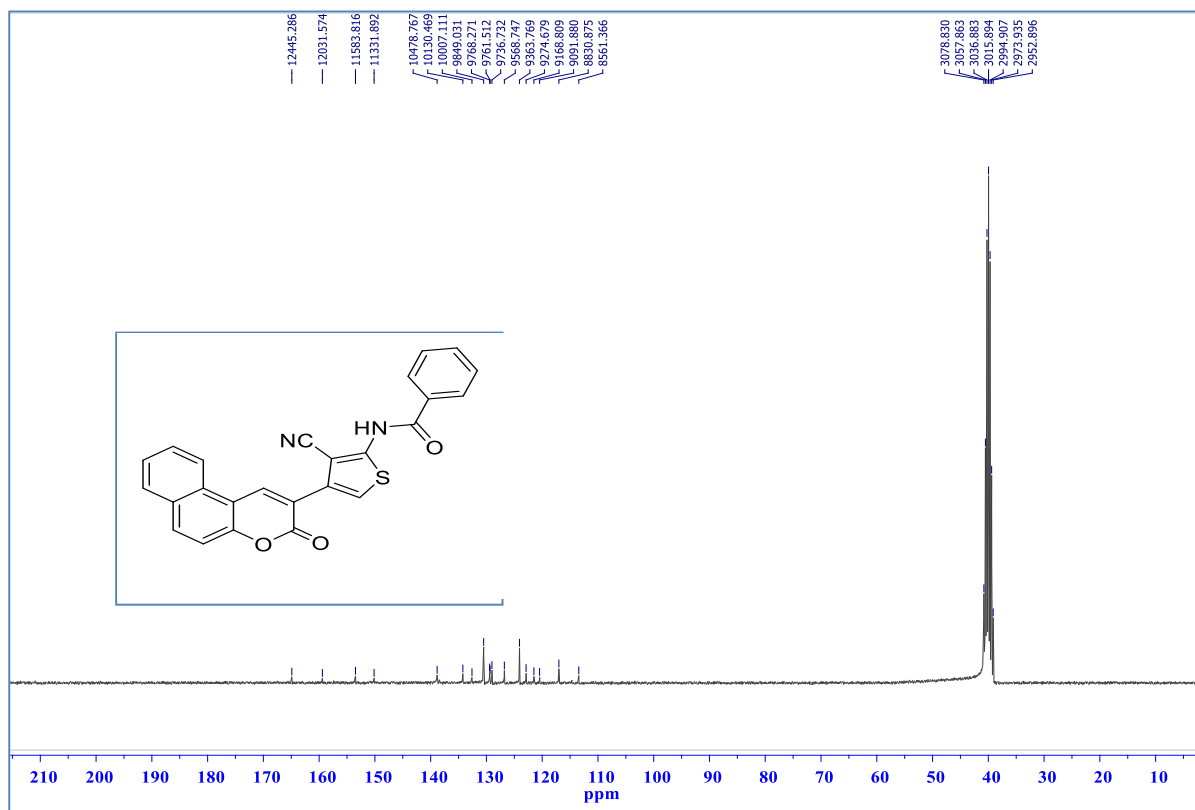


Figure 4.2.3.  $^{13}\text{C-NMR}$  (DMSO- $d_6$ ) Spectrum of 32

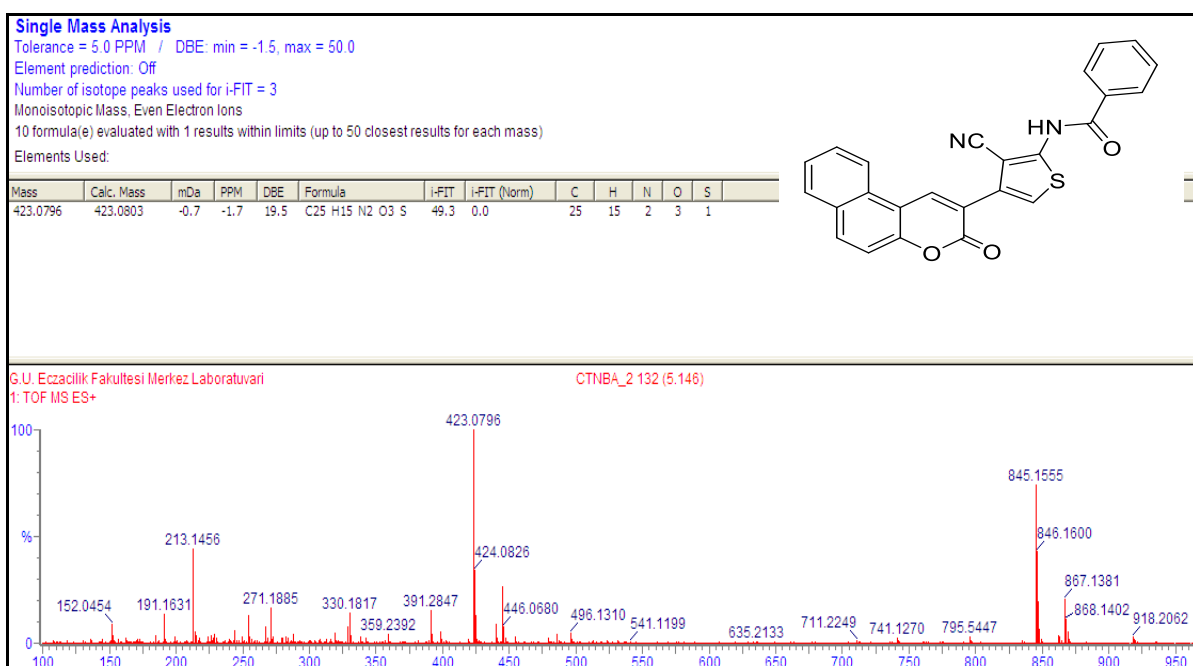


Figure 4.2.4. HRMS Spectrum of 32

Appendix-4. (Continues) FT-IR,  $^1\text{H-NMR}$ ,  $^{13}\text{C-APT}$ , HRMS for the Amides, the Sulfonamide, and the Urea 31-35

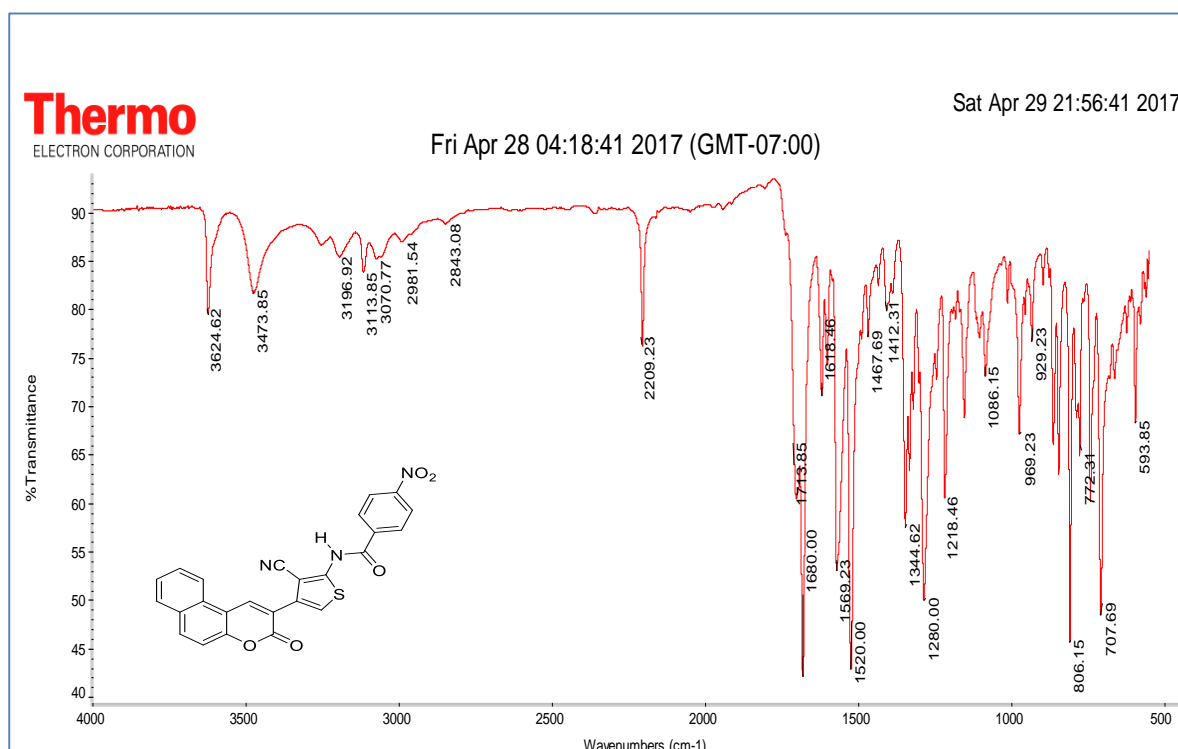


Figure 4.3.1. FT-IR Spectrum of 33

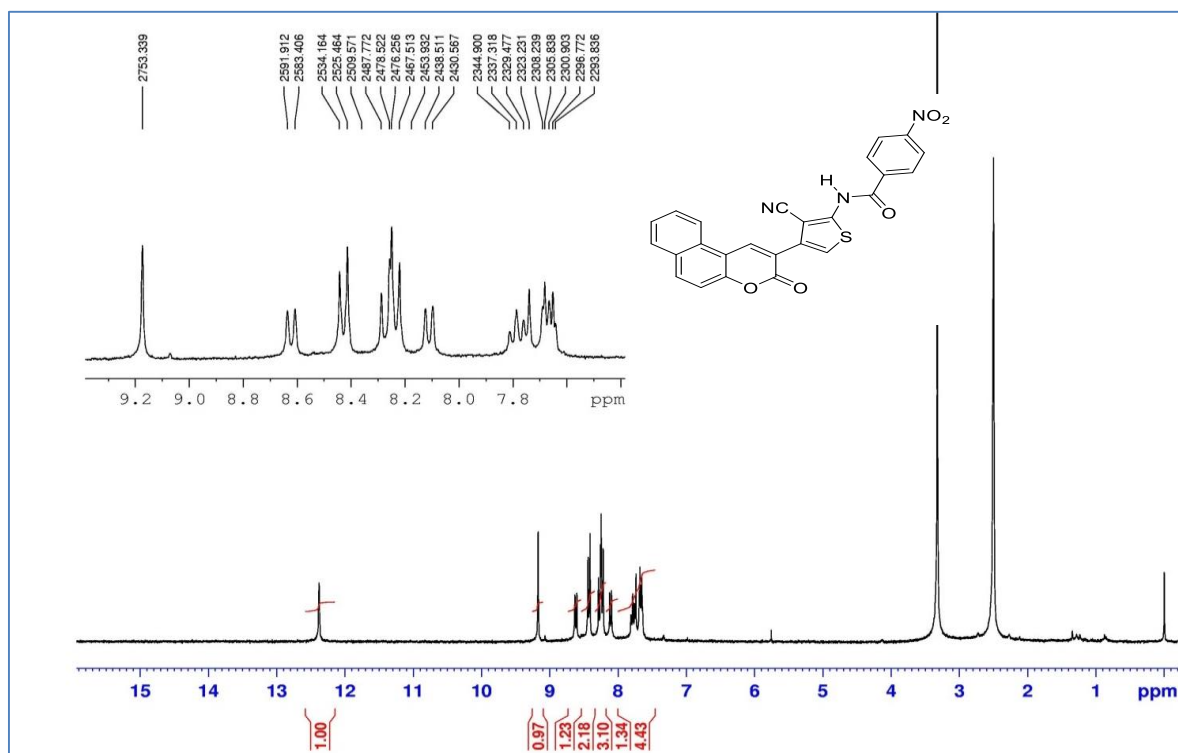


Figure 4.3.2.  $^1\text{H-NMR}$  ( $\text{DMSO-}d_6$ ) Spectrum of 33

Appendix-4. (Continues) FT-IR,  $^1\text{H-NMR}$ ,  $^{13}\text{C-APT}$ , HRMS for the Amides, the Sulfonamide, and the Urea 31-35

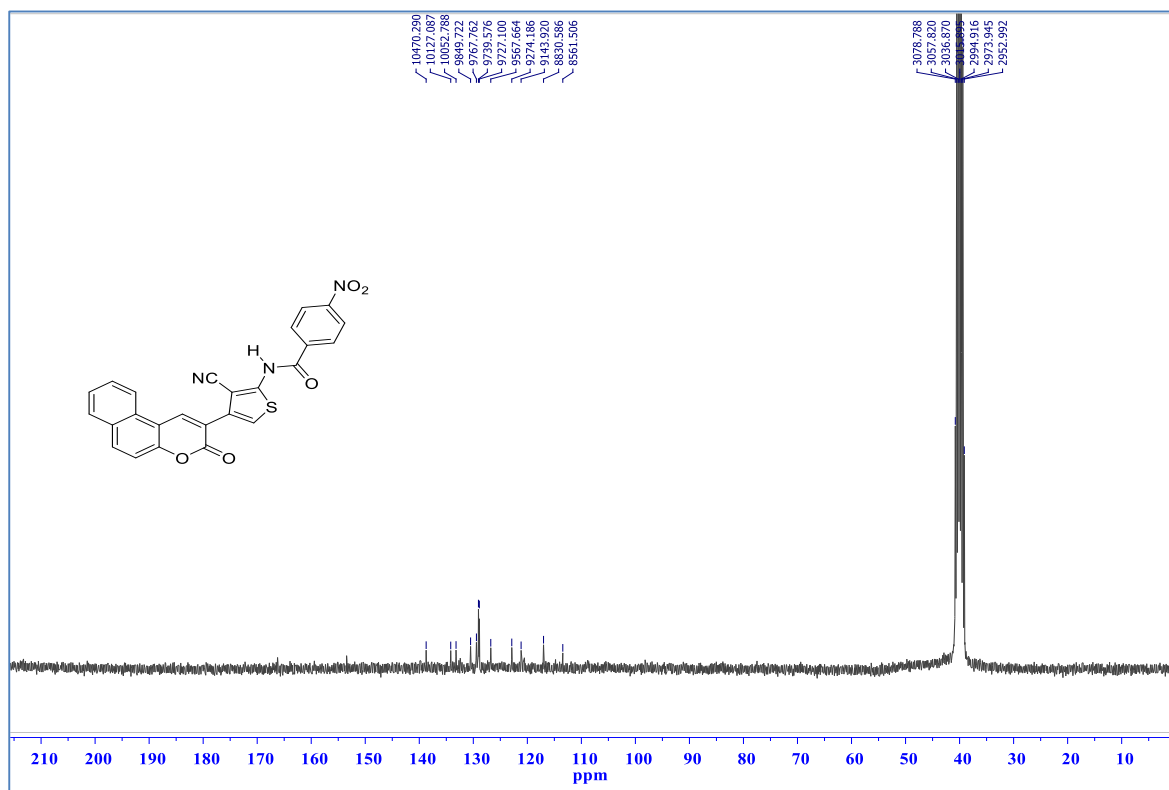


Figure 4.3.3.  $^{13}\text{C-APT}$  ( $\text{DMSO-}d_6$ ) Spectrum of 33

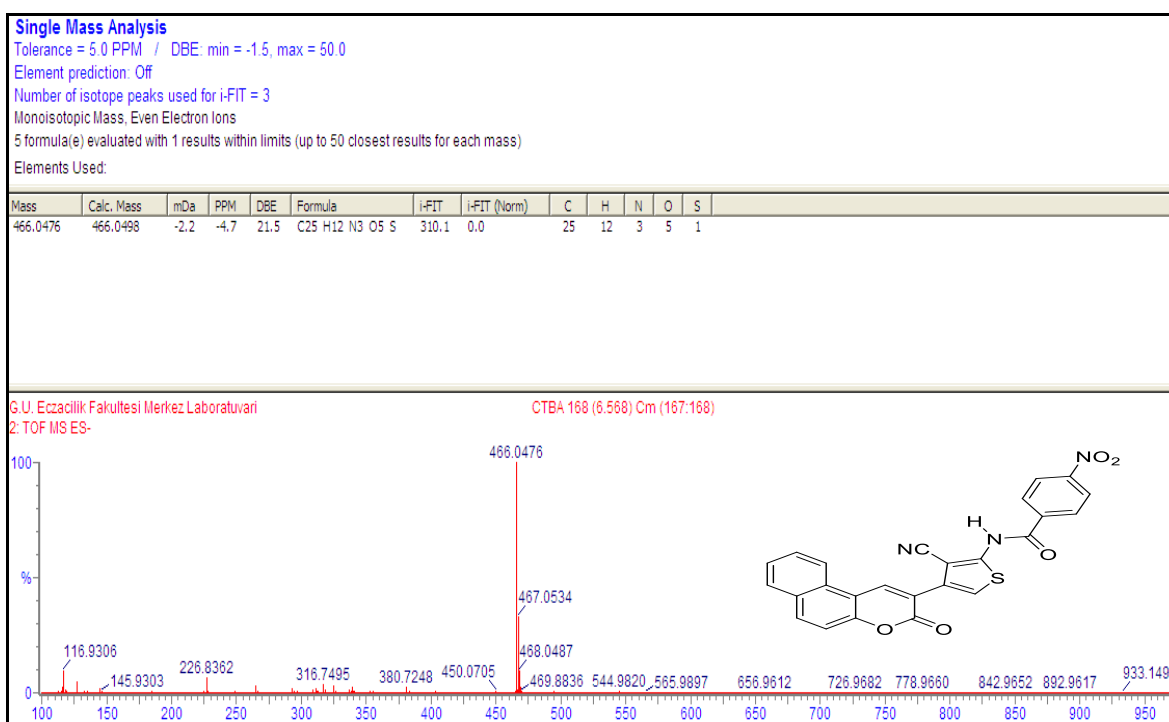


Figure 4.3.4. HRMS spectrum of 33

Appendix-4. (Continues) FT-IR,  $^1\text{H-NMR}$ ,  $^{13}\text{C-APT}$ , HRMS for the Amides, the Sulfonamide, and the Urea 31-35

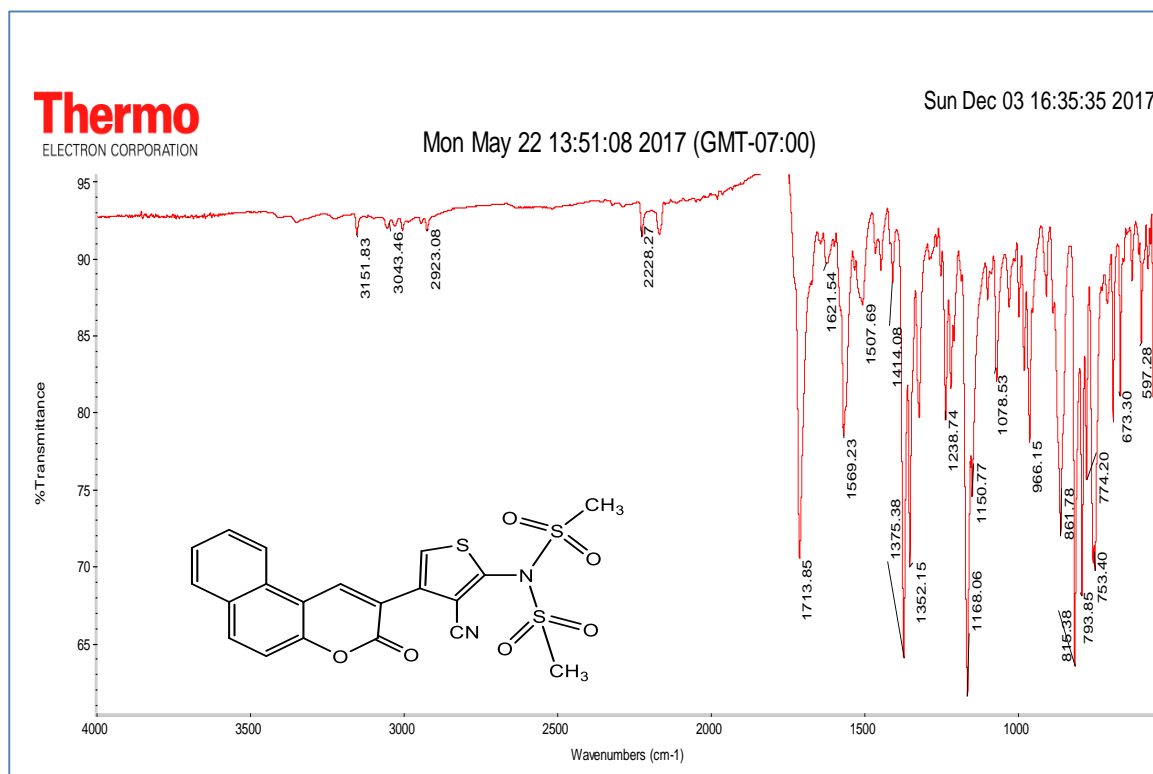


Figure 4.4.1. FT-IR Spectrum of 34

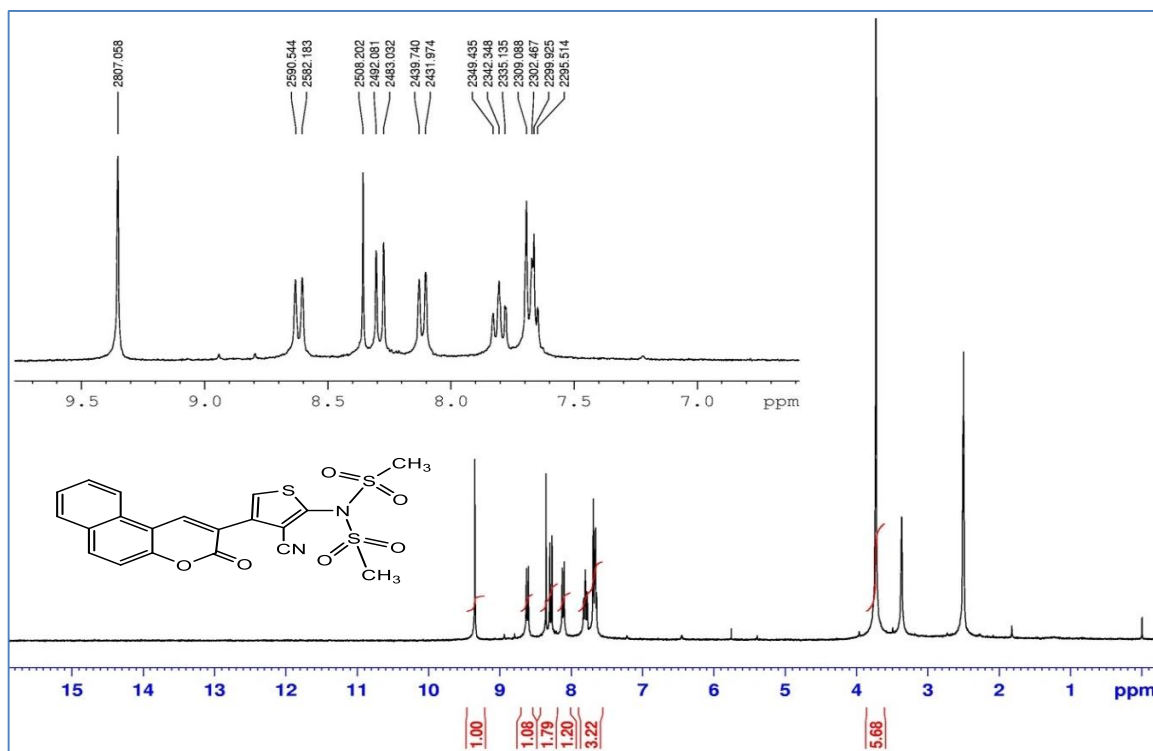


Figure 4.4.2.  $^1\text{H-NMR}$  ( $\text{DMSO-}d_6$ ) Spectrum of 34

Appendix-4. (Continues) FT-IR,  $^1\text{H-NMR}$ ,  $^{13}\text{C-APT}$ , HRMS for the Amides, the Sulfonamide, and the Urea 31-35

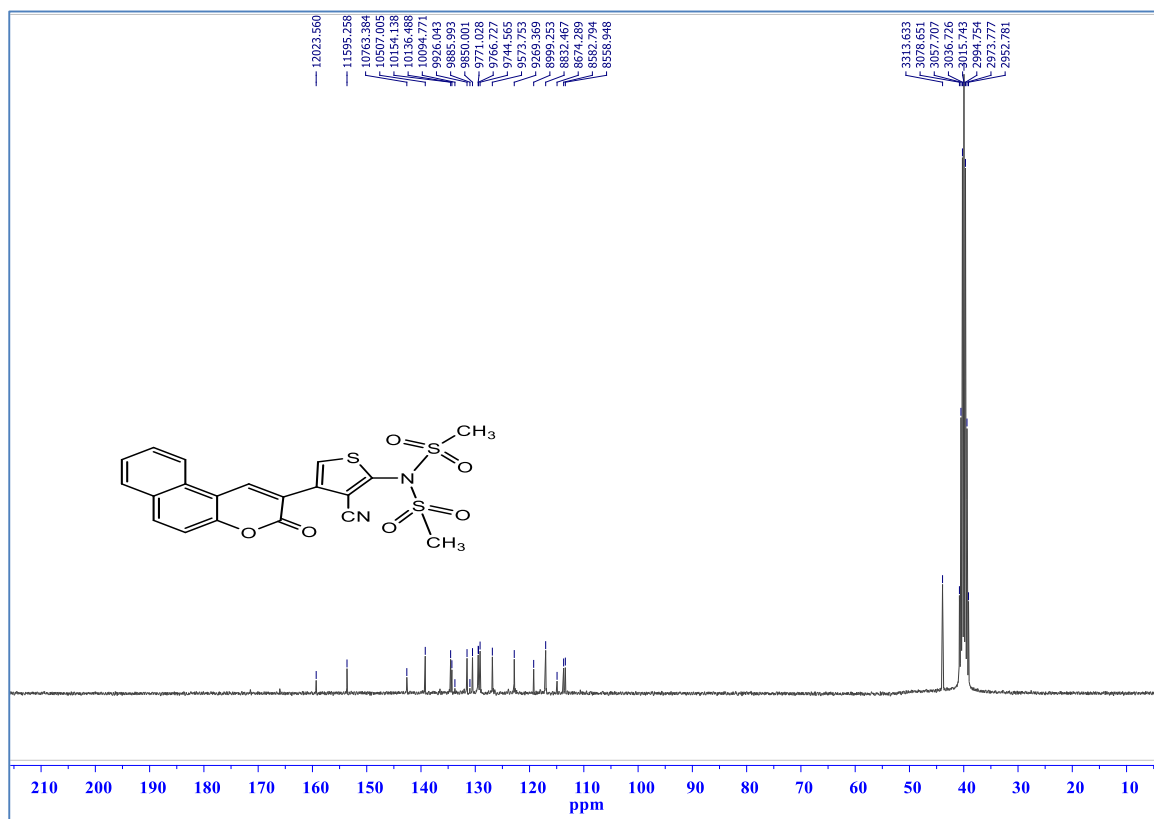


Figure 4.4.3.  $^{13}\text{C-APT}$  ( $\text{DMSO-}d_6$ ) Spectrum of 34

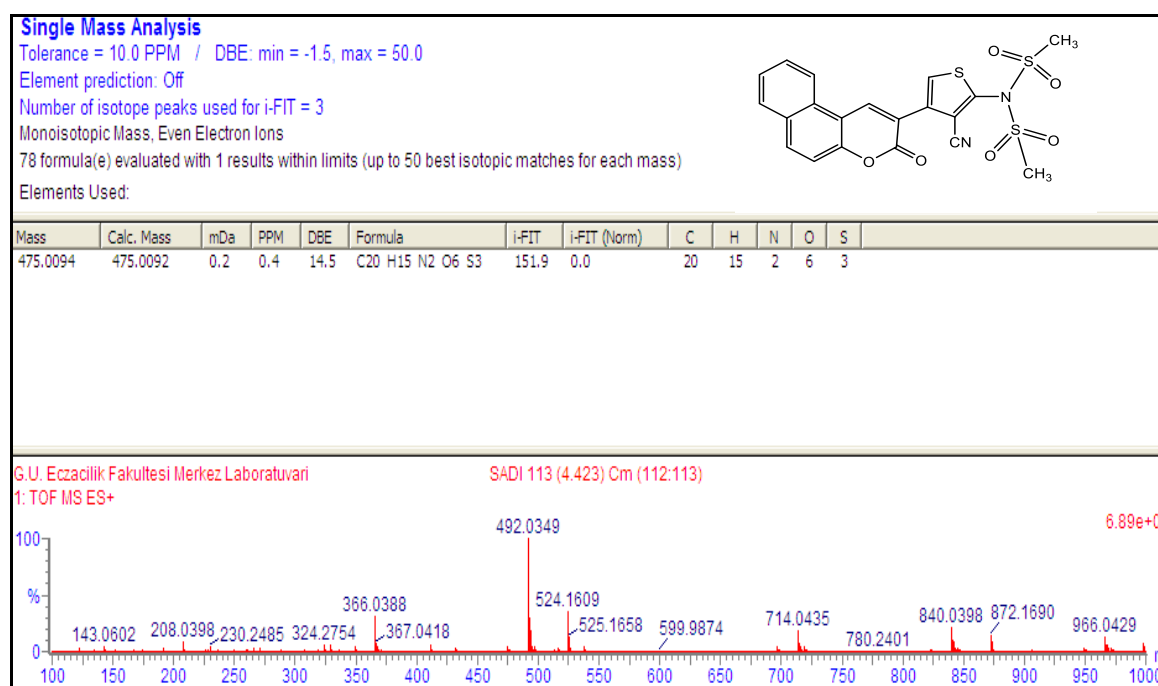


Figure 4.4.4. HRMS Spectrum of 34

Appendix-4. (Continues) FT-IR,  $^1\text{H-NMR}$ ,  $^{13}\text{C-APT}$ , HRMS for the Amides, the Sulfonamide, and the Urea 31-35

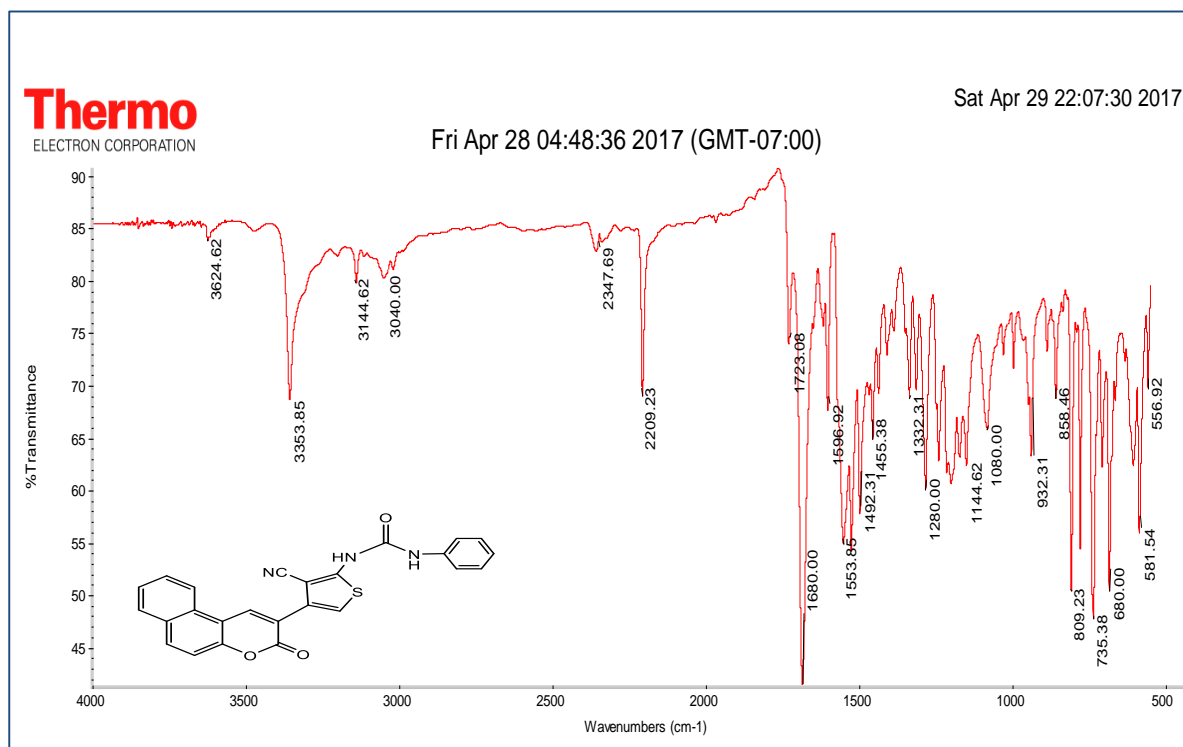


Figure 4.5.1. FT-IR Spectrum of 35

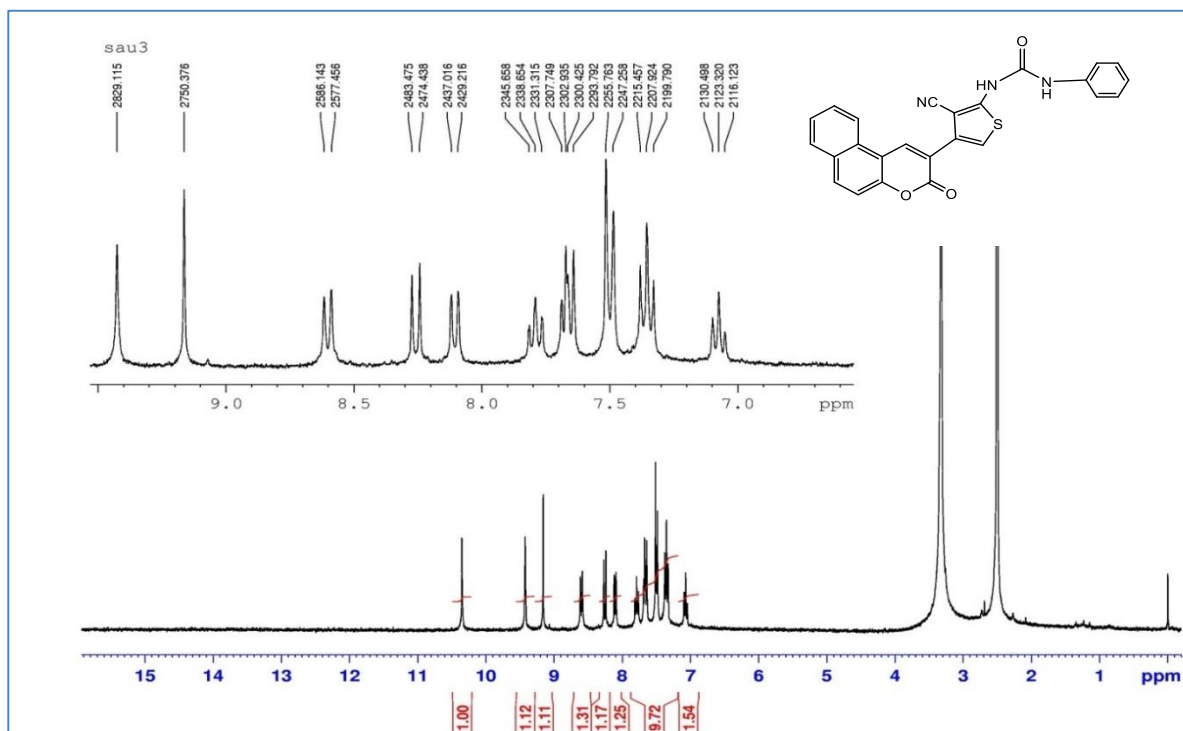


Figure 4.5.2.  $^1\text{H-NMR}$  ( $\text{DMSO-}d_6$ ) Spectrum of 35

Appendix-4. (Continues) FT-IR,  $^1\text{H-NMR}$ ,  $^{13}\text{C-APT}$ , HRMS for the Amides, the Sulfonamide, and the Urea 31-35

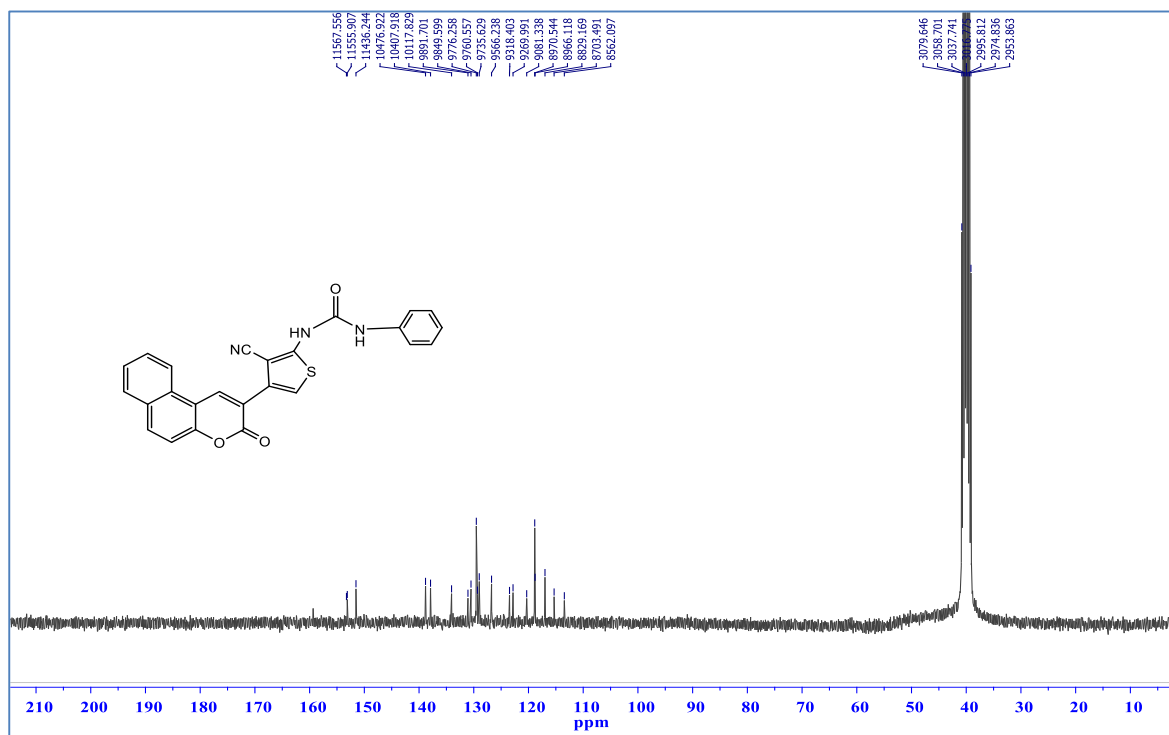


Figure 4.5.3.  $^{13}\text{C-APT}$  ( $\text{DMSO-}d_6$ ) Spectrum of 35

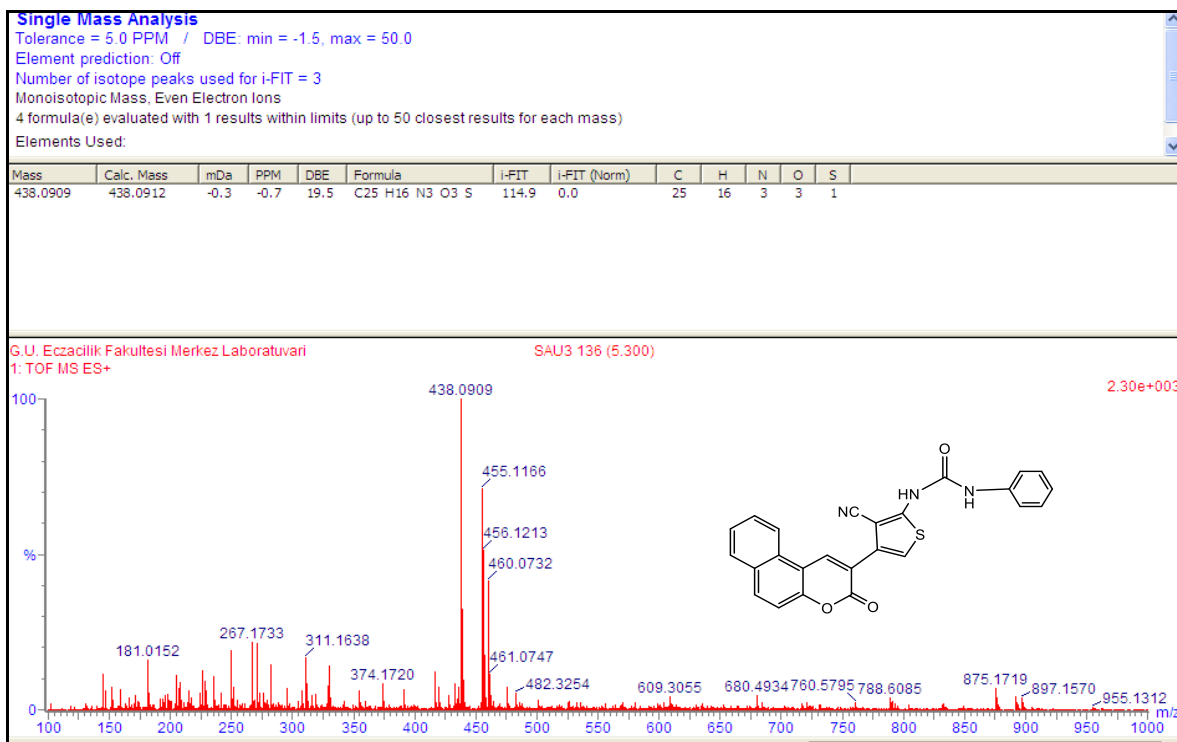


Figure 4.5.4. HRMS spectrum of 35

Appendix-5. Results Tables, Physicochemical Properties, Comparative Analyses of Data for all the Synthesized compounds

Table 5.1. Physicochemical properties of the 3-Acetyloumarins synthesized by Conventional Method

Precursor	Product Obtained	Reaction time (h)	Yield <sup>a</sup> (%)	Appearance	Melting Point (°C)	Literature Melting Point (°C) [Reference]
S1	1	5	92	White Powder	124-126	120-122 [215]
S2	2	5	98	Light Yellow	234-236	233–235[215]
S3	3	6	90	Light Yellow Powder	151-152	204-206[217]
S4	4	5	90	Dark Green Powder	243-245	254-256 [79]
S5	5	5	90	Yellow powder	208-210	152-154[215]
S6	6	6	90	Light Yellow Powder	173-175	171– 172[218]
S7	7	6	90	Yellow Powder	240-242	234–236 [218]
S8	8	6	90	Yellow Powder	158-160	135–137[216]
S9	9	5.5	92	Light Yellow Powder	181-182	172–172[218]
S10	10	5	94	Light Yellow Powder	189-190	189-190[218]

<sup>a</sup>Yields refer to isolated pure products

Appendix-5. (Continues). Results Tables, Physicochemical Properties, Comparative Analyses of Data for all the synthesized compounds

Table 5.2. Physicochemical Properties of the 3-Acetyloumarins synthesized via Microwave-Assisted Irradiation (300 W, 80 °C) Procedure

Precursor	Product obtained	Reaction time (min)	Yield <sup>a</sup> (%)	Appearance	Melting Point (°C)	Literature Melting Point (°C) [Reference]
S1	1	1	97	White powder	124-126	120-122[215]
S2	2	1	100	Light Yellow Powder	234-236	233-235[215]
S3	3	1	95	Light Yellow powder	208-210	204-206[217]
S4	4	1	94	Dark Green Powder	243-245	254-256[218]
S5	5	1.5	95	Yellow Powder	151-152	152-154[79]
S6	6	1	90	Light Yellow powder	173-175	171-172[218]
S7	7	2	96	Yellow powder	240-242	234-236[218]
S8	8	2	95	Yellow Powder	158-160	135-137[216]
S9	9	1.5	93	Light Yellow Powder	181-182	172-172[218]
S10	10	1.5	97	Light Yellow powder	189-190	189-190[218]

<sup>a</sup>Yields refer to isolated pure products

Appendix-5. (Continues). Results Tables, Physicochemical Properties, Comparative Analyses of Data for all the synthesized compounds

Table 5.3. Physicochemical Properties of the Malononitriles Synthesized via Conventional Procedure

Precursor	Product obtained	Reaction time (h)	Yield <sup>a</sup> (%)	Appearance	Melting Point (°C)	Literature Melting Point (°C) [Reference]
1	11	5	89	Yellow powder	164-166	162-164[70]
2	12	4	90	Light Yellow powder	204-206	203-205[70]
3	13	5	88	Light Yellow powder	185-187	185-187 [70]
4	14	4.5	89	Golden Yellow powder	248-250	- <sup>b</sup>
5	15	5	90	Dark Red Crystals	145-146	161-162[79]
6	16	4	80	Yellow powder	187-189	- <sup>b</sup>
7	17	4.5	90	Dark Yellow powder	235-237	- <sup>b</sup>
8	18	5	88	Yellow powder	152-154	- <sup>b</sup>
9	19	4	85	Light Yellow powder	171-173	171-173[70]
10	20	4	90	Dark Brown powder	236-238	- <sup>b</sup>

<sup>a</sup>Yields refer to isolated pure products

-<sup>b</sup>New compound

Appendix-5. (Continues). Results Tables, Physicochemical Properties, Comparative Analyses of Data for all the Synthesized compounds

Table 5.4. Physicochemical Properties of Malononitriles Synthesized via Microwave Irradiation Power of 300W at different Temperatures

Precursor	Product obtained	Reaction time (min)	Temperature (°C)	Yield <sup>a</sup> (%)	Appearance	Melting Point (°C)	Literature Melting Point (°C) [Reference]
1	11	1	90	95	Yellow powder	164-166	162-164[70]
2	12	1	90	98	Light Yellow powder	204-206	203-205[70]
3	13	1.5	110	93	Light Yellow powder	185-187	185-187 [70]
4	14	1	110	96	Golden Yellow powder	248-250	- <sup>b</sup>
5	15	1.25	100	97	Dark Red Crystals	145-146	161-162[79]
6	16	1.5	100	90	Yellow powder	187-189	- <sup>b</sup>
7	17	2	90	96	Dark Yellow powder	235-237	- <sup>b</sup>
8	18	1.5	100	97	Yellow powder	152-154	- <sup>b</sup>
9	19	1.5	100	96	Light Yellow powder	171-173	171-173[70]
10	20	2	110	93	Dark Brown powder	236-238	- <sup>b</sup>

<sup>a</sup>Yields refer to isolated pure products    <sup>b</sup>New compound

Appendix-5. (Continues). Results Tables, Physicochemical Properties, Comparative Analyses of Data for all the Synthesized compounds

Table 5.5. Physicochemical Properties of the Coumarin-thiophenes synthesized via Conventional Procedure

Precursor	Product Obtained	Reaction time (h)	Yield <sup>a</sup> (%)	Appearance	Melting Point (°C)	Literature Melting Point (°C) [Reference]
11	21	2	90	Bright Yellow Powder	241-243	240-242[70]
12	22	2	90	Light Yellow Powder	213-215	212-215[70]
13	23	3	89	Dark Yellow Powder	253-255	>250[70]
14	24	2	83	Golden Yellow Powder	293-295	- <sup>b</sup>
15	25	2	88	Dark Pink Powder	211-213	211-213[79]
16	26	3	80	Light Yellow Powder	208-210	- <sup>b</sup>
17	27	3	86	Dark Yellow Powder	304-306	- <sup>b</sup>
18	28	3	87	Light Yellow Powder	215-217	- <sup>b</sup>
19	29	2.5	90	Golden Yellow Powder	148-150	147-149[70]
20	30	3	90	Dark Yellow Powder	275-277	- <sup>b</sup>

<sup>a</sup>Yields refer to isolated pure products      <sup>b</sup>New compound

Appendix-5. (Continues). Results Tables, Physicochemical Properties, Comparative Analyses of Data for all the Synthesized compounds

Table 5.6. Physicochemical Properties of the Coumarin-thiophenes synthesized via Microwave Irradiation (450 W, 80 °C) procedure in Stepwise

Precursor	Product obtained	Reaction time (min)	Yield <sup>a</sup> (%)	Appearance	Melting Point (°C)	Literature Melting Point (°C) [Reference]
11	21	3	96	Bright Yellow Powder	241-243	240-242[70]
12	22	2	95	Light Yellow Powder	213-215	212-215[70]
13	23	3	94	Dark Yellow Powder	253-255	>250[70]
14	24	3	92	Golden Yellow Powder	293-295	- <sup>b</sup>
15	25	3	95	Dark Pink Powder	211-213	211-213[79]
16	26	2.5	95	Light Yellow Powder	208-210	- <sup>b</sup>
17	27	3	92	Dark Yellow Powder	304-306	- <sup>b</sup>
18	28	3	95	Light Yellow Powder	215-217	- <sup>b</sup>
19	29	3	96	Golden Yellow Powder	148-150	147-149[70]
20	30	3	95	Dark Yellow Powder	275-277	- <sup>b</sup>

<sup>a</sup>Yields refer to isolated pure products

-<sup>b</sup>New compound

Appendix-5. (Continues). Results Tables, Physicochemical Properties, Comparative Analyses of Data for all the synthesized compounds

Table 5.7. Physicochemical Properties of other derivatives Synthesized via Conventional Procedure

Precursors	Product obtained <sup>a</sup>	Reaction time (h)	Yield <sup>b</sup> (%)	Appearance	Melting Point (°C)
30 + AC <sup>c</sup>	31	18	94	Light Pink powder	238-240
30 + BC <sup>c</sup>	32	16	90	Light Pink powder	308-310
30 + NBC <sup>c</sup>	33	18	90	Dark Yellow powder	310-312
30 + SC <sup>c</sup>	34	17	92	Dark Yellow powder	172-174
30 + IB <sup>d</sup>	35	16	91	Dark Yellow powder	278-280

<sup>a</sup>New compound ; <sup>b</sup>Isolated pure products; <sup>c</sup>Room temperature condition; <sup>d</sup>Reflux at 65 °C

Table 5.8. Physicochemical Properties of other derivatives Synthesized via Microwave-Enhanced Irradiation Procedure

Precursors	Product Obtained <sup>a</sup>	Reaction time (min)	Yield <sup>b</sup> (%)	Appearance	Melting Point (°C)
30 + AC <sup>c</sup>	31	3	98	Light Pink powder	238-240
30 + BC <sup>c</sup>	32	3.5	95	Light Pink powder	308-310
30 + NBC <sup>c</sup>	33	3	94	Dark Yellow powder	310-312
30 + SC <sup>c</sup>	34	3.5	96	Dark Yellow powder	172-174
30 + IB <sup>c</sup>	35	3	94	Dark Yellow powder	278-280

<sup>a</sup>New compound ; <sup>b</sup>Isolated pure products; <sup>c</sup>450 W, 130 °C

## CURRICULUM VITAE

### Personal Information

Surname, Name : YAHAYA, Issah  
 Nationality : Ghana  
 Date and Place of Birth : 28.01.1982, Kumasi/Ghana  
 Marital status : Married  
 Phone number : 0 (534) 686 67 28  
 E-mail : issah.yahaya@gazi.edu.tr



### Education

Degree	School/ Program	Graduation Date
Doctoral (Ph.D)	Gazi University/Chemistry	2018
Masters (M.Phil.)	KNUST/ Pharm. Chemistry	2013
Undergraduate (BSc)	UCC/Chemistry	2007

### Work Experience

Year	Place of Work	Position
2007-2013	T.I. AMASS Girls'	Chemistry Teacher
2012-2012	Aspee Pharmaceuticals	QA/QC Manager/Chemist
2014-2015	Özel Seviye Koleji	English Skills Teacher
2015-To Date	Özel Aşıyan Koleji	English Skills Teacher

### Foreign Language

Turkish

### Publications

Yanar, U., Babür, B., Pekyılmaz, D., Yahaya, I., Aydın, B., Dede, Y., and Seferoğlu, Z. (2016). A fluorescent coumarin-thiophene hybrid as a ratiometric chemosensor for anions: Synthesis, photophysics, anion sensing and orbital interactions. *Journal of Molecular Structure*, 1108, 269-277.

### Hobbies

Playing Football, Playing Table-Tennis, Playing Draught, Swimming, etc.



*GAZİ GELECEKTİR..*